University of Liverpool
School of Environmental Sciences
Marine Electrochemistry Group

Chemical speciation of iron with humic ligands in estuarine and coastal waters

Doctoral Dissertation

Mahmoud Mohammad Abu Alhaija

September- 2015

Supervisors:

Professor C.M.G van den Berg

Doctor P. Salaün

ACKNOWLEDGEMENTS

I would never have been able to finish my dissertation without the guidance and support of my supervisor Professor Constant Van den berg.

Firstly, I would like to express my deepest gratitude to my supervisors, Professor C. M.G van den Berg and Dr. Pascal Salaün, for their excellent guidance, caring, patience, and providing me with an excellent atmosphere for doing research and in the end their friendship. I would also like to acknowledge the University of Jordan for financially supporting me during my study.

My deepest thanks to my wife, Wad Farah. She was always there cheering me up and stood by me through the good and bad times.

Also, I would like to thank my colleague Hannah Whitby, who was as an excellent friend, was always willing to help and give her best suggestions. It would have been a lonely lab without her.

Thank you to Paula Houghton, Carmel Pinnington, Karen Li and Susan Jones for all your help and support.

Finally, I would also like to thank my parents (Mohammad Abualhaija and Abla abualhaija), sister (Maysa), and brothers (Ahmad, Ehab, Ammar, Odai, and Ala'a). They were always supporting me and encouraging me with their best wishes.

ABSTRACT

Iron in coastal and sea water is readily complexed with organic matter (ligands) causing the formation of different species of iron, which affects its biogeochemistry. For this reason it is of interest to determine iron speciation in addition to its concentration. The chemical speciation of iron in coastal and sea water is typically determined by cathodic stripping voltammetry (CSV), making use of ligand competition between an electroactive ligand added to obtain the CSV signal and the natural ligand to determine the complex stability of the natural species. This thesis aims to identify the main ligand responsible for binding iron. Thereto, I first set out to improve the existing method of iron speciation in seawater using salicylaldoxime (SA) (as an added competing ligand) and subsequently used this method to determine the complex stability and concentration of the unknown Fe-binding ligands. Using another CSV method the concentration of humic substances (HS) was determined in samples from estuarine, coastal, shelf and ocean origin. Particular attention was given in this dissertation to the comparison between humic substances and natural Fe-binding ligands in all samples.

The improved SA method has a much better sensitivity due to two effects: 1) the use of dissolved oxygen (DO) as an oxidant was found to give a catalytic effect; this improved the sensitivity greatly, and also stabilized the pH. 2) the analytical conditions of using SA were re-optimised and best sensitivity is now obtained at 5 µM SA (~5 x less than the pre-existing method). Interpretation of the experiments showed that the complex responsible for adsorption on the mercury drop electrode is FeSA, whereas the $FeSA_2$ species does not adsorb. The complex stability for complexes of Fe with SA (FeSA and $FeSA_2$), in pH 8 seawater, were calibrated over a range of SA concentrations and salinities. The similarity of the stability constants (log $K'_{Fe'SA}$ and log $B'_{Fe'SA2}$) determined via calibration against EDTA to those calibrated without EDTA shows that the speciation of Fe with SA and EDTA is well understood. The improved method is applied to a mixed depth Celtic Sea sample, and two GEOTRACES samples from the Atlantic, at a SA concentration of 5 µM. Ligand concentrations were 1.47 and 1.49 nM in the GEOTRACES water (log $K'_{Fe'L}$ values of 11.1 and 11.9) and 2.53 nM in the Celtic Sea water (log $K'_{Fe'L}$ =11.5). Application of the method to ligands added to seawater gave log $K'_{Fe'L}$ values of 11.6 $\pm$0.1 for humic acid (Suwannee River) and 12.2 $\pm$0.3 for a siderophore (desferrioxamine B).

The improved SA method was also applied to samples from the Mersey estuary and Liverpool

Bay (salinity between 19 and 32). The concentration of unknown Fe-binding ligands was virtually the same as that of Fe-binding humics and both are greater than [Fe] in all samples, indicating that there was an excess of the ligand concentration and that almost the entire ligand concentration (95%) could be ascribed to humic substances. The average complex stability (log $K'_{Fe'L}$) was 11.2 $\pm$ 0.1, the same as for the iron-humic species (log $K'_{Fe'\text{-}SRHA}$). Copper additions demonstrated competition between Cu and Fe for the natural ligands.

Multiple analytical windows (MAWs) were used to determine the iron speciation in the Mersey estuary by varying the concentration of salicylaldoxime (SA). Data fitting of the individual titrations was compared to fitting of all data simultaneously (MAW fitting) giving good agreement. Individual titration fitting as well as the MAW fitting demonstrated the presence of only one ligand class in all samples (which was identified as humic substance in the previous work). Measurement of the composition of dissolved organic carbon (DOC) indicates the presence of terrestrial as well as microbial sources of organic matter in the estuary. The fraction of HS in the DOC amounted to between 47 and 25 % between salinities of 19 and 31.

Application of the improved method to samples from the shelf and the Atlantic ocean (vertical profile) shows that the Fe-binding ligands concentration is greater than Fe concentration in all shelf and ocean samples. The complex stability of the Fe species in the Atlantic and over the shelf is identical within a narrow range of log $K'_{Fe'L}$ values of 11.2 $\pm$ 0.1 (Atlantic profile) and 11.2 $\pm$ 0.2 for the shelf samples. Comparison of the iron-binding humics and complexing ligands shows that the humic substances account for 95 to 98 % of the total ligand for iron in the shelf and ocean waters. This revolutionary finding challenges the paradigm that iron-binding ligands largely originate from in-situ production by microorganisms and much facilitates the modeling of the background ligand concentration that controls the global oceanic distribution of Fe.

Data fitting of the complexometric titrations in all samples from the estuarine, coastal, shelf and ocean origin demonstrated the presence of only one ligand class.

ABBREVIATIONS AND SYMBOLS

Acronyms

AL	Added competing ligand
ASV	Anodic stripping voltammetry
BIX	Biological index
CDOM	Chromophoric dissolved organic matter
CLE-ACSV	Competing ligand exchange- cathodic stripping voltammetry
CE	Counter electrode
CL	Concentration of ligands
CSV	Cathodic stripping voltammetry
Cu-HS	Copper- binding humics
DFB	Desferrioxamine B
dFe	Dissolved iron
DHN	2,3-dihydroxynaphthalene
DO	Dissolved oxygen
DOC	Dissolved organic carbon
DOM	Dissolved organic matter
DP	Differential pulse mode
EDTA	Ethylenediaminetetraacetic acid
EPS	Exopolysaccharides
FA	Fulvic acid
Fe’	Inorganic iron
Fe-HS	Iron- binding humics
FI	Fluorescence index
HA	Humic acid
HDPE	High density polyethylene
HIX	Humidification index
HMDE	Hanging mercury drop electrode
HNLC	High nutrient, low chlorophyll
HS	Humic substances
IHSS	International humic substances society
KMS	KINETEQL Multiwindow Solver
L	Ligand
LAT/Lat	Latitude
L_{Cu}	Copper complexing ligands
LDPE	Low density polyethylene
L_{Fe}	Iron complexing ligands
LoD	Limit of detection
LON/Lon	Longitude
L_T	Total concentration of natural ligands
M	Metal
MAWs	Multiple analytical windows
MCC or ProMCC	A new windows-based, user friendly program for the determination of metal complexation parameters (L and K’) and for theoretical simulation of metal complexometric titration
ML	Metal- ligand complex
MQ	Milli-Q water
NN	1-nitroso-2-napthol
NOM	Natural organic matter

PFA	Perfluoroalkoxy alkane
PTFE	Polytetrafluoroethylene (Teflon)
RE	Reference electrode
RMSE	Root mean square error
SA	Salicylaldoxime
Sal	Salinity
SAW	Single analytical window
SPM	Suspended particulate matter
SRFA	Suwannee river fulvic acid
SRHA	Suwannee river humic acid
STN / Stn	Station
TAC	2-(2-thiazolylazo)-p-cresol
TDN	Total dissolved nitrogen
UVSW	Ultraviolet digestion Sea Water
VA	Voltammetric Apparatus
WE	Working electrode

Experimental symbols

(k)	Kinetic rate constant
K	Conditional stability constant
S	Sensitivity
S_{Max}	Maximum sensitivity
R_{AL}	The ratio of sensitivity at a given analytical window to the highest sensitivity
mM	Millimolar
µM	Micromolar
nM	Nanomolar
pM	Picomolar
A	Ampere
nA	Nano ampere
i_{p0}	initial peak height
$i_{P,}$ Ip	Peak current
Ip^{Cal}	Calculated peak current
$i_{p\ max}$	Maximum peak current
(km)	Kilometer
(m)	Meter
(mm)	Millimeter
(µm)	Micrometer
(m^3)	Cubic meter
(h)	Hour
(s)	Second
SD	Standard deviation
t_{dep} / d. t	Deposition time
V	Volt
mV	Millivolt
(α)	Side reaction coefficient
°C	Degree Celsius

CONTENTS

PAPERS RESULTING FROM THE EXPERIMENTS CARRIED OUT AND DESCRIBED IN THIS DISSERTATION

Abualhaija, M.M. and van den Berg, C.M.G., 2014. Chemical speciation of iron in seawater using catalytic cathodic stripping voltammetry with ligand competition against salicylaldoxime. Marine Chemistry, 164(0): 60-74.

Abualhaija, M.M., Whitby, H. and van Den Berg, C.M.G., 2015. Competition between copper and iron for humic ligands in estuarine waters. Marine Chemistry, 172(0): 46-56.

Mahmood, A., **Abualhaija, M.M.,** van den Berg, C.M.G. and Sander, S., 2015. Organic speciation of dissolved iron in estuarine and coastal waters at multiple analytical windows. Marine Chemistry, Submitted.

Abualhaija, M.M., van den Berg, C.M.G., Lohan, L., Rijkenberg, M. and Statham, P., 2015. Identification of iron-binding substances in the oceans. In preparation for Nature Geoscience.

Contributions to this thesis:

In chapters (2, 3 and 5), I prepared all data and graphs as well as the drafts for international journals under supervision of my supervisor professor C.M.G van den berg. In chapter 4, I collaborated with Abida Mahmood (New Zealand-Otago University). I did part of this work, including calibrations of stability constants (log $K'_{Fe'SA}$ and log $B'_{Fe'SA2}$), help Abida to use and set up the new SA method, supervise the measurements and calculations of the individual complexation titrations step by step and make comments on this paper. Van den Berg co-wrote the papers that were submitted and devised the speciation modeling.

THESIS STRUCTURE

The CSV method for iron speciation in seawater using (SA) was improved in this thesis, and applied to samples from coastal, estuarine, shelf and open ocean waters.

Chapter 1: General introduction.

Brief: General introduction to the iron and organic ligands in coastal and sea water and CSV methods for iron speciation and humic substances.

Chapter 2: Chemical speciation of iron in seawater using catalytic cathodic stripping voltammetry with ligand competition against salicylaldoxime.

Brief: The sensitivity of the existing CSV method for Fe speciation in seawater using salicylaldoxime (SA) was improved by measuring in the presence of air-oxygen which was found to a give catalytic effect. The complex stability of Fe' with SA (FeSA and $FeSA_2$) was calibrated independently against and without EDTA. FeSA2 was found not to adsorb on the electrode, but FeSA does instead. The improved method was tested on samples from the Atlantic ocean.

Chapter 3: Competition between copper and iron for humic ligands in estuarine waters.

Brief: The new SA method is applied to samples from the Mersey estuary and Liverpool bay, to determine iron speciation and humic substances at different salinity, The complex stability of Fe' with SA was also calibrated over a range of salinity (19 to 32) to enable iron speciation in estuarine waters. The competition between copper and iron for humic ligands was studied in this chapter.

Chapter 4: Organic speciation of dissolved iron in estuarine and coastal waters at multiple analytical windows.

Brief: The multiple analytical windows were used with the improved method in the same samples from the Mersey estuary and Liverpool Bay, 5 detection windows defined by setting the concentration of the competing ligand (SA) at 5, 10, 15, 25 and 50 µM to determine the speciation of iron and the possibility of finding more than one ligand (ligand

classes) in these waters.

Chapter 5: Identification of iron-binding substances in the oceans.

Brief: The improved method is also applied to samples from the shelf and vertical ocean profile (Atlantic ocean) to determine the iron speciation and humic substances in these waters. Measurements of ligand concentrations and humic concentrations show agreements, suggesting that humic substances and unknown complexing ligands are one and the same.

1

Chapter 1
Introduction

1. INTRODUCTION

1.1. Iron distribution, limitation, and sources in coastal and sea waters

Iron is the fourth most abundant element in the earth's crust (Taylor, 1964; Wedepohl, 1995) after oxygen (O), silicon (Si) and aluminium (Al). Despite that, iron exists at extremely low concentrations in oceanic surface waters (0.02 to 1 nM), whereas its concentrations increase by orders of magnitude in transects from the open ocean to coastal waters (Martin and Gordon, 1988; Wu and Luther III, 1996). Iron distribution in coastal and sea waters is controlled by different processes, including differences in rate of iron inputs (i.e. rivers, shelf sediments, atmospheric deposition and hydrothermal vents), biological uptake, complexation with organic ligands, remineralisation and scavenging on sinking particles.

River input is the dominant source of trace metals (including iron) in estuarine waters (Bruland et al., 2014), but the majority of dissolved iron in river water exists as colloidal particles (Fox, 1988; Wen et al., 1999). The concentration of dissolved iron in estuarine waters decreases with increasing salinity, due to estuarine waters mixing with seawater and the increase in concentration of major cations, the colloidal iron flocculated with organic matter, forming particulate matter that sinks to the sediments. Previous work (Boyle et al., 1977; Sholkovitz, 1976; Sholkovitz et al., 1978) described the scavenging of Fe (as iron oxyhydroxides) in salinity gradients in estuarine systems due to flocculation with humic substances (HS) during estuarine mixing, removing more than 90% of the dissolved Fe and lowering its concentration from 0.5–10 μ mol/L in freshwaters (Nagai et al., 2007), to the 1-20 nmol/L range in coastal water.

Coastal waters are enriched in iron compared to the open ocean due to their proximity to shelf sediments and terrestrial sources (Johnson et al., 1997), since the majority of dissolved iron is lost through estuarine flocculation and precipitation processes (Boyle et al., 1977). Resuspended shelf sediments combined with the upwelling process are the dominant sources to coastal surface waters (Johnson et al., 1999), and this may explain the gradient of surface dissolved Fe concentration from shelf and coastal to open ocean. Atmospheric deposition is the dominant source of iron in ocean waters (Duce and Tindale, 1991), followed by shelf sediments, hydrothermal vents and upward mixing and advection of

deeper waters (Conway and John, 2014; Klunder et al., 2012; Tagliabue et al., 2010).

The vertical distribution of dissolved iron in seawater has a nutrient-like profile due to its biological function (Martin and Gordon, 1988), dissolved iron concentration in surface waters usually < 0.2 nM, then its concentration increases gradually to ~0.7 nM in deep waters (Boyd and Ellwood, 2010; Johnson et al., 1997). Several vertical profiles of dissolved iron concentration have been published previously, for example two of those profiles, were in the north Pacific (Martin et al., 1989) and north Atlantic (Conway and John, 2014) (Fig. 1.1), with low concentrations of dissolved Fe in surface waters ~ 0.05 nM in the north Pacific compared to higher concentrations in the north Atlantic ~ 0.3 nM, then Fe concentrations gradually increase at 1000 m depth to ~ 0.7 nM in the north Pacific and ~ 0.8 in the north Atlantic, and then decrease slightly in both profiles to ~ 0.6 nM at 4000 m (Fig. 1.1). Dissolved iron concentrations in the deep Pacific and Atlantic are nearly similar (Biller and Bruland, 2012) and the complexation with organic ligands controls the residual Fe and scavenging processes (Völker and Tagliabue, 2015).

The distributions and concentrations of iron in seawater are controlled by several processes where the chemical forms (speciation) affect transport and internal cycling. Generally the Fe concentrations in ocean surface waters are regulated by Fe inputs (atmospheric deposition) and removal (biological uptake and scavenging processes). Scavenging processes result in the transport of dissolved Fe from the surface waters to deeper waters with subsequent remineralisation at depth. Below the productive waters the oxygen is consumed due to organic matter respiration and weak ocean ventilation forming oxygen minimum zone (Karstensen et al., 2008), as a result of low oxygen concentration, the dissolved Fe concentration is enhanced and stabilized by organic ligands (Hopkinson and Barbeau, 2007). Remineralisation, hydrothermal vents, scavenging process as well as organic complexation control iron concentrations in deep waters. Ocean mixing processes also affect the distribution of iron in ocean waters (i.e. Tagliabue et al., 2014). (Boyd and Ellwood, 2010) noted that the remineralisation process is significant at (300-1000 m) depth, whereas the scavenging process is significant at (> 1000 m) depth. The scavenging process is an important process because it acts throughout the water column and affects the iron distribution and removes iron at concentrations greater than solubility limit (Johnson et al., 1997).

The low solubility of inorganic species (Fe') (~10 pM) (Liu and Millero, 2002), biological

uptake and adsorption on sinking particulate material are the main reasons for iron removal from seawater. The scavenging process can be defined as the process of metal removal due to its adsorption on particulate materials with relatively high affinity surface sites and settling with these particles to the deep ocean (Bruland et al., 2014; Turekian, 1977). Chemical and biological scavenging processes lower the dissolved Fe concentration unless organic complexation plays a role by stabilizing iron against these processes (Kuma et al., 1996). Thus iron complexation with organic ligands plays a critical role in determining Fe distribution (Tagliabue and Völker, 2011; Völker and Tagliabue, 2015). Fe concentrations in the deep Pacific and Atlantic are nearly similar reflecting a balance between Fe removal and supply processes with stabilization through ligands.

Fe is an essential element required for the synthesis of chlorophyll and several proteins involved in many life processes, such as photosynthesis, respiration and nitrogen fixation (Moore and Doney, 2007; Raven et al., 1999; Sunda et al., 1991). It is well known that Fe deficiency limits primary productivity in large areas of the world's oceans in region known as HNLC (high nutrient, low chlorophyll) (Martin and Fitzwater, 1988; Martin and Gordon, 1988), even in some coastal upwelling regions (Biller and Bruland, 2014).

HNLC areas (such as, the equatorial and subarctic Pacific and the Southern Ocean) are rich of macronutrients such as nitrate, phosphate and silicate, but have low phytoplankton growth; this restriction of growth in these areas is attributed to the iron deficiency (Boyd et al., 2007; Martin and Fitzwater, 1988).

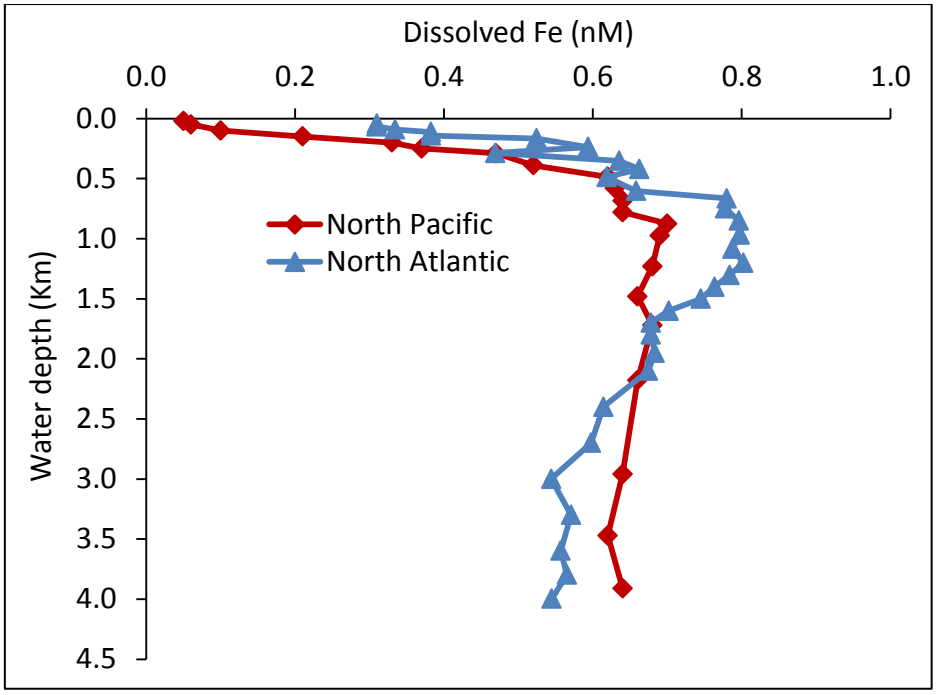

Figure 1.1. Typical profiles of dissolved iron in the north Pacific (cruise: VERTEX VII, station 7) (Martin et al., 1989) and north Atlantic (cruise: US GEOTRACES North Atlantic GA03, station 6) (Conway and John, 2014).

In 1990 John Martin published the "Iron Hypothesis", in which he proposed that increased iron deposition by atmospheric input in HNLC regions could promote primary production; consequently it has a significant influence on the global carbon cycling and earth's climate (Martin, 1990). Several previous studies have used the iron fertilisation approach (iron fertilisation experiments) to test the iron hypothesis in ocean surface waters, such as equatorial Pacific Ocean (IronEx) (Coale et al., 1996; Martin et al., 1994), Subarctic Northeast Pacific (Boyd et al., 2005) and Southern Ocean (SOIREE) (Boyd and Law, 2001) by intentional introduction of low concentrations of iron to the surface ocean waters to stimulate a phytoplankton growth. Most of these studies have supported the iron hypothesis and demonstrated that the additions of the iron to the surface ocean waters provide a significant increase in phytoplankton productivity and reduce atmospheric carbon dioxide.

The major inputs of iron in ocean waters are from atmospheric deposition (Duce and Tindale, 1991; Jickells et al., 2005), river runoffs and continental shelf sediments (Johnson et al., 1997; Moore and Braucher, 2008), hydrothermal vents (Klunder et al., 2012; Tagliabue et al., 2010; Wu et al., 2011) and ice melting (Lannuzel et al., 2007; Wang et al., 2014). Whereas the main removal pathways of iron in ocean waters are biological uptake and scavenging on settling particles (Bergquist et al., 2007; Tortell et al., 1999).

1.2. Iron chemistry and bioavailability in seawater

Iron occurs in seawater in two oxidation states: the soluble ferrous form Fe (II) in chemically reducing conditions (Landing and Westerlund, 1988) or when subject to photochemical reactions (Laglera and Van den Berg, 2007; Miller and Kester, 1994), whereas the ferric form Fe (III), is the thermodynamically stable form in oxygenated waters. The reduced form, Fe (II), is found in oxic surface waters at extremely low concentrations (pM or less) due to the rapid oxidation (in hours) to Fe (III) by O_2 and H_2O_2. The lower concentrations of Fe in open ocean waters are attributed to its poor solubility (~10 pM as inorganic Fe at pH 8 seawater (Liu and Millero, 2002)), whereas its solubility in coastal water is about an order of magnitude higher than that in the Open Ocean (Kuma et al., 1996). Fe is found in higher concentrations than expected by its solubility due to the presence of organic matter (ligands). So we all appreciate the role of the natural ligands.

Iron complexation with organic ligands increases its solubility and prevents its hydrolysis and precipitation, thus keeps it in the dissolved phase (Kuma et al., 1998; Kuma et al., 1996b; Liu and Millero, 2002). The inorganic speciation of Fe (III) is dominated by its hydrolysis behaviour (Waite, 2001). It has been demonstrated that over 99 % of dissolved iron in coastal and ocean waters is complexed with organic ligands (Gledhill and Van Den Berg, 1994; Rue and Bruland, 1995; van den Berg, 1995).

The availability of Fe to microorganisms is linked with its speciation. Iron in surface water exists as Fe complexed with organic ligands and free inorganic iron (Fe II and Fe III). Redox transitions involve oxidation of Fe(II) (by dissolved oxygen in surface water) and reduction of Fe(III) (by photochemical process). Fe(III) complexes with organic ligands dominate the chemical speciation of iron in coastal and seawater (Gledhill and van den Berg, 1994; Rue and Bruland, 1995; van den Berg, 1995). An important question remains how microorganisms can access organically bound Fe. Fe(II) in shelf water has also (like Fe(III)) been shown to be stabilised with organic matter (Statham et al., 2012) which probably contributes to its longevity.

It has been shown that phytoplankton can access organically bound iron using specific mechanisms (Maldonado and Price, 1999); these mechanisms involve the reduction of organically bound Fe by specific reductases at the surface of the cell (Maldonado and Price, 1999, Maldonado., et al., 2006). Hutchins and coauthors have shown that not all forms of

organically bound iron are equally available to different groups of phytoplankton (Hutchins et al., 1999). Photochemical reduction of organically bound Fe is an important process retaining Fe in surface waters and increasing its availability to microorganisms (Rijkenberg et al., 2005; Tagliabue and Arrigo, 2006). The inorganic form of iron is the most bioavailable form as it can be taken up directly by phytoplankton (Morel et al., 2008).

The speciation of copper is similar to that of iron in that its speciation in seawater is dominated by organic complexation (Bruland et al., 2000; Buck and Bruland, 2005; Kogut and Voelker, 2003). Phytoplankton release copper binding ligands in response to copper toxicity, thus affecting the copper speciation (Moffett et al., 1997). Copper is a redox active transition metal acts as a cofactor in enzymes that catalyse other redox reactions, thus it is a vital metal for growth (Maldonado., et al., 2006). It has been shown that the uptake rate of organically bound iron by phytoplankton is dependent on copper availability; as the Fe (II) produced by reductases is re-oxidized by a copper containing ferroxidase during the Fe transport to the cell membrane (Maldonado., et al., 2006).

Competition between copper and iron (as demonstrated in chapter 3) could affect the bioavailability of both metals to microorganisms. Increases in the copper concentration could lead to increasing competition with Fe for natural ligands and displace Fe from Fe-L complexes thus increasing inorganic Fe, thus affecting the bioavailability of both metals. For example domoic acid, is known to be complexed with copper and iron in seawater (Rue and Bruland, 2001) suggesting that metal competition could play a role. It has been suggested that Fe uptake by Pseudo-nitzschia is regulated by both domoic acid and copper (Wells et al., 2005), which could possibly be explained by competition reactions.

1.3. What are the natural ligands in seawater?

Iron is an essential micronutrient element required by phytoplankton such as photosynthetic microalgae. Photosynthesis is the process of converting light energy (from Sun), into chemical energy and then the chemical energy is stored as organic compounds (e.g. $C6H_{12}O_6$ or CH_2O), which are synthesized from the inorganic carbon dioxide (CO_2) and water (H_2O).

Fe is also a required element for marine microorganisms, such as bacteria (Tortell et

al., 1999). These organisms are responsible for degradation and remineralisation of sinking organic matter. Organic matter (like algae and fecal pellets) and their breakdown products contain several molecules which have high chemical attractions to bind Fe. These molecules are called ligands and are responsible to keep iron dissolved in seawater; consequently preventing its hydrolysis and precipitation (Kuma et al., 1996).

The compositions of these ligands are still largely unknown, and may consist of many compounds, "Ligands soup", this term is given to ligands in seawater and is "based on the notion that almost any organic matter, after suitable 'cooking', will most likely generate metal-binding ligands" (Hunter and Boyd, 2007). The possible sources of these ligands (Ligand soup) in seawater are generally ascribed to biological activities (such as, (1) breakdown of sinking organic particulate matter, (2) ligands produced by marine bacteria, such as saccharides and siderophores) and terrestrial inputs (transported organic matter from rivers and continental shelves) (Bauer et al., 2002; Hwang et al., 2004; Macrellis et al., 2001).

It has been reported that the Fe-binding organic ligands during the iron fertilisation experiment (IronEx II) in the equatorial Pacific Ocean are produced rapidly in response to small iron additions (Rue and Bruland, 1997). Furthermore during the iron fertilisation experiment (SOIREE) in the polar Southern Ocean (Boyd et al., 2000), one data point inside the patch of the fertilisation experiment has shown an increase of ligand concentration from 3.5 nM (until 11 day after the start of experiment) to 8.5 nM (At day 12), but one data point is not enough to decide if the ligands are produced or not and this may need further investigations and it will be an interesting area for the future studies to verify whether the Fe-binding ligands are produced during the iron fertilisation experiments or not.

Several ligands have been proposed as Fe (III)-binding ligands in coastal and sea water, such as siderophores (Mawji et al., 2008; Velasquez et al., 2011), porphyrin (IX) (Heme B) (Gledhill, 2014), saccharides (Hassler et al., 2011a; van der Merwe et al., 2009) and humic substances (Batchelli et al., 2010; Laglera and van den Berg, 2009).

Siderophores are low-molecular weight, high-affinity Fe (III)-binding ligands produced by marine bacteria (Macrellis et al., 2001; Velasquez et al., 2011; Vraspir and Butler, 2009). Siderophores have been found at very low concentrations (pM) in coastal and sea water (Mawji et al., 2008; Velasquez et al., 2011), and they have been shown to be produced by

marine bacteria in culture (Martinez et al., 2003). (Mawji et al., 2008) have identified and quantified two types of siderophores (ferrioxamine G and ferrioxamine B) in the Atlantic Ocean waters, with concentrations up to 20 pM, and represent between 0.2 and 5 % of the dissolved Fe pool if these siderophores are fully complexed in seawater. An example of siderophores is shown in Fig. 1.2 below:

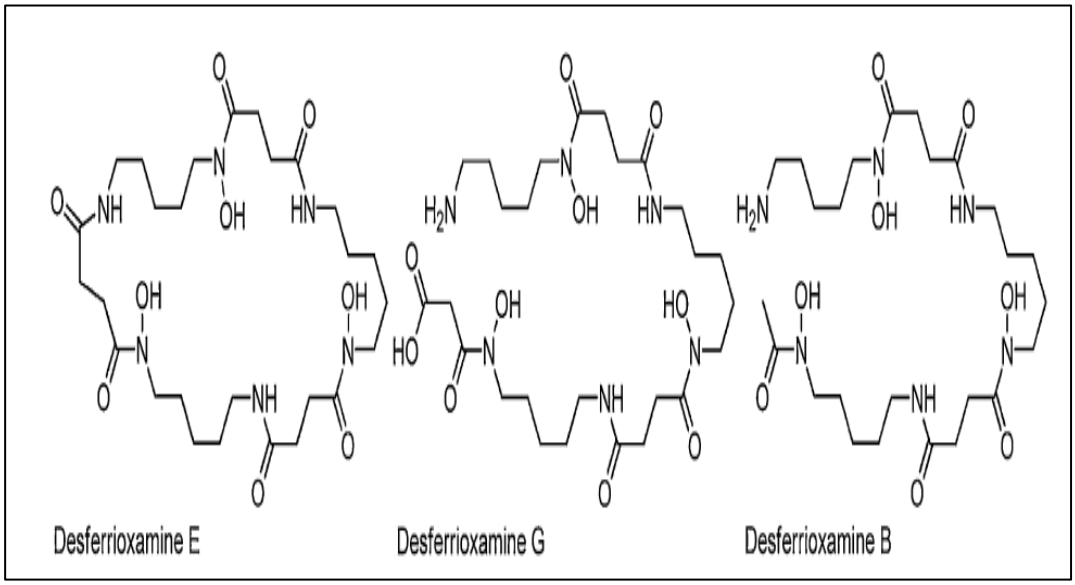

Figure 1.2. Structures of marine Siderophores (deffeioxamine E, G and B) (Butler and Theisen, 2010).

Porphyrins are biologically produced molecules (Hutchins et al., 1999). Porphyrin (IX) was used as a model ligand in seawater with values of Log $K'_{Fe'L1}$ =12 (Rue and Bruland, 1995) and 12.4 (Witter et al., 2000a), thus it has been proposed as a potential Fe-binding ligand and may contribute to Fe ligand pool in seawater (Hunter and Boyd, 2007; Rue and Bruland, 1995; Witter et al., 2000a). Recent studies have found protoporphyrin (heme b) in phytoplankton and marine particulate material (Gledhill, 2014; Honey et al., 2013) and in river waters (Vong et al., 2007). The structure of marine protoporphyrin (heme b) is shown in Fig. 1.3 below:

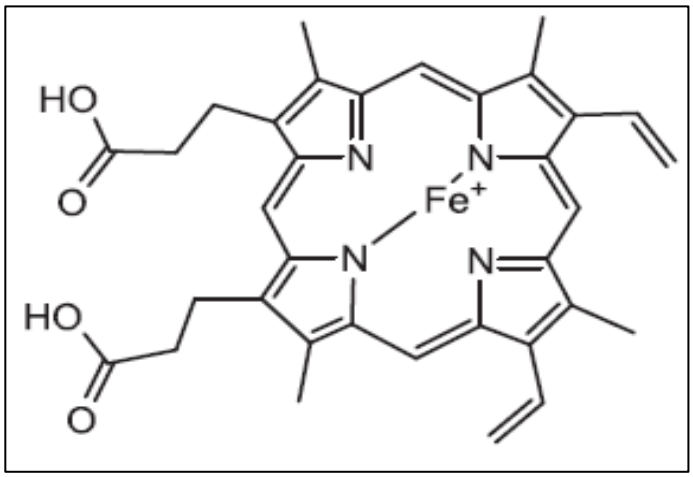

Figure 1.3. Structure of marine protoporphyrin (heme b) (Gledhill, 2014).

Exopolysaccharides are high molecular weight compounds secreted by micro-organisms (such as, marine bacteria) (Hassler et al., 2011a; Poli et al., 2010), recently have been shown that saccharide additions enhance iron bioavailability and iron uptake by marine phytoplankton, and hence saccharide compounds may also contribute to Fe ligand pool (Hassler et al., 2011b). The proposed structure of extracellular polysaccharide is shown in Fig. 1.4 below:

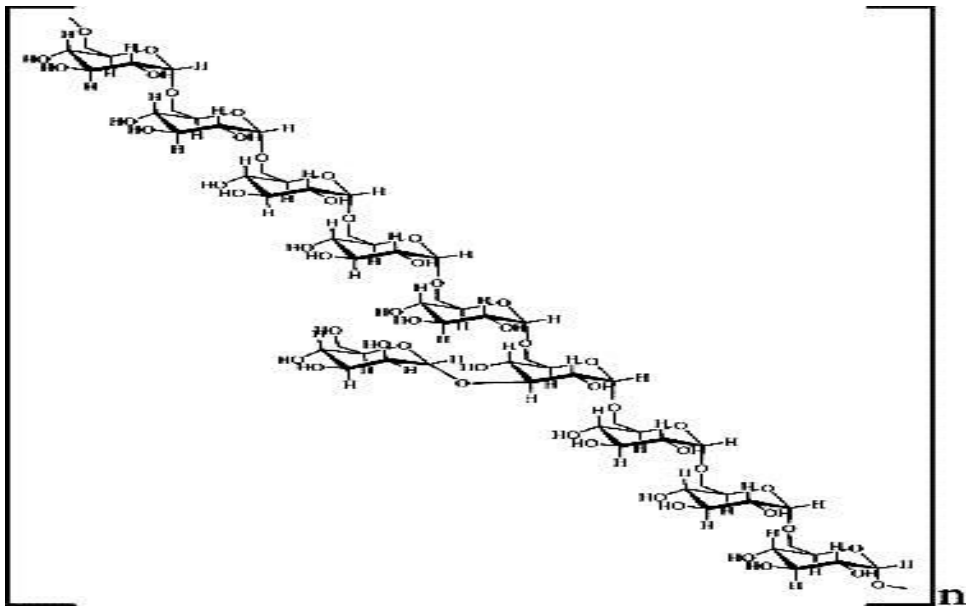

Figure 1.4. Proposed structure of the extracellular polysaccharide produced by by *A. versicolor* (Chen et al., 2013).

Humic substances (HS) are important constituents of natural organic matter (NOM) in soil and aquatic environments, and account for a significant portion of dissolved organic

carbon (DOC) in the aquatic system (Frimmel, 2005). The possible sources of HS in the aquatic system are attributed to terrestrial sources and biological by-products in the water body (Frimmel, 2005). Fluorescence data of HS shows that humic substances are wide-spread in the oceans (Heller et al., 2013). Humic substances in seawater can be divided depending on their solubility into two major components, fulvic acid (FA), this component is soluble in water at all pH, and humic acid (HA), which is insoluble in water under acidic condition (pH < 2).

Humic substances are strong candidates for the iron complexation in coastal and sea water because they have high attraction to complex with iron (Laglera and van den Berg, 2009) and they are resistant to degradation (refractory organic matter) with long residence time (centuries to millennia) (Buffle, 1990). The model structure of humic acid is shown in Fig. 1.5 below:

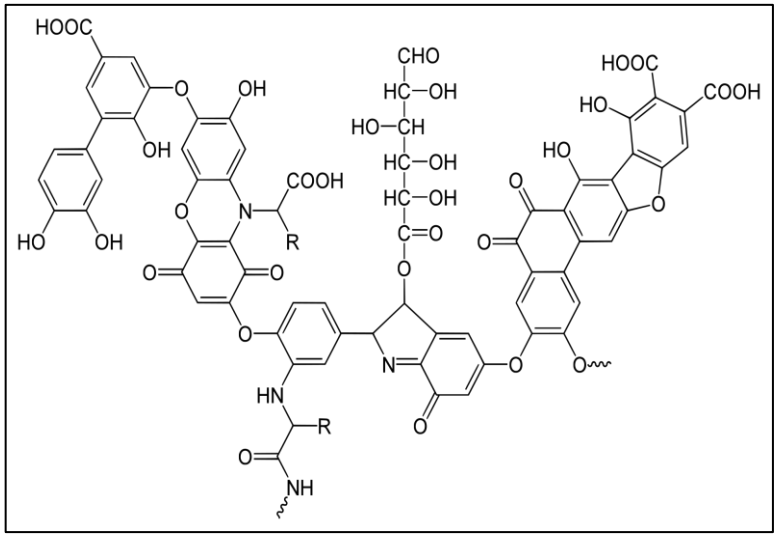

Figure 1.5. Model structure of humic acid (Stevenson, 1994).

1.4. Determination of humic substances (HS)

The quantification and characterisation of aquatic HS has been studied using several methods, including spectroscopic methods (e.g. fluorescence) (Heller et al., 2013; Kumke et al., 1998; Senesi et al., 1991), elemental analysis (Abbt-Braun and Frimmel, 2002; Huffman and Stuber, 1985), chemiluminescence (Tian et al., 2005) and voltammetric response of Fe-HS complex (Laglera et al., 2007).

Laglera et al. (2007) developed an electrochemical method that enables the direct

measure of humic like substances in seawater by cathodic stripping voltammetry (CSV). This method basically measures the response of Fe-HS complex in presence of bromate to enhance the sensitivity of the Fe-HS response through a catalytic effect, and then HS is calibrated using Suwannee River fulvic acid (SRFA) standard (Laglera et al., 2007). Using this method it has been suggested that the HS may account for the entire iron-binding ligands in coastal waters and the co-variation of Fe with HS indicates that the iron is transported from estuarine and coastal to the sea waters stabilized with HS (Laglera and van den Berg, 2009).

The concentration of humic substances in the present study was determined by cathodic stripping voltammetry (CSV) in the presence of bromate as developed previously (Laglera et al., 2007), with a small difference where the voltammetric apparatus was air-pressurised instead of nitrogen as used for the Fe determination (Abualhaija and van den Berg, 2014), as the response for Fe-HS was not affected by the dissolved oxygen (DO). The concentration of humic substances was determined after the addition of sufficient Fe to saturate the free humic substances followed by detection of the Fe-HS by CSV method. Calibration of humic substances was by standard additions of Suwannee River humic acid (SRHA). The deposition potential was 0 V, with a deposition time between 20 and 180 s depending on the ambient Fe and HS concentrations. The scans were initiated from 0 V to -1 V and were in the differential-pulse (DP) mode (see Chapter 3).

1.5. Determination of natural ligands (L) by cathodic stripping voltammetry (CSV)

Complexation by organic matter dominates the chemical speciation of the biogenic metals copper, zinc, cobalt and iron in seawater (Ellwood and Van den Berg, 2001; Gledhill and Van Den Berg, 1994; Laglera and van den Berg, 2003; Saito and Moffett, 2001; van den Berg et al., 1987). This complexation is important because it affects the availability of metals to organisms, for instance by facilitating the uptake of iron (Hassler et al., 2015; Maldonado and Price, 1999).

Speciation procedures for trace metals in seawater are based either on anodic stripping voltammetry (ASV) (Plavšić et al., 1982) or cathodic stripping voltammetry (CSV) (Van Den Berg, 1984). The advantages of voltammetric stripping methods (ASV and CSV) are high sensitivity, small sample volume (10 ml or so), possibility of performing shipboard

measurements (Buffle et al., 2005) and the capability of analysing chemical speciation directly. The possible disadvantage of voltammetric methods is the potential of interference from organic substances (Laglera et al., 2011). The CLE-CSV method can be used to determine the complex stability (Log K'_{FeL}) and concentration of natural ligands, but its resolution with respect to the identity of different natural compounds is restricted if these compounds have similar complex stability. For instance the log K for Fe with a siderophores like DFB is 12.2 (chapter 2) whilst for humic acid it is 11.2. Other siderophores may have complex stability similar to DFB so it may be difficult to identify those. Other compounds that can be identified by CSV are various thiols (cysteine, glutathione, thioacetamide) and sulphide (Al-Farawati and Van Den Berg, 2001; Laglera and van den Berg, 2003; Le Gall and van den Berg, 1998).

The ASV method can be used to determine metals that are electroplated at the electrode and this method is not suitable for iron determination, as iron cannot be reduced to the metallic state and electroplated at the electrode. Consequently the CSV method is the most common method for determination of iron and iron speciation. The ASV method does not require addition of competing ligand and can be used to measure the concentration of labile metal without added competing ligand. Pseudopolarography can be used to determine complex stabilities of copper and lead complexes from the half-wave potential (Gibbon-Walsh et al., 2012). But this is not suitable for iron due to insufficient sensitivity (Mikkelsen et al., 2006).

CSV of iron involves a pre-concentration step in which an iron-binding ligand (AL) is added to the seawater sample to form an electro-active adsorptive complex with Fe (III). Then this complex (FeAL) is adsorbed onto a mercury electrode (hanging mercury drop electrode (HDME)) at a specific potential (deposition step). The amount of adsorbed complex is determined by a reducing potential scan (stripping step) using the CSV method, and this amount is directly proportional to the concentration of dissolved FeAL, and thus the dissolved FeAL is related to the concentration of Fe and AL.

Competition for iron between added ligand and natural complexing ligand is the basis for the speciation methods. Catechol was the first reported competitive added ligand for the determination of iron in seawater using CSV method (Van Den Berg and Huang, 1984), but catechol method has a high detection limit, and it is not suitable for oceanic samples. More

recent, four different competitive added ligands have been reported for Fe speciation: 1-nitroso-2 naphthol (NN) (Gledhill and Van Den Berg, 1994), salicylaldoxime (SA) (Rue and Bruland, 1995), 2-(2-thiazoly-lazo)-*p*-cresol (TAC) (Croot and Johansson, 2000) and 2,3-dihydroxynaphthalene (DHN) (van den Berg, 2006) (Table 1.1). In NN method the pH is adjusted to 6.9 using PIPES buffer, while in SA, DHN and TAC methods is adjusted to seawater pH (pH=8) using borate or EPPS buffer.

In the present work, the pre-existing SA method was re-visited and improved (Abualhaija and van den Berg, 2014), with different findings and different interpretation for the adsorptive electroactive species (see Chapter 2).

The voltammetric apparatus used in the present study consisted of a Metrohm 663 VA Stand connected to a μAutolab III potentiostat, which was computer-controlled using the GPES 4.9 (general-purpose-electrochemical-software) software. The working electrode was a hanging mercury drop electrode (HMDE), Ag | AgCl electrode filled with 3M KCl was used as a reference electrode, whereas a glassy carbon rod was the counter electrode. The voltammetric stand was connected to compressed air at 1 bar (Abualhaija and van den Berg, 2014). Voltammetric scans were in differential-pulse mode. Each sample was scanned 3 times, and the average value was recorded as a peak height. Examples of the voltammetric scans are shown in (Fig. 1.6). The peak for Fe-HA and Fe-SA is at similar potential near -0.48 V but that for Fe-SA requires catalysis by dissolved oxygen and that for Fe-HA requires bromate for catalysis.

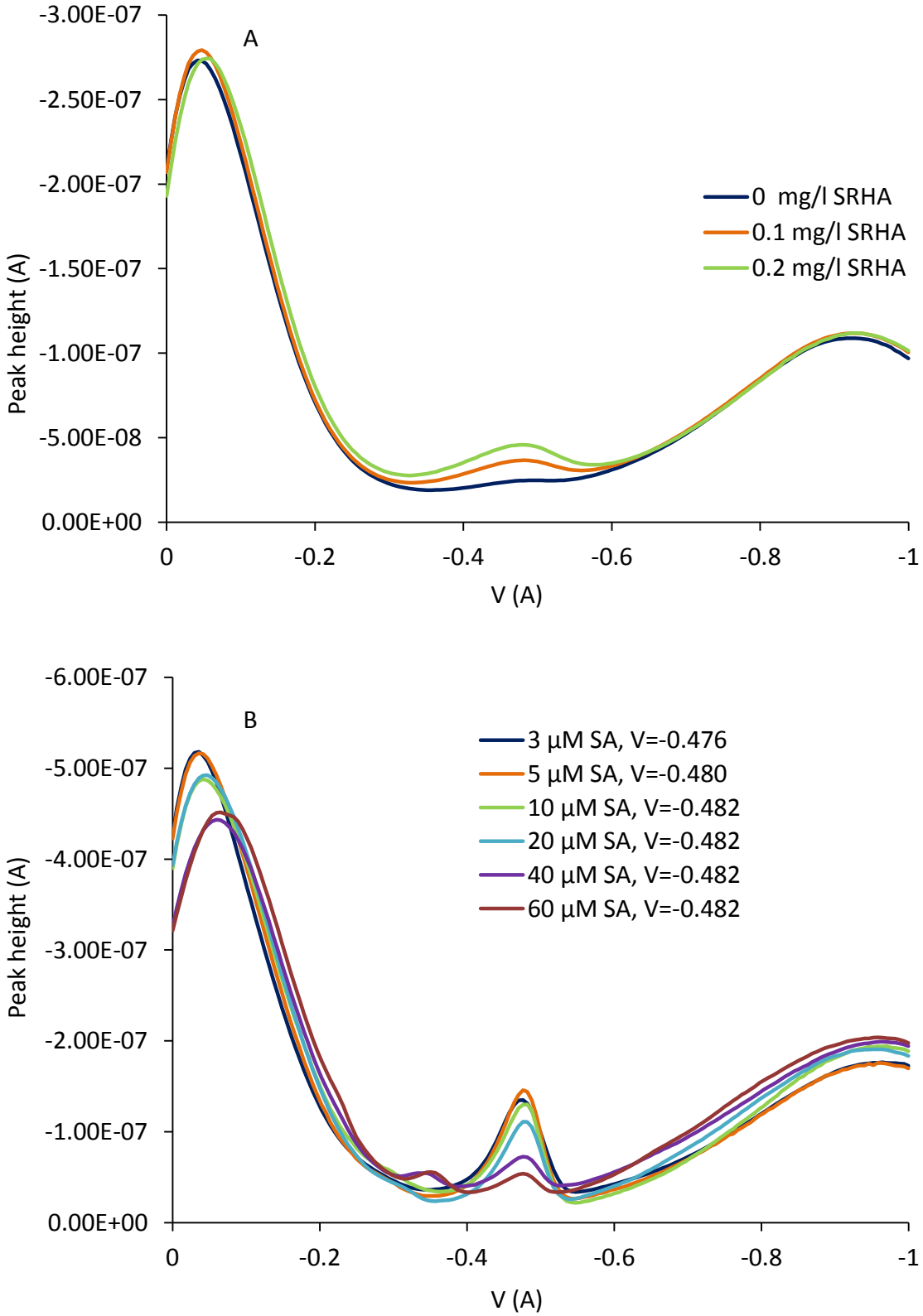

Figure 1.6. Examples of voltammetric scans, A) Fe-HS scans at a constant concentration of Fe and different concentrations of SRHA (0, 0.1 and 0.2 mg/l). B) Fe-SA scans at a constant Fe concentration and different concentrations of SA (3, 5, 10, 20, 40 and 60 µM SA).

Table 1.1: Overview of the organic speciation of iron: Location, Method, ligand concentrations and conditional stability constants (with respect to $Fe^{'}$) compiled from the literature. The originally published values of Log K'_{Fe3+L} were converted to Log $K'_{Fe'L}$ using Log αFe'=10.

Location	Depth (m)	Reference	Method	Ligand concentration (nM)	Stability constant Log $K'_{Fe'L}$	Other
Mersey estuary and Liverpool bay (Irish Sea)	2	This study, (Abualhaija et al., 2015)	SA Air-O_2	6.1-105.0	11.1-11.4	
North Atlantic-Celtic Sea	2 and 75	This study, (Abualhaija and van den Berg, 2014)	SA Air-O_2	1.47-2.53	11.1-11.9	Log $K'_{Fe'HA}$=11.6 Log $K'_{Fe'DFB}$=12.2
North Atlantic- Celtic sea- shelf samples Western North Atlantic- vertical profile	2-195 26-3346	This study	SA Air-O_2	0.69-3.07 1.45-2.13	11.0-11.6 11.0-11.3	
San Francisco Bay, California	2-64	(Bundy et al., 2015)	SA	L1: 9.2-139.5 L2: 11.3-121.2 L3: 16.0-88.8 L4: 45.3-163.3	Log $K'_{Fe'L1}$: 12.2-13.2 Log $K'_{Fe'L2}$: 11.0-12.0 Log $K'_{Fe'L3}$: 10.3-11.0 Log $K'_{Fe'L4}$: 9.2-9.9	Multiple analytical window
off the coast of northern and central California: surface and benthic boundary layer (BBL) samples	2-339	(Bundy et al., 2014)	SA	L1: 3.4-16.2 L2: 2.6-15.8 L3: 2.0-24.5 L4: 13.9-68.8	Log $K'_{Fe'L1}$: 12.1-12.4 Log $K'_{Fe'L2}$: 11.2-11.9 Log $K'_{Fe'L3}$: 10.4-11.0 Log $K'_{Fe'L4}$: 9.3-10.0	Multiple analytical window
High latitude North Atlantic Ocean	5-2237	(Mohamed et al., 2011)	TAC	0.24-3.15	11.47-13.86	
Southern Ocean	15-1000	(Ibisanmi et al., 2011)	TAC	0.47-1.51	11.00-11.95	
Northeast Atlantic Ocean	26-3998	(Thuroczy et al., 2010)	TAC	0.65-1.76	11.68-13.00	
Southern Ocean-Atlantic Sector	20-1000	(Boye et al., 2010)	TAC	0.58-0.86	11.00-12.86	
Northeast Atlantic Ocean- Humic rich coastal water.	1	(Batchelli et al., 2010)	TAC	46.5-604.4	10.23-11.97	
- Irish Sea- Coastal water - Pacific Ocean (SAFe)	15 600-1000	(Laglera and van den Berg, 2009)	DHN	7.5-11.5 1.0-5.2	10.9-11.2 11.0-12.4	Log $K'_{Fe'HA}$=11.1 Log $K'_{Fe'FA}$=10.6
Tropical Northeast Atlantic Ocean	3	(Rijkenberg et al., 2008)	TAC	0.82-1.46	11.94-13.41	
NW Pacific	2	(Kondo et al., 2008)	TAC	0.29-2.02	11.9-12.5	
Southern Ocean-Indian Sector	20-2500	(Gerringa et al., 2008)	TAC	0.08-1.61	11.0-12.8	
Eastern Tropical North Pacific	2-200	(Hopkinson and Barbeau, 2007)	TAC	0.2-1.6	12.1-12.8	
Bering Sea-Alaska	2-57	(Buck and Bruland, 2007)	SA	L1: 0.4-18.0 L2: 1.2-15	Log $K'_{Fe'L1}$: 11.1-12.0 Log $K'_{Fe'L2}$: 9.7-10.8	

Scheldt Estuary, NE Atlantic	1-2	(Gerringa et al., 2007)	TAC	38.8-526.0	9.59	
Northwest Pacific Ocean (Sulu, Philippine, Celebes, and South China Seas)	5-5357	(Kondo et al., 2007)	TAC	0.43-1.46	12.0-13.8	
Columbia River-Northeast Pacific	2-31	(Buck et al., 2007)	SA	L1: 1.0-55.8 L2: 0.4-9.0	Log $K'_{Fe'L1}$: 11.8-13.9 Log $K'_{Fe'L2}$: 10.7-11.8	
Central North Pacific (from Hawaii to San Diego)	3-1000	(van den Berg, 2006)	DHN bromate	0.86-2.45	11.4-12.3	Model ligands Log $K'_{Fe'DFB}$ = 11.54
Southwest Pacific Ocean	1–2m	(Tian et al., 2006)	TAC	0.66-1.72	12.2-13.1	
Northeast Atlantic Ocean- Canary Basin	10-152	(Gerringa et al., 2006)	TAC	0.8-4.8	9.7-12.7	
Northwest Atlantic Ocean	5-5256	(Cullen et al., 2006)	TAC	L1: 0.81-1.14 L2: 1.11-2.11	Log $K'_{Fe'L1}$: 12.7-13.1 Log $K'_{Fe'L2}$: 11.5-11.9	
Northeast Atlantic Ocean	10-2000	(Boye et al., 2006)	NN	1.17-3.52	10.36-12.25	
Atlantic Sector-Southern Ocean	20-100	(Boye et al., 2005)	TAC	0.60-3.52	11.1-13.0	
Atlantic Sector-Southern Ocean	10-1500	(Croot et al., 2004)	TAC, NN	0.9-3.0	11.4-13.5	
Mississippi River	1-2	(Powell and Wilson-Finelli, 2003)	TAC	4.3-64.1	10.4-12.3	
Northeast Atlantic	~ 2	(Boye et al., 2003)	NN	1.60-3.88	10.5-11.4	
Peconic Estuary ,North Atlantic	5	(Gobler et al., 2002)	NN	17-209	12.9-14.5	
Atlantic sector-Southern Ocean	20-4500	(Boye et al., 2001)	NN	0.37-1.39	10.9-13.0	
South and Equatorial Atlantic	1-5300	(Powell and Donat, 2001)	SA	0.33-2.54	11.1-14.2	
Arabian sea	25-600	(Witter et al., 2000b)	NN	1.47-6.33	11.6-12.5	
Atlantic Sector-Southern Ocean	5-110	(Croot and Johansson, 2000)	TAC	2.4-17.6	10.7-11.1	Model ligands Log $K'_{Fe'DFB}$ = 16.5
Northwest Atlantic Ocean	11-2874	(Witter and Luther, 1998)	NN	1.67-4.62	12.2-12.9	
Equatorial Pacific	15	(Rue and Bruland, 1997)	SA	L1: 0.31-1.75 L2: 0.19-2.00	Log $K'_{Fe'L1}$: 11.2-13.0 Log $K'_{Fe'L2}$: 10.60-11.91	
Western Mediterranean	20-2586	(van den Berg, 1995)	NN (H_2O_2/SDS)	3.6-13.0	9.4-10.5	
Central North Pacific	20-2000	(Rue and Bruland, 1995)	SA	L1: 0.37-1.00 L2: 1.3-2.8	Log $K'_{Fe'L1}$: 12.7-13.2 Log $K'_{Fe'L2}$: 11.3-11.8	Model ligands Log $K'_{Fe'DFB}$ >13 Log $K'_{Fe'protoporphyrin-IX}$= 12
North Atlantic and Menai Straits	2-1002	(Gledhill and Van Den Berg, 1994)	NN (H_2O_2/SDS)	3.0-10.1	8.85-11.55	

1.5.1. Catalytic effects in CSV

In some of the previous CSV methods (such as using NN and DHN for the adsorptive competing species), an oxidant has been added to enhanced the reduction peak resulted from the re-oxidation of Fe (II) formed in the stripping step. For example, hydrogen peroxide (H_2O_2) was used in NN method (Gledhill and Van Den Berg, 1994) and bromate ($BrO3^-$) in NN (Aldrich and van den Berg, 1998) and DHN (van den Berg, 2006) methods, and more recent bromate ($BrO3^-$) was used to enhanced the response of Fe complexed with humic substances (Laglera et al., 2007). In the present study dissolved oxygen (DO) was used as an oxidant which causes catalytic effect (Abualhaija and van den Berg, 2014) (see Chapter 2).

1.5.2. Experimental aspects

The concentrations of Fe-binding ligands and conditional stability constants ($K'_{Fe'L}$), were determined in the present work using the updated SA method (Abualhaija and van den Berg, 2014), after a competing equilibrium has been established between the added ligand (SA), natural Fe-binding ligands and Fe′. Complexing ligand titration procedures as determined in (Abualhaija and van den Berg, 2014), a large buffered seawater sample (pH 8.18 NBS scale) using borate buffer was divided into subsamples usually in pre-conditioned PFA (perfluoroalkoxy alkane) (Savillex, Cole-Parmer) vials or (Sterilin) tubes. Two or three of the vials were 0 added Fe, whereas increasing amount of Fe was added to the other subsamples. The iron and natural complexing ligands were allowed to equilibrate for 10 min (up to 2 h) at room temperature. Then 5 µM SA was added to the subsamples, which were left to equilibrate overnight, and then the labile Fe was determined in each of the subsamples using the CSV method. All vials, containers as well as voltammetric cell used in the titrations were conditioned typically 3 times prior to a titration (see Chapter 2).

1.5.3. Data interpretation with respect to one or more ligands

The Fe-binding ligands are typically described as one ligand class (L), two different classes (L1 and L2) and recently more than two classes (L1, L2, L3….) (Table 1.1). Ligand classes have been identified depending on the values of conditional stability constants (log $K'_{Fe'L}$), where strong ligands (L1) have values of log $K'_{Fe'L} > 12$, whilst weak ligands (L2, L3….)

with log $K'_{Fe'L}$ values <12. From the literature studies, strong ligands are generally found in oceanic surface waters and are proposed to be from biological origin (Gledhill and Buck, 2012), whereas weak ligands exist in whole water column and may have different sources include biological product, humic substances, resuspended sediments and degradation of strong organic ligands (Hassler et al., 2011a; Hunter and Boyd, 2007; Laglera and van den Berg, 2009).

1.5.4. The α-coefficient and effects of iron speciation

Conditional stability constants of the Fe-binding ligands can be expressed with respect to Fe' or Fe^{3+}, according to this relationship $K_{Fe3+L} = K_{Fe'L} \times \alpha_{Fe'}$, it is possible to convert K_{Fe3+L} to $K_{Fe'L}$ or vice versa using the value of $\alpha Fe'$ (α-coefficient for inorganic iron), where $\alpha_{Fe'} = [Fe'] / [Fe^{3+}]$. $\alpha_{Fe'}$ varies with pH and salinity values (Byrne et al., 1988), the value of $\alpha_{Fe'} = 10^{10}$ was used in the present work at seawater pH. The calculated value of $\alpha_{Fe'}$ using the constants from (Liu and Millero, 2002) was $10^{9.98}$ (Abualhaija and van den Berg, 2014), which is almost the same as that found previously at seawater pH (Hudson et al., 1992), whereas the calculated value at different salinities (from 4 to 35) was between $10^{9.98}$ and $10^{10.28}$ (Abualhaija et al., 2015) (Chapter 3). All Conditional stability constants of the Fe-binding ligands in the present work are expressed with respect to Fe'.

The competitive strength between the added ligand and natural ligands depends on the inorganic side reaction coefficient of Fe with added (α_{FeAL}) and natural ligands (α_{FeLi}). The analytical detection window of the CSV method is described as (α_{FeAL}), the value of α_{FeAL} can be changed by varying the concentration of the added ligand or by using a different added ligand that forms complexes with Fe´.

To select the detection window of the CSV method it is very important to know that the added ligand should outcompete the inorganic complexes of Fe with OH^- and shouldn't outcompete the natural ligands, that means the value of αFeAL should be significantly greater than the value of αFe´ but less than or equal to the value of αFeL_i. The detection window using the new SA method (Abualhaija and van den Berg, 2014) is expressed as:

$$\alpha FeSA = K_{Fe'SA} \times [SA] + B_{Fe'SA2} \times [SA^2].$$

Multiple detection windows were used in this thesis (chapter 4), 5 detection windows were used by setting the concentration of the competing ligand (SA) at 5, 10, 15, 25 and 50 μM to determine the iron speciation and the effect of varying the detection window on the iron speciation in samples from the Mersey estuary and Liverpool Bay.

Speciation measurements of iron including ligand concentrations and conditional stability constants in some of the previous literatures have been compiled in Table 1.1. The ligand concentrations and conditional stability constants in the present study are comparable with the most of the studies in Table 1.1.

1.6. Specific aims of this dissertation

- Improving the chemical speciation of iron in seawater (Chapter 2).
- Testing the hypothesis that humic substances are the predominant ligands for iron in estuarine and coastal (Chapter 3), shelf and open ocean waters (Chapter 5).
- To demonstrate the competition between copper and iron for the natural ligands in estuarine, coastal (Chapter 3) as well as in sea waters.
- To verify whether the iron speciation is dominated by one or more ligands (chapter 4).

1.7. References

Abbt-Braun, G. and Frimmel, F.H., 2002. The Relevance of Reference Materials: Isolation and General Characterization. Wiley-VCH, Weinheim.

Abualhaija, M.M. and van den Berg, C.M.G., 2014. Chemical speciation of iron in seawater using catalytic cathodic stripping voltammetry with ligand competition against salicylaldoxime. Marine Chemistry, 164(0): 60-74.

Abualhaija, M.M., Whitby, H. and van den Berg, C.M.G., 2015. Competition between copper and iron for humic ligands in estuarine waters. Marine Chemistry, 172(0): 46-56.

Aldrich, A.P. and van den Berg, C.M.G., 1998. Determination of iron and its redox speciation in seawater using catalytic cathodic stripping voltammetry. Electroanalysis, 10(6): 369-373.

Batchelli, S., Muller, F.L.L., Chang, K.-C. and Lee, C.-L., 2010. Evidence for Strong but Dynamic Iron−Humic Colloidal Associations in Humic-Rich Coastal Waters. Environmental Science & Technology, 44(22): 8485-8490.

Bauer, J.E., Druffel, E.R.M., Wolgast, D.M. and Griffin, S., 2002. Temporal and regional variability in sources and cycling of DOC and POC in the northwest Atlantic continental shelf and slope. Deep Sea Research Part II: Topical Studies in Oceanography, 49(20): 4387-4419.

Bergquist, B.A., Wu, J. and Boyle, E.A., 2007. Variability in oceanic dissolved iron is dominated by the colloidal fraction. Geochimica et Cosmochimica Acta, 71(12): 2960-2974.

Biller, D.V. and Bruland, K.W., 2012. Analysis of Mn, Fe, Co, Ni, Cu, Zn, Cd, and Pb in seawater using the Nobias-chelate PA1 resin and magnetic sector inductively coupled plasma mass spectrometry (ICP-MS). Marine Chemistry, 130: 12-20.

Biller, D.V. and Bruland, K.W., 2014. The central California Current transition zone: a broad region exhibiting evidence for iron limitation. Progress in Oceanography, 120: 370-382.

Boyd, P.W. and Ellwood, M.J., 2010. The biogeochemical cycle of iron in the ocean. Nature Geoscience, 3(10): 675.

Boyd, P.W. et al., 2007. Mesoscale Iron Enrichment Experiments 1993-2005: Synthesis and Future Directions. Science (Classic), 315(5812): 612.

Boyd, P.W. and Law, C.S., 2001. The Southern Ocean Iron RElease Experiment (SOIREE)—introduction and summary. Deep Sea Research Part II: Topical Studies in Oceanography, 48(11–12): 2425-2438.

Boyd, P.W. et al., 2005. The evolution and termination of an iron-induced mesoscale bloom in the northeast subarctic Pacific. Limnology and Oceanography, 50(6): 1872-1886.

Boyd, P.W. et al., 2000. A mesoscale phytoplankton bloom in the polar Southern Ocean stimulated by iron fertilization. Nature, 407: 695-702.

Boye, M. et al., 2006. The chemical speciation of iron in the north-east Atlantic Ocean. Deep-Sea Research Part I-Oceanographic Research Papers, 53(4): 667-683.

Boye, M. et al., 2003. Horizontal gradient of the chemical speciation of iron in surface waters of the northeast Atlantic Ocean. Marine Chemistry, 80(2-3): 129-143.

Boye, M. et al., 2010. Significant portion of dissolved organic Fe complexes in fact is Fe colloids. Marine Chemistry, 122(1–4): 20-27.

Boye, M. et al., 2005. Major deviations of iron complexation during 22 days of a mesoscale iron enrichment in the open Southern Ocean. Marine Chemistry, 96(3–4): 257-271.

Boye, M. et al., 2001. Organic complexation of iron in the Southern Ocean. Deep-Sea Research Part I-Oceanographic Research Papers, 48(6): 1477-1497.

Boyle, E., Edmond, J. and Sholkovitz, E., 1977. The mechanism of iron removal in estuaries. Geochimica et Cosmochimica Acta, 41(9): 1313-1324.

Bruland, K.W., Middag, R. and Lohan, M.C., 2014. 8.2 - Controls of Trace Metals in Seawater. In: H.D.H.K. Turekian (Editor), Treatise on Geochemistry (Second Edition). Elsevier, Oxford, pp. 19-51.

Bruland, K.W., Rue, E.L., Donat, J.R., Skrabal, S.A. and Moffett, J.W., 2000. Intercomparison of voltammetric techniques to determine the chemical speciation of dissolved copper in a coastal seawater sample. Analytica Chimica Acta, 405(1-2): 99-113.

Buck, K.N. and Bruland, K.W., 2005. Copper speciation in San Francisco Bay: A novel approach using multiple analytical windows. Marine Chemistry, 96(1–2): 185-198.

Buck, K.N. and Bruland, K.W., 2007. The physicochemical speciation of dissolved iron in the Bering Sea, Alaska. Limnology and Oceanography, 52(5): 1800-1808.

Buck, K.N., Lohan, M.C., Berger, C.J.M. and Bruland, K.W., 2007. Dissolved iron speciation in two distinct river plumes and an estuary; implications for riverine iron supply. Limnology and Oceanography, 52(2): 843-855.

Buffle, J., 1990. The analytical challenge posed by fulvic and humic compounds. Analytica Chimica Acta, 232(1): 1-2.

Buffle, J., Tercier-Waeber, M.L., Buffle, J. and Tercier-Waeber, M.L., 2005. Voltammetric environmental trace-metal analysis and speciation: from laboratory to in situ measurements. TrAC Trends in Analytical Chemistry, 24(3): 172.

Bundy, R.M. et al., 2015. Iron-binding ligands and humic substances in the San Francisco Bay estuary and estuarine-influenced shelf regions of coastal California. Marine Chemistry, 173: 183-194.

Bundy, R.M., Biller, D.V., Buck, K.N., Bruland, K.W. and Barbeau, K.A., 2014. Distinct pools of dissolved iron-binding ligands in the surface and benthic boundary layer of the California Current. Limnology and Oceanography, 59(3): 769-787.

Butler, A. and Theisen, R.M., 2010. Iron(III)–siderophore coordination chemistry: Reactivity of marine siderophores. Coordination chemistry reviews, 254(3-4): 288-296.

Byrne, R.H., Kump, L.R. and Cantrell, K.J., 1988. The influence of temperature and pH on trace metal speciation in seawater. Marine Chemistry, 25(2): 163-181.

Chen, Y. et al., 2013. Structural elucidation of an extracellular polysaccharide produced by the marine fungus Aspergillus versicolor. Carbohydrate Polymers, 93(2): 478-483.

Coale, K.H. et al., 1996. A massive phytoplankton bloom induced by an ecosystem-scale iron fertilization experiment in the equatorial Pacific Ocean. Nature, 383: 495-501.

Conway, T.M. and John, S.G., 2014. Quantification of dissolved iron sources to the North Atlantic Ocean. Nature, 511(7508): 212-215.

Croot, P.L., Andersson, K., Öztürk, M. and Turner, D.R., 2004. The distribution and speciation of iron along 6°E in the Southern Ocean. Deep Sea Research Part II: Topical Studies in Oceanography, 51(22–24): 2857-2879.

Croot, P.L. and Johansson, M., 2000. Determination of Iron Speciation by Cathodic Stripping Voltammetry in Seawater Using the Competing Ligand 2-(2-Thiazolylazo)-p-cresol (TAC). Electroanalysis, 12(8): 565-576.

Cullen, J.T., Bergquist, B.A. and Moffett, J.W., 2006. Thermodynamic characterization of the partitioning of iron between soluble and colloidal species in the Atlantic Ocean. Marine Chemistry, 98(2–4): 295-303.

Duce, R.A. and Tindale, N.W., 1991. Atmospheric transport of iron and its deposition in the ocean. Limnology and Oceanography, 36(8): 1715-1726.

Dupont, C.L., Nelson, R.K., Bashir, S., Moffett, J.W. and Ahner, B.A., 2004. Novel copper-binding and nitrogen-rich thiols produced and exuded by Emiliania huxleyi. Limnology And Oceanography, 49(5): 1754-1762.

Ellwood, M.J. and Van den Berg, C.M.G., 2001. Determination of organic complexation of cobalt in seawater by cathodic stripping voltammetry. Marine Chemistry, 75(1-2): 33-47.

Fox, L.E., 1988. The solubility of colloidal ferric hydroxide and its relevance to iron concentrations in river water. Geochimica et Cosmochimica Acta, 52(3): 771-777.

Frimmel, F.H., 2005. Aquatic Humic Substances. In: Martin Hofrichter. and A. Steinbüchel. (Editors), Biopolymers: Lignin, Humic Substances and Coal. Wiley-VCH Verlag GmbH & Co. KGaA.

Gerringa, L.J.A. et al., 2008. Fe-binding dissolved organic ligands near the Kerguelen Archipelago in the Southern Ocean (Indian sector). Deep-Sea Research Part II: Topical Studies in Oceanography, 55(5-7): 606-621.

Gerringa, L.J.A. et al., 2007. Kinetic study reveals weak Fe-binding ligand, which affects the solubility of Fe in the Scheldt estuary. Marine Chemistry, 103(1–2): 30-45.

Gerringa, L.J.A., Veldhuis, M.J.W., Timmermans, K.R., Sarthou, G. and de Baar, H.J.W., 2006. Co-variance of dissolved Fe-binding ligands with phytoplankton characteristics in the Canary Basin. Marine Chemistry, 102(3–4): 276-290.

Gibbon-Walsh, K., Salaun, P. and van den Berg, C.M.G., 2012. Pseudopolarography of Copper Complexes in Seawater Using a Vibrating Gold Microwire Electrode. Journal of Physical Chemistry A, 116(25): 6609-6620.

Gledhill, M., 2014. The detection of iron protoporphyrin (heme b) in phytoplankton and marine particulate material by electrospray ionisation mass spectrometry – comparison with diode array detection. Analytica Chimica Acta, 841(0): 33-43.

Gledhill, M. and Buck, K.N., 2012. The organic complexation of iron in the marine environment: a review. Frontiers in Microbiology, 3: 69-86.

Gledhill, M. and Van Den Berg, C.M.G., 1994. Determination of Complexation of Iron(III) with Natural Organic Complexing Ligands in Seawater Using Cathodic Stripping Voltammetry. Marine Chemistry, 47(1): 41-54.

Gobler, C.J., Donat, J.R., Consolvo Iii, J.A. and Sañudo-Wilhelmy, S.A., 2002. Physicochemical speciation of iron during coastal algal blooms. Marine Chemistry, 77(1): 71-89.

Hassler, C.S., Alasonati, E., Mancuso Nichols, C.A. and Slaveykova, V.I., 2011a. Exopolysaccharides produced by bacteria isolated from the pelagic Southern Ocean — Role in Fe binding, chemical reactivity, and bioavailability. Marine Chemistry, 123(1–4): 88-98.

Hassler, C.S. et al., 2015. Iron associated with exopolymeric substances is highly bioavailable to oceanic phytoplankton. Marine Chemistry, 173(0): 136-147.

Hassler, C.S., Schoemann, V., Nichols, C.M., Butler, E.C.V. and Boyd, P.W., 2011a. Saccharides enhance iron bioavailability to Southern Ocean phytoplankton. Proceedings of the National Academy of Sciences of the United States of America (PNAS), 108(3): 1076.

Heller, M.I., Gaiero, D.M. and Croot, P.L., 2013. Basin scale survey of marine humic fluorescence in the Atlantic: Relationship to iron solubility and H2O2. Global Biogeochemical Cycles, 27(1): 88-100.

Honey, D.J. et al., 2013. Heme b in marine phytoplankton and particulate material from the North Atlantic Ocean. Marine Ecology Progress Series, 483: 1.

Hopkinson, B.M. and Barbeau, K.A., 2007. Organic and redox speciation of iron in the eastern tropical North Pacific suboxic zone. Marine Chemistry, 106(1–2): 2-17.

Hudson, R.J.M., Covault, D.T. and Morel, F.M.M., 1992. Investigations of iron coordination and redox reactions in seawater using 59Fe radiometry and ion-pair solvent extraction of amphiphilic iron complexes. Marine Chemistry, 38(3–4): 209-235.

Huffman, E.W.D. and Stuber, H.A., 1985. Analytical Methodology for Elemental Analysis of Humic Substances. John Wiley & Sons, New York.

Hunter, K.A. and Boyd, P.W., 2007. Iron-binding ligands and their role in the ocean biogeochemistry of iron. Environmental Chemistry, 4(4): 221-232.

Hutchins, D.A., Witter, A.E., Butler, A. and Luther, G.W., III, 1999. Competition among marine phytoplankton for different chelated iron species. Nature, 400(6747): 858-861.

Hwang, J. et al., 2004. Temporal variability of Δ14C, δ13C, and C/N in sinking particulate organic matter at a deep time series station in the northeast Pacific Ocean. Global biogeochemical cycles, 18(4).

Ibisanmi, E., Sander, S.G., Boyd, P.W., Bowie, A.R. and Hunter, K.A., 2011. Vertical distributions of iron-(III) complexing ligands in the Southern Ocean. Deep Sea Research Part II: Topical Studies in Oceanography, 58(21–22): 2113-2125.

Jickells, T.D. et al., 2005. Global Iron Connections Between Desert Dust, Ocean Biogeochemistry, and Climate. Science (Classic), 308(5718): 67.

Johnson, K.S., Gordon, R.M. and Coale, K.H., 1997. What controls dissolved iron concentrations in the world ocean? Marine Chemistry, 57(3–4): 137-161.

Karstensen, J., Stramma, L. and Visbeck, M., 2008. Oxygen minimum zones in the eastern tropical Atlantic and Pacific oceans. Progress in Oceanography, 77(4): 331-350.

Klunder, M.B., Laan, P., Middag, R., de Baar, H.J.W. and Bakker, K., 2012. Dissolved iron in the Arctic Ocean: Important role of hydrothermal sources, shelf input and scavenging removal. Journal of Geophysical Research: Oceans, 117(C4): C04014.

Kogut, M.B. and Voelker, B.M., 2003. Kinetically inert Cu in coastal waters. Environmental Science & Technology, 37(3): 509-518.

Kondo, Y., Takeda, S. and Furuya, K., 2007. Distribution and speciation of dissolved iron in the Sulu Sea and its adjacent waters. Deep Sea Research Part II: Topical Studies in Oceanography, 54(1–2): 60-80.

Kondo, Y. et al., 2008. Organic iron (III) complexing ligands during an iron enrichment experiment in the western subarctic North Pacific. Geophysical Research Letters, 35(12): L12601.

Kuma, K., Katsumoto, A., Kawakami, H., Takatori, F. and Matsunaga, K., 1998. Spatial variability of Fe(III) hydroxide solubility in the water column of the northern North Pacific Ocean. Deep Sea Research Part I: Oceanographic Research Papers, 45(1): 91-113.

Kuma, K., Nishioka, J.U.N. and Matsunaga, K., 1996. Controls on iron(III) hydroxide solubility in seawater: The influence of pH and natural organic chelators. Limnology and Oceanography, 41(3): 396.

Kumke, M.U., Abbt-Braun, G. and Frimmel, F.H., 1998. Time-resolved fluorescence measurements of aquatic natural organic matter (NOM). Acta Hydrochimica et Hydrobiologica, 26(2): 73-81.

Laglera, L.M., Battaglia, G. and van den Berg, C.M.G., 2007. Determination of humic substances in natural waters by cathodic stripping voltammetry of their complexes with iron. Analytica Chimica Acta, 599(1): 58-66.

Laglera, L.M., Battaglia, G. and van den Berg, C.M.G., 2011. Effect of humic substances on the iron speciation in natural waters by CLE/CSV. Marine Chemistry, 127(1-4): 134-143.

Laglera, L.M. and van den Berg, C.M.G., 2003. Copper complexation by thiol compounds in estuarine waters. Marine Chemistry, 82(1–2): 71-89.

Laglera, L.M. and Van den Berg, C.M.G., 2007. Wavelength dependence of the photochemical reduction of iron in Arctic seawater. Environmental Science & Technology, 41(7): 2296-2302.

Laglera, L.M. and van den Berg, C.M.G., 2009. Evidence for geochemical control of iron by humic substances in seawater. Limnology and Oceanography, 54(2): 610-619.

Landing, W.M. and Westerlund, S., 1988. The solution chemistry of iron(II) in Framvaren fjord. Marine Chemistry, 23: 329-343.

Lannuzel, D., Schoemann, V., de Jong, J., Tison, J.-L. and Chou, L., 2007. Distribution and biogeochemical behaviour of iron in the East Antarctic sea ice. Marine Chemistry, 106(1–2): 18-32.

Le Gall, A.-C. and van den Berg, C.M.G., 1998. Folic acid and glutathione in the water column of the North East Atlantic. Deep-Sea Research Part I-Oceanographic Research Papers, 45: 1903-1918.

Liu, X. and Millero, F.J., 2002. The solubility of iron in seawater. Marine Chemistry, 77(1): 43-54.

Macrellis, H.M., Trick, C.G., Rue, E.L., Smith, G. and Bruland, K.W., 2001. Collection and detection of natural iron-binding ligands from seawater. Marine Chemistry, 76(3): 175-187.

Maldonado, M.T. and Price, N.M., 1999. Utilization of iron bound to strong organic ligands by plankton communities in the subarctic Pacific Ocean. Deep Sea Research Part II: Topical Studies in Oceanography, 46(11–12): 2447-2473.

Martin, J.H., 1990. Glacial-interglacial CO2 change: The iron hypothesis. Paleoceanography, 5(1): 1-13.

Martin, J.H. et al., 1994. Testing the iron hypothesis in ecosystems of the equatorial Pacific Ocean. Nature, 371: 123-129.

Martin, J.H. and Fitzwater, S.E., 1988. Iron deficiency limits phytoplankton growth in the north-east Pacific subarctic. Nature, 331(6154): 341-343.

Martin, J.H. and Gordon, R.M., 1988. Northeast Pacific iron distributions in relation to phytoplankton productivity. Deep-Sea Research, 35: 177-196.

Martin, J.H., Gordon, R.M., Fitzwater, S. and Broenkow, W.W., 1989. Vertex: phytoplankton/iron studies in the Gulf of Alaska. Deep Sea Research Part A. Oceanographic Research Papers, 36(5): 649.

Martinez, J.S. et al., 2003. Structure and Membrane Affinity of a Suite of Amphiphilic Siderophores Produced by a Marine Bacterium. National Academy of Sciences, pp. 3754.

Mawji, E. et al., 2008. Hydroxamate Siderophores: Occurrence and Importance in the Atlantic Ocean. Environmental Science & Technology, 42(23): 8675.

Mikkelsen, O., van den Berg, C.M.G. and Schroder, K.H., 2006. Determination of labile iron at low nmol L-1 levels in estuarine and coastal waters by anodic stripping voltammetry. Electroanalysis, 18(1): 35-43.

Miller, W.L. and Kester, D., 1994. Photochemical iron reduction and iron bioavailability in seawater. Journal of Marine Research, 52(2): 325-343.

Moffett, J.W., Brand, L.E., Croot, P.L. and Barbeau, K.A., 1997. Cu speciation and cyanobacterial distribution in harbors subject to anthropogenic Cu inputs. Limnology and Oceanography, 42(5): 789.

Mohamed, K.N., Steigenberger, S., Nielsdottir, M.C., Gledhill, M. and Achterberg, E.P., 2011. Dissolved iron(III) speciation in the high latitude North Atlantic Ocean. Deep-Sea Research Part I, 58: 1049-1059.

Moore, J.K. and Braucher, O., 2008. Sedimentary and mineral dust sources of dissolved iron to the world ocean. Biogeosciences, 5(3): 631-656.

Moore, J.K. and Doney, S.C., 2007. Iron availability limits the ocean nitrogen inventory stabilizing feedbacks between marine denitrification and nitrogen fixation. Global Biogeochemical Cycles, 21(2).

Morel, F., ccedil, ois, M.M., Kustka, A.B. and Shaked, Y., 2008. The role of unchelated Fe in the iron nutrition of phytoplankton. Limnology and Oceanography, 53(1): 400.

Nagai, T., Imai, A., Matsushige, K., Yokoi, K. and Fukushima, T., 2007. Dissolved iron and its speciation in a shallow eutrophic lake and its inflowing rivers. Water Research, 41(4): 775-784.

Plavšić, M., Krznarić, D. and Branica, M., 1982. Determination of the apparent copper complexing capacity of seawater by anodic stripping voltammetry. Marine Chemistry, 11(1): 17-31.

Poli, A., Anzelmo, G. and Nicolaus, B., 2010. Bacterial Exopolysaccharides from Extreme Marine Habitats: Production, Characterization and Biological Activities. Marine Drugs, 8(6): 1779-1802.

Powell, R.T. and Donat, J.R., 2001. Organic complexation and speciation of iron in the South and Equatorial Atlantic. Deep Sea Research Part II: Topical Studies in Oceanography, 48(13): 2877-2893.

Powell, R.T. and Wilson-Finelli, A., 2003. Importance of organic Fe complexing ligands in the Mississippi River plume. Estuarine, Coastal and Shelf Science, 58(4): 757-763.

Raven, J.A., Evans, M.C.W. and Korb, R.E., 1999. The role of trace metals in photosynthetic electron transport in O2-evolving organisms. Photosynthesis Research, 60: 111-149.

Rijkenberg, M.J.A. et al., 2005. The influence of UV irradiation on the photoreduction of iron in the Southern Ocean. Marine Chemistry, 93(2–4): 119-129.

Rijkenberg, M.J.A. et al., 2008. Changes in iron speciation following a Saharan dust event in the tropical North Atlantic Ocean. Marine Chemistry, 110(1–2): 56-67.

Rue, E. and Bruland, K., 2001. Domoic acid binds iron and copper: a possible role for the toxin produced by the marine diatom Pseudo-nitzschia. Marine Chemistry, 76(1-2): 127-134.

Rue, E.L. and Bruland, K.W., 1995. Complexation of iron(III) by natural organic ligands in the central North Pacific as determined by a new competitive ligand equilibration/adsorptive cathodic stripping voltammetric method. Marine Chemistry, 50(1-4): 117-138.

Rue, E.L. and Bruland, K.W., 1997. The role of organic complexation on ambient iron chemistry in the equatorial Pacific Ocean and the response of a mesoscale iron addition experiment. Limnology and Oceanography, 42(5): 901-910.

Saito, M.A. and Moffett, J.W., 2001. Complexation of cobalt by natural organic ligands in the Sargasso Sea as determined by a new high-sensitivity electrochemical cobalt speciation method suitable for open ocean work. Marine Chemistry, 75(1–2): 49-68.

Senesi, N., Miano, T. and Provenzano, M., 1991. Fluorescence spectroscopy as a means of distinguishing fulvic and humic acids from dissolved and sedimentary aquatic sources and

terrestrial sources. In: B. Allard, H. Borén and A. Grimvall (Editors), Humic Substances in the Aquatic and Terrestrial Environment. Lecture Notes in Earth Sciences. Springer Berlin Heidelberg, pp. 63-73.

Sholkovitz, E., 1976. Flocculation of dissolved organic and inorganic matter during the mixing of river water and seawater. Geochimica et Cosmochimica Acta, 40(7): 831-845.

Sholkovitz, E., Boyle, E. and Price, N., 1978. The removal of dissolved humic acids and iron during estuarine mixing. Earth and Planetary Science Letters, 40(1): 130-136.

Statham, P.J., Jacobson, Y. and van den Berg, C.M.G., 2012. The measurement of organically complexed Fe-II in natural waters using competitive ligand reverse titration. Analytica Chimica Acta, 743: 111-116.

Stevenson, F.J., 1994. Humus chemistry: genesis, composition, reactions. John Wiley & Sons.

Sunda, W.G., Swift, D.G. and Huntsman, S.A., 1991. Low iron requirement for growth in oceanic phytoplankton. Nature, 351(6321): 55-57.

Tagliabue, A. and Arrigo, K.R., 2006. Processes governing the supply of iron to phytoplankton in stratified seas. Journal of Geophysical Research: Oceans (1978–2012), 111(C6).

Tagliabue, A. et al., 2010. Hydrothermal contribution to the oceanic dissolved iron inventory. Nature Geosci, 3(4): 252-256.

Tagliabue, A. et al., 2014. Surface-water iron supplies in the Southern Ocean sustained by deep winter mixing. Nature Geosci, 7(4): 314-320.

Tagliabue, A. and Völker, C., 2011. Towards accounting for dissolved iron speciation in global ocean models. Biogeosciences, 8(10): 3025-3039.

Taylor, S.R., 1964. Abundance of chemical elements in the continental crust: a new table. Geochimica et Cosmochimica Acta, 28(8): 1273-1285.

Thuroczy, C.E. et al., 2010. Speciation of Fe in the eastern North Atlantic Ocean. Deep-Sea Research. Part I: Oceanographic Research Papers, 57(11): 1444-1453.

Tian, F. et al., 2006. Organic iron(III) speciation in surface transects across a frontal zone: the Chatham Rise, New Zealand. Marine & Freshwater Research, 57(5): 533.

Tian, Y.H., Song, Q.J. and Hua, Z.Z., 2005. Flow Injection Determination of Humic Acid with Chemiluminescence Detection. Analytical letters, 38(14): 2439.

Tortell, P.D., Maldonado, M.T., Granger, J. and Price, N.M., 1999. Marine bacteria and biogeochemical cycling of iron in the oceans. FEMS Microbiology Ecology, 29(1): 1-11.Turekian, K.K., 1977. The fate of metals in the oceans. Geochimica et Cosmochimica Acta, 41(8): 1139-1144.

Van Den Berg, C.M.G., 1984. Determination of the Complexing Capacity and Conditional Stability-Constants of Complexes of Copper(Ii) with Natural Organic-Ligands in Seawater by Cathodic Stripping Voltammetry of Copper Catechol Complex-Ions. Marine Chemistry, 15(1): 1-18.

Van Den Berg, C.M.G., 1995. Evidence for Organic Complexation of Iron in Seawater. Marine Chemistry, 50(1-4): 139-157.

van den Berg, C.M.G., 2006. Chemical speciation of iron in seawater by cathodic stripping voltammetry with dihydroxynaphthalene. Analytical Chemistry, 78(1): 156-163.

Van Den Berg, C.M.G. and Huang, Z.Q., 1984. Determination of Iron in Seawater Using Cathodic Stripping Voltammetry Preceded by Adsorptive Collection with the Hanging Mercury Drop Electrode. Journal of Electroanalytical Chemistry, 177(1-2): 269-280.

van den Berg, C.M.G., Merks, A.G.A. and Duursma, E.K., 1987. Organic complexation and its control of the dissolved concentrations of copper and zinc in the Scheldt estuary. Estuarine, Coastal and Shelf Science, 24(6): 785-797.

van der Merwe, P. et al., 2009. Biogeochemical observations during the winter–spring transition in East Antarctic sea ice: Evidence of iron and exopolysaccharide controls. Marine Chemistry, 115(3–4): 163-175.

Velasquez, I. et al., 2011. Detection of hydroxamate siderophores in coastal and Sub-Antarctic waters off the South Eastern Coast of New Zealand. Marine Chemistry, 126(1–4): 97-107.

Völker, C. and Tagliabue, A., 2015. Modeling organic iron-binding ligands in a three-dimensional biogeochemical ocean model. Marine Chemistry, 173(0): 67-77.

Vong, L., Laës, A. and Blain, S., 2007. Determination of iron–porphyrin-like complexes at nanomolar levels in seawater. Analytica Chimica Acta, 588(2): 237-244.

Vraspir, J.M. and Butler, A., 2009. Chemistry of Marine Ligands and Siderophores. Annual Review of Marine Science, 1(1): 43-63.

Waite, T.D., 2001. Thermodynamics of the iron system in seawater. In: D.R. Turner and K.A. Hunter (Editors), The Biogeochemistry of Iron in Seawater. Wiley, New York, pp. 291–342.

Wang, S., Bailey, D., Lindsay, K., Moore, J.K. and Holland, M., 2014. Impact of sea ice on the marine iron cycle and phytoplankton productivity. Biogeosciences, 11(17): 4713-4731.

Wedepohl, H.K., 1995. The composition of the continental crust. Geochimica et Cosmochimica Acta, 59(7): 1217-1232.

Wells, M.L., Trick, C.G., Cochlan, W.P., Hughes, M.P. and Trainer, V.L., 2005. Domoic acid: The synergy of iron, copper, and the toxicity of diatoms. Limnology and Oceanography, 50(6): 1908-1917.

Wen, L.-S., Santschi, P., Gill, G. and Paternostro, C., 1999. Estuarine trace metal distributions in Galveston Bay: importance of colloidal forms in the speciation of the dissolved phase. Marine Chemistry, 63(3–4): 185-212.

Witter, A.E., Hutchins, D.A., Butler, A. and Luther Iii, G.W., 2000a. Determination of conditional stability constants and kinetic constants for strong model Fe-binding ligands in seawater. Marine Chemistry, 69(1–2): 1-17.

Witter, A.E., Lewis, B.L. and Luther Iii, G.W., 2000b. Iron speciation in the Arabian Sea. Deep Sea Research Part II: Topical Studies in Oceanography, 47(7–8): 1517-1539.

Witter, A.E. and Luther, G.W., 1998. Variation in Fe-organic complexation with depth in the Northwestern Atlantic Ocean as determined using a kinetic approach. Marine Chemistry, 62(3–4): 241-258.

Wu, J. and Luther III, G.W., 1996. Spatial and temporal distribution of iron in the surface water of the northwestern Atlantic Ocean. Geochimica et cosmochimica acta, 60(15): 2729-2742.

Wu, J., Wells, M.L. and Rember, R., 2011. Dissolved iron anomaly in the deep tropical–subtropical Pacific: Evidence for long-range transport of hydrothermal iron. Geochimica et Cosmochimica Acta, 75(2): 460-468.

2

Chapter 2
Chemical speciation of iron in seawater using catalytic cathodic stripping voltammetry with ligand competition against salicylaldoxime

This chapter is adapted from: Abualhaija, M.M. and van den Berg, C.M.G., 2014. Chemical speciation of iron in seawater using catalytic cathodic stripping voltammetry with ligand competition against salicylaldoxime. Marine Chemistry, 164(0): 60-74.

2. CHEMICAL SPECIATION OF IRON IN SEAWATER USING CATALYTIC CATHODIC STRIPPING VOLTAMMETRY WITH LIGAND COMPETITION AGAINST SALICYLALDOXIME

Abstract

The chemical speciation of iron in seawater is typically determined by cathodic stripping voltammetry (CSV) making use of ligand competition between an electroactive ligand added to obtain the CSV signal and the natural ligand to determine the complex stability of the natural species. Different procedures differ in the added ligand that is selected. Recent findings have suggested that several of these procedures suffer from interference by humic substances, which are now known to be ubiquitous in coastal and ocean waters. We re-optimise here CSV of iron speciation using salicylaldoxime (SA) in seawater, finding differences with the pre-existing method, and a different interpretation for the electroactive species. The main findings are that optimum sensitivity is obtained at ~5 x less SA, that the complex responsible for adsorption on the electrode is FeSA, that the $FeSA_2$ species does not adsorb, and that the sensitivity of the method is much improved in the presence of dissolved oxygen (DO) through a catalytic effect (Fe^{II} acts as catalyst for the reduction of DO). The complex stability for complexes of Fe' with SA (FeSA and $FeSA_2$), in pH 8 seawater, is calibrated over a range of SA concentrations between 1 and 40 µM SA against EDTA and between 1 and 100 µM SA without EDTA. Data fitting of the EDTA data gave log $K'_{Fe'SA}$ = 6.50 ±0.04 and log $B'_{Fe'SA2}$ = 10.85 ±0.08. The data fits agree with the formation of an electroactive species FeSA which is superseded by a non-electroactive $FeSA_2$ at [SA] > 5 µM. Independent calibration of these stability constants on the basis of the formation of FeSA in competition only with the hydroxide species of Fe^{III}, between 1 and 100 µM SA, without EDTA, gave values of log $K'_{Fe'SA}$ = 6.52 ± 0.01 and log $B'_{Fe'SA2}$ = 10.72 ±0.03. These are the values we propose for the constants as they are independent of any uncertainties in the speciation with EDTA. The similarity of these constants to those determined via calibration against EDTA shows that the speciation of Fe with SA and EDTA is well understood. The re-optimised method is applied to a mixed depth Celtic Sea sample, and two GEOTRACES samples from the Atlantic, at a SA concentration of 5 µM. Ligand concentrations were 1.47 and 1.49 nM in the GEOTRACES water (log $K'_{Fe'L}$ values of 11.1 and 11.9) and 2.53 nM in the Celtic Sea water (log $K'_{Fe'L}$ =11.5). Application of the method to ligands added to seawater

gave log $K'_{Fe'L}$ values of 11.6 ± 0.1 for humic acid (Suwannee River) and 12.2 ±0.3 for a siderophore (desferrioxamine B). Measurement of the rate of dissociation of the complex of Fe with the natural ligand in Celtic seawater gave a value of k_{FeL} = 0.00133 ± 0.0002 s^{-1}. The half-life of this reaction is 8.7 minutes. This means that a reaction time of 1 h is required after the addition of SA prior to analysis.

2.1. Introduction

Iron is one of the bioactive elements in the oceans and is essential to marine microorganisms, its uptake causing depletion in ocean surface waters (Martin and Gordon, 1988). This depletion is the reason for limitation of primary productivity in about half of the global oceans (Behrenfeld and Kolber, 1999; Martin et al., 1991; Moore et al., 2002). In spite of being the 4th most abundant element in the earth's crust (Wedepohl, 1995), the oceanic concentration of iron is low (typically <1 nM in deep waters) which is caused by its poor solubility (~0.01 nM as inorganic Fe in pH 8 seawater (Liu and Millero, 2002)) and biological uptake. The poor solubility is the reason that iron tends to be removed from solution in estuarine and coastal waters, and is transported from land to the open ocean largely via the atmosphere rather than from fluvial sources.

It has been demonstrated that organic complexation increases Fe solubility (Kuma et al., 1996; Millero, 1998). For this reason the chemical speciation of iron is fundamental to understanding its marine geochemistry. Iron occurs in seawater in two oxidation states: 2-valent in chemically reducing conditions (Landing and Westerlund, 1988) or when subject to photochemical reactions (Laglera and van den Berg, 2007; Miller and Kester, 1994), whilst the 3-valent, Fe^{III}, is predominant in the presence of oxygen. This work is on Fe^{III}, as it is the predominant species in seawater in the presence of air. All measurements of organic speciation of Fe thus far have been in the presence of air (Buck et al., 2012; Croot and Johansson, 2000; Gledhill and van den Berg, 1994; Rue and Bruland, 1995) (apart from the brief detection step which often requires partial oxygen removal) and are therefore for Fe^{III}, apart from a recent method to determine the concentration of organic Fe^{II}-binding ligands (Statham et al., 2012). Organic complexation of Fe is one of the parameters studied as part of the GEOTRACES program and methods for its measurement are still subject to

development and intercomparison (Buck et al., 2012). The result of that intercomparison was encouraging (reasonable agreement between methods) but also showed problems (some titrations showed variability).

All Fe^{III} speciation methods make use of cathodic stripping voltammetry (CSV) and the methods can use each of several ligands: 1-nitroso-2-napthol (NN) (Gledhill and van den Berg, 1994), 2-(2-thiazolylazo)-p-cresol (TAC) (Croot and Johansson, 2000), salicylaldoxime (SA) (Rue and Bruland, 1995) and 2,3-dihydroxynaphthalene (DHN) (van den Berg, 2006) have been used successfully. In each case the added ligand forms a complex (FeAL) with Fe^{III} that adsorbs on the mercury electrode. The amount of adsorbed complex is determined by a reducing potential scan using cathodic stripping voltammetry (CSV), and this amount is directly related to the concentration of dissolved FeAL, which in turn is directly related to the concentration of Fe and AL via the sensitivity which is calibrated by means of internal iron standard additions. This is used to obtain the concentration of reactive Fe at a constant concentration of AL.

Competition for iron between AL and natural complexing ligands is the basis for the speciation methods. In each case the free Fe^{III} (that not bound by the natural ligands) is bound by the added ligand and detected. Correction is made for the free Fe^{III} that is bound by the added ligand and which causes equilibria to shift. The procedures vary in that sometimes the sensitivity is increased by adding an oxidant which causes a catalytic effect: NN has been used without oxidant (Gledhill and van den Berg, 1994; Witter et al., 2000), with hydrogen peroxide (van den Berg, 1995) and with bromate (Aldrich and van den Berg, 1998), and DHN with bromate (van den Berg, 2006). Measurements using these ligands can be without oxidant, but then a much longer adsorption time has to be included prior to the voltammetric scan, which may lead to electrode saturation and non-linearity of response: for instance the peak height increases linearly with adsorption time to 8 min for 1.6 nM Cu complexed with SA (Campos and van den Berg, 1994), and up to 30 min for 2.5 nM Fe (Rue and Bruland, 1995). The sensitivity of the method using TAC is sufficient without the need for an added oxidant.

Recent work has suggested that Fe^{III} in seawater is complexed with humic substances (HS) (Laglera and van den Berg, 2009). Fe^{III}-HS in seawater gives a response in CSV which is catalysed by bromate (Laglera et al., 2007). This peak overlaps with that obtained using

DHN/bromate, which interferes with the use of this ligand for Fe speciation in the presence of HS. Further work on HS has also shown interference with Fe speciation using TAC and NN, but that SA and DHN (without bromate) can be used (Laglera et al., 2011). On the other hand, TAC was used recently and apparently successfully for Fe speciation in the presence of HS (Batchelli et al., 2010). This is important as HS occurs in all seawater, though the concentration in ocean waters is low. The presence of the HS could be part of the reason for the small differences found between methods tested for the GEOTRACES intercalibration programme (Buck et al., 2012).

The un-catalysed DHN method has poor sensitivity, whilst the un-catalysed SA method has been used successfully in the past, e.g. (Rue and Bruland, 1995). The SA method has problems which have been un-reported and are not understood, and which make it difficult to use. Nevertheless the SA method is being used for Fe speciation (Buck and Bruland, 2007; Buck et al., 2007) with apparently good results. We have re-visited the SA method to resolve the outstanding issues and improve the method.

2.1.1 Existing Fe speciation method using salicylaldoxime

2.1.1.1. Equilibration time

The original SA method (Rue and Bruland, 1995) has been modified slightly, and re-calibrated, for estuarine waters (Buck et al., 2007). The Fe added for the complexing ligand titration (0 – 5 nM Fe) is allowed to equilibrate with the seawater and natural ligands before the SA addition, which was added after a first equilibration period. 1 h equilibration was used after the Fe addition to the seawater (2 h in the Buck version), and a further 10-15 min equilibration after the addition of SA (27.5 µM (Buck et al., 2007; Rue and Bruland, 1995) and 25 µM SA (Buck et al., 2007)). A much longer equilibration period between the added ligand, the iron and the natural ligands is used in the other CLE-CSV methods, which is typically overnight (Croot and Johansson, 2000; Gledhill and van den Berg, 1994; Witter et al., 2000), though then everything is equilibrated simultaneously which can be expected to take longer (because the free iron concentration is lowered by the added ligand) than the sequential equilibration used with SA. The TAC method uses the sequential principle but still equilibrates overnight (Croot and Johansson, 2000).

2.1.1.2. Removal of dissolved oxygen

The updated SA method (Buck et al., 2007) does not remove dissolved oxygen (DO) during the voltammetric Fe measurement, while the other methods remove DO as it normally interferes with voltammetric measurement.

2.1.1.3. Decreasing response

The SA method stipulates that just one mercury drop is dispensed (Rue and Bruland, 1995) which is unusual as automated voltammeters normally dispense several before using a fresh one, and the apparatus, or software, may require modification (the software of the Bioanalytical Systems (BAS) voltammeter does not require modification). The use of a single drop was to avoid an apparent decrease in the response when a scan was repeated using the same solution, which was ascribed to adsorption on the mercury drops in the cell (Rue and Bruland, 1995). The drop-size of the systems used for iron speciation can vary by a factor of 8 (Buck et al., 2012), so this aspect is tested in this work. Any decrease due to Fe removal as a result of adsorption on the voltammetric cell is eliminated if a conditioned cell is used. Because of the decreasing response, repeat measurements for Fe-SA on aliquots of a titration are carried out in separate aliquots, whereas other CLE-CSV methods repeat the scans in the same cell. This decreasing response is an inconvenience of the SA method as it affects repeat scans, calibrations and standard additions, and its cause is at least in part resolved here.

A second problem with the existing CSV method using SA is a large variability in the sensitivity between samples from different depths (much lower sensitivity for deeper samples) (Buck et al., 2012). A possible explanation is the presence of surface-active compounds but these probably occur at lower levels in deep waters than in surface waters. Oceanic surfactant concentrations in surface waters are low at <0.02 mg L^{-1} (Croot et al., 2007) suggesting that these are probably not the cause of the difference. Solutions for both problems are suggested in this work. An improved method is developed with much better sensitivity, and the method is re-calibrated over an extensive range of SA concentrations, now allowing measurement at several detection windows, e.g. (Bundy et al., 2014).

2.1.2. Identity of the adsorptive iron species with SA and effect on calibration

The previous work (Rue and Bruland, 1995) decided on the basis of a literature review that $FeSA_2$ is the species that predominates and therefore adsorbs on the electrode. It is important that this is correct as otherwise the calibration would only be valid at a single calibrated concentration of SA (27.5 μM in this case). The papers cited (Burger and Egyed, 1965; Burger et al., 1965) discuss Fe^{II}-SA species and not the Fe^{III} species occurring in the presence of dissolved oxygen (DO) and detected by CSV. It can therefore not be a priori assumed that the relevant Fe-SA species is $FeSA_2$. More recent work (Mohanty et al., 1994) is consistent with formation of a 1:1 species of Fe^{III} with SA. The 1:1 (Fe:SA) species is formed first unless the 1:2 (Fe:2SA) species is stabilized such as by pi-orbital bonding, for which there is no evidence for Fe^{III}. This work will demonstrate through modeling that the voltammetric data fits adsorption of the 1:1 species, whilst the $FeSA_2$ species is formed at higher [SA], does not adsorb and is the cause for decreased sensitivity.

SA is a bidentate chelating agent with two functional groups: hydroxyl and oxime (-HC=N-OH) (Tshuma et al., 2007). The speciation of Fe with SA is complicated by the formation of mixed ligand species (OH as well as SA) (Keeney et al., 1984) as well as species of the type FeSAx. The mixed FeOHSA species is likely in view of the high stability of the Fe-hydroxide species (pK_a = 2.6 (Liu and Millero, 1999) for the first hydroxyl species of Fe, $FeOH^{2+}$) and this would tend to increase the stability of the 1:1 ratio of Fe and SA as it would have a neutral charge. Higher order $FeSA_x$ species (with or without OH) become more important at higher concentrations of SA (Egneus, 1972) and OH groups are added with increasing pH (Keeney et al., 1984). It is therefore likely that a species of the type FeOHSA, which is 1:1 with respect to Fe and SA and which has a zero ionic charge, is formed before a species of the type $FeOHSA_2$, or $FeSA_2$, and the second species will be formed at higher concentration of SA. SA has long been used for the colorimetric determination of Fe^{III} (Howe and Mellon, 1940; Reddy and Rao, 1979) and is also used as corrosion inhibitor with associated formation of polynuclear complexes (Smith et al., 2003). The acidity constants (pK values) for SA are 1.2 (pK_{a1}), 8.55 (pK_{a2}) and 11.73 (pK_3) (valid for ionic strength of 0.5, similar to seawater) (Tshuma et al., 2007), indicating that the SA ligand is partially protonated at pH 8, the pH of seawater. The complex stability with Fe^{III} can be expected to be pH dependent due to protonation of SA as well as major cation ion competition and variation in the

hydroxide speciation of Fe.

2.1.3. Effect of electrode size on sensitivity

The sensitivity, S, is commonly expressed as nA nM^{-1} min^{-1} which is suitable for a given electrode of constant size. S varies with the mercury drop size unless it is normalised to the surface area of the electrode (e.g. nA nM^{-1} min^{-1} mm^{-2}) as the CSV response is directly related to the area of the mercury drop (van den Berg and Huang, 1984b). Without this correction the sensitivity between different makes of electrode cannot be readily compared. The limit of detection is not determined by the drop size but by the signal to noise ratio and presence of interfering responses, and the findings of this work are valid for all electrodes and drop sizes.

2.2. Methods

2.2.1. Apparatus

The voltammetric system was a μAutolab-III potentiostat (Ecochemie, Netherlands) connected to a hanging mercury drop electrode (HMDE, Metrohm VA663, Switzerland), the voltammetric system was connected to a PC via a 663 IME interface and was computer-controlled using the GPES 4.9 (general-purpose-electrochemical-software) software. The electrodes in the stand were a standard HMDE cartridge, a glassy carbon counter electrode and a double-junction, reference electrode with the bridge (Teflon) and reference cartridge filled with 3 M KCl. The size of the mercury drops was set to 3 (the largest setting) with a surface area of ~0.5 mm^2. The stirrer was a rotating PTFE rod, set to stirring speed 5. The voltammetric cell was PTFE.

The electrode stand was initially pressurised using N_2 at 1 Bar, but this was later modified to air (from a cylinder) at 1 Bar. In some of our experiments the N_2-blanketing was blocked by closing a valve but this was found to cause problems with the making of the mercury drops. In the new method, with the air-pressurised system, samples were blanketed with air during the analyses.

Voltammetric scans were in the differential-pulse mode similar to previously published

work (Rue and Bruland, 1995), with a shorter interval and modulation time providing improved sensitivity. The adsorption potential was 0 V, adsorption time 120 s, equilibration time 10 s (unstirred), modulation time 0.004 s, interval time 0.1 s, step potential 6 mV, modulation amplitude 50 mV; the scan was from 0 to -0.85 V.

The mercury drop renewal was reduced to just a single drop per measurement for some experiments (the standard setting is 5 drops, of which the last one is used), whilst in the final procedure 3 drops are dispensed, to minimise the mercury in the cell and wastage, not to minimise adsorption on waste mercury as this did not occur. This involved making a minor change in the GPES software: using a text editor (notepad), open the file SYSDEF40.INP (in the Autolab directory); in line 29 change the number from 5 to 3. However, measurements were found to work just as well with any number of drops.

Seawater (0.2 µm filtered) was UV-digested to prepare organic-free UV-SW using a home-built apparatus with a 125-W high-pressure mercury vapour lamp (1 h) (Van Den Berg, 2014), using 30 mL quartz sample tubes. This system was tested to break down 8 mg L^{-1} HA added to seawater.

Sample (LDPE, Nalgene) and reagent bottles (Sterilin, polyethylene, Fisher Scientific) were soaked in hot detergent (1 week), then in acid (1 M HCl 1 week) and finally filled with 0.01 M HCl, or left to soak. Salinity measurements were made using an Autosal Salinometer 8400B.

2.2.2. Reagents

Milli-Q water (Millipore, UK) of 18 MΩ.cm resistivity was used to prepare reagents and for dilutions. Metal standard solutions from atomic absorption standard solutions (BDH, UK) were diluted with water and HCl was added (10 µL 9M HCl /10 mL) to a pH of 2. The HCl was trace analysis grade (Fisher Scientific), and the ammonia was Optima grade (Fisher Scientific). Buffer solutions were 1 M boric acid/ 0.35 M ammonia (final pH 8.18 after 100x dilution in seawater). The pH was on the NBS pH scale. Stock solutions of SA (Acros, Fisher Scientific, 98% purity) were 0.1 M SA in 0.1 M HCl and in methanol (equal results were obtained), which were diluted with water as required. These were stored in polyethylene bottles.

Seawater from the Celtic Sea (salinity 35.0) was used for optimisation experiments. This was collected 30/06/2012, at 48.33 ^{o}N / 9.43 ^{o}W, and was stored in a 50 L carboy covered with black plastic.

Model ligands were Suwannee River humic acid (SRHA) and DFB (deferoxamine, mesylate salt, Sigma Aldrich, purity ≥92.5%, molecular weight 656.8) which were dissolved in water: the SRHA stock solution contained 1 g L^{-1}, and the DFB stock solution was 0.1 M, both diluted with MQ as required. The DFB concentration was not corrected for its composition purity.

GEOTRACES samples 7556 and 8047 were collected by Geoffrey Smith (Ocean Sciences, University of California Santa Cruz): Bottle #7556: at Station 18 from a depth of 75 m on 12/1/2011 at 24.149 deg N by 40.222 deg W. Bottle #8047 was collected from the GeoFish (~2 m depth) upon arrival at Station 24 on 12/9/11 at 17.484 deg N by 24.691 deg W. These were filtered (0.2 μm) and then stored frozen.

2.2.3. Modified procedure to determine total dissolved Fe

The water was filtered (0.2 μm Sartobran cartridge) and stored acidified if used only for metal determination, or frozen if used for speciation. Total Fe concentrations were determined after acidification (20 μL of 50 % HCl into 10 mL seawater to give pH 1.9) of the seawater, SA was added (5 μM SA), and the sample allowed to stand for several hours. Then ammonia was added to approximately neutralise the pH and the buffer (final concentration 10 mM borate) was added. 10 mL of the seawater was pipetted into the voltammetric cell. The solution was air-purged (2 min) prior to the first scan, if it was suspected to be out of equilibrium (for instance by UV-digestion), and air-blanketed. Repeat scans and scans after iron additions were made in the same solution without changing the cell and without further purging. Three voltammetric scans were made using an adsorption time of typically 2 min. The Fe response was measured by the software before initiating the next scan. More scans were made if the peak height of the scans varied more than a few %, and the solution was replaced if there was a systematic change, for instance as a result of Fe adsorption on an un-conditioned cell. The first iron standard addition was made sufficient to at least double the original peak and three more scans were made. A second iron standard addition was made

to confirm the sensitivity if necessary. The sensitivity was calculated from the increase in response and used to calculate the Fe concentration in the sample.

2.2.4. Calibration of the conditional stability constants for SA with Fe in seawater ($K'_{Fe'SA}$ and $B'_{Fe'SA2}$) by competition with EDTA

Fe (5 nM) was added to UV-SW (120 mL) buffered with borate pH buffer to pH 8.18. 10 mL aliquots of this water were transferred to polyethylene vessels (30 mL Sterilin) and EDTA (final concentration between 0 and 5 µM EDTA in 12 separate steps) was added to the water. This was equilibrated for about 15 min. Then SA was added to each aliquot and left to equilibrate overnight before detection of Fe-SA was initiated. The response for Fe-SA was determined by CSV (2 min adsorption time at 0 V). The solutions were air-purged 2 min prior to the first measurement. Three scans were made to determine the response for Fe-SA at each SA concentration, and the average result was used. In separate experiments the calibration against EDTA was repeated at SA concentrations of 1, 2, 5, 10, 20, 30 and 40 µM SA.

2.2.5. Calibration without EDTA

The response for Fe was measured at various concentrations of SA. In this case the experiment was carried out in the voltammetric cell: 10 mL of UV-SW was placed in the cell, the Fe concentration was raised, in separate experiments, to 1, 3 and 10 nM Fe, the water was air-purged (120 s) and SA was added from 1 to 100 µM SA. 5 min reaction time was allowed after each addition and 3 scans were made using an adsorption time of 120 s at 1 and 3 nM Fe, and of 30 s at 10 nM Fe.

2.2.6. Procedure to determine the concentration of unknown iron complexing ligands: complexing ligand titrations

Borate buffer was added to 150 mL seawater (final concentration 10 mM giving pH_{NBS} 8.18). 12 10-ml aliquots of this water were pipetted into polyethylene (Sterilin) tubes (30 mL), containing Fe additions to give a range 0 to 8 nM Fe. Two of the tubes were 0 added Fe.

The iron and natural complexing ligands were allowed to equilibrate 10 min (up to 2 h) at room temperature. Then 5 µM SA was added to the aliquots, which were left to equilibrate overnight (at least 6 h), and then the water was transferred to the voltammetric cell (PTFE). The Sterilin tubes and other containers used for the titrations were conditioned typically 3x prior to a titration by setting up and discarding the titration about 3 h later or after overnight equilibration. Usually the third one was measured although the titration was repeated. The same tubes were used at the same Fe concentration each time. It may be necessary to re-condition the tubes between samples, or repeat the titration, if significant differences in concentrations of Fe and L are anticipated between one sample and the next. The voltammetric cell was conditioned 3 times with seawater without added Fe, with 5 µM SA, prior to the start of a titration. The iron complexed with the added SA was determined by CSV, using a 2 min adsorption time. Linear least square regression of $[Fe_{labile}]/[FeL]$ as a function of $[Fe_{labile}]$ was used to obtain values for the concentration of iron binding ligands (C_L) from the slope and the conditional stability constant (K'_{FeL}) from the Y-axis intercept, according to this relationship (van den Berg, 2006):

$$[Fe_{labile}]/[FeL]=[Fe_{labile}]/C_L + (\alpha_{Fe}+\alpha_{FeSA}+\alpha_{FeSA2})/(C_L K'_{FeL}) \quad (1)$$

analogous to that used before (van den Berg, 2006). The data was corrected for the extent of undersaturation of L (Turoczy and Sherwood, 1997).

Comparative data fitting was carried out using software from Dario Omanovic (Omanović et al., 2015), which fits the data simultaneously to several fitting methods, linear and non-linear, using the same theory as that used in this work.

2.3. Results

2.3.1. Preliminary optimization

CSV of Fe using the existing SA method (25 µM SA, pH 8.2, no purging) (Buck et al., 2007) using N_2 blanketing as in the original method (Rue and Bruland, 1995) showed that the Fe peak decreased rapidly, decreasing by more than half within 5 min, and to near-zero after about 15 min (Fig. 2.1). This decrease could be one of the reasons that, using that method (Rue and Bruland, 1995), repeat scans needed to be carried out in separate aliquots. According to the modified method (Buck et al., 2007) the solution (Fig. 2.1) is not purged,

which meant that measurement is relatively quick which minimizes the decrease in the Fe-response in the first scan. This decrease was investigated in further experiments.

In preliminary experiments we attempted to add an oxidant to improve the sensitivity by a catalytic effect, and to perhaps also stabilize the response. The response of Fe-SA was not enhanced by bromate, but it was increased by hydrogen peroxide (H_2O_2). As dissolved oxygen (DO) is reduced to H_2O_2 at the electrode at potentials <-0.1 V and might therefore have a similar effect, we attempted to increase, or at least stabilise, the sensitivity, by stabilising the concentration of DO in the solution. Automated mercury electrode stands typically include a facility for purging with nitrogen (N_2): this includes the Metrohm VA663 stand used here, the BASi model used for the intercomparison study (Buck et al., 2012) and the PAR303 electrode used elsewhere (Rue and Bruland, 1995). The purging is software controlled and was switched off in our preliminary experiments (Fig. 2.1). All electrodes have

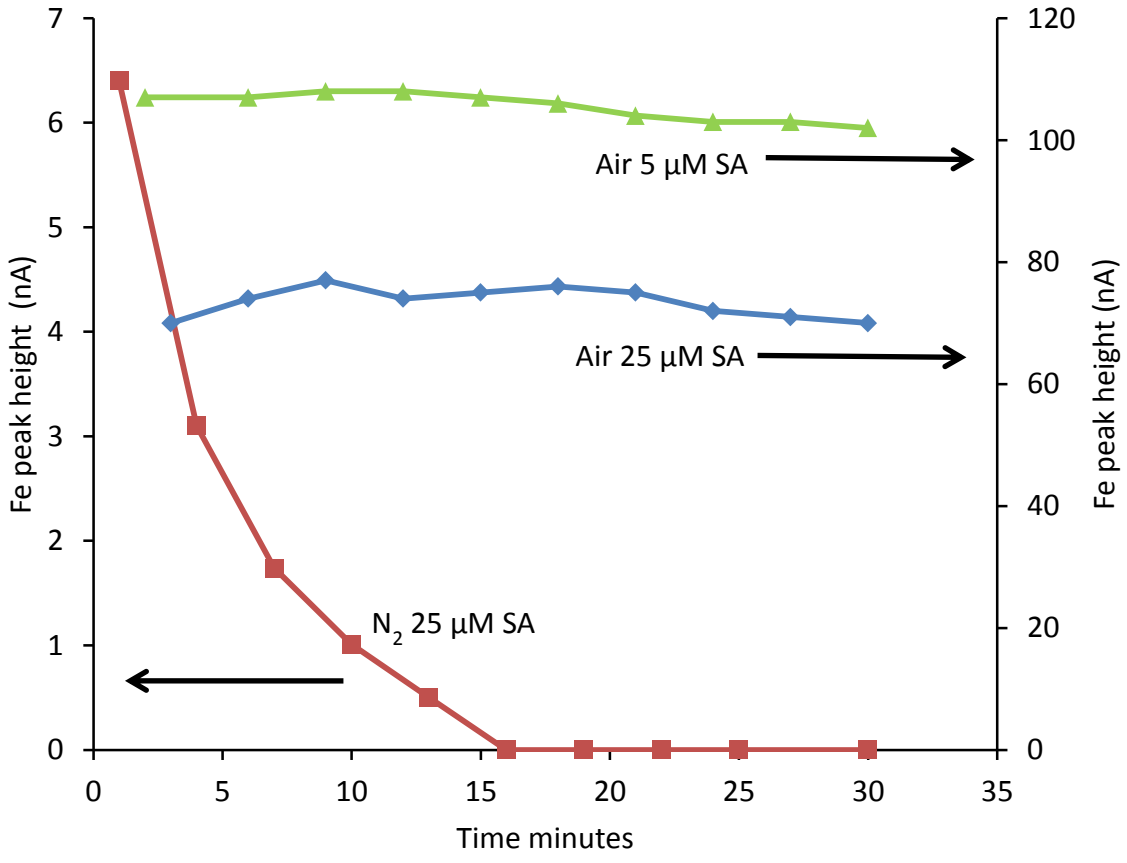

Figure 2.2. Fe peak height as a function of time using the existing method (left hand scale, response decreasing) and using the new method (right hand scale, stable response). The concentration of iron was 5 nM, the seawater had been UV-digested and contained 10 mM borate pH buffer, pH 8.18, the adsorption time was 120 s. The electrode was pressurised using N_2 in the old method, using air in the new method. The concentration of SA was 5 µM or 25 µM as indicated. The peak height using the air system was not affected by repeating the measurement or by adding 50 mercury drops into the cell.

a facility for a N_2-blanket, and this can be difficult to switch off as it is supposed to be permanent. This means that the voltammetric cell is covered with N_2, which gradually removes the DO in the sample. The N_2 blanket was initially switched off in the Metrohm stand by closing its control valve (tightening a screw): this simple procedure was found to much stabilise the response for Fe-SA. However, it also caused the drop control to malfunction causing irregularity. For this reason the electrode stand was connected to an air supply (set to 1 Bar) instead of N_2, which meant that the stand was run in its standard configuration but with air-O_2 blanketing. This produced a drastic improvement: repeat scans for Fe-SA were now stable, without a systematic decrease, and the sensitivity was much better (about 15x) than it was using the N_2 blanket (Fig. 2.1, right hand scale). A drawback of this modification of the electrode stand was a more rapid oxidation of mercury in the electrode cartridge, necessitating more frequent (monthly) cleaning of the cartridge by filtration of the mercury.

These experiments demonstrated that DO (like H_2O_2) much increases the CSV response for Fe-SA, and that its gradual removal as a result of blanketing with N_2 is a possible contributory cause for the decrease in response seen in the original work (Rue and Bruland, 1995) (if removal of DO was not complete) and also in our previous work and that of others (unpublished) who tried without success to get the method to work. Secondly, the scans using our system were now reproducible and could be repeated many times over without a change in sensitivity.

The DO is already present in the samples (except if they are anoxic) and therefore the purging and blanketing with air does not introduce an artefact in the metal speciation, whilst addition of H_2O_2 (or bromate which is used for CSV of Fe-DHN) would increase the redox potential of the system to above that of air-equilibrated seawater. The lack of understanding of the effect of DO in the previous work may have affected all parameters fundamental to the method for Fe detection and speciation. For this reason these were re-optimised in subsequent experiments.

The finding that the results are stable in our system with air purging and an air blanket has not solved all reported peak decreases as Buck's system (Buck et al., 2007) was not connected to N_2 (or air) and still had a problem of a decreasing peak. The BAS electrode (used by Buck) and the PAR electrode (used by Rue and Bruland) have mercury drops with a

surface area ~8x larger than those of the Metrohm system (Buck et al., 2012). We tested for possible Fe-SA adsorption on waste mercury drops by dispensing 50 drops and repeating the measurement: the response for 5 nM Fe was not changed by this mercury addition, suggesting that this effect was negligible in our case. We subsequently measured the response for Fe (5 nM) in UV-SW over a long period (16 h) using automated measurement (4 scans every 30 min), which showed no systematic decrease: the averaged response was 75.5 ±1.5 nA (n=132).

2.3.2. Optimisation of the concentration of SA used for CSV of Fe

The pH was set to pH_{NBS} 8.18 as this is close to the natural pH of seawater in equilibrium with air, and borate pH buffer was used as it is inorganic and can be UV-digested to remove possible interfering organic matter, and as the borate binds metals very weakly in seawater (Byrne and Thompson, 1997; van den Berg, 1984). This buffer therefore has advantages over for instance TRIS buffer, which has a pK_a of 8.07 in seawater (Ramette et al., 1977) as this tends to compete for Fe and lower the response, and POPSO buffer with a pK_a value of ~7.8. UV-digestion of the borate buffer stock solution was found to improve the CSV sensitivity so this was made part of the preparation procedure.

Variation of the concentration of SA in UV-SW (pH 8.18) containing 10 nM Fe showed the response for Fe-SA to increase from 0.5 to 5 µM SA, after which the response decreased again (Fig. 2.2). This maximum at 5 µM SA was surprising as it is at a much lower concentration of SA than found previously (27.5 µM SA) (Rue and Bruland, 1995). The experiment was repeated at lower concentrations of Fe (1 and 3 nM Fe), and gave the maximum response at the same SA concentration (Fig. 2.2). The experiment was repeated with different batches of SA (from different bottles, including newly purchased), prepared in 0.1 M HCl and in methanol, in each case giving the same result. 27.5 µM SA was the concentration selected for Fe speciation in the original work (Rue and Bruland, 1995), and 25 µM (Buck et al., 2007), as this was thought to be the optimal level. The complex stability of Fe-SA has been calibrated for that same concentration. However, our data shows that this level of SA gives a relatively poor response for Fe and this response is easily improved by lowering its concentration to 5 µM SA.

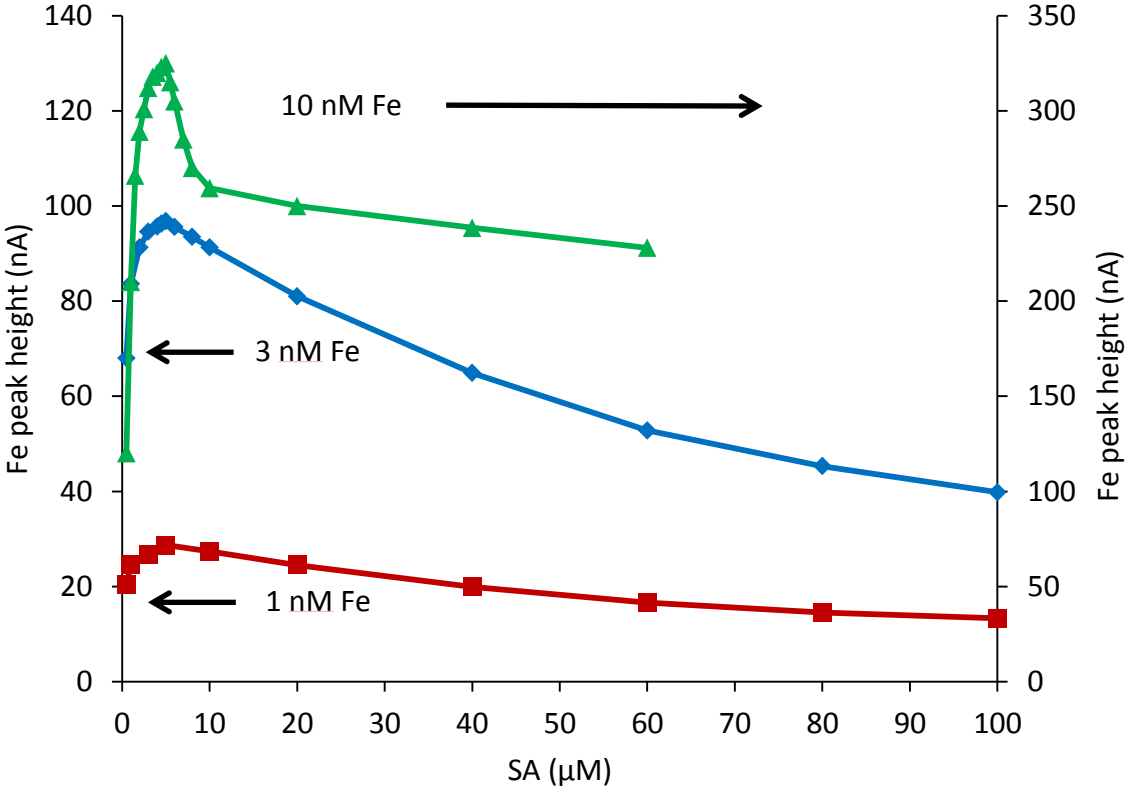

Figure 2.3: Optimisation of SA concentration: the diagram shows the response for 1, 3 and 10 nM Fe as a function of the concentration of SA. The adsorption time was 2 min. Maximum response is obtained at 5 µM SA, compared to 27.5 µM in the existing method (Rue and Bruland, 1995).

2.3.3. Variation of other parameters

Variation of the deposition potential showed that best response for Fe-SA was obtained after deposition at 0 V (Fig. 2.3A). This potential is close to the oxidation potential of mercury in seawater, which limits the positive potential range. Its relatively positive value suggests that the adsorbing Fe-SA species has a neutral or a negative charge, as a positively charged species would be expected to adsorb less well at positive potentials. This potential is essentially the same as that used before (Buck et al., 2007; Rue and Bruland, 1995).

Oxidants were added to investigate whether the response could be further improved. Bromate, known to increase the peak height for Fe in presence of DHN (Obata and van den Berg, 2001) did not increase the peak height for FeSA. Hydrogen peroxide was found to much improve the sensitivity. The data shows that the response increased linearly with the hydrogen peroxide concentration to ~2 mM H_2O_2 (Fig 2.3B), after which the response levelled off and started to decrease. The sensitivity is enhanced according to the following

mechanism (Kolthoff and Parry, 1951):

Fe^{III}-SA + e- → Fe^{II}-SA (2)

Fe^{II}-SA + H_2O_2 → Fe^{III}-SA + $HO^{\cdot}$ + OH^- (3)

The hydroxyl radical may also oxidise Fe^{II}:

Fe^{II} + $HO^{\cdot}$ → Fe^{III} + OH^- (4)

At high levels of H_2O_2 the $HO^{\cdot}$ may lead to self-destruction of the H_2O_2 (reactions 5 and 6):

HO. + H_2O_2 → H_2O + $HO_2^{\cdot}$ (5)

HO_2. + H_2O_2 → O_2 + H_2O + $HO^{\cdot}$ (6)

Reaction (3) is rate determining (Kolthoff and Parry, 1951) which is the reason that the peak height increases linearly with the concentration of H_2O_2. A similar linear increase was found previously for the system of Fe/NN/H_2O_2 (Yokoi and van den Berg, 1992). The half-wave potential for the reduction of H_2O_2 (~-0.8 V) is more negative than the oxidation potential of Fe^{II} (~-0.4 V) which explains why Fe^{II} catalyses the reduction of H_2O_2 (via the Fenton reaction). The actual reaction is complicated because of the generation of free radicals (Florence, 1984; Millero and Sotolongo, 1989) but the catalysed reaction involves the exchange of just one electron. The levelling off of the increase and the decrease at levels above 2 mM H_2O_2, could be due to self-destruction of H_2O_2 (equations 5 and 6) or due to a possible oxidation of the dissolved SA or both in view of the decrease.

The experiment was carried out without purging of the solution which was air-equilibrated, therefore containing ~200 µM O_2. The oxygen is reduced to H_2O_2 at the electrode at potentials <~-0.2 V in pH 8 seawater, and therefore has the same effect as H_2O_2 added to the seawater:

O_2 + $2H^+$ + $2e^-$ → H_2O_2 (7)

The response for Fe was approximately doubled by the addition of 0.6 mM H_2O_2. Clearly it is possible to reach high sensitivity for Fe by the addition of H_2O_2, but this has the drawback that any natural ligands with a tendency to oxidation could be altered, which might affect determination of the Fe speciation. For this reason, and because the sensitivity for Fe in the presence of air was sufficiently high, H_2O_2 was not used for the purpose of Fe speciation.

2.3.4. pH effect

The pH was varied between 7.1 and 8.8 to evaluate its effect on the sensitivity. The SA concentration was set to 5 μM and the concentration of Fe was 3 nM. The sensitivity was found to increase up to pH 8.24 above which it decreased (Fig 2.3 C). The increase was a factor of 2 from pH 7.7 to pH 8.24, which is the pH range found in seawater from deep sea to surface waters. It is therefore possible to study the speciation of Fe over the entire range of pH values naturally occurring. However, in this work the pH was set to 8.18 (NBS scale) as this is close to that for seawater in equilibrium with air, and this pH was buffered by the addition of borate to the water.

The reason for the increase in sensitivity with increasing pH is not obvious from the equations. It suggests that reaction (2) or (3) is affected in this pH region. The decrease at pH values > 8.24 may be due to competition between OH- and SA for complexation with Fe^{III}. It is therefore possible that a different pH profile would be obtained at a lower or higher concentration of SA, but this was not further investigated.

2.3.5. Effect of the equilibration time between inorganic Fe and SA

SA was added to UV-SW which had been pre-equilibrated overnight with 5 nM Fe. Due to the low solubility of Fe the majority of the Fe would have been present as colloidal Fe-hydroxide, which explains the slow reaction rate found (Fig. 2.3D). The signal for FeSA gradually increased until it stabilised after ~10 min. After a longer reaction time (>30 min) the signal started to decrease which was ascribed to adsorption on the voltammetric cell. A stable response over several hours is obtained if the cell is previously equilibrated with seawater of the same Fe concentration in the presence of SA. Subsequent calibration showed that all Fe was recovered during the 10 min equilibration period indicating that the SA re-dissolves the colloidal Fe. Additions of dissolved Fe (from an acidified standard) gave an immediate signal increase and stable response demonstrating that the reaction between inorganic, dissolved Fe and SA is rapid (within seconds).

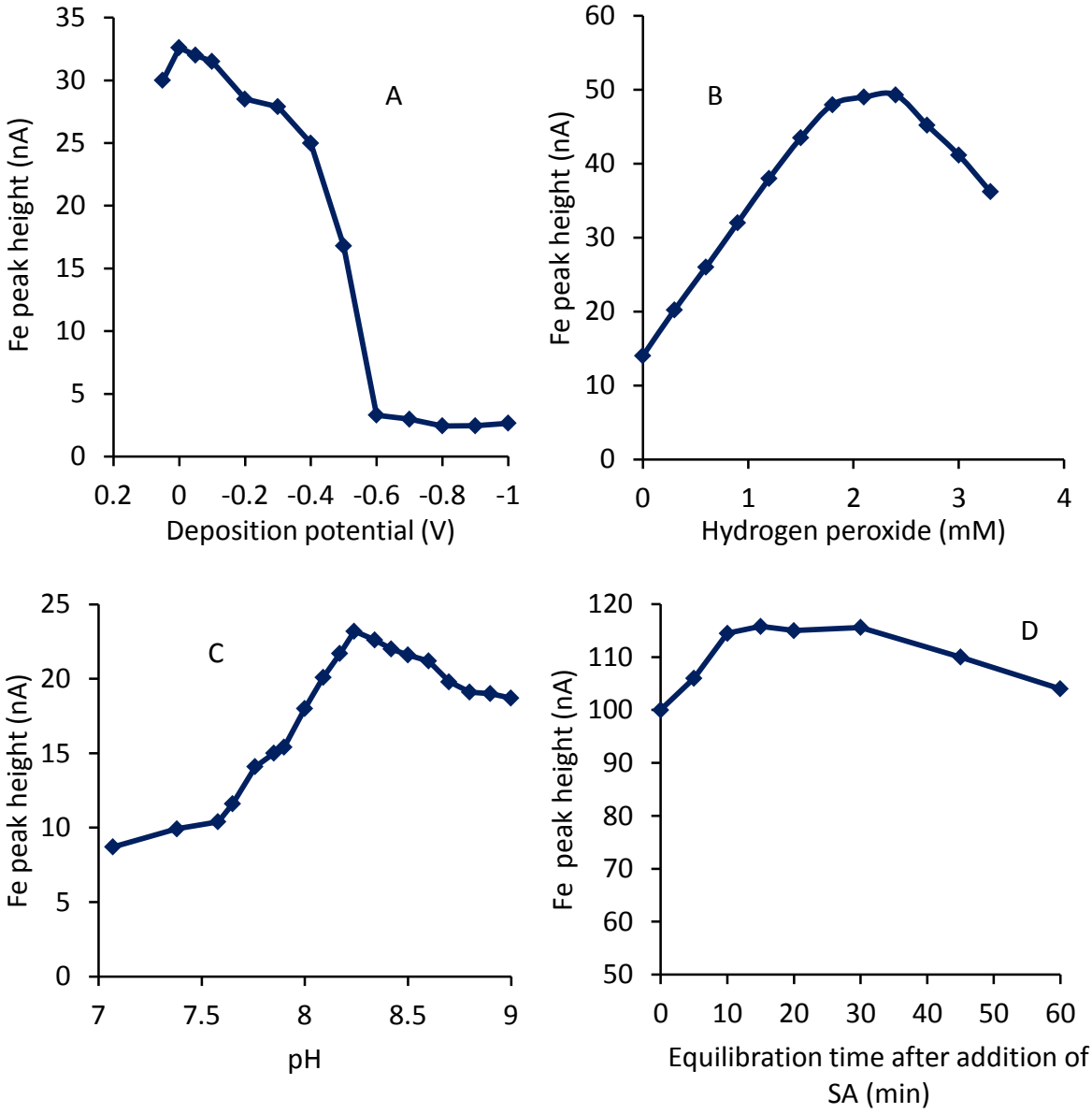

Figure 2.4. Optimisation of analytical parameters in UV-digested seawater, containing 5 nM Fe, 10 mM borate buffer, pH 8.18 and 5 μM SA; the deposition time was 2 min at 0 V unless indicated differently. Solutions were blanketed with air. A) Effect of varying the deposition potential. B) Effect of adding H_2O_2 to the solution. C) Effect of varying the pH; the pH was varied by adding ammonia (1 M) to seawater that had first the pH lowered by additions of HCl (1 M). D) Effect of varying the reaction time between inorganic, mostly colloidal, Fe and 5 μM SA; the seawater had first been allowed to equilibrate overnight with 5 nM Fe in the voltammetric cell.

2.3.6. Kinetic effects of Fe complexation with natural ligands and EDTA

The reaction of SA with Fe consists of complexation of inorganic Fe, which leads to dissociation of natural organic complexes of Fe with ligands L. The two processes were tested individually to ensure that equilibrium conditions were met during the measurements.

Measurement of the CSV response for inorganic Fe immediately after addition of 5 μM SA showed the peak height increase over ~10 minutes after which it stabilised (Fig. 2.3D). The seawater had been UV-digested to remove any organic ligands, and 5 nM Fe had been equilibrated overnight, which ensured supersaturation of the seawater with inorganic Fe due to its poor solubility (Liu and Millero, 1999). ~90% of the response was achieved with the first scan, which was carried out within 2 min after the SA addition, indicating that the freshly precipitated Fe-hydroxide was highly reactive. The peak height started to decrease after 30 min of repeated measurements in the voltammetric cell, which was probably due to adsorption on the cell. The response for a solution of 5 nM Fe and 5 μM SA stored in a polyethylene bottle (which had previously been conditioned with water of the same composition) was constant for several hours indicating that Fe can be equilibrated for an extended period with SA in seawater without loss of sensitivity or loss of Fe. The kinetic effect shown here is for reaction of colloidal Fe-hydroxides, as the reaction between SA and freshly added, dissolved Fe', is immediate.

To prevent possible decreases as a result of adsorption on bottle and cell walls, all speciation experiments were carried out after conditioning of the containers until stability was obtained.

2.3.7. Rate coefficient for dissociation of the EDTA complex and the complex of natural ligand L with Fe in seawater

The reaction rate of organically complexed Fe with SA was tested with a model ligand (EDTA) and with Fe complexed with natural (unknown) ligands present in the seawater. Fe (5 nM) was pre-equilibrated with EDTA (2 μM EDTA) in UV-SW for periods of 3 h, overnight and 3 days) and the response for Fe-SA measured after addition of SA (5 μM). About 20% of the Fe was found to be complexed with the EDTA equilibrated for 3 h, 2 min after the SA addition, indicating that the EDTA had not reached equilibrium. >90% of the Fe was EDTA-bound after overnight equilibration, and further equilibration over 3 d did not increase this further indicating that equilibrium had been obtained after overnight equilibration, in agreement with a previous finding of 7 h to reach equilibrium between EDTA and Fe in UV-SW (Wu and Luther III, 1995).

The addition of SA to the pre-equilibrated Fe-EDTA causes some of the Fe' to become complexed with SA which causes a decrease in the concentration of Fe-EDTA and formation of Fe-SA until a new equilibrium is attained. The reaction was followed by measurement of the peak current (i_p, which reflects the concentration of Fe-SA) which increased as a function of time until it stabilised at $i_p = i_{pmax}$ when equilibrium had been reached between SA, Fe' and EDTA. At each moment during this period the response was normalised to the maximum response (from >50 min):

$$X = i_p / i_{pmax} \quad (8)$$

The equilibrium concentration of Fe-SA was computed from the total concentration of Fe (C_{Fe} = 5 nM) and the balance of the α-coefficients:

$$[Fe\text{-}SA]_{equil} = C_{Fe}\, \alpha_{Fe'\text{-}SA} / (\alpha_{Fe'\text{-}SA} + \alpha_{Fe'EDTA} + \alpha_{Fe'}) \quad (9)$$

Here $\alpha_{Fe'\text{-}SA}$ is the overall α-coefficient for Fe complexed with SA, $\alpha_{Fe'EDTA}$ for Fe and EDTA and $\alpha_{Fe'}$ for inorganic complexation of Fe. All α-coefficients are on the Fe' scale which means that $\alpha_{Fe'}$ here is 1. At each point in time the concentration of Fe-SA is given as a fraction of the maximal $[Fe\text{-}SA]_{equil}$:

$$[Fe\text{-}SA]_t = X\, [Fe\text{-}SA]_{equil} \quad (10)$$

The concentration of Fe' in equilibrium with $[Fe\text{-}SA]_t$ and C_{SA} (the total added SA) was calculated from

$$[Fe']_t = [Fe\text{-}SA]_t / \alpha_{Fe'\text{-}SA} \quad (11)$$

The residual concentration of Fe-EDTA decreased as a function of time and was calculated from the balance of total Fe (C_{Fe}), [Fe-SA] and [Fe'] at each point in time:

$$[Fe\text{-}EDTA]_t = C_{Fe} - [Fe\text{-}SA]_t - [Fe']_t \quad (12)$$

and shown in Figure 2.4A. The rate coefficient, k_d (s^{-1}), for dissociation of EDTA-bound Fe was obtained from the slope of a plot of $\ln[Fe\text{-}EDTA]_t$ as function of time (Croot and Heller, 2012; Witter et al., 2000) (Fig. 2.4A).

Values for the reaction rate coefficient for Fe-EDTA dissociation were found of 0.000172 s^{-1} (overnight equilibration) and 0.000167 s^{-1} (3 d equilibration) giving a half-life of 68 min for the Fe-EDTA dissociation. The value for the rate coefficient found here is greater

than that found previously (~2 x 10^{-6} s^{-1}) when Fe-EDTA was reacted with sulfoxine (Hudson et al., 1992), suggesting that possibly direct ligand exchange took place between the Fe-EDTA and SA. Nevertheless, the reaction rate is slow indicating that long equilibration times are necessary: a reaction time of ~7 h should be used to be within 1% of equilibrium with EDTA. The ln[FeEDTA] diagram for the 3 h equilibration experiment was non-linear as only about 30% of the Fe had reacted with the EDTA, so the dissociation reaction was near to equilibrium when the SA was added. However, the first few data points suggested a similar half-life of the reaction.

The dissociation rate of Fe complexed with natural ligands (half-life= 8.7) was quicker than with EDTA (half-life= 68 min) (Fig. 2.4B). The Fe response for FeSA in presence of FeL was found to increase gradually reaching apparent stability after ~40 min. In this case the seawater was from the Celtic Sea and the concentration of Fe had been raised to 1.5 nM (from a background level of 0.5 nM Fe) to obtain a significant peak at the beginning of the reaction, and the cell had been conditioned and the experiment repeated several times to obtain a reproducible result. The ligand concentration in the water was determined (by complexing ligand titration) to be 2.5 nM, which meant that nearly all Fe was complexed by L. In view of the fast reaction (instantaneous) for Fe' with SA, the 40 min reaction time is due to a slow dissociation of FeL.

The rate coefficient of dissociation of FeL (k_{FeL}) was calculated from the slope of a plot of ln[FeL] as a function of time (s) (Fig. 2.4B inset), where concentrations of FeL were calculated from the difference of the final response (when nearly all FeL is converted to FeSA) and the actual response. The plot for ln[FeL] as a function of time was linear indicating that it is a pseudo-first order reaction (FeSA is formed much quicker than FeL dissociates, which means that the FeL dissociation is rate limiting), giving a value of k_{FeL} = 0.00133 ± 0.0002 s^{-1}. The half-life of this reaction is 8.7 minutes suggesting that the SA is reacting with FeL via an associative mechanism (appendix (Croot and Heller, 2012)).

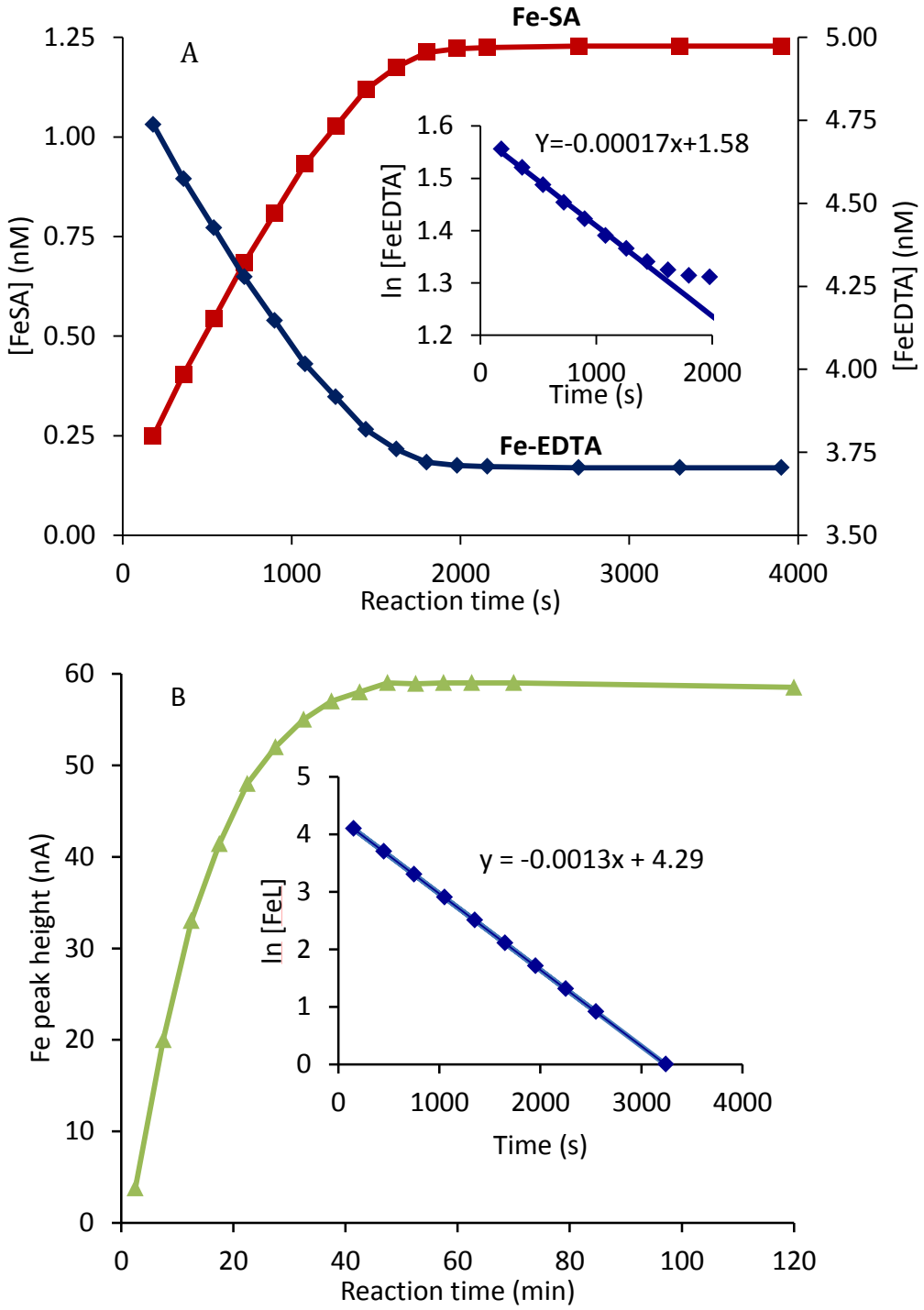

Figure 2.5. Reaction time of Fe with 2 µM EDTA (A) and unknown ligand L (B), present at 2.53 nM (log $K'_{Fe'L}$ = 11.5). The concentration of Fe was 5 nM in A and 1.14 nM in B. The diagrams show that the peak height for FeSA increases as a function of time after addition of 5 µM SA. The concentration of FeL, used for the inserted diagrams, was calculated from the difference between the total [Fe] and the [Fe-SA] calculated from the response.

2.3.8. Interferences

SA can be expected to complex other metals beside Fe in seawater. However, complexes are likely to be weakened as a result of competition with H^+ and the abundance of Ca^{2+} and Mg^{2+}. Copper is known to give a peak with SA (Campos and van den Berg, 1994) which is apparent at -0.3 V, about 0.2 V more positive than that for Fe. The peak separation is sufficient for good quantification of the two peaks. The CSV response for Cu is poor in the presence of air, but the Cu-SA species still adsorbs on the electrode giving a relatively broad and low peak. Additions of Cu to UV-seawater (120 s adsorption time, 10 nM Fe) showed that the peak for Fe decreased when [Cu]>25 nM. This suggests that Cu could potentially interfere by lowering the sensitivity for Fe during Fe-complexing ligand titrations of deep ocean waters at long deposition times (typically 120-300 s (Buck et al., 2012)) especially at the higher SA concentration used in that work.

Surface-active organic matter decreases the sensitivity for Fe as a result of competitive adsorption on the electrode. Triton X-100, used as model compound for non-ionic surfactants, was found to decrease the response for Fe (2 min adsorption time) by 20 % (0.5 mg/L Triton), 25 % (1 mg/L) and 30 % (2 mg/L Triton). A variable decrease in sensitivity is therefore expected for seawater as this is thought to contain between 0.1 and 2 mg/L of surface active compounds similar to Triton-X-100 (Cosovic et al., 1977). In view of lower levels, up to 0.02 mg/L for upper water column waters from the Southern Ocean (Croot et al., 2007) in ocean waters, this effect may there be minor. This type of interference is common for all CSV methods, though it is not always mentioned, and is especially important for speciation as the water is analysed without UV-digestion; the effect on Fe-SA is similar to that obtained for Cu with SA (Campos and van den Berg, 1994). The suppression of the peak height by surfactants could incorrectly be interpreted by strong complexation unless the sensitivity is determined.

2.3.9. Calibration of $K'_{Fe'SA}$ and $B'_{Fe'SA2}$ by titrations with SA with and without competition with EDTA

The complex stability of Fe with SA was calibrated by two procedures, based on measurement of the reactive species of Fe-SA (peak height for Fe in the presence of SA) with

and without competition against EDTA. EDTA was selected as its complex stability with Fe is known and side-reactions with the major cations in seawater can be taken into account. The inorganic speciation of iron is dominated by hydroxide formation and was calculated using an ion-pairing model with the stability constants for Fe^{III}-OH species from Liu and Millero (Liu and Millero, 1999). The constants used for the calculation are shown in Table 2.1. The K values from (Martell and Smith, 1974) are valid for an ionic strength of 0.1 M, and those from (Arena et al., 1983) were calculated for an ionic strength of 0.7 M using their equations (their experiments were for ionic strengths between 0.17 and 0.77 M). The Martell and Smith values were not adjusted to the ionic strength of seawater because the Davies equation is not valid beyond ionic strength 0.1 M. The side reaction coefficient of EDTA with the major cations and pH in seawater using the Arena constants (Arena et al., 1983) is 8.41 (log value) compared to 7.97 using constants corrected to the seawater ionic strength using the Davies equation (Croot and Johansson, 2000) and 8.6 using uncorrected Martell and Smith constants. The species FeOH.EDTA was taken into account and increased the value for α_{FeEDTA} by a factor 4. The inorganic α_{Fe} was calculated as 9.98 (log value) at the experimental pH (pH_{NBS} = 8.18) using the constants from Liu and Millero, which is almost the same as that (log α_{Fe} = 10) found experimentally (Hudson et al., 1992). The value of 10 is used here as elsewhere (Croot and Johansson, 2000; Rue and Bruland, 1995). The thus calculated conditional stability constant for complexation of inorganic iron (Fe') by EDTA in seawater of pH_{NBS} 8.18 was log $K'_{Fe'EDTA}$ = 6.7, which is very close to the value of 6.8 obtained in pH 8.26 synthetic seawater (Hudson et al., 1992) indicating that this modeling fits previous data well. The α-coefficient for complexation of Fe' by 1 μM EDTA in seawater calculated using these constants is 28.8 (Table 2.1).

Because greatest sensitivity is obtained for Fe at 5 μM SA, at first this SA concentration was selected for calibration of the α-coefficient ($\alpha_{Fe'\text{-}SA}$) and from this the value for the stability constant, by competition against EDTA. This determination was repeated at several SA concentrations, between 1 and 40 μM SA, in order to evaluate whether the adsorptive Fe complex is of the type FeSA or $FeSA_2$, to re-calibrate the α-coefficient for the SA concentration used in previous work (27.5 μM SA), and to verify whether SA may be suitable for reverse metal titrations in which the concentration of the added ligand is varied without metal additions (Nuester and van den Berg, 2005).

Table 2.1. log K values used in this work to calculate the speciation in seawater, and sample values for the α-coefficients calculated with these constants for given conditions.

Species	**log K values**	**Reference**
$Fe(OH)^{2+}$	-2.58	(Liu et al., 1992)
$Fe(OH)_2^{+}$	-6.64	(Liu et al., 1992)
$Fe(OH)_3^{0}$	-14.9	(Liu et al., 1992)
$Fe(OH)_4^{-}$	-23.5	(Liu et al., 1992)
Fe^{3+}EDTA	25.1	(Martell and Smith, 1974)
Ca^{2+}EDTA	10.4	(Arena et al., 1983)
Mg^{2+}EDTA	8.56	(Arena et al., 1983)
Fe^{3+}EDTA'	16.7	Seawater of Sal 35, calculated using the Arena et al (1983) data.
FeEDTA /FeOHEDTA . H	7.49	(Martell and Smith, 1974)
	Calculated α-values	
log α_{EDTA}	8.41	Seawater of Sal 35
log $\alpha_{Fe3+EDTA}$	11.46	for 1 µM EDTA
log $\alpha_{Fe'}$	10.0	
log $\alpha_{Fe'EDTA}$	1.46	for 1 µM EDTA ($\alpha_{Fe'EDTA}$ = 28.8),

The stability of Fe-SA was calibrated in separate experiments in seawater with 5 nM Fe, at levels of SA of 1, 2, 5, 10, 20, 30 and 40 µM by equilibration with EDTA, which was added to levels of 0, 0.05, 0.1, 0.3, 0.5, 1, 2, 3 and 5 µM EDTA up to 5 µM SA. The EDTA titration was extended to 20 µM EDTA at higher [SA].

In seawater containing Fe, SA and competing ligand EDTA, the metal is distributed across the various species, inorganic and organic. Assuming that two species are formed (FeSA and $FeSA_2$), and either one, or both, may be responsible for the Fe peak, the following relationship exists at equilibrium between the EDTA and SA, having species without EDTA in the numerator and all species in the denominator:

$$X = (\alpha_{FeSA} + \alpha_{FeSA2} + \alpha_{Fe}) / (\alpha_{FeSA} + \alpha_{FeSA2} + \alpha_{Fe} + \alpha_{FeEDTA}) \qquad (13)$$

where $\alpha_{FeSA} = K'_{FeSA} \times [SA]$, $\alpha_{FeSA2} = B'_{FeSA2} \times [SA]^2$ and $\alpha_{Fe\text{-}SA}$ = the overall α-coefficient for Fe with SA = $\alpha_{FeSA} + \alpha_{FeSA2}$. The two constants (K'_{FeSA} and B'_{FeSA2}) are for the reaction of Fe^{3+} with SA in seawater of the experimental pH and salinity. Eqn. (13) is analogous to that used before (van den Berg, 1985) but with the inclusion of the inorganic species of Fe.

Experimental measurements of X (Eqn. 13) were obtained from $X = i_p / i_{pmax}$ where i_p is

the peak height for Fe-SA (any species of Fe with SA) in the presence of EDTA, and i_{pmax} the maximum peak height that is obtained without EDTA. X = 1 when [EDTA] = 0. Values for K'_{FeSA} and B'_{FeSA2} were calculated (separately individually and simultaneously) from minimisation (using Solver in Excel) of the least squares difference between the actual X-values obtained from titration with EDTA and those calculated from the estimated values for the constants according to Eqn. 13.

The results of the titrations of SA with EDTA at various SA concentrations are shown in Fig 2.5. The peak height of each experiment was normalised to that at zero EDTA. The actual peak heights for the experiment at 10, 20, 30 and 40 µM SA were lower than those for 5 µM SA as the sensitivity is greatest for 5 µM SA (Fig. 2.2). The relative peak heights decrease in each experiment with increasing concentration of EDTA (Fig. 2.5), which is in line with expectation as the EDTA competes for Fe with the SA, so the response should decrease regardless of which species adsorbs. The halfway point of the titrations with EDTA (where the normalised response is 0.5 in Fig. 2.5) was reached at a higher concentration of EDTA as SA increased from 1 to 40 µM SA. This is to be expected as the α-coefficient for Fe-SA ($\alpha_{Fe\text{-}SA}$) increases with the concentration of SA, which means that more EDTA is required to increase α_{FeEDTA} to the same level. The values of α_{FeEDTA} and $\alpha_{Fe\text{-}SA}$ are equal when the relative response has been lowered to 0.5, which can be used to obtain a first estimate for the value of $\alpha_{Fe\text{-}SA}$.

The curves shown in Fig. 2.5, approximately connecting the data points, were calculated by modelling the titrations using the fitted values for K'_{FeSA} and B'_{FeSA2} in each experiment, and the good data fit demonstrates the quality of the fitting.

Values for $K'_{Fe'SA}$ and $B'_{Fe'SA}$ were obtained by dividing K'_{FeSA} and B'_{FeSA2} by α_{Fe} ($=10^{10}$). The log $K'_{Fe'SA}$ values were found to lie in a small range (log $K'_{Fe'SA}$ = 6.53 ± 0.03 with log $B'_{Fe'SA2}$ = 10.2 ± 0.6) for SA concentrations between 1 and 40 µM (Table 2.2). However, the data fit as a function of EDTA was found to be insensitive for $B'_{Fe'SA2}$ therefore giving a large standard deviation. The reason for the small influence of $B'_{Fe'SA2}$ on $\alpha_{Fe'\text{-}SA}$ is that α_{FeSA2} (=1.3) < α_{FeSA} (= 16.6) at 5 µM SA.

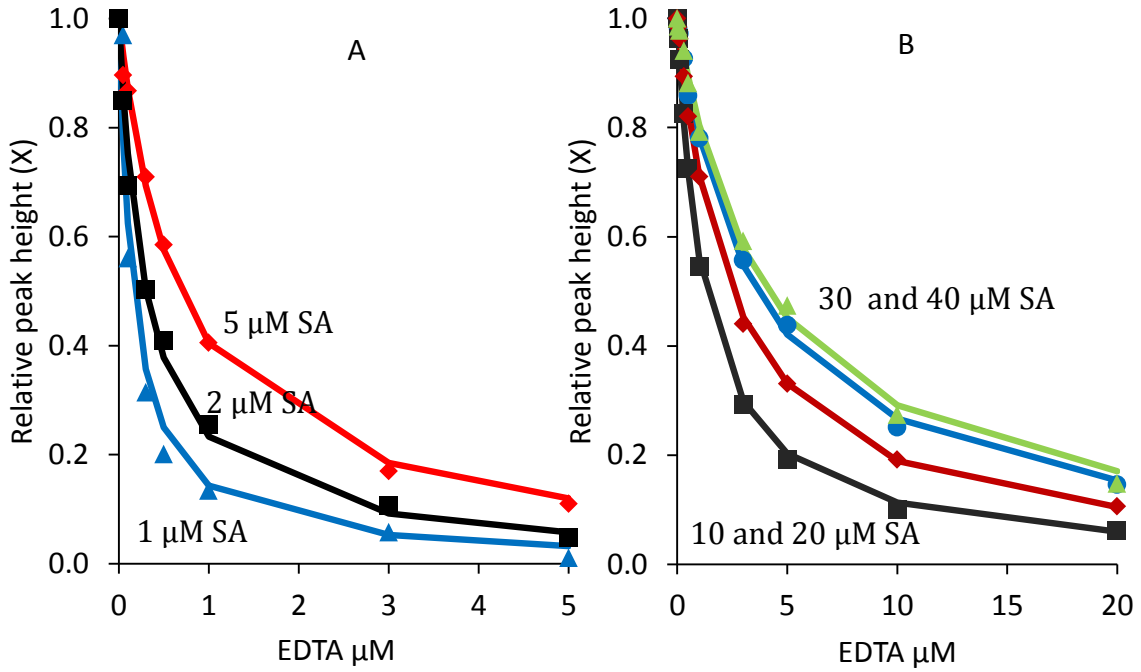

Figure 2.6. Calibration of $K'_{Fe'SA}$ and $B'_{Fe'SA2}$ by titration of various levels of SA with EDTA in UV-digested seawater set to pH_{NBS} 8.18 using borate buffer. The data have been normalized by plots of the ratio X (peak height / max peak height) as a function of the concentration of EDTA. The curves were calculated using the values for $K'_{Fe'SA}$ and $B'_{Fe'SA2}$ obtained from the least squares regression of the data according to Eqn. 13. The values found for $K'_{Fe'SA}$ and $B'_{Fe'SA2}$ are in Table 2.2. A) X as a function of [EDTA] at 1,2 and 5 µM SA; B) X as a function of [EDTA] at 10, 20, 30 and 40 µM SA.

Table 2.2. Values for $K'_{Fe'SA}$ and $B'_{Fe'SA}$ obtained by titrations of Fe-SA with EDTA at constant SA and Fe, and by titrations with SA at constant EDTA. Data fitting as function of [EDTA] and as function of [SA]. The sensitivity (S) is in nA nM^{-1} min^{-1}. The titrations with EDTA and SA are shown in Fig. 2.5. The values for $K'_{Fe'SA}$ and $B'_{Fe'SA2}$ were converted from K'_{Fe3+SA} and $B'_{Fe3+SA2}$ values using log $\alpha_{Fe'}$ = 10. The standard deviation for log $B_{Fe'SA2}$ is 0.6 when fitted as function of EDTA. The 0-EDTA values for $K'_{Fe'SA}$ and $B'_{Fe'SA2}$ at 5 nM Fe agreed well with the values for 1 and 3 nM Fe. Previous work calibrated $B'_{Fe'SA2}$ against EDTA and assumed that only $FeSA_2$ was present: B'_{FeSA2} = 10.98 (Rue and Bruland, 1995) and 11.1 (Buck et al., 2007).

		Titrations with EDTA at constant SA and 5 nM Fe. EDTA varied from 0 to 5 µM for =<5 µM SA and from 0 to 20 µM EDTA at higher SA. Data fitted as function of EDTA.	
Experimental concentration of SA and sensitivity (S) (nA nM^{-1} Min^{-1})		**log $K'_{Fe'SA}$**	**Log $B'_{Fe'SA2}$**
1 µM SA	S = 3.5	6.54	11.0
1 µM SA		6.54	10.9
2 µM SA	S = 3.8	6.55	10.9
2 µM SA		6.56	10.9
5 µM SA	S = 4.4	6.53	9.9
5 µM SA		6.54	10.0
10 µM SA	S = 3.8	6.54	9.8
20 µM SA	S = 3.1	6.53	9.5
30 µM SA	S = 2.8	6.53	9.5
40 µM SA	S = 2.6	6.46	9.8
Average value		**6.53 ± 0.03**	**10.2 ± 0.6**
		Same data but with data fitting as a function of [SA] at constant [EDTA]	
EDTA µM		**log $K'_{Fe'SA}$**	**Log $B'_{Fe'SA2}$**
0		6.51	10.72
0.05		6.53	10.81
0.1		6.50	10.75
0.3		6.44	10.83
0.5		6.55	10.90
1		6.52	10.90
3		6.49	10.92
5		6.46	10.95
Average		**6.50 ± 0.04**	**10.85 ± 0.08**
		Titration with SA from 0 – 100 µM SA, without EDTA	
At 1 nM Fe		6.53	10.70
At 3 nM Fe		6.51	10.75
At 5 nM Fe		6.51	10.72
Average values		**6.52 ± 0.01**	**10.72 ± 0.03**

Plots (Fig. 2.2 and 2.6) of the response as a function of [SA] rather than of [EDTA] show an initial increase followed by a decrease at high [SA]. This decrease is consistent with the formation of a higher order Fe-SA species that does not adsorb. The most simple chemical model that describes this is that a species of the type FeSA adsorbs, whilst the subsequent species, $FeSA_2$, does not adsorb. This can be modelled theoretically using equation 14: in this case $X = i_p / i_{pmax}$ is defined as follows:

$$X = \alpha_{FeSA} / (\alpha_{FeSA} + \alpha_{FeSA2} + \alpha_{Fe} + \alpha_{FeEDTA}) \quad (14)$$

The data of the competition experiments against EDTA were re-arranged and are shown as function of SA in Fig. 2.6A, showing variation in X as function of [SA] at 6 concentrations of EDTA. Values for K'_{FeSA} and B'_{FeSA2} were fitted using equation 14. A complication in this case is that the maximum peak current, $i_{pmax,}$, is not reached because of the presence of Fe' and $FeSA_2$ in the denominator. Therefore X <1 when [EDTA] = 0:

$$\text{At 0 EDTA: } X = \alpha_{FeSA} / (\alpha_{FeSA} + \alpha_{FeSA2} + \alpha_{Fe}) \quad (15)$$

i_{pmax} was therefore one of the fitted parameters. The curves shown (Fig. 2.6A) were calculated using the fitted values for i_{pmax}, K'_{FeSA} and B'_{FeSA2}, and demonstrate a good data fit. The value for log $K'_{Fe'SA}$ was found to be 6.50 ± 0.04, and log $B'_{Fe'SA2}$ = 10.85 ± 0.08 (Table 2.2). The log $K'_{Fe'SA}$ value is slightly less (0.03 units) than that found by fitting as function of EDTA, but the value for $B'_{Fe'SA2}$ is larger and has a smaller standard deviation. The main advantage of this way of fitting is that it is sensitive to both K'_{FeSA} and B'_{FeSA2}.

2.3.10. Calibration of $K'_{Fe'SA}$ and $B'_{Fe'SA}$ without EDTA

The calibration of $K'_{Fe'SA}$ and $B'_{Fe'SA2}$ at 0 µM EDTA (Fig. 2.6B and Table 2.2) showed excellent agreement with the values obtained in the presence of EDTA, indicating that it is possible to calibrate the value for $\alpha_{Fe\text{-}SA}$ without competition against a secondary organic ligand. The reason this is possible is because of the high stability of the inorganic species (hydroxide predominantly) which is well defined using the constants from Liu and Millero (Liu and Millero, 1999). This finding was used to calibrate the constants for FeSA and $FeSA_2$ using two further experiments where SA was added to UV-seawater containing 1 nM Fe and 3 nM Fe, buffered to pH_{NBS} 8.18 as before, without a competing ligand (no EDTA). These titrations were carried out in the voltammetric cell, with just 5 min equilibration time after

each SA addition, which was sufficient as the reaction between SA and inorganic Fe is complete within seconds. The three SA titrations (one for 5 nM Fe using equilibrated aliquots as part of the EDTA titrations) are shown in Fig. 2.6B. These data were used to fit parameters to Eqn. 15 to obtain values for i_{pmax}, $K'_{Fe'SA}$ and $B'_{Fe'SA2}$ (Table 2.2).

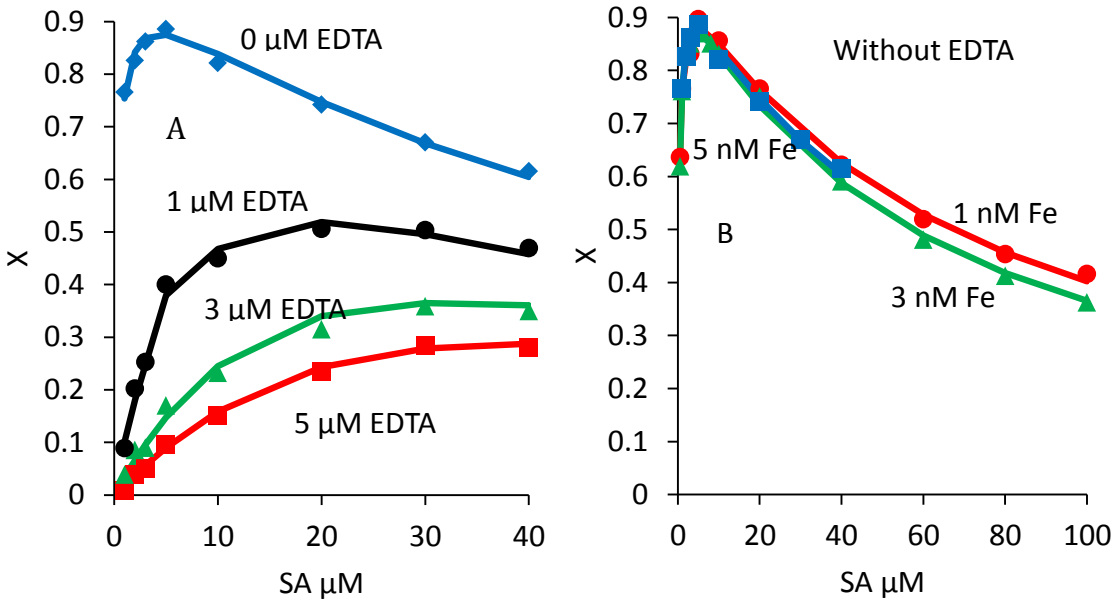

Figure 2.7. A) Data as shown in Fig. 5, but now data fitting as a function of SA using Eqn. 14. X is shown as function of [SA]. The curves were calculated using the values for i_{pmax}, $K'_{Fe'SA}$ and $B'_{Fe'SA2}$ obtained from the least squares regression of the data according to Eqn. 14. The values found for $K'_{Fe'SA}$ and $B'_{Fe'SA2}$ are in Table 2.2; B) additions of SA to UV-seawater without EDTA. X is shown as a function of [SA]. The curves are calculated using the fitted values for $K'_{Fe'SA}$ and $B'_{Fe'SA2}$.

2.3.11. Application to seawater samples and model ligands

The new method (using air and at the most sensitive condition of 5 µM SA) was tested by determination of the concentration Fe, Fe-binding ligands, and their conditional stability constant, $K'_{Fe'L}$, in several seawater samples, and for ligands (humic acid and a siderophore) added to seawater. Determination of Fe in reference seawater samples (SAFe) showed that the concentration of Fe is correctly determined at low and higher concentration of Fe (Table 2.4). The standard deviation of Fe (± 8 - 10 pM for separate analyses, using 5 scans for the sample and 3 scans after the Fe addition for calibration) in SAFe seawater containing 92 pM Fe, suggests a limit of detection of 24 - 30 pM Fe using a deposition time of 3 min. It should be possible to lower the limit of detection to ~10 pM Fe by extending the deposition time to 9 min.

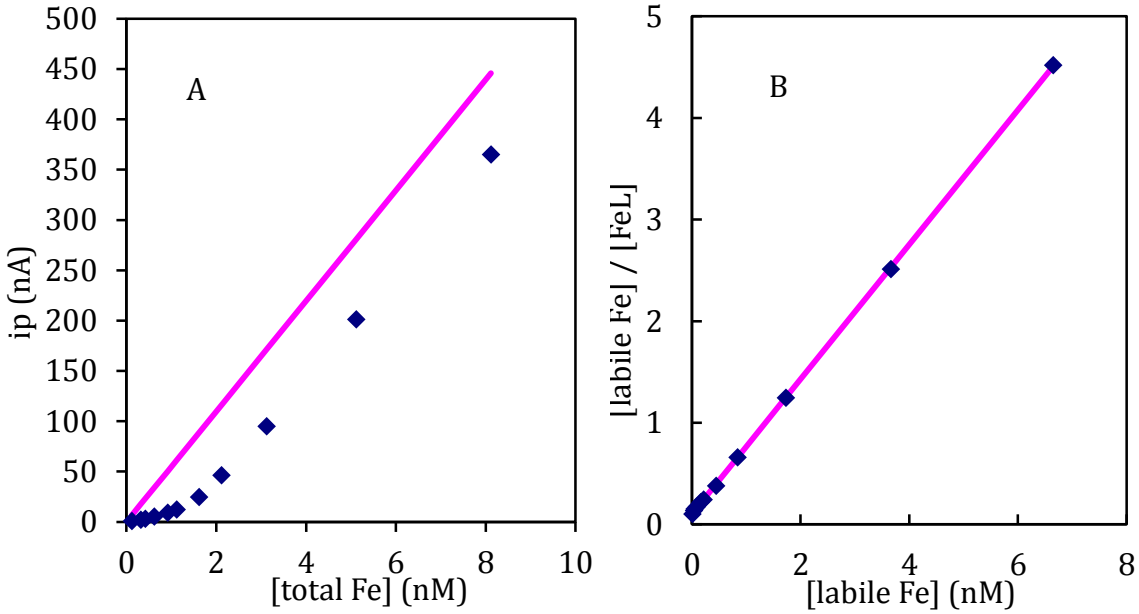

Figure 8. Complexing ligand titrations of Geotraces sample 7556 (Atlantic seawater; depth 75 m). The initial concentration was 0.12 nM Fe. A) Peak height as function of the concentration of total dissolved Fe. B) Linearisation of the data. The ligand concentration and stability constants for this and other samples are shown in Table 2.4.

The concentration of complexing ligands was determined by titration with Fe using overnight equilibration to ensure that the previously complexed FeL was equilibrated with the added SA (Fig. 2.7). The GEOTRACES samples were found to contain 1.47 ± 0.01 (bottle 7556) and 1.49 ±0.17 nM (bottle 8047) of ligands (Table 2.4). The peak height (Fig. 2.7) in the beginning of the titration, for Fe < C_L, shows strong suppression, due to the detection window being low. Values for the peak height for FeSA could nevertheless be measured for the lowest concentrations of Fe, illustrating the good sensitivity of the method. The data linearization (Fig. 2.7B) shows little or no curvature suggesting that a single complexing ligand dominates the speciation. Calculation of the ligand concentration using only the first 3 data points of sample 7556 ([Fe] < 0.42 nM) gave a ligand concentration of 0.78 nM (originally 1.47 nM for the entire data range) with a value for log $K'_{Fe'L}$ of 11.4, compared to 11.1 for the entire titration. The difference suggests that perhaps a second ligand is present in this water, but the difference is small.

Two model ligands (Suwannee River humic acid and a siderophore (DFB)) were added to UV-digested seawater (UV-SW). Ligand concentrations and stability constants were determined and are shown in Table 2.4.

2.4. Discussion

2.4.1. Changes to the CSV method and effects

The method for the chemical speciation of Fe in seawater using CSV with SA has been updated, resulting in a better understanding of the reaction mechanism, improved sensitivity, stable response and calibration over a large concentration range of SA. The mechanism of the electrochemical reaction has now been elucidated: the method is subject to a catalytic reaction in which the reduction product (Fe^{II}), which is produced from Fe^{III}-SA, is re-oxidised during the scan by DO. The sensitivity is therefore maximised by ensuring that the water is saturated with air, and can be improved by bubbling with air if it is undersaturated, or by adding H_2O_2. Use of H_2O_2 could lead to oxidation of natural ligands, so this is not recommended. Similarly the sensitivity would be enhanced by purging and blanketing with a gas mixture with a higher partial pressure of O_2, but we found there to be no need as the sensitivity of the method is sufficient using air-oxygen. The good reproducibility with repeat scans (without the previously observed decrease in the peak height (Rue and Bruland, 1995)) using an air-blanketed solution has as major advantages that repeat scans can be carried out without solution renewal and the sensitivity calibrated by the standard addition method in the cell. This much facilitates the speciation procedure and the method to determine dissolved Fe.

The main improvement in the method is the use of air blanketing, and air purging if necessary, which was found to improve the sensitivity by a factor of 15 over that in a non-purged but N_2-blanketed cell (first scan in Fig. 2.1). The sensitivity of the updated method for the determination of dissolved Fe is much better than before, resulting in a limit of detection of 24-30 pM Fe using a 180 s adsorption time in air-equilibrated seawater (from 3xSD of separate determinations of Fe in SAFe-S reference seawater, Table 2.4). This limit can be lowered to (8-10) pM Fe by extending the adsorption time to 9 min.

2.4.2. Possible adsorption of Fe-SA on waste mercury drops

If the amount of Fe-SA that adsorbs on a mercury drop during a measurement is similar to that of Fe-catechol complexes (~10^{-10} mol cm^{-2}) (Van Den Berg and Huang, 1984a), this would amount to at most ~3 pmol at electrode saturation (for a large mercury drop of 3

mm^2), equivalent to 0.3 nM Fe in a 10 mL cell. A relatively high Fe concentration, or a long deposition time, would be required to achieve such high density, well outside the linear range. The Fe is returned to solution during the scan but could conceivably adsorb again on waste mercury and account for some or all of the decrease seen before amounting to a few % of the peak height per waste drop (Rue and Bruland, 1995).

Our experiment where dispensing 50 mercury drops had no effect on the peak height for Fe in subsequent measurements suggests that adsorption on waste mercury was negligible in our system. This was confirmed by a stable response even when measurements were continued over 16 h. The amount of mercury in the cell at the end of this experiment was equivalent to 446 drops, the volume of which is equivalent to ~22 drops of the large variety as used in other systems (Buck et al., 2012). The conclusion of these experiments is that adsorption on waste mercury is negligible at this level of Fe and it is unlikely that there is adsorption on mercury also in systems with a large mercury drop, though the relative effect would be magnified at lower [Fe]. A solution to this problem apparently affecting some systems would therefore be to choose the smallest mercury drop setting.

An alternative explanation for decreasing peaks in systems without an air blanket might be DO removal due its reduction at the electrode during the deposition step and scan. The current during the deposition step (at 0 V) on our system was -0.2 µA, which over 120 s is equivalent to 2.4 x 10^{-5} coulombs, which is equivalent to a reduction of 2.5 x 10^{-10} moles of DO over 120 s. The concentration of DO (~250 µM) is equivalent to 2.5 x 10^{-6} moles in 10 mL, which means a decrease in DO of ~0.01% for each measurement, which is negligible even if this DO would not be replenished without air-blanket. The effect would be larger at a longer deposition time and with the larger mercury drop electrodes used in some laboratories (Buck et al., 2012). However, this effect does not account for the much larger decrease in the Fe-SA peak seen before.

2.4.3. Calibration of $K'_{Fe'SA}$ and $B'_{Fe'SA2}$ with and without competition with EDTA

The speciation of Fe^{III} with SA is complicated by the formation of mixed species with OH: FeOHSA (Keeney et al., 1984). This species is included here for convenience in the 1:1 Fe-SA species, but it is not specified further. Effects of competition for SA by H^+, Ca^{2+} and

Mg^{2+} and ionic strength effects are also not specified and are part of the conditional stability constants for Fe with SA as they are for Cu (Campos and van den Berg, 1994).

The value of $\alpha_{Fe\text{-}SA}$ was calibrated by competition against EDTA at [SA] between 1 and 40 µM, and used to obtain values for $K'_{Fe'SA}$ and $B'_{Fe'SA2}$. The data fit as a function of [EDTA] was found to be insensitive for the value for $B'_{Fe'SA2}$ which is caused by the overall α-coefficient occurring above and below the division (Eqn 13). The fit of the same data as function of [SA] (Eqn. 14) was found to be sensitive to both $K'_{Fe'SA}$ and $B'_{Fe'SA2}$, giving a similar value for $K'_{Fe'SA}$ but a larger value for $B'_{Fe'SA2}$ with a smaller standard deviation (Table 2.2). The diagrams (Fig. 2.6A) show that Eqn. 14 describes the data well.

The data fit without EDTA involved fitting 3 parameters ($K'_{Fe'SA}$, $B'_{Fe'SA2}$ and i_{pmax}) to Eqn. 15, whereas only 2 parameters are fitted in presence of EDTA according equation 13. The number of data points was increased to 18 by extending the range of SA concentrations that were tested without EDTA, compared to 8 data points for the titrations with EDTA. The data fit for 0 µM EDTA (Fig. 2.6A) gave values for $K'_{Fe'SA}$ and $B'_{Fe'SA2}$ that matched the values in the presence of EDTA (Table 2.2). This means that the response for Fe as a function of [SA] without EDTA (Fig. 2.2) can be used for independent calibration of the stability constants (independent of an organic competing ligand). The normalised response for Fe to additions of SA between 1 and 100 µM shows good agreement for various concentrations of Fe in seawater (freshly UV-digested): the relative response was the same for 1, 3 and 5 nM Fe until 5 µM SA, with minor divergence at higher [Fe], possibly due to partial precipitation of inorganic Fe during the experiment. The SA titrations at 1 and 3 nM Fe were carried out by SA additions to the voltammetric cell, with only brief equilibration (5 min after each SA addition), whereas for 5 nM Fe the calibration were carried out with overnight equilibration for each point as part of the calibrations against EDTA. The stability constants, fitted using Eqn. 15, were close to those obtained by competition against EDTA (Table 2.2) but with a narrower standard deviation: $\log K'_{Fe'SA} = 6.52 \pm 0.01$ and $\log B'_{Fe'SA2} = 10.72 \pm 0.03$.

The excellent agreement between the calibrations of the complex stability in the presence and absence of EDTA indicates that the values for α_{Fe} and α_{FeEDTA} in Eqn. 15 are apparently correctly modelled and are internally consistent. The difference is greatest (0.13 log units) for $\log B'_{Fe'SA2}$, which is of significance at SA concentrations > 5 µM. We recommend that the values obtained without EDTA are adopted as these are independent

from any errors in the modelling of the speciation of EDTA, and are only affected by errors in $\alpha_{Fe} = 10^{10}$, which cannot be avoided as it is part of the equation with or without EDTA.

The data fitting (Fig. 2.6A) is consistent with a model in which the FeSA species adsorbs on the electrode, whereas $FeSA_2$ does not adsorb. This explains the maximum in sensitivity for the detection of inorganic Fe at 5 µM SA (Fig. 2.1) and it also explains the decrease at higher [SA]. Using the values for the stability constants it was calculated that $FeSA_2$ becomes significant at [SA] > 4.4 µM, which is close to the experimental value of 5 µM SA (Fig. 2.2) where the peak height is greatest.

An interesting finding is that, whilst the maximum response (X in Fig. 2.6A) is attained at 5 µM SA without EDTA, this maximum shifts to a higher concentration of SA in the presence of EDTA: the maximum is located at 20 µM SA for 1 µM EDTA, and at 30 µM SA at 3 µM EDTA. Competition by natural complexing matter is a possible reason why previous work(Rue and Bruland, 1995) found a maximum response at a much higher [SA] (27.5 µM) than found here (5 µM SA) suggesting that their seawater was not organic free. On the other hand a small pH difference may have played a role.

The calibration of the stability constants is valid for 1 µM < [SA] < 100 µM, which is equivalent to values for $\alpha_{Fe\text{-}SA}$ between 3.4 and 856 (Table 2.3). Taking into account poor sensitivity at 1 and 100 µM SA, the detection window for Fe speciation can realistically be varied between 6 and 300, or about two orders of magnitude. Best sensitivity is obtained at 5 µM SA, in spite of a larger peak height in early points of a titration with Fe at a higher concentration of SA up to ~25 µM SA. Complexing ligand titrations at 5 µM SA will show better differentiation between inorganic Fe and organically complexed Fe than at a higher concentration of SA. On the other hand, it will be interesting to study the effect of variation in the detection window. This may shed light on whether more than one complexing ligand is present in seawater samples.

2.4.4. Comparison of the new values of $K'_{Fe'SA}$ and $\alpha_{Fe'SA}$ to previous calibrations and implications.

Values for $\alpha_{Fe'\text{-}SA}$ were calculated for the SA concentrations used in these experiments and are shown in Table 2.3. At 27.5 µM SA (the SA concentration recommended previously

(Rue and Bruland, 1995)) $\alpha_{Fe'\text{-}SA}$ = 131, a little greater than that ($\alpha_{Fe'\text{-}SA}$ = 73) found previously (Rue and Bruland, 1995). At 25 µM SA $\alpha_{Fe'\text{-}SA}$ = 116, greater than the value (79) from (Buck et al., 2007). These differences affect $K'_{Fe'L}$ values, not ligand concentrations. K' values are normally presented on a log-scale when the difference between the new and old calibrations is equivalent to between 0.17 and 0.25 log units. The previous calibrations (Buck et al., 2007; Rue and Bruland, 1995) therefore agree reasonably with the new one at the same concentration of SA (25 or 27.5 µM).

Table 2.3. Comparison of the overall α-coefficient for Fe with SA ($\alpha_{Fe\text{-}SA}$) calculated using the constants from this work, with values determined in previous work.

[SA]	**Calculated values for $\alpha_{Fe'SA}$**	**Previous work**
2 µM SA	6.8	
5 µM SA	17.9	
25 µM SA	116	79 (using log $B_{Fe'SA2}$=11.1) (Buck et al., 2007)
27.5 µM SA	131	73 (Rue and Bruland, 1995)
50 µM SA	297	
100 µM SA	856	

The previous calibrations cannot be extended to different concentrations of SA as they were calibrated at a single concentration of SA (25 µM (Rue and Bruland, 1995) or 27.5 µM SA (Buck et al., 2007)). Calibration at a single concentration of SA is of use to get a value for the overall $\alpha_{Fe'\text{-}SA}$ but not for $\alpha_{Fe'SA}$ and $\alpha_{Fe'SA2}$. Without this information it is not possible to determine which type of complex, FeSA or $FeSA_2$, occurs in solution. Our data fitting showed that either constant, $K'_{Fe'SA}$ or $B'_{Fe'SA2}$, but not both, could be fitted to the voltammetric response as a function of [EDTA] for a given concentration of SA. Differences became apparent only when the concentration of SA was varied and then the correct fits were obtained for $K'_{Fe'SA}$ and $B'_{Fe'SA2}$ (Fig. 2.6 and Table 2.2).

The new conditions that are recommended here (air-blanketing and if necessary air-purging if samples are not already in equilibrium with air, a lower concentration of SA, and different stability constants to calculate $\alpha_{Fe'\text{-}SA}$), give better sensitivity than before, and stable conditions also when samples derive from anoxic waters. An additional effect is that the

detection window is moved from 116 to 18. This means that complexation of Fe by ligands in seawater causes greater suppression of the CSV response, which may make for higher resolution. The peak height may be very low if Fe is complexed by very strong ligands such as siderophores but this is offset to some extent by better sensitivity.

A further outcome of this work is that, using the calibrated values for $K'_{Fe'SA}$ and $B'_{Fe'SA2}$ it is now possible to vary the detection window at which Fe speciation is determined by varying the concentration of SA between 1 and 100 μM, as the value for $\alpha_{Fe'\text{-}SA}$ can now be calculated correctly. However, the possibility to detect stronger bound Fe at higher [SA] is lowered by the decreasing sensitivity at [SA]>5 μM.

2.4.5. Reaction kinetics

The dissociation rate of the complex of Fe^{III} with ligands, L, in seawater was determined to be quite slow with a value for the rate coefficient of k_{FeL} = 0.00133 ± 0.0002 s^{-1}. The half-life of this reaction is 8.7 minutes. This means that a reaction time of >1 h is required to reach 99% of the equilibrium condition between FeL and added SA. Interestingly, recent experiments using SA (Buck et al., 2007) found that the response stabilised after 1.5 h, which is similar to that calculated here. Other work using TAC has found that an even longer reaction time of 6 h is required to reach equilibrium for the exchange of iron between natural ligands and TAC (Croot and Heller, 2012) possibly suggesting that TAC does not make use of an associative mechanism whilst SA does. Different species may have varying dissociation rates, and our work confirms that a long equilibration time is of the essence. The reaction time to reach 99% of the equilibrium condition between SA and Fe complexed with L is significantly (about 9x) greater than that (10 -15 min) recommended in the previous work using SA (Buck et al., 2007; Rue and Bruland, 1995). This previous work based their recommendation on the observed rate at which added Fe is bound by L and subsequently bound with SA. Our measurement shows that this is not valid for any Fe already complexed with L at the beginning of the titration, which affects low Fe concentrations < the concentration of the natural ligand, whereas any Fe in excess would tend to react much more quickly. The effect of using an equilibration time that is too short would cause an underestimation of the Fe that is bound by the added SA, and therefore an overestimate of

the complex stability for low Fe levels. Therefore, use of a short equilibration time could lead to the apparent presence of a second ligand that binds Fe strongly, at low Fe levels. This would confirm recent work using radiotracers that showed that the larger pool of weaker ligands can react more quickly (Croot and Heller, 2012).

2.4.6. Complex stability of DFB and humic substances

An equilibration time of 4 h had been allowed after the Fe addition, followed by overnight equilibration after the addition of SA, to ensure that equilibrium was attained for this complexing ligand. The concentration of DFB (3 nM based on its molecular weight) was reflected in an Fe-binding ligand concentration of ~2.6 nM. The complex stability was $\log K'_{Fe'DFB}$ = ~12.2 (Table 2.4), which compares to values of >13 (Rue and Bruland, 1995) (determined by CSV using the early SA method), 11.6 (Witter et al., 2000) (determined by CSV using NN as ligand) and 11.8 (Maldonado et al., 2005) (determined by CSV using TAC as ligand). Much greater values have also been found: for instance $\log K'_{Fe'DFB}$ ~ 16 (Hudson et al., 1992) and too strong for determination using TAC (Croot and Johansson, 2000). The value determined here was at the edge of the detection window: $\alpha_{Fe'SA}$ = 17.9 at 5 µM SA, whereas $\alpha_{Fe'DFB}$ =~10^3 at 3 nM DFB, i.e. 55 times greater (at a factor of 100 about 1% of the Fe occurs as FeSA, which could be considered to be near to the limit of detection (van den Berg and Donat, 1992)). The first 4 points of the titration with Fe (up to 0.5 nM Fe) were below the limit of detection due to the masking by DFB. The complex formation rate of DFB with Fe^{III} in seawater is much faster than with EDTA (Hudson et al., 1992) suggesting that our measurement should have reached equilibrium, in spite of the high complex stability. The good agreement between the ligand concentration found by titration and from the molecular weight shows that equilibrium had indeed been attained.

The Fe-binding ligand concentration for 0.2 mg L^{-1} HA was 6.1 nM (Table 2.4), equivalent to a binding capacity of ~31 nmol mg^{-1} HA. This is in very good agreement with that (32 nmol mg^{-1} SRHA) found previously from the increase of the Fe-HA peak added to seawater (Laglera and van den Berg, 2009). We found here using CSV that $\log K'_{Fe'HA}$ = 11.6 $\pm$ 0.1, somewhat larger than a value of 11.1 found by direct measurement of the peak height for FeHA with competition against EDTA (Laglera and van den Berg, 2009). The ligand

concentration found for the DFB (2.59 – 2.64 nM) approximately matched that expected for 1:1 binding between Fe and DFB.

Table 2.4. Concentrations of Fe in reference seawater and results of complexing ligand titrations. The Celtic Sea sample represents seawater from several depths, filtered and then stored in a 50 L container; it has a salinity of 35.0. The Geotraces samples had been stored frozen at natural pH. Standard deviations in the ligand concentrations were calculated from data fitting. The purity of the DFB was ≥92.5%. The concentration of Fe in the UV-seawater used for the DFB and HA titrations was 0.45 ± 0.05 nM.

Fe in reference seawater	**Fe found (nM)**	**Reference value (nmol/kg)**	**Log $K'_{Fe'L}$**
SAFe S	0.092 ± 0.008	0.090 ± 0.007	
SAFe D1	0.69 ± 0.05	0.67 ± 0.07	
SAFe D2	0.93 ± 0.03	0.90 ± 0.02	
Seawater samples	**[Fe_d] (nM)**	**C_L (nM)**	**Log $K'_{Fe'L}$**
Celtic	0.66 ± 0.04	2.53 ± 0.02	11.5 ± 0.2
Geotraces 8047	0.12 ± 0.01	1.49 ± 0.17	11.9 ± 0.1
Geotraces 7556	0.12 ± 0.01	1.47 ± 0.01	11.1 ± 0.01
Potential ligands added to UV-SW		**C_L (nM)**	**Log $K'_{Fe'L}$**
DFB (3 nM)		2.59 ± 0.41	12.17 ± 0.26
DFB (3 nM)		2.64 ± 0.45	12.15 ± 0.27
HA (0.2 mg L^{-1})		6.1 ± 0.2	11.6 ± 0.1
HA (0.2 mg L^{-1})		6.1 ± 0.2	11.7 ± 0.1

2.4.7. Iron speciation in Atlantic samples

Titrations of Atlantic samples (GEOTRACES and Celtic Sea) showed the presence of 1.47 to 2.53 nM of ligands with values for log $K'_{Fe'L}$ from 11.1 to 11.9 (Table 2.4), overlapping with the complex stability of SR-HA (log $K'_{Fe'HA}$=11.6) and less than that for DFB (log $K'_{Fe'DFB}$=12.2). This preliminary comparison of ligands suggests that the bulk of the natural ligands do not include siderophores of the type of DFB. Siderophores have been found previously in surface ocean waters at levels <20 pM (Velasquez et al., 2011); such low picomolar levels of siderophores would be hard to detect by this method as their concentration is much less than that of iron.

Acknowledgements

We are grateful for two water samples that were collected using trace metal clean techniques by Geo Smith, from the laboratory of Ken Bruland (UCSC) during a GEOTRACES cruise, and used here to test the method. A large (50 L) water sample was obtained from the Celtic Sea by Hannah Whitby (Ocean Sciences, Liverpool) during a cruise with the Discovery in 2012 (PI Jonathan Sharples, Liverpool University). The research of Mahmoud Abualhajia was funded by the University of Jordan. We used software of Dario Omanovic (Zagreb, Croatia) for comparative data fitting of the ligand titrations. We acknowledge comments from Peter Croot and anonymous referees that were beneficial to this paper.

2.5. References

Aldrich, A.P. and van den Berg, C.M.G., 1998. Determination of iron and its redox speciation in seawater using catalytic cathodic stripping voltammetry. Electroanalysis, 10: 369-373.

Arena, G., Musumeci, S., Purrello, R. and Sammartano, S., 1983. Calcium-EDTA and magnesium-EDTA complexes - stability constants and their dependence on temperature and ionic strength. Thermochimica Acta, 61(1-2): 129-138.

Batchelli, S., Muller, F.L.L., Chang, K.C. and Lee, C.L., 2010. Evidence for Strong but Dynamic Iron-Humic Colloidal Associations in Humic-Rich Coastal Waters. Environmental Science & Technology, 44(22): 8485-8490.

Behrenfeld, M.J. and Kolber, Z.S., 1999. Widespread iron limitation of phytoplankton in the South Pacific Ocean. Science, 283: 840-843.

Buck, K.N. and Bruland, K.W., 2007. The physicochemical speciation of dissolved iron in the Bering Sea, Alaska. Limnology and Oceanography, 52(5): 1800-1808.

Buck, K.N., Lohan, M.C., Berger, C.J.M. and Bruland, K.W., 2007. Dissolved iron speciation in two distinct river plumes and an estuary: Implications for riverine iron supply. Limnology and Oceanography, 52(2): 843-855.

Buck, K.N. et al., 2012. The organic complexation of iron and copper: an intercomparison of competitive ligand exchange-adsorptive cathodic stripping voltammetry (CLE-ACSV) techniques. Limnology and Oceanography-Methods, 10: 496-515.

Bundy, R.M., Biller, D.V., Buck, K.N., Bruland, K.W. and Barbeau, K.A., 2014. Distinct pools of dissolved iron-binding ligands in the surface and benthic boundary layer of the California Current. Limnology and Oceanography, 59(3): 769-787.

Burger, K. and Egyed, I., 1965. Some theoretical and practical problems in the use of organic reagents in chemical analysis—V: Effect of electrophilic and nucleophilic substituents on the stability of salicylaldoxime complexes of transition metals. Journal of Inorganic and Nuclear Chemistry, 27(11): 2361-2370.

Burger, K., Ruff, F., Ruff, I. and Egyed, I., 1965. Some theoretical and practical problems in the use of organic reagents in chemical analysis. 6. Hydrogen bridges and donor pi bonds in salicylaldoxime complexes of transition metals. Acta Chimica Academiae Scientarium Hungaricae, 46(1): 1-&.

Byrne, R.H. and Thompson, S.W., 1997. Ferric borate formation in aqueous solution. Journal of Solution Chemistry, 26(7): 729-734.

Campos, M.L.A.M. and van den Berg, C.M.G., 1994. Determination of copper complexation in sea water by cathodic stripping voltammetry and ligand competition with salicylaldoxime. Analytica Chimica Acta, 284: 481-496.

Cosovic, B., Zutic, V. and Kozarac, Z., 1977. Surface-active substances in the sea surface microlayer by electrochemical methods. Croatica Chemica Acta, 50: 229-241.

Croot, P.L. and Heller, M.I., 2012. The importance of kinetics and redox in the biogeochemical cycling of iron in the surface ocean. Frontiers in microbiology, 3.

Croot, P.L. and Johansson, M., 2000. Determination of iron speciation by cathodic stripping voltammetry in seawater using the competing ligand 2-(2-thiazolylazo)-p-cresol (TAC). Electroanalysis, 12(8): 565-576.

Croot, P.L., Passow, U., Assmy, P., Jansen, S. and Strass, V.H., 2007. Surface active substances in the upper water column during a Southern Ocean Iron Fertilization Experiment (EIFEX). Geophysical Research Letters, 34(3).

Egneus, B., 1972. Investigations of dioximes and their metal complexes: A survey of the literature since 1963. Talanta, 19(11): 1387-1419.

Florence, T.M., 1984. The production of hydroxyl radical from hydrogen-peroxide. Journal of Inorganic Biochemistry, 22: 221-230.

Gledhill, M. and van den Berg, C.M.G., 1994. Determination of complexation of iron(III) with natural organic complexing ligands in seawater using cathodic stripping voltammetry. Marine Chemistry, 47(1 SU -): 41-54.

Howe, D.E. and Mellon, M.G., 1940. Colorimetric determination of iron with salicylaldoxime. Industrial and Engineering Chemistry, 12: 448-450.

Hudson, R.J.M., Covault, D.T. and Morel, F.M.M., 1992. Investigations of iron coordination and redox reactions in seawater using Fe-59 radiometry and ion-pair solvent-extraction of amphiphilic iron complexes. Marine Chemistry, 38(3-4): 209-235.

Keeney, M.E., Osseoasare, K. and Woode, K.A., 1984. Transition-metal hydroxyoxime complexes. Coordination Chemistry Reviews, 59(SEP): 141-201.

Kolthoff, I.M. and Parry, E.P., 1951. Catalytic Polarographic Waves of Hydrogen Peroxide .1. The Kinetic Wave for the Ferric Iron Hydrogen Peroxide System. Journal of the American Chemical Society, 73(8): 3718-3723.

Kuma, K., Nishioka, J. and Matsunaga, K., 1996. Controls on iron(III) hydroxide solubility in seawater: The influence of pH and natural organic chelators. Limnology and Oceanography, 41(3): 396-407.

Laglera, L.M., Battaglia, G. and van den Berg, C.M.G., 2007. Determination of humic substances in natural waters by cathodic stripping voltammetry of their complexes with iron. Analytica Chimica Acta, 599(1): 58-66.

Laglera, L.M., Battaglia, G. and van den Berg, C.M.G., 2011. Effect of humic substances on the iron speciation in natural waters by CLE/CSV. Marine Chemistry, 127(1-4): 134-143.

Laglera, L.M. and van den Berg, C.M.G., 2007. Wavelength Dependence of the Photochemical Reduction of Iron in Arctic Seawater. Environmental Science & Technology, 41(7): 2296-2302.

Laglera, L.M. and van den Berg, C.M.G., 2009. Evidence for geochemical control of iron by humic substances in seawater. Limnology and Oceanography, 54(2): 610-619.

Landing, W.M. and Westerlund, S., 1988. The solution chemistry of iron(II) in Framvaren fjord. Marine Chemistry, 23: 329-343.

Liu, R.M., Liu, D.J. and Sun, A.Y., 1992. Studies on the application of photochemical reactions in a flow injection system. Part 2. Simultaneous determination of iron(II) and iron(III) based on the photoreduction of the iron(III)-phenanthroline complex. Analyst, 117: 1767-1770.

Liu, X. and Millero, F.J., 1999. The solubility of iron hydroxide in sodium chloride solutions. Geochimica et Cosmochimica Acta, 63(19-20): 3487-3497.

Liu, X. and Millero, F.J., 2002. The solubility of iron in seawater. Marine Chemistry, 77(1): 43-54.

Maldonado, M.T., Strzepek, R.F., Sander, S. and Boyd, P.W., 2005. Acquisition of iron bound to strong organic complexes, with different Fe binding groups and photochemical reactivities, by

plankton communities in Fe-limited subantarctic waters. Global Biogeochemical Cycles, 19(4).

Martell, A.E. and Smith, R.W., 1974. Critical stability constants. Volume 1: Amino acids. Plenum Press, New York.

Martin, J.H. and Gordon, R.M., 1988. Northeast Pacific iron distributions in relation to phytoplankton productivity. Deep-Sea Research, 35: 177-196.

Martin, J.H., Gordon, R.M. and Fitzwater, S.E., 1991. THE CASE FOR IRON. Limnology and Oceanography, 36(8): 1793-1802.

Miller, W.L. and Kester, D., 1994. Photochemical iron reduction and iron bioavailability in seawater. Journal of Marine Research, 52(2): 325-343.

Millero, F.J., 1998. Solubility of Fe(III) in seawater. Earth and Planetary Science Letters, 154(1-4): 323-329.

Millero, F.J. and Sotolongo, S., 1989. The oxidation of Fe(II) with H2O2 in seawater. Geochimica et Cosmochimica Acta, 53: 1867-1873.

Mohanty, R.K., Das, A.K. and Das, M., 1994. Study on kinetics and mechanism of reaction of iron(III) with salicylaldoxime and ortho-hydroxyacetophenoneoxime in HClO4-NaClO4 media. Indian Journal of Chemistry Section a-Inorganic Bio-Inorganic Physical Theoretical & Analytical Chemistry, 33(10): 932-936.

Moore, J.K., Doney, S.C., Glover, D.M. and Fung, I.Y., 2002. Iron cycling and nutrient-limitation patterns in surface waters of the World Ocean. Deep-Sea Research Part Ii-Topical Studies in Oceanography, 49(1-3): 463-507.

Nuester, J. and van den Berg, C.M.G., 2005. Determination of metal speciation by reverse titrations. Analytical Chemistry, 77(1): 11-19.

Obata, H. and van den Berg, C.M.G., 2001. Determination of picomolar levels of iron in seawater using catalytic cathodic stripping voltammetry. Analytical Chemistry, 73(11): 2522-2528.

Ramette, R.W., Culberson, C.H. and Bates, R.G., 1977. Acid-base properties of tris(hydroxymethyl) aminomethane (tris) buffers in seawater from 5 to 40 C. Analytical Chemistry, 49: 867-870.

Reddy, P.B.S. and Rao, S.B., 1979. Extraction photometric-determination of iron(III) with salicylaldoxime. Current Science, 48(7): 298-299.

Rue, E.L. and Bruland, K.W., 1995. Complexation of iron(III) by natural organic-ligands in the central north pacific as determined by a new competitive ligand equilibration adsorptive cathodic stripping voltammetric method. Marine Chemistry, 50(1-4): 117-138.

Smith, A.G., Tasker, P.A. and White, D.J., 2003. The structures of phenolic oximes and their complexes. Coordination Chemistry Reviews, 241(1): 61-85.

Statham, P.J., Jacobson, Y. and van den Berg, C.M.G., 2012. The measurement of organically complexed Fe-II in natural waters using competitive ligand reverse titration. Analytica Chimica Acta, 743: 111-116.

Tshuma, J. et al., 2007. Spectrophotometric determination of acidity constants of salicylaldoxime in aqueous solution at 25 degrees C and ionic strength of 0.5 M controlled with NaCl. Spectrochimica Acta Part a-Molecular and Biomolecular Spectroscopy, 66(4-5): 879-883.

Turoczy, N.J. and Sherwood, J.E., 1997. Modification of the van den Berg/Ruzic method for the investigation of complexation parameters of natural waters. Analytica Chimica Acta, 354(1-3): 15-21.

Van Den Berg, C.M., 2014. UV digestion apparatus. http://pcwww.liv.ac.uk/~sn35/Site/UV_digestion_apparatus.html.

van den Berg, C.M.G., 1984. Speciation of boron with Cu2+, Zn2+, Cd2+ and Pb2+ in 0.7 M KNO3 and in sea-water. Geochimica et Cosmochimica Acta, 48(12): 2613-2617.

van den Berg, C.M.G., 1985. Determination of the zinc complexing capacity in seawater by cathodic stripping voltammetry of zinc APDC complex-ions. Marine Chemistry, 16(2): 121-130.

van den Berg, C.M.G., 1995. Evidence for organic complexation of iron in seawater. Marine Chemistry, 50(1-4): 139-157.

van den Berg, C.M.G., 2006. Chemical speciation of iron in seawater by cathodic stripping voltammetry with dihydroxynaphthalene. Analytical Chemistry, 78(1): 156-163.

van den Berg, C.M.G. and Donat, J.R., 1992. Determination and data evaluation of copper complexation by organic ligands in sea water using cathodic stripping voltammetry at varying detection windows. Analytica Chimica Acta, 257: 281-291.

Van Den Berg, C.M.G. and Huang, Z.Q., 1984a. Determination of iron in seawater using cathodic stripping voltammetryu preceded by adsorptive collection with the hanging mercury drop electrode. Journal of Electroanalytical Chemistry, 177(1-2): 269-280.

van den Berg, C.M.G. and Huang, Z.Q., 1984b. Determination of uranium (VI) in sea water by cathodic stripping voltammetry of complexes with catechol. Analytica Chimica Acta, 164: 209-222.

Velasquez, I. et al., 2011. Detection of hydroxamate siderophores in coastal and Sub-Antarctic waters off the South Eastern Coast of New Zealand. Marine Chemistry, 126(1-4): 97-107.

Wedepohl, K.H., 1995. The composition of the continental crust. Geochimica et Cosmochimica Acta, 59: 1217-1232.

Witter, A.E., Hutchins, D.A., Butler, A. and Luther, G.W., 2000. Determination of conditional stability constants and kinetic constants for strong model Fe-binding ligands in seawater. Marine Chemistry, 69(1-2): 1-17.

Wu, J. and Luther III, G.W., 1995. Complexation of Fe(III) by natural organic ligands in the Northwest Atlantic Ocean by a competitive ligand equilibration method and a kinetic approach. Marine Chemistry, 50: 159-177.

Yokoi, K. and van den Berg, C.M.G., 1992. The determination of iron in seawater using catalytic cathodic stripping voltammetry. Electroanalysis, 4: 65-69.

3

Chapter 3
Competition between copper and iron for humic ligands in estuarine waters

This chapter is adapted from: Abualhaija, M.M., Whitby, H. and van den Berg, C.M.G., 2015. Competition between copper and iron for humic ligands in estuarine waters. Marine Chemistry, 172(0): 46-56.

3. COMPETITION BETWEEN COPPER AND IRON FOR HUMIC LIGANDS IN ESTUARINE WATERS

Abstract

We determined the concentration of iron- and copper-binding humic substances (Fe-HS and Cu-HS) in estuarine waters along with the concentrations of iron- and copper-complexing ligands (L_{Fe} and L_{Cu}). Suwannee River humic acid (SRHA) was used as a humic standard. The complex stability of Fe with salicylaldoxime (SA) was calibrated for salinities between 4 and 35 and fitted to linear equations to enable Fe speciation in estuarine waters: $K'_{Fe'SA} = -2.98 \times 10^4 \times Sal + 4.60 \times 10^6$ and $\log B'_{Fe'SA2} = -1.41 \times \log Sal + 12.85$. The concentration of Cu-HS in waters from the Mersey estuary and Liverpool bay was less than the overall ligand concentration ($[Cu\text{-}HS]/L_{Cu} = 0.69 \pm 0.05$) suggesting that a second ligand was of importance to Cu complexation. The concentration of Fe-HS was virtually equal to the total ligand concentration for Fe ($[Fe\text{-}HS]/L_{Fe} = 0.95 \pm 0.16$) confirming that humics are responsible for Fe complexation in these waters. The concentration of HS determined from Fe-HS was within 4 % of that found from Cu-HS, confirming that the same substance is detected. The average complex stability ($\log K'_{Fe'L}$) was 11.2 ± 0.1, the same as for $\log K'_{Fe'\text{-}SRHA}$. Copper additions demonstrated competition between Cu and Fe for the HS-type ligands. This competition was used to determine the complex stability for the Cu-HS species, giving a value of 10.6 ± 0.4 for $\log K'_{Cu'HS}$, which is nearly a unit less than the complex stability, $\log K'_{Cu'L} = 11.4 \pm 0.2$, found for all Cu ligands (the HS and the unknown ligand combined). The competition affects the complexation of both metals with HS-type ligands. Extrapolation of the concentration of Fe-HS to an ocean salinity of 35 gives a residual level of 0.05 mg HS L^{-1}, equivalent to an Fe-binding ligand concentration of 1.5 nM. If HS-type ligands are confirmed to be ubiquitous in coastal or ocean waters, competition reactions could be of importance to the bioavailability of both metals to marine microorganisms.

3.1. Introduction

Iron (Fe) and copper (Cu) occur complexed with organic matter in waters from estuarine and oceanic origin (Buck et al., 2007; Campos and van den Berg, 1994; Gledhill and van den Berg, 1994; Muller and Batchelli, 2013; Rue and Bruland, 1995; Sander et al., 2014; van den Berg, 1995) in spite of competition by the major cations that occur at concentrations typically 10^6 times greater. Metal complexation is important because it affects the metal geochemistry and bioavailability. The main removal pathway of freshly added metals in estuarine and coastal waters is by scavenging with suspended particulate matter (SPM) (Achterberg et al., 1999; Ellwood et al., 2008; Li et al., 1984), in addition to biological uptake in ocean waters (Balistrieri et al., 1981). Dissolved complexation reactions are in competition with the removal processes (Turner et al., 1998; van den Berg et al., 1987). Complexation also affects availability to microorganisms leading to feedback reactions, as exemplified by releases of exopolysaccharides from marine bacteria (Hassler et al., 2011), and other ligands (Eldridge et al., 2004; Weaver et al., 2003). Importantly, the solubility of Fe is enhanced by organic complexation (Schlosser and Croot, 2009) causing the element to remain in solution allowing more time for uptake by microorganisms.

Copper (Cu) speciation in seawater is dominated by organic complexation (Bruland et al., 2000; Buck and Bruland, 2005; Kogut and Voelker, 2003). Thiols have been identified as one type of Cu-binding ligands (Dupont et al., 2004; Laglera and van den Berg, 2003; Le Gall and van den Berg, 1998) and humic substances (HS) are likely another ligand (Kogut and Voelker, 2001; Muller and Batchelli, 2013; Shank et al., 2004; Xue and Sigg, 1999). Cu-binding ligands (Skrabal et al., 1997) and thiols (Chapman et al., 2009) have been shown to emanate from pore-waters into shallow surface waters. Cu-HS species have recently been shown to occur in estuarine waters (Whitby and van den Berg, 2014).

The complex stability is a function of the stability constant (K'_{CuL}), which is conditional upon side-reactions of the ligand with competing cations, and the ligand concentration. Natural waters containing ligands of various sources (terrestrial, break down products of plant materials, and in-situ produced by microorganisms), contain a mixture of ligands that form strong as well as weak complexes, that can be crudely subdivided into ligand classes. Log K'_{CuL} values vary between ligand classes, typically ranging from log $K'_{Cu'L}$ = 8-10 for weak ligands (L2 type) (Donat et al., 1994; Moffett et al., 1990) to as high as log $K'_{Cu'L}$ = 15 for

strong ligands (L1 type) (Bundy et al., 2013) (these constants were converted to the Cu' scale using a value for $\alpha_{Cu'}$ of ~20 valid for pH 8 seawater (Whitby and van den Berg, 2014)). Suwannee River humic acid (SRHA) gives a log $K'_{Cu'SRHA}$ = 10.7 in seawater (Kogut and Voelker, 2001; Whitby and van den Berg, 2014). Estuarine waters have been reported to have ligands for Cu with a complex stability of log $K'_{Cu'L}$ ranging from 11-16 (Muller and Batchelli, 2013) encompassing that of HS but also several thiol compounds (Dryden et al., 2007).

The speciation of iron (Fe) is, like Cu, dominated by organic complexation and it tends to occur >99% complexed with organic matter in sea (Gledhill and van den Berg, 1994; Rue and Bruland, 1995; van den Berg, 1995) and estuarine waters (Batchelli et al., 2010; Rijkenberg et al., 2006). Siderophores (low-molecular weight, high-affinity Fe(III)-binding ligands secreted by bacteria) (Macrellis et al., 2001; Mawji et al., 2011; Velasquez et al., 2011) and humic substances (Laglera and van den Berg, 2009) have been reported as Fe-binding ligands. Certain natural ligands, such as domoic acid, are known to be complexed with both copper and iron in seawater (Rue and Bruland, 2001) suggesting that metal competition could play a role. It has been suggested that Fe uptake by Pseudo-nitzschia is regulated by both domoic acid and copper (Wells et al., 2005), which could possibly be explained by competition reactions.

Speciation measurement is generally by cathodic stripping voltammetry (CSV) making use of competition between an added ligand, which forms an electroactive complex, and natural complexing matter. Using this technique the concentration and complex stability of natural complexing ligands of Cu and Fe have been determined in estuarine (Buck et al., 2007; Gerringa et al., 2007), coastal (Buck and Bruland, 2005; Muller and Batchelli, 2013; Sander et al., 2014) and ocean waters (Buck et al., 2012; Rue and Bruland, 1995; van den Berg, 1995). Competition between the metals for ligands occurring in natural waters has not been demonstrated though competition has been shown between Fe, Cu (Whitby and van den Berg, 2014), Al and Co for complexation with Suwannee River humic substances (SRHA and SRFA) added to seawater (Yang and Van den Berg, 2009).

It is possible to determine specific ligands in seawater on the basis of the specific CSV response of their metal species. This has been used to identify Cu binding thiols (Al-Farawati and Van Den Berg, 2001; Le Gall and van den Berg, 1993), Cu and Fe binding humic substances (Laglera et al., 2007; Whitby and van den Berg, 2014), and various sulfur species

(Luther III and Ferdelman, 1993; Rozan et al., 2000).

Using the ligand competition method it has not been possible to investigate competition between metals for natural complexing ligands because the added competing ligand affects the speciation of all metals. Here we make use of the signal for specific ligands (humic substances present in the seawater) to investigate competition between Cu and Fe for these ligands in estuarine and coastal waters. Concentrations of copper and iron binding ligands were determined separately using ligand competition techniques and from the signal for Cu-HS and Fe-HS.

3.2. Experimental

3.2.1. Equipment

Voltammetric apparatus was a µAutolab-III potentiostat (Ecochemie, Netherlands) connected to a hanging mercury drop electrode (HMDE, Metrohm 663VA), the voltammetric system was computer-controlled using the GPES 4.9 software. The reference electrode was Ag/AgCl with a 3 M KCl salt bridge, and the counter electrode was a glassy carbon rod. The stirrer was a rotating PTFE rod. GPES software was used to control the instrument. Apparatus used for Cu detection used nitrogen for oxygen removal, whereas apparatus used for Fe and Fe-speciation was pressurised using air (Abualhaija and van den Berg, 2014) in order to ensure that the concentration of dissolved oxygen (DO) was constant during the measurements. The software was changed to discard 2 mercury drops (instead of 4) between scans. Water used for rinsing and dilution of reagents (MQ) was purified by reverse osmosis (Millipore) and deionisation (Milli-Q). Glass and PTFE voltammetric cells used for total metal determination were cleaned using 0.1 M HCl and rinsed with deionised water followed by UV-digested sample before measurements. Vessels used for titrations were MQ-rinsed about once a week but were not normally rinsed between titrations to minimise de-conditioning. pH measurements (Metrohm models 605 and 827) were calibrated against pH 7 and pH 4 standards on the NBS pH scale. The reference section of the combined pH electrode was filled with 3 M KCL. Total dissolved metal concentrations were determined by CSV after 1 h UV-digestion of acidified samples (20 µL 50% HCl (10 mL)$^{-1}$) either in 30-mL PTFE-capped quartz sample tubes using a 125-W UV system (fitted with a high-pressure

mercury vapour lamp) (Van Den Berg, 2014) or in the voltammetric cell with a horizontal UV lamp. pH neutralisation was by addition of ammonia and borate pH buffer. UV absorbance of dissolved humic matter was measured on a Jenway 7315 spectrophotometer set to 355 nm in polystyrene cells of 1 cm path length. Background correction was against UV seawater. The absorbance of each station was compared to a calibration curve of HA standards to quantify the HS in samples, similar to that used for chromophoric dissolved organic matter (CDOM) (Chanudet et al., 2006; Hong et al., 2005; Laglera et al., 2007).

3.2.2. Reagents

Cu and Fe standard solutions were atomic absorption spectrometry standard solutions (BDH SpectrosoL grade) diluted with MQ water; HCl was added to a pH of 2. Typically 20 mL was prepared of these solutions, which were stable and were replaced only when the level ran low. An aqueous stock solution containing 0.1 M salicylaldoxime (SA) was prepared in 0.1 M HCl. Reference humic and fulvic acid used for calibrations were Suwannee River HA (International Humic Substances Society (IHSS) Standard II 2S101H) and FA (IHSS standard II 2S101F), which were dissolved in MQ water to a concentration of 0.1 g L^{-1} and stored in the dark at 4 ◦C when not in use. 1 M sodium bicarbonate (Sigma Aldrich) in MQ water was diluted to 2 mM and used to dilute seawater to lower salinity. A pH buffer containing 1 M boric acid (Aristar grade) and 0.35 M ammonia (MOS grade, Fisher Scientific) was UV-irradiated for 45 min to remove organic contaminants. A bromate stock solution containing 0.4 M potassium bromate (Fisher Scientific) was used for the determination of Fe-binding HS. Contaminating metals were removed from the buffer and bromate solutions by overnight equilibration with 100 µM MnO_2 (van den Berg, 1982) and then filtered (0.2 µm inorganic membrane, Whatman); 100 µL of the buffer in 10 mL seawater gave a pH_{NBS} of 8.18.

All sample containers were cleaned in 3 steps: first by soaking for 1 week in 1 % detergent in warm MQ-water, followed by soaking for 1 week in 1 M HCl (Analar grade), and finally by soaking at least 1 week in 0.1 M HCl (Analar grade). Containers were then rinsed in MQ-water and stored partially filled with 0.01 M HCl (high-purity grade).

3.2.3. Sample collection and storage

Samples from the Mersey Estuary and Liverpool Bay (Irish Sea) were collected using a peristaltic pump. The water inlet tubing was held away from the vessel, the RV Marisa, (May 2013 and April 2014) and the water was used to first rinse (3 x) and then fill a 5-L high-density polyethylene (HDPE) container at each station. The suspended matter was allowed to settle overnight in the laboratory and the supernatant water was filtered through an in-line 0.2 µm filtration cartridge (Sartobran, Whatman) using a peristaltic pump, and stored in the dark at 4 ^{o}C in 0.5 L HDPE bottles.

3.2.4. Procedure to determine total dissolved copper (Cu) and iron (Fe)

Acidified (pH 2) sample aliquots were UV-digested (1 h) in a PTFE voltammetric cell with the lamp placed immediately above the sample in a PTFE housing separated by a sheet of quartz from the sample, prior to pH neutralization with ammonia and pH buffering using the borate/ammonia buffer. Fe and Cu were determined by CSV as optimised previously (Abualhaija and van den Berg, 2014; Campos and van den Berg, 1994). CSV conditions for Cu were a deposition potential of -0.15 V (30 s), using a 1-s potential-jump to -1.3 V to desorb any residual organic matter and Fe species, followed by 9 s equilibration at -0.15 V prior to the voltammetric scan to -0.7 V (differential-pulse (DP) mode, modulation time 40 ms, modulation amplitude 50 mV, step potential 5 mV, interval time 0.1 s) in the presence of 20 µM SA. CSV of Fe used the DP mode in the presence of 5 µM SA, with an adsorption potential of 0 V (60 s) followed by the scan to -1 V.

3.2.5. Procedures to determine copper- and iron-binding HS (Cu-HS and Fe-HS) using CSV

The concentration of Cu-HS was determined after addition of sufficient copper (usually 50 nM Cu) to saturate the HS followed by detection of the Cu-HS by CSV (Whitby and van den Berg, 2014). Calibration was by internal standard additions of SRHA. Low salinity samples with very high HS concentrations were diluted to 10 or 50 % in UV-SW to increase the linear range. The deposition potential was +0.05 V, with a deposition time between 10 and 60 s depending on the concentration of HS. The quiescence time was 9 s and scans were

initiated from 0 V and terminated at -0.75 V. The scanning parameters were differential-pulse (DP) mode, modulation time 40 ms, modulation amplitude 50 mV, step potential 5 mV and interval time 0.1 s. A background scan using a one-second deposition time was subtracted from the analytical scan to eliminate the peak for inorganic Cu adjacent to the Cu-HS peak (Whitby and van den Berg, 2014).

The concentration of Fe-HS was determined by CSV in the presence of bromate (Laglera et al., 2007). The voltammetric apparatus was air-pressurised as for the Fe determination, as the response for Fe-HS was not affected by the DO. Bromate (0.4 M final concentration) was added to improve the sensitivity for the Fe-HS. The concentration of Fe-HS was determined after addition of sufficient Fe (typically 50 nM) to saturate the HS followed by detection of the Fe-HS complexes by CSV. Calibration was by standard additions of SRHA. Samples with high Fe and humic concentrations (low salinity samples) were diluted with UV-SW 10 or 50 % to get the concentrations in the linear range. The deposition potential was 0 V, and the deposition time was between 20 and 120 s, depending on ambient dissolved Fe and Fe-binding humic concentrations.

3.2.6. Procedure to determine Cu and Fe complexing ligand concentrations

The concentration of Cu and Fe complexing ligands in the samples was determined in separate titrations with ligand competition against SA (Abualhaija and van den Berg, 2014; Campos and van den Berg, 1994). Approximately 150 mL sample was transferred to a 250-mL low-density polyethylene bottle (LDPE) (Nalgene), 0.01 M borate buffer and 1, 2 or 10 µM SA (actual concentration depending on the detection window) was added for Cu. 10 mL aliquots of the solution were pipetted into 14 25-mL PFA (perfluoroalkoxy alkane) (Savillex, Cole-Parmer) vials with lid. Cu was added to each vial in steps of progressively increasing concentration from 0 nM to 150 nM. These were then left to equilibrate overnight (or for a minimum of 8 h). The labile Cu concentration (i.e. that bound with the added SA) in each cell was then determined by CSV using 30 s adsorption. The deposition potential was -0.15 V, followed by a 9-s quiescence period and the scan initiated at the same potential (no potential jumps were used). The scan was in DP-mode as for total Cu.

The concentration of Fe complexing ligands was determined by titration with Fe in the

presence of 5 µM SA and borate pH buffer (Abualhaija and van den Berg, 2014) using a method modified from that before (Buck et al., 2007; Rue and Bruland, 1995). The 10-mL sample aliquots were equilibrated in polyethylene (Sterilin) tubes (30 mL), containing Fe additions to give a range 0 to 70 nM Fe. Two of the tubes were 0 added Fe. The iron and natural complexing ligands were allowed to equilibrate 10 min (up to 2 h) at room temperature. 5 µM SA was then added to the aliquots, which were left to equilibrate overnight prior to the determination of labile Fe by CSV in a PTFE voltammetric cell.

Vials used for the titrations were conditioned typically 3 times prior to a titration by setting up and discarding the titration about 3 h later or after overnight equilibration. The third one was measured and was repeated to check for further improvement. The voltammetric cell was conditioned 3 times with seawater with SA without added Cu or Fe prior to the start of a titration.

Data interpretation was using the van den Berg/Ruzic linearization procedure (Campos and van den Berg, 1994; van den Berg, 2006). A first estimate for S from the last three data points was improved using the modelled linearisation, with correction of the sensitivity for under-saturation of L (Turoczy and Sherwood, 1997). Comparative calculations were carried out using MCC software (Omanović et al., 2015) which fits the data simultaneously to several fitting methods, linear and non-linear and also corrects for under-saturation of L.

3.2.7. Calibration of the conditional stability constants for Fe-SA complexation ($K'_{Fe'SA}$ and $B'_{Fe'SA2}$) in seawater at different salinities

The complex stability of Fe-SA was calibrated at several salinities by monitoring by CSV the concentration of Fe-SA as a function of the concentration of SA (Abualhaija and van den Berg, 2014). UV-SW (Sal 35) was diluted with MQ, containing 2 mM HCO_3^-, to achieve salinities of 4, 11, 20, 26 and 35. 10 mL of the water was pipetted into the voltammetric cell with 10 mM borate buffer, 5 µM SA and 5 nM Fe. The water was air-purged (120 s) and SA was added in steps from 1 to 100 µM SA. A 5-min reaction time was allowed after each addition and 3 scans were made using an adsorption time of 120 s.

3.2.8. Cu competition with Fe for HS in estuarine waters

The CSV signal for Fe-HS was obtained as before: 10 ml seawater was put in the voltammetric cell and 100 µL borate buffer (pH_{NBS} 8.18), 100 nM Fe and 1 ml bromate (0.4 mM final concentration) were added. Cu additions were then made whilst monitoring the response for the Fe-HS species using an adsorption time of 30-60 s. Five minutes equilibration time was allowed after each copper addition. Repeated measurements with zero-added copper were used to obtain a value for the initial peak height of the experiment (i_{p0}).

3.3. Results

3.3.1. Calibration of K'_{FeSA} and B'_{FeSA2} for various salinities

The concentration and complex stability of Cu and Fe complexes with ligands in seawater is determined by ligand competition against SA. The complex stability for Cu with SA has been calibrated over a salinity range (Campos and van den Berg, 1994) and was used in this work: log K'_{CuSA} = 10.12 - 0.37 log Sal, and log B'_{CuSA2} = 15.78 - 0.53 log Sal. Similar to Cu, two SA-species are also known to exist for Fe with SA (FeSA and $FeSA_2$), but in the case of Fe only one of these, FeSA, is electroactive (Abualhaija and van den Berg, 2014). The complex stability of FeSA and $FeSA_2$ has been calibrated for seawater of salinity 35 (Abualhaija and van den Berg, 2014) but not yet for estuarine waters at lower salinity. For this reason values for of K'_{FeSA} and B'_{FeSA2} were calibrated here at salinities between 4 and 35. Values for K'_{FeSA} and B'_{FeSA2} were fitted to the response for 5 nM Fe in UV-digested seawater diluted to several salinities and in the presence of SA at concentrations between 1 and 100 µM. The data was expressed as a ratio, X, of the actual response (i_p) over the maximum response (i_{pmax}): $X = i_p / i_{pmax}$.

Values for K'_{FeSA} and B'_{FeSA2} were fitted using Solver in Excel (version 2011) to the following model of the response for Fe as function of the concentration of SA (Abualhaija and van den Berg, 2014):

$$X = \alpha_{FeSA} / (\alpha_{FeSA} + \alpha_{FeSA2} + \alpha_{Fe}) \quad (1)$$

where $\alpha_{FeSA} = K'_{Fe'SA} \times [SA]$ and $\alpha_{FeSA2} = B'_{Fe'SA2} \times [SA]^2$. I_{pmax} was one of the fitted parameters

as it is never reached because of a decrease in the voltammetric response with increasing concentration of SA due to increasing significance of $FeSA_2$ compared to that of FeSA. The effect of varying the concentration of SA on the response for Fe is shown at various salinities in Fig. 3.1. The curves in the diagram were calculated using the fitted values for the constants. The maximum in the response moves to a lower concentration of SA with decreasing salinity indicating that the stability of $FeSA_2$ increases compared to that of FeSA at a lower concentration of SA. A general increase in complex stability may be expected with decreasing salinity if there is significant competition by Ca^{2+} and Mg^{2+}. The values for $K'_{Fe'SA}$ were found to increase slightly, and those for $B'_{Fe'SA2}$ more strongly, with decreasing salinity, from 3.5 x 10^6 to 4.5 x 10^6 and from $10^{10.7}$ to $10^{12.0}$ respectively (Fig. 3.1) indicating that there was competition by the major cations.

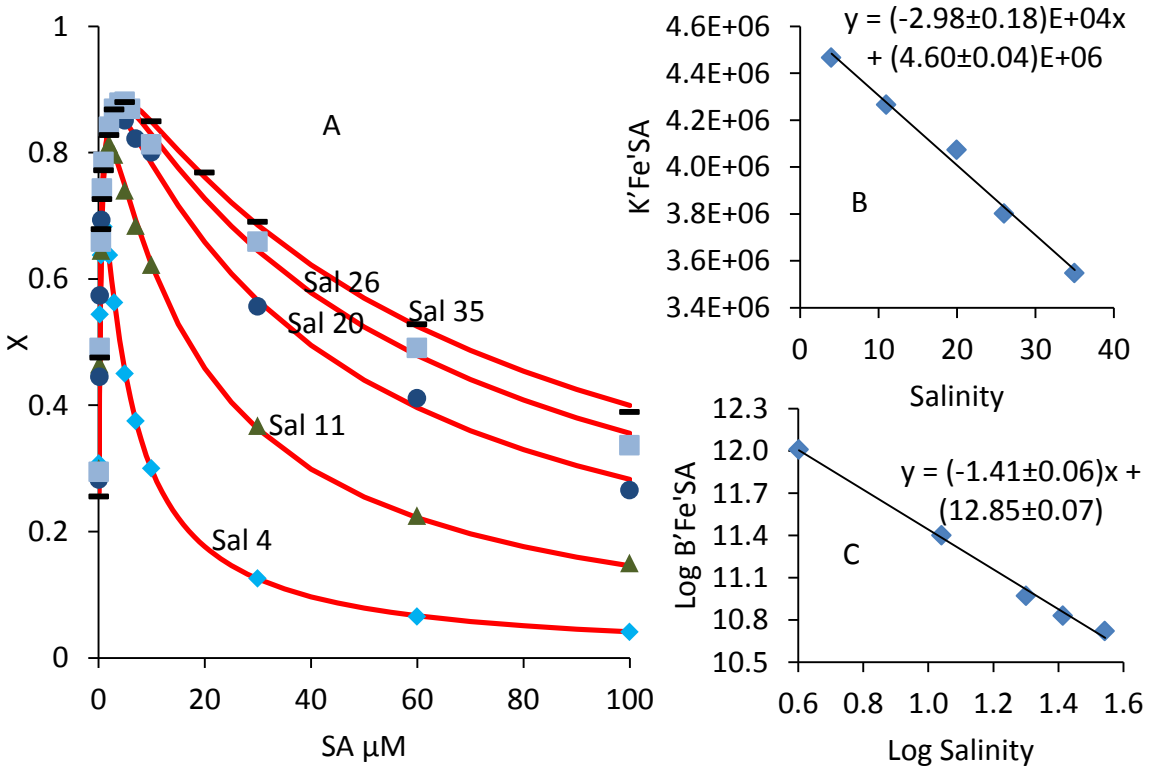

Figure 3.1. Calibration of $K'_{Fe'SA}$ and $B'_{Fe'SA2}$ by titrations of 5 nM Fe with SA in water of salinities between 4 and 35. A) Plots of the relative voltammetric response, $X = i_p / i_{pmax}$ as a function of [SA]. The lines were calculated using the fitted values for the constants. B and C): Plots of the fitted values for $K'_{Fe'SA}$ and $B'_{Fe'SA2}$ as a function of the salinity. The line through the data represents the data fit.

The K´ values were found to fit a straight line as function of the salinity, whereas the B values were fitted as a log-log diagram. The values found for the constants are summarised in Table 3.1 and the data fits to salinity are shown in Fig. 3.1B and C.

The constants were used to calculate the overall α-coefficient for Fe with SA ($\alpha_{Fe\text{-}SA}$) including FeSA and $FeSA_2$) and used to obtain complex stability for FeL in this study. Values for these α-coefficients are compared to values obtained using the original constants (Buck et al., 2007) at two concentrations of SA and four salinities in Table 3.2.

Table 3.1. Values of $K'_{Fe'SA}$ and $B'_{Fe'SA2}$ at different salinities. These constants were calibrated by measurement of the concentration of FeSA as a function of [SA] added to seawater of given salinity at pH_{NBS} 8.18.

Equations for $K'_{Fe'SA}$ and $B'_{Fe'SA2}$ as function of Salinity. **$K'_{Fe'SA}$= (-2.98±0.18) x10^4 × Sal+ (4.60±0.04) x10^6.** **Log $B'_{Fe'SA2}$= (-1.41±0.06) × Log Sal + (12.85±0.07).**					
Salinity	**Experimental Log $K'_{Fe'SA}$**	**Calculated Log $K'_{Fe'SA}$ using equations**	**Experimental Log $B'_{Fe'SA2}$**	**Calculated Log $B'_{Fe'SA2}$ using equations**	**Log $\alpha_{Fe'}$ at pH_{NBS} 8.18**
4	6.65	6.65	12.01	12.00	10.28
11	6.63	6.63	11.40	11.38	10.10
20	6.61	6.60	10.97	11.02	10.00
26	6.58	6.58	10.83	10.85	9.98
35	6.55	6.55	10.72	10.67	9.98

Table 3.2. Calculated values for the overall α-coefficient for Fe complexation with SA, comprising FeSA and $FeSA_2$ ($\alpha_{Fe\text{-}SA}$) using the new stability constants for $K'_{Fe'SA}$ and $B'_{Fe'SA2}$, and the previous value (Buck et al., 2007) that uses only $B'_{Fe'SA2}$, and the ratio of the new and previous α-coefficients.

[SA] (M)	**Salinity**	**$\alpha_{Fe\text{-}SA}$**	**$\alpha_{new}/\alpha_{previous}$**
5 x 10^{-6}	2	89	11.87
5 x 10^{-6}	10	28	6.84
5 x 10^{-6}	20	23	7.04
5 x 10^{-6}	35	19	7.27
30 x 10^{-6}	2	2534	9.35
30 x 10^{-6}	10	377	2.52
30 x 10^{-6}	20	213	1.85
30 x 10^{-6}	35	149	1.59

3.3.2. Complexing ligands, Cu-HS and Fe-HS in the estuarine waters

Cu and Fe complexing ligands were determined by CSV with ligand competition against SA. The ligand concentrations are on basis of Cu and Fe-equivalents (nM). Concentrations of Cu-HS and Fe-HS were determined by CSV and calibrated using SRHA on the mg/L scale (Table 3.3).

HS concentrations were found to be stable for several months when stored in the dark at 4◦C. HS in STN 6 was measured in May 2013, Sept 2013 and Feb 2014 using voltammetry and found to be 0.90, 0.90 and 0.89 mg L^{-1} respectively. STN 6 was also measured using UV spectrophotometry in May 2014 giving 0.91 mg/L. All samples measured using UV spectrophotometry in May 2014 were within 11 % of the values measured by voltammetry a year earlier.

Table 3.3. Comparative concentrations of metals and humic substances in estuarine and coastal samples: Fe (nM), Cu (nM), Fe-HS (mg HS/l), Cu-HS (mg HS/l) and UV-HS (mg HS/l). n.d. means not determined. LoD is limit of detection which was ~0.5 mg/l for the UV method.

Station	Salinity	Fe (nM)	Cu (nM)	Fe-HS (mg/l)	Cu-HS (mg/l)	UV-HS (mg/L)
1	18.8	86.0	54.3	3.3	n.d.	2.6
2	20.0	54.0	54.5	2.3	2.5	2.6
3	22.2	42.0	43.3	1.8	1.6	n.d.
4	26.3	34.7	38.0	1.4	1.5	1.7
5	28.8	27.7	31.1	1.1	1.4	1.2
6	30.9	22.4	20.7	1.0	0.9	0.9
7	32.2	4.9	11.6	0.1	0.3	<LoD

Some Cu-complexing capacity titrations showed the possibility of the presence of two individual ligand classes but due to the high organic matter content obscuring the CuSA peak at low total Cu, the initial titration points were often difficult to measure and were unreliable. For this reason, it was only possible to accurately measure total ligand rather than separate ligand classes. The Cu-complexing ligands, Cu-HS and dissolved Cu follow the same pattern (Fig. 3.2A): decreasing with increasing salinity towards much lower concentrations in the seawater endmember.

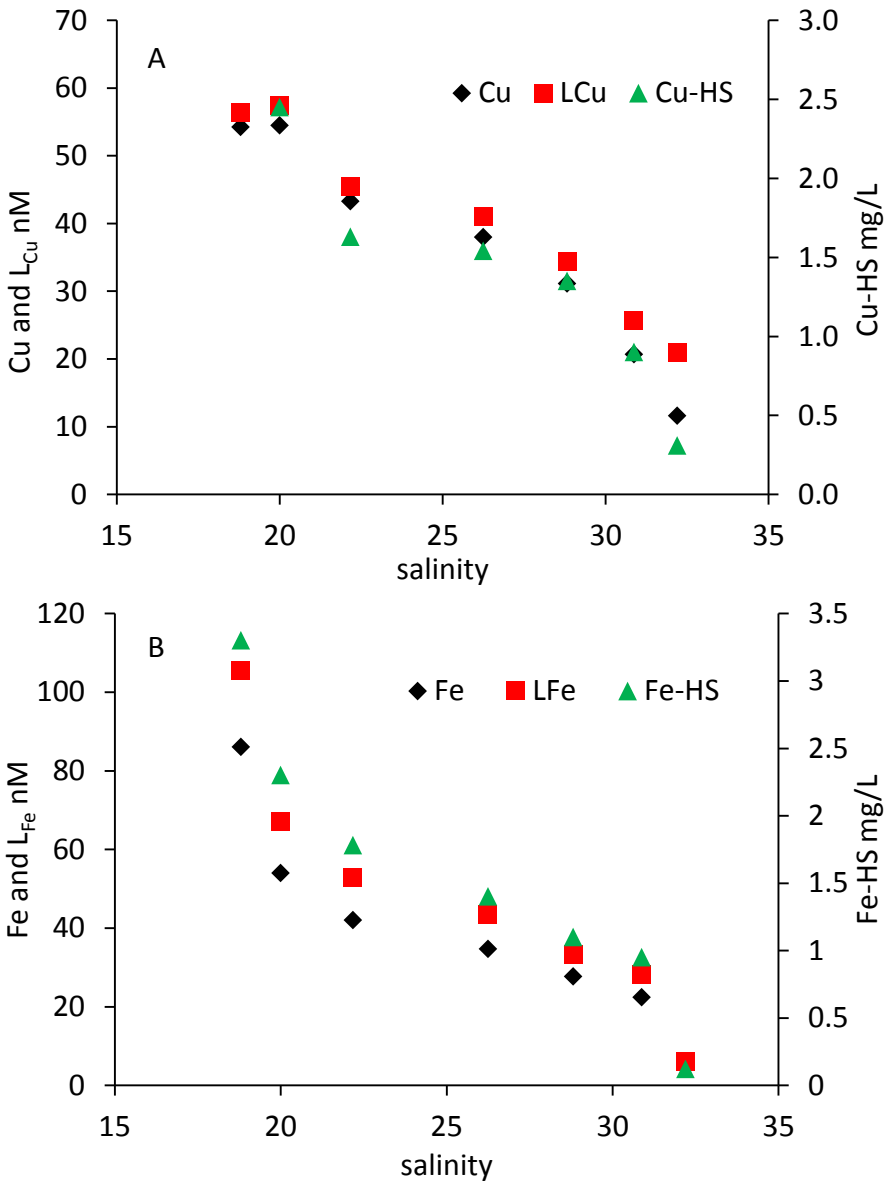

Figure 3.2. A) Concentrations of Cu, L_{Cu} (nM scale) and Cu-HS (right-hand mg/L scale) as function of the salinity. B) Concentrations of Fe, L_{Fe} (nM scale) and Fe-HS (right-hand mg/L scale) as function of the salinity.

The seawater end-member sample (salinity 32.2) was taken in Liverpool Bay (Irish Sea) about 15 mile from the mouth of the estuary, where the water was clear and contained much less suspended matter than in the estuary, and had a dissolved Cu concentration of 11.6 nM. The concentrations of Cu-HS had previously been determined in the same samples (Whitby and van den Berg, 2014) and are compared here to Fe-HS and the complexing ligands of Cu (L_{Cu}) and Fe (L_{Fe}). The concentration of L_{Cu} was greater than the Cu concentration in all samples, and therefore likely in control of the geochemistry of Cu (van den Berg et al., 1987).

The pattern for Fe-HS was similar to the Cu species in that [Fe], L_{Fe} and [Fe-HS] co-vary, and with a ligand concentration greater than the dissolved [Fe]. However, there are differences in the specific distributions.

The concentrations of HS (mg/L scale) found after complexation with Cu (Cu-HS) were the same as those of Fe-HS as evidenced from a plot of [Cu-HS] versus [Fe-HS] (on the mg/L scale) which has a slope of 1.04 ±0.1 (Fig. 3.3A). The good agreement between these two independent measurements suggests that the same HS is detected, and the similarity of the UV-HS values (Table 3.3) suggests that approximately the total concentration of HS is detected in spite of possible competition between metals (this is except for the high salinity, end-member, sample which was below the limit of detection (~0.5 ppm) of the UV method at salinity 32).

The ligand concentrations for Cu and Fe were similar but not identical, the concentration of L_{Cu} generally being greater than that of L_{Fe}. A plot of one against the other (Fig. 3.3B) has a significant intercept on the axis for L_{Cu}, at zero L_{Fe}. This finding suggests that a second ligand may be present for Cu, amounting to ~15 nM at the high salinity end, and which is in addition to the Cu-binding HS. This second ligand was not apparent in the titrations, as the CuSA peak at low [Cu] was difficult to measure. We have not been able to identify the second ligand experimentally, but thiols are known to occur in seawater (Al-Farawati and Van Den Berg, 2001; Tang et al., 2000) and act as ligand for Cu^{I} (Leal and Van den Berg, 1998). The data point for L_{Cu} at the highest concentration of L_{Fe} deviates from the linear relationship (Fig. 3.3B): a possibility is that competition has played a role here as the concentration of L_{Cu} may have been underestimated at the high concentration of Fe in this sample.

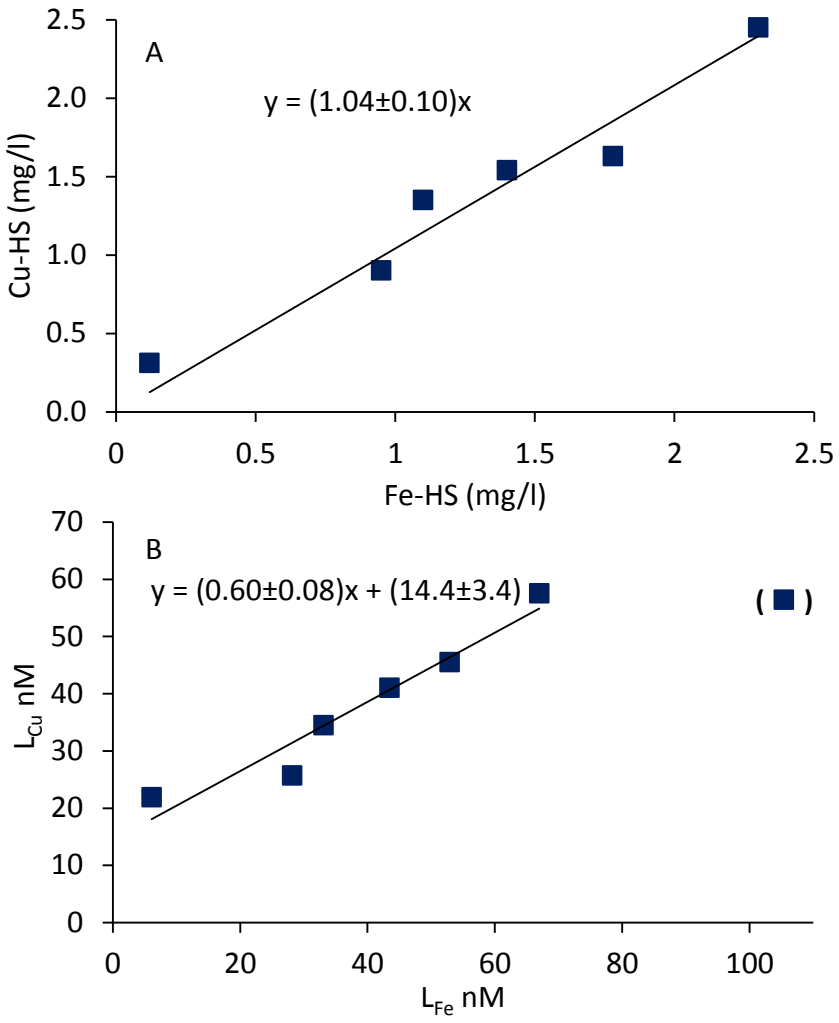

Figure 3.3. A) Comparison of Cu and Fe-binding HS (mg/L scale), and B) comparison of Cu and Fe-binding ligands in the estuarine waters.

The concentrations of Cu-HS and Fe-HS, which had been calibrated by additions of SRHA, were converted to the nanomolar scale by multiplication with their metal binding capacity for the SRHA reference material (Table 3.4). The Cu-binding capacity of this particular batch of SRHA is 18.0 ± 0.4 nmol/mg SRHA (Whitby and van den Berg, 2014), whereas the Fe-binding capacity is 30.6 ± 0.6 nmol/mg SRHA (Abualhaija and van den Berg, 2014) nearly the same as that (32 nmol/mg SRHA) found previously for a different batch of SRHA (Laglera and van den Berg, 2009).

Table 3.4. Values of L_{Fe} (nM), L_{Cu} (nM), Log $K'_{Fe'L}$ and Log $K'_{Cu'L}$ from complexation titrations data; Fe-HS mg/L converted to nM using a binding capacity of 30.6 Fe nmole/mg HA (Abualhaija and van den Berg, 2014), and Cu-HS mg/L converted to nM using a binding capacity of 18 Cu nmole/mg HA (Whitby and van den Berg, 2014).

Station	Salinity	L_{Fe} (nM)	L_{Cu} (nM)	Log $K'_{Fe'L}$	Log $K'_{Cu'L}$	Fe-HS (nM)	Cu-HS (nM)
1	18.8	105	56.4	11.1	11.6	101	
2	20.0	67	57.5	11.1	11.4	70	44
3	22.2	53	45.4	11.3	11.5	54	29
4	26.3	43	41.0	11.3	11.4	43	28
5	28.8	33	34.4	11.4	11.0	34	24
6	30.9	28	25.6	11.3	11.4	29	16
7	32.2	6	21.9	11.3	11.9	4	5.6

Because the ligand concentrations are greater than the metal concentrations, it is likely that the metals and ligands co-vary, potentially the ligands controlling the estuarine geochemistry of the metals. This was tested by plotting the metal concentration as a function of the concentration of the ligands and the HS (Fig. 3.4A and 3.4B). The data shows that the Cu-binding ligand concentration is greater than dissolved Cu in all stations (shown as a function of salinity in Fig. 3.2A) and the dissolved Cu varies linearly as a function of Cu-HS and L_{Cu}. The Cu complexing ligand concentration are similar to the copper concentration: $[Cu]/L_{Cu}$ = 0.92±0.06), and the concentrations of Cu-HS are systematically less than the concentration of Cu-binding ligands: $[Cu\text{-}HS]/L_{Cu}$ = 0.69 ± 0.05 (Fig. 3.4A and Table 3.4) (excluding the high salinity end-member which was taken a year later and had a lower than expected concentration of Cu). This indicates that, although the estuarine HS constitute the majority of the Cu-binding ligands, other ligands are able to complex the Cu as well.

The concentration of L_{Fe} was virtually the same as that of Fe-HS ($[FeHS]/L_{Fe}$ = 0.95±0.16) and both are greater than [Fe], indicating that there was an excess of the ligand concentration and that almost the entire ligand concentration (95%) can be ascribed to HS of a similar nature (metal binding capacity, complex stability) to SRHA.

A plot of Fe as function of L_{Fe} is straight (Fig. 3.4B), indicating that the Fe and L co-vary ($[Fe]/L_{Fe}$ = 0.81 ± 0.02) but the ligand concentration is always greater than [Fe].

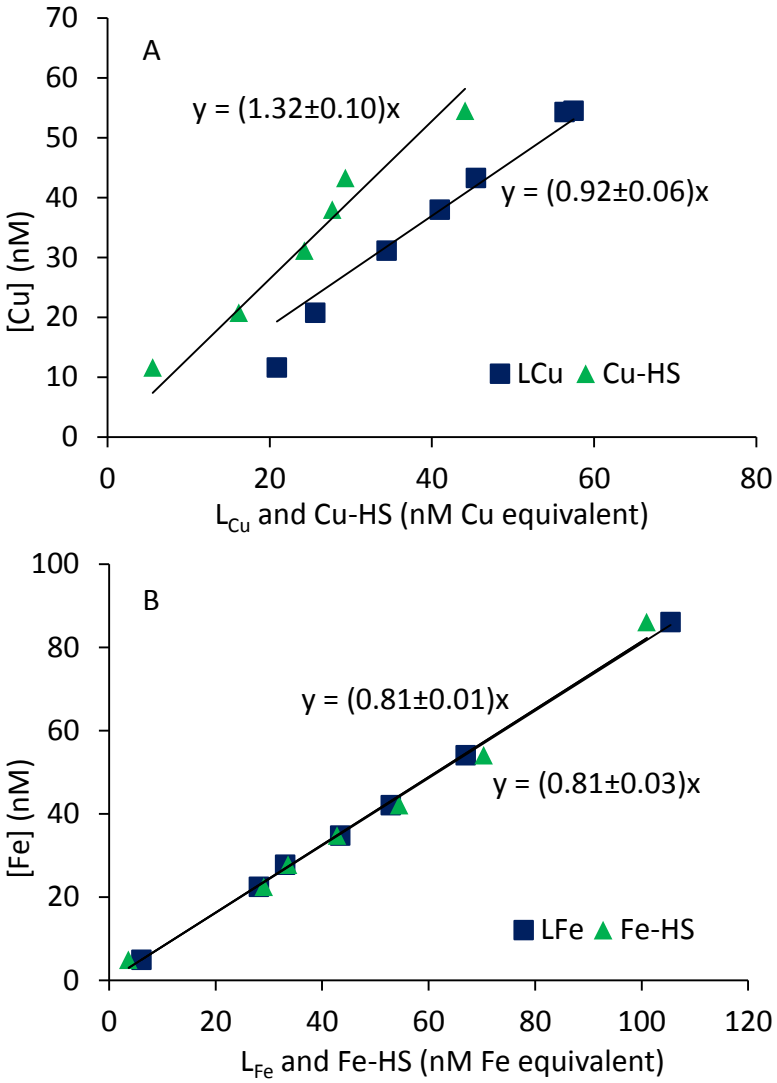

Figure 3.4. A) Comparison of the concentration of Cu to that of Cu-binding HS and ligands. B) Comparison of the concentration of Fe to that of Fe-binding HS and ligands. The slope of the data is indicated in the diagrams. The [Cu] was greater than [Cu-HS] but less than L_{Cu}, whereas the [Fe] was less than [Fe-HS] and L_{Fe}.

3.3.3. Comparison between Cu- and Fe- binding ligands and HS

A diagram of [Cu-HS] as a function of L_{Cu} has an intercept on the X-axis (the ligand axis) of 11 nM (Fig. 3.5A) indicating that a major component of the Cu binding ligands is different from HS. This is perhaps not surprising as thiols in estuarine waters are a known ligand for Cu, binding it as Cu^{I} (Leal and Van den Berg, 1998) and with only weak complex stability with divalent or trivalent metals: they are therefore detected as Cu-binding ligands by competition against SA, but not as Fe-binding ligands.

The data points for [Fe-HS] are nearly the same as those for [L_{Fe}] causing them to be superimposed in Fig. 3.4B. A diagram of [Fe-HS] as function of L_{Fe} (Fig. 3.5B) shows a linear relationship with a slope of near unity (0.98 ±0.04) and an intercept that is <1 nM ligands confirming that nearly the entire ligand concentration for Fe consists of HS. On this basis it is possible to calculate the amount of Fe that can be bound by estuarine HS from the ratio of LFe/[Fe-HS] (the Fe-HS on the mg/L scale), which gives a value of 30.3 ±1.0 nmol/mg HS. This value is the same (within the standard deviation) as the ratio (30.6) at which Fe is bound by SRHA (Abualhaija and van den Berg, 2014) indicating that the HS occurring in estuarine waters and the SRHA have the same binding capacity for Fe on the mg/L scale.

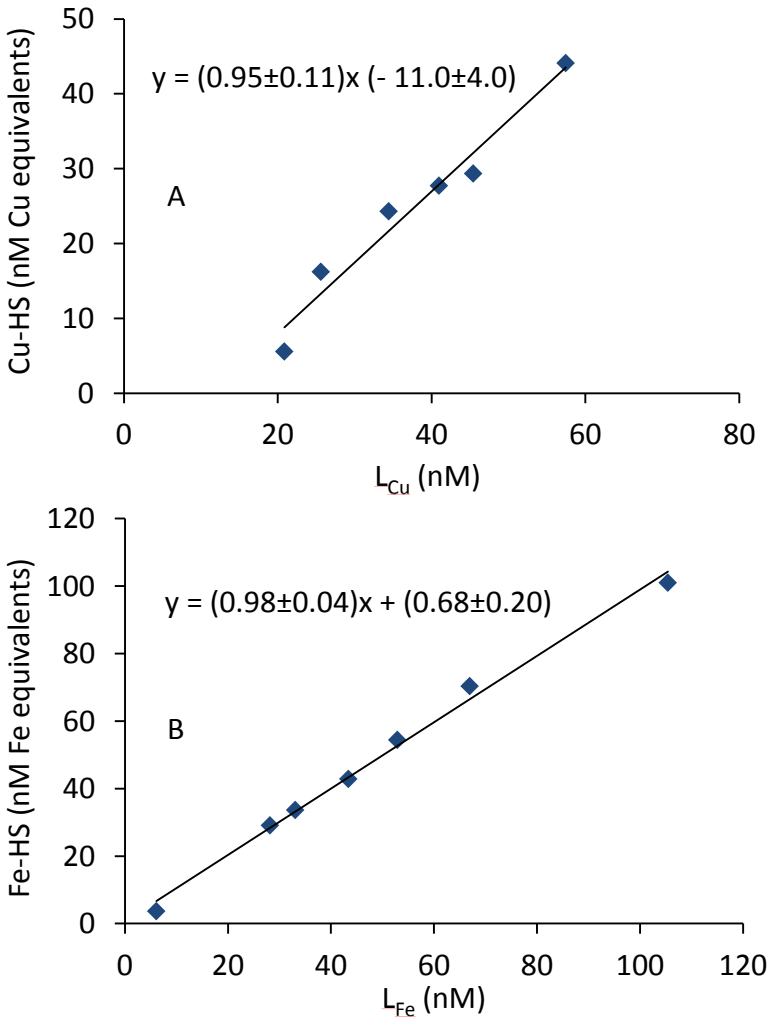

Figure 3.5. Comparison of the concentrations of Fe-binding and Cu-binding HS to the concentration of Cu -binding ligands (A) and Fe -binding ligands (B). The slopes are close to unity but there is a large intercept on the X-axis for the Cu data. The metal concentrations are shown in Table 3.3. The ligand concentration for Fe is virtually the same as the concentration of HS, whilst for Cu a large intercept indicates the presence of a second ligand.

3.3.4. Competition between Cu and Fe for complexation with HS in estuarine water

The measurements of HS in samples from the Mersey estuary using Fe and Cu indicated the presence of Fe-HS and Cu-HS species: this means that the HS is being complexed with Cu as well as Fe, suggesting that competition is possible between these metals for complexation with the HS. Competition between Cu, Co and Al with Fe has previously been demonstrated for SRHA and SRFA (Yang and Van den Berg, 2009). Because the HS are the sole ligand for Fe in these waters (within 95%), it is possible to determine competition between Cu and Fe for these ligands from the effect of copper additions on the response for the estuarine Fe-HS. This competition method has previously been used to determine the stability of Cu complexation with SRHA and SRFA (Yang and Van den Berg, 2009) and the principle of the method is the same. The data was interpreted using the theory developed previously (Yang and Van den Berg, 2009) modified for the use of marine HS by using the ligand concentrations ($[L_{Fe}]$ as determined by titrations) for the mass balance required for the competition modelling, to get a value for the total ligand concentration. The difference between L_{Fe} and [Fe-HS] is <5% so this introduced only a minor change. Curve fitting was used to fit a $K'_{Cu'HS}$ value to all data simultaneously after initially calculating a value for each data point.

The concentration of Fe-HS was found to decrease in response to the copper additions (Fig. 3.6) suggesting that Cu caused Fe to be released from Fe-HS as a result of competitive complexation. The copper additions were over a large range from nM to µM: the high range was necessary to obtain a good data fit, but [Fe-HS] was responding already at Cu additions in the nM range, indicating that the effect is of importance at the concentrations typical for estuarine conditions. The copper additions at low salinity were lower than those at higher salinity this could be due to increase competitions by major cations with increasing salinity. The complex stability for the Cu-HS (values for the conditional stability constant $K'_{Cu'HS}$) calculated from the competition titrations, is summarised in Table 3.5. These are an order of magnitude lower than the complex stabilities for total Cu ligands in the samples, further supporting the presence of another, stronger, ligand for Cu, such as thiols.

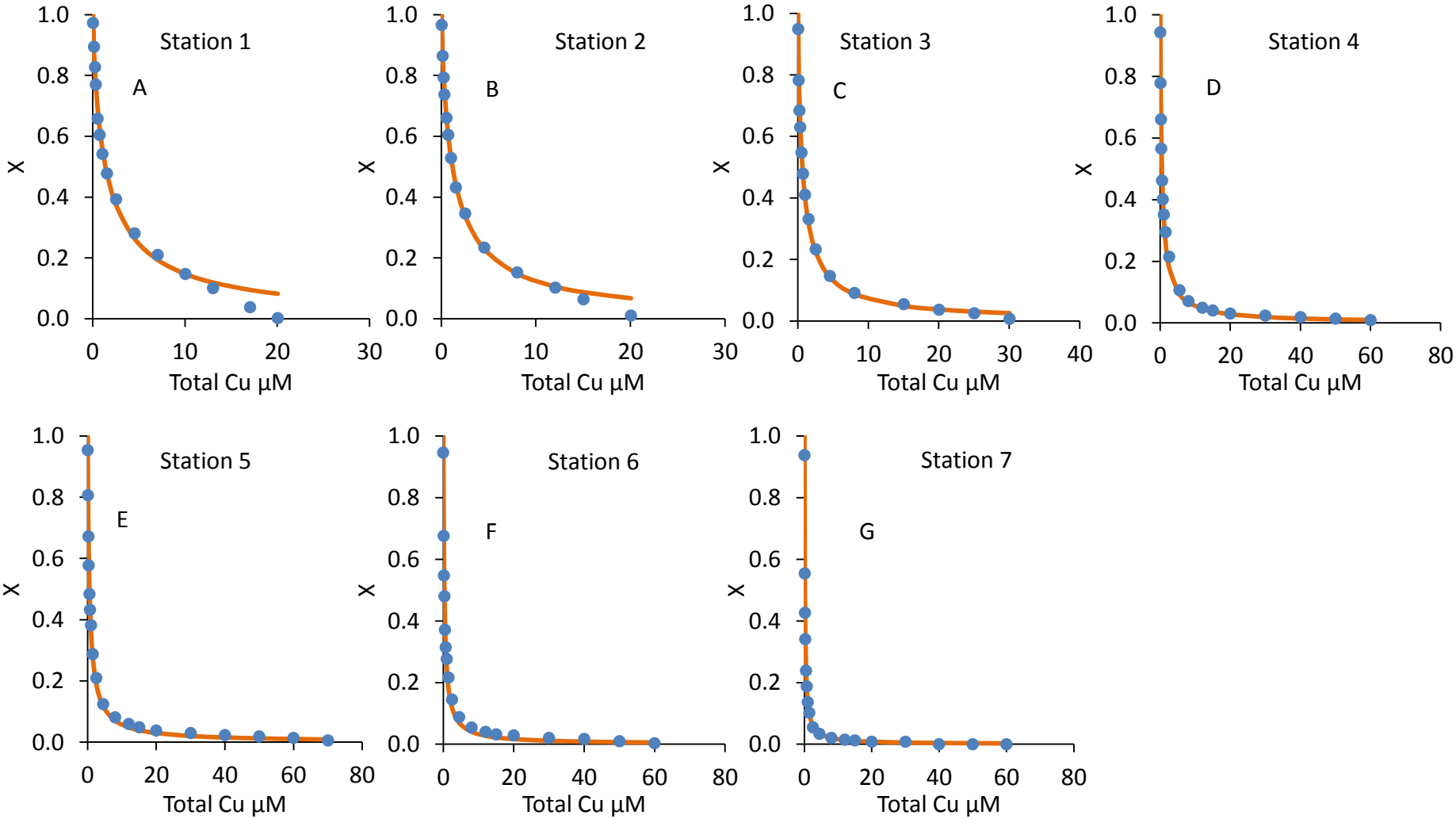

Figure 3.6. Effect of Cu additions on the response for the natural Fe-HS species in each sample, as a result of competition of Cu with the complexation of HS by Fe. The curves represent the data fit through the data, which was used to obtain values for the complex stability, $K'_{Cu'HS}$, for Cu with HS. Values for $K'_{Fe'HS}$ needed for this calculation were obtained using separate complexing ligand titrations. The values for $K'_{Fe'HS}$ are in Table 3.4 and those for $K'_{Cu'HS}$ in Table 3.5.

Table 3.5: Conditional stability constants (log $K'_{Cu'HS}$) from Cu competition with Fe for HS in estuarine and coastal waters. The fitted values are compared to log $K'_{Cu'L}$ values from complexing ligand titrations carried out in the same samples. The values for log $K'_{Cu'L}$ are representative for all ligands whereas the values for log $K'_{Cu'HS}$ are for the HS species only. The values for $\alpha_{Cu'}$ were calculated for pH_{NBS} 8.2 using an ion-pairing model to provide free concentrations of the major anions (CO_3^{2-}, HCO_3^-, SO_4^{2-}), concentrations of H^+ on the NBS, free and SW scale, and total concentrations of CO_3^{2-} and HCO_3^- on the seawater scale.

Station	**Salinity**	**Log $K'_{Cu'HS}$ from values for $K'_{Fe'L}$ by Cu competition**	**Log $K'_{Cu'L}$ from CuL titrations**	**$\alpha_{Cu'}$**
1	18.8	10.2	11.6	14
2	20.0	10.1	11.4	14
3	22.2	10.5	11.5	15
4	26.3	10.7	11.4	17
5	28.8	10.7	11.0	18
6	30.9	10.9	11.4	19
7	32.2	11.1	11.9	19
Calculation of values for $\alpha_{Cu'}$				
pK'_{CuOH} = 8.11 (H_F scale) pK'_{CuOH2} = 15.9 (H_F scale)			Ionic strength corrected (Turner et al., 1981) and adjusted to match at Sal 35 the constants from (van den Berg, 1984)	
log $K'_{CuB(OH)4}$ = 3.45			(van den Berg, 1984)	
log$K'_{CuCO3sw}$ =6.74-542.1/T =4.89			(Soli and Byrne, 1989)	
log$B'_{Cu(CO3SW)2}$ =7.58			(Byrne and Miller, 1985; Soli and Byrne, 1989)	

3.4. **Discussion**

3.4.1. Re-calibration of $K'_{Fe'SA}$ and $B'_{Fe'SA2}$ as function of the salinity

The stability constants, $K'_{Fe'SA}$ and $B'_{Fe'SA2}$, were re-calibrated as a function of salinity between 4 and 35 to enable use of SA for ligand competition at low salinities as occurring in estuarine waters. The values for the constants were fitted to the response as a function of [SA] without the need for addition of an organic competing ligand (typically EDTA) thus eliminating problems related to uncertainties in its complex stability as a function of salinity (Abualhaija and van den Berg, 2014). The inorganic speciation of Fe ($\alpha_{Fe'}$)as a function of the ionic strength (salinity) and temperature is well known (Liu and Millero, 1999). The value for log $\alpha_{Fe'}$ varied between 10.28 (Sal 4) and 9.98 (Sal 35) (Table 3.1) and was used for the calibration. The water of Sal < 35 consisted of UV-digested seawater of Sal 35 diluted with 2 mM HCO_3^- in MQ to maintain a realistic constant alkalinity. The pH was kept at 8.18 (NBS

scale) using borate/ammonia buffer. The values for $K'_{Fe'SA}$ and $\log B'_{Fe'SA2}$ were fitted to linear equations as a function of salinity to enable interpolation and extrapolation:

$$K'_{Fe'SA} = (-2.98 \pm 0.18) \times 10^4 \times Sal + (4.60 \pm 0.04) \times 10^6 \quad (2)$$

$$\log B'_{Fe'SA2} = (-1.41 \pm 0.06) \times \log Sal + (12.85 \pm 0.07) \quad (3)$$

The change in $B'_{Fe'SA2}$ as a function of Sal was much greater than in $K'_{Fe'SA}$ and was therefore fitted using a log-log function (Eqn. 3). Values calculated for K' and B' at salinity 35 using these equations match the previous values at the same salinity (Abualhaija and van den Berg, 2014): the reference value for $\log K'_{Fe'SA}$ is 6.52, compared to 6.55 from equation (2), and the reference value for $\log B'_{Fe'SA2}$ is 10.72 (Abualhaija and van den Berg, 2014), compared to 10.67 using equation (3). The stability of the 1:1, Fe-SA, complex was found to increase a small amount (0.1 units in $\log K'_{Fe'SA}$) when the salinity was decreased from 35 to 4, whereas the value of $\log B'_{Fe'SA2}$ increased from 10.7 to 12.0 over the same salinity range (Table 3.1).

Previously it was thought that the CSV response for Fe was based on the concentration of $FeSA_2$ (Buck et al., 2007; Rue and Bruland, 1995), whereas recent data shows that FeSA is the adsorptive species and formation of $FeSA_2$ is the cause for a decrease in the sensitivity (nA peak-height $(nM\ Fe)^{-1}$) when [SA] increases above the optimal concentration (Abualhaija and van den Berg, 2014). The lower salinity data in this work confirms that scenario: the relative sensitivity (X) can be seen to decrease with increasing [SA] at each salinity tested (Fig. 3.1A) when [SA] is greater than an optimal concentration. This optimal concentration can be seen to move to a lower [SA] with decreasing salinity, whilst at the same time the maximum sensitivity at each salinity also decreases. This decrease in the maximum sensitivity is somewhat counter-intuitive as it might be expected that the complex stability and therefore the complexation of Fe by SA should increase with decreasing salinity due to less competition by the major cations. The values for $K'_{Fe'SA}$ and $B'_{Fe'SA2}$ do indeed increase with decreasing salinity (Fig. 3.1A and B) indicating that the complexation of Fe by SA, and its complex stability, increase with decreasing salinity. However, the overall sensitivity diminishes because the stability of the $FeSA_2$ species increases more rapidly than that of FeSA. The comparative change means that the FeSA species is increasingly outcompeted by the $FeSA_2$ species at lower salinity, which explains the shape of the sensitivity curves (Fig. 3.1A). The maximum response at low salinity is obtained at [SA] = 1 µM (for Sal = 4) whereas

the response is greatest at 5 µM SA at a salinity of 35. The concentration of SA was kept constant at 5 µM SA in this work to standardise the analyses.

3.4.2. Fe and Cu-binding humics in estuarine waters

The concentrations of Cu-HS and Fe-HS were measured here independently by voltammetry using either the peak for the Cu-HS or the Fe-HS species. The results shown were calibrated against SRHA and separate tests showed that the sensitivity was the same using SRFA: the mg/L concentrations of HS are therefore independent on whether SRFA or SRHA is used.

A difference between the two species (Cu-HS and Fe-HS) is that the Cu-HS was determined after saturation with Cu and the Fe-HS after saturation with Fe. The good agreement in the data (Fig. 3.3A and Table 3.3) shows that either method can be used to determine marine HS. The peak for Cu-HS is near to the peak for free Cu', which requires careful elimination by subtracting a blank scan and by minimising the Cu addition. Detection of Fe-HS does not suffer from this complication and is therefore arguably easier to determine, but the Fe-HS peak could be unstable due to precipitation of the excess inorganic Fe. The limit of detection (LoD) of the Fe-HS method was 3 µg/l HS using a 240 s adsorption time in seawater. A higher LoD of 100 µg/l has been quoted for the CuHS (Whitby and van den Berg, 2014).

Conversion of the Fe-HS and Cu-HS from the mg/L to the nM scale would be simple if there was a single metal binding capacity of the HS. Our data shows that there are differences in the numbers of Cu and Fe binding sites on SRHA: 18 nanomole Cu/mg SRHA (Whitby and van den Berg, 2014) compared to ~31 nanomole Fe/mg SRHA (Abualhaija and van den Berg, 2014; Laglera and van den Berg, 2009). SRFA binds at a different ratio from SRHA: the ratio for Cu (16 nmole Cu/mg SRFA) is the same as on the SRHA, whereas the number of Fe-binding sites on SRFA is approximately half that on the SRHA: 17.6 nanomole Fe/mg SRFA, compared to 32 nmole Fe/mg SRHA (Laglera and van den Berg, 2009). The SRHA binds nearly twice as much Fe as Cu, which might suggest that the Fe-HA complex is 2:1 (Fe_2-HA) whereas the Cu complex is 1:1, or that two sites are available for Fe on the SRHA. The SRFA data is then consistent with a 1:1 species for Fe-SRFA and Cu-SRFA.

Not knowing whether the HS in estuarine waters are like FA or HA complicates the conversion of FeHS to the nanomolar scale, necessary to compare to the ligand concentrations (as the ratios are the same for Cu-FA and Cu-HA it makes no difference for the Cu-HS). The nanomolar concentrations in Table 3.4 were calculated using the ratios for SRHA. The nanomolar concentrations of the Cu-HS and Fe-HS in Table 3.4 differ because of the different complexation ratios. The data in Fig. 3.5B was plotted using a binding capacity of 30.6 nmole Fe (mg HA^{-1}) as valid for SRHA. The slope of nearly unity (0.98) confirms that the Fe-binding ratio of the marine HS of 30.3 $\pm$1 nmole Fe/mg HS is nearly the same as that for SRHA, indicating that the HS in these waters behaves as HA rather than FA which has a lower binding ratio of near 17 nmole Fe/mg FA (Laglera and van den Berg, 2009).

The concentration of HS (Cu and Fe-bound) is decreasing with increasing salinity, largely in-line with what is known about HS (Sholkovitz et al., 1978). Extrapolation of the concentration of HS in the Mersey waters to a salinity of 35 gives an estimated value of 0.05 mg HS L^{-1}, which is, coincidentally in view of the noise in the data, the same as that found for residual HS in the Amazon outflow (Sholkovitz et al., 1978). A value of 0.2 mg HS L^{-1} is found by extrapolation of the Cu-HS data.

3.4.3. Fe and Cu complexing ligands in estuarine waters

Ligand concentrations had been determined by metal titration in presence of SA, which therefore constitutes a method that is independent of the HS determination. The concentration of the iron binding ligand (L_{Fe}) was > [Fe] in all samples: [Fe] / L_{Fe} = 0.81 $\pm$ 0.02. This makes sense as any Fe in excess of the ligand concentration would tend to precipitate due to the low solubility of inorganic Fe (~10^{-11} M (Liu and Millero, 1999)) until the remainder is kept in solution by the excess of ligands. The plot of Fe as function of L_{Fe} is linear (Fig. 3.4B) showing the strong effect of organic complexation on the geochemistry of Fe found previously for estuarine waters (Laglera and van den Berg, 2009).

The Cu concentration is also controlled by complexation: [Cu]/ L_{Cu} = 0.92 $\pm$ 0.06 for stations collected in May 2013, which is greater than the ratio ([Cu]/ L_{Cu} = 0.5) found for the high salinity end member collected in May 2014.

Comparison with the concentrations of Fe-HS and Cu-HS (Fig. 3.5) shows that the Fe-

HS constitutes all the ligands for Fe ([Fe-HS] = 0.98 x L_{Fe} + 0.68) whereas a much larger intercept on the ligand-axis is obtained for Cu suggesting that a significant proportion is not from HS. The concentration of Cu-binding HS was on average 0.69 ± 0.05 x L_{Cu}, indicating that on average about 30% of the Cu binding ligands is not from HS origin. Again there was a discrepancy in the high salinity end member value, where the concentration of Cu-binding HS was 0.3, much lower than the ratio of 0.7 determined at the other stations the previous year. Other than the end member station, the copper binding ligands are largely, but not exclusively, from humic origin. The discrepancy makes sense as thiols also occur in estuarine waters, are a ligand for Cu (Tang et al., 2000) and apparently tend to account for a higher percentage of Cu ligands at higher salinity. Although it was not possible to accurately model two ligand classes for these samples, we are currently working on samples where we can distinguish between thiols and humics as competing ligands for Cu in estuarine water. Co-variation of the Cu concentration with complexing ligands, and the effect on the Cu geochemistry, has been found before in waters from the Scheldt estuary (van den Berg et al., 1987) and elsewhere (Muller and Batchelli, 2013; Oldham et al., 2014; Plavsic et al., 2009).

The average value of log $K'_{Fe'L}$ between salinity 18.8 and 32.2 was 11.2±0.1, similar to that found for SRHA added to seawater (11.6 ±0.1 and 11.1) (Abualhaija and van den Berg, 2014; Laglera and van den Berg, 2009) and also similar to the complex stability (log $K'_{Fe'L}$ = 11.1) of ligands in coastal waters (Laglera and van den Berg, 2009). Other work on estuarine waters found log K'_{FeL} varying between 11.1 and 13.9, the highest values greater than found here but which could be due to measurements at much lower salinity (1.4-5.6) (Buck et al., 2007).

3.4.4. Metal competition for the HS

The competition experiments demonstrated competition between Cu and Fe for HS in the marine environment. The competition data were used to get a value for the complex stability of Cu with the HS: an average value of 10.6±0.4 was found for log$K'_{Cu'HS}$, which compares to a value of 11.5±0.3 for log$K'_{Cu'L}$ from the Cu-complexing ligand titrations against SA. There is therefore a significant difference between the value for $K'_{Cu'HS}$ and $K'_{Cu'L}$ which must be due to greater stability of complexes with other organic ligands. It can be speculated

that other species of Cu may be thiols which are known to form more stable complexes with complex stability ($logK'_{Cu'L}$) values of 12-14 (Laglera and van den Berg, 2003). The value of $logK'_{Cu'HS}$ (10.6±0.4) from the competition data is very similar to that ($logK'_{Cu'HS}$ = 10.7) for Cu complexation with riverine humics (SRHA) (Whitby and van den Berg, 2014) confirming that the HS in the Mersey behaves similar to SRHA.

3.4.5. Implications of the findings of this work

The new values for $K'_{Fe'SA}$ and $B'_{Fe'SA2}$ obtained at salinities between 4 and 35 give a significantly larger value for the α-coefficient for complexation of Fe by SA than calculated based on the previous values for $B'_{Fe'SA2}$ (Buck et al., 2007) alone (Table 3.2). Calculation of α-coefficients and comparison to that calculated using the previous complex stability shows that the difference is a factor of ~9 at a salinity of 2 at 30 µM SA (the correct α-coefficient is 9 times larger), whilst the difference at higher salinity is less but still important (Table 3.2). It is of special importance to use the correct stability constants when the detection window is varied as the ratio of the new and old α-coefficients varies with the concentration of SA: the ratio changes from 7.3 to 1.6 (Sal 35), or from 11.9 to 9.4 (Sal 2) when [SA] is raised from 5 to 30 µM (Table 3.2). Using the old constants would lead to a shift in the detected $K'_{Fe'L}$ with the detection window, that could be incorrectly attributed to the presence of more than one ligand.

The co-variation between Cu and Fe with the ligand concentration shows that the geochemistry of both metals in the Mersey estuary is controlled by organic complexation, as has been found previously for Cu (Buck and Bruland, 2005; Oldham et al., 2014; Sander et al., 2014; van den Berg et al., 1987) and Fe (Boye et al., 2003; Buck et al., 2007; Bundy et al., 2014) in estuarine and seawater. The similarity of the concentrations of Fe-binding HS to the ligand concentration shows that nearly the entire ligand concentration is represented by HS. The concentration of Cu-binding HS is less than the Cu-binding ligand concentration indicating that a second ligand plays a role for Cu. The competition experiments show that complexation of Fe by ligands is affected by competition by Cu (Fig. 3.6).

The concentration of HS (mg L^{-1}) found as Cu-HS and Fe-HS is the same (Table 3.3). This means that the HS that is binding these metals is the same. This is confirmed by the

competition experiments (Fig. 3.6) that show that Cu competes with Fe and displaces it from Fe-HS when added in sufficient quantity. Competition occurs when [Cu'] > [Fe'] because of the similarity of $K'_{Fe'HS}$ and $K'_{Cu'HS}$ (log $K'_{Cu'HS}$ = 11.1 and log $K'_{Fe'HS}$ = 11.3 at Sal 32, Table 3.5). This competition may cause the complexation of Fe with HS to be carefully balanced.

The excess of Fe over the ligand concentration in all samples causes the [Fe] to diminish with time due the low solubility of inorganic Fe as the water travels through the estuary and beyond. The ligand concentration in the high salinity end member (6 nM) is only slightly larger than the Fe concentration (5 nM). Competition by Cu, and variations therein due to variations in the concentration of thiols, could vary the amount of HS available for complexation with Fe and could therefore affect the geochemistry of Fe. Similarly, the competition by Cu can be expected to affect the availability of Fe to microorganisms in seawater if this relationship plays a role in open sea conditions. Extrapolation of the concentration of Fe-HS to an ocean salinity of 35 gives a residual level of 0.05 mg HS L^{-1}, equivalent to Fe-binding ligand concentration of 1.5 nM, which is similar to Fe-binding ligand concentrations found in ocean waters (Boye et al., 2005). Extrapolation of Cu-HS gives a residual level of 0.2 mg HS L^{-1} in seawater equivalent to a Cu-binding ligand concentration of 3.6 nM, which is comparable to levels found in ocean waters (Moffett and Dupont, 2007). Further work is required to confirm whether HS is an important ligand for Cu as well as Fe in ocean waters, and whether terrestrial HS is transported from land to the ocean.

Acknowledgements

The research of Mahmoud Abualhaija is financed by a scholarship from the University of Jordan, and that of Hannah Whitby by a scholarship of the Natural Environment Research Council ((NE/K500975/1). We thank the crew of the Marisa (David Annett and Philip Robson) for assistance with sample collection.

3.5. References

Abualhaija, M.M. and van den Berg, C.M.G., 2014. Chemical speciation of iron in seawater using catalytic cathodic stripping voltammetry with ligand competition against salicylaldoxime. Marine Chemistry, 164(0): 60-74.

Achterberg, E.P., Colombo, C. and van den Berg, C.M.G., 1999. The distribution of dissolved Cu, Zn, Ni, Co and Cr in English coastal surface waters. Continental Shelf Research, 19(4): 537-558.

Al-Farawati, R. and Van Den Berg, C.M.G., 2001. Thiols in coastal waters of the western North Sea and English Channel. Environmental Science & Technology, 35(10): 1902-1911.

Balistrieri, L.S., Brewer, P.G. and Murray, J.W., 1981. Scavenging residence times of trace metals and surface chemistry of sinking particles in the deep ocean. Deep-Sea Research, 28 A: 101-121.

Batchelli, S., Muller, F.L.L., Chang, K.C. and Lee, C.L., 2010. Evidence for Strong but Dynamic Iron-Humic Colloidal Associations in Humic-Rich Coastal Waters. Environmental Science & Technology, 44(22): 8485-8490.

Boye, M. et al., 2003. Horizontal gradient of the chemical speciation of iron in surface waters of the northeast Atlantic Ocean. Marine Chemistry, 80(2-3): 129-143.

Boye, M. et al., 2005. Major deviations of iron complexation during 22 days of a mesoscale iron enrichment in the open Southern Ocean. Marine Chemistry, 96(3-4): 257-271.

Bruland, K.W., Rue, E.L., Donat, J.R., Skrabal, S.A. and Moffett, J.W., 2000. Intercomparison of voltammetric techniques to determine the chemical speciation of dissolved copper in a coastal seawater sample. Analytica Chimica Acta, 405(1-2): 99-113.

Buck, K.N. and Bruland, K.W., 2005. Copper speciation in San Francisco Bay: A novel approach using multiple analytical windows. Marine Chemistry, 96(1-2): 185.

Buck, K.N., Lohan, M.C., Berger, C.J.M. and Bruland, K.W., 2007. Dissolved iron speciation in two distinct river plumes and an estuary: Implications for riverine iron supply. Limnology and Oceanography, 52(2): 843-855.

Buck, K.N. et al., 2012. The organic complexation of iron and copper: an intercomparison of competitive ligand exchange-adsorptive cathodic stripping voltammetry (CLE-ACSV) techniques. Limnology and Oceanography-Methods, 10: 496-515.

Bundy, R.M., Barbeau, K.A. and Buck, K.N., 2013. Sources of strong copper-binding ligands in Antarctic Peninsula surface waters. Deep-Sea Research Part Ii-Topical Studies in Oceanography, 90: 134-146.

Bundy, R.M., Biller, D.V., Buck, K.N., Bruland, K.W. and Barbeau, K.A., 2014. Distinct pools of dissolved iron-binding ligands in the surface and benthic boundary layer of the California Current. Limnology and Oceanography, 59(3): 769-787.

Byrne, R.H. and Miller, W.L., 1985. Copper(II) carbonate complexation in seawater. Geochimica et Cosmochimica Acta, 49: 1837-1844.

Campos, M.L.A.M. and van den Berg, C.M.G., 1994. Determination of copper complexation in sea water by cathodic stripping voltammetry and ligand competition with salicylaldoxime. Analytica Chimica Acta, 284: 481-496.

Chanudet, V., Filella, M. and Quentel, F., 2006. Application of a simple voltammetric method to the determination of refractory organic substances in freshwaters. Analytica Chimica Acta, 569(1-2): 244-249.

Chapman, C.S., Capodaglio, G., Turetta, C. and van den Berg, C.M.G., 2009. Benthic fluxes of copper, complexing ligands and thiol compounds in shallow lagoon waters. Marine Environmental Research, 67(1): 17-24.

Donat, J.R., Lao, K.A. and Bruland, K.W., 1994. Speciation of dissolved copper and nickel in South San Francisco Bay: a multi-method approach. Analytica Chimica Acta, 284(3): 547-571.

Dryden, C.L., Gordon, A.S. and Donat, J.R., 2007. Seasonal survey of copper-complexing ligands and thiol compounds in a heavily utilized, urban estuary: Elizabeth River, Virginia. Marine Chemistry, 103(3-4): 276-288.

Dupont, C.L., Nelson, R.K., Bashir, S., Moffett, J.W. and Ahner, B.A., 2004. Novel copper-binding and nitrogen-rich thiols produced and exuded by Emiliania huxleyi. Limnology And Oceanography, 49(5): 1754-1762.

Eldridge, M.L. et al., 2004. Phytoplankton community response to a manipulation of bioavailable iron in HNLC waters of the subtropical Pacific Ocean. Aquatic Microbial Ecology, 35(1): 79-91.

Ellwood, M.J., Wilson, P., Vopel, K. and Green, M., 2008. Trace metal cycling in the Whau Estuary, Auckland, New Zealand. Environmental Chemistry, 5(4): 289-298.

Gerringa, L.J.A. et al., 2007. Kinetic study reveals weak Fe-binding ligand, which affects the solubility of Fe in the Scheldt estuary. Marine Chemistry, 103(1-2): 30-45.

Gledhill, M. and van den Berg, C.M.G., 1994. Determination of complexation of iron(III) with natural organic complexing ligands in seawater using cathodic stripping voltammetry. Marine Chemistry, 47(1 SU -): 41-54.

Hassler, C.S., Alasonati, E., Nichols, C.A.M. and Slaveykova, V.I., 2011. Exopolysaccharides produced by bacteria isolated from the pelagic Southern Ocean - Role in Fe binding, chemical reactivity, and bioavailability. Marine Chemistry, 123(1-4): 88-98.

Hong, H.S., Wu, J.Y., Shang, S.L. and Hu, C.M., 2005. Absorption and fluorescence of chromophoric dissolved organic matter in the Pearl River Estuary, South China. Marine Chemistry, 97(1-2): 78-89.

Kogut, M.B. and Voelker, B.M., 2001. Strong copper-binding behavior of terrestrial humic substances in seawater. Environmental Science & Technology, 35(6): 1149-1156.

Kogut, M.B. and Voelker, B.M., 2003. Kinetically inert Cu in coastal waters. Environmental Science & Technology, 37(3): 509-518.

Laglera, L.M., Battaglia, G. and van den Berg, C.M.G., 2007. Determination of humic substances in natural waters by cathodic stripping voltammetry of their complexes with iron. Analytica Chimica Acta, 599(1): 58-66.

Laglera, L.M. and van den Berg, C.M.G., 2003. Copper complexation by thiol compounds in estuarine waters. Marine Chemistry, 82(1-2): 71-89.

Laglera, L.M. and van den Berg, C.M.G., 2009. Evidence for geochemical control of iron by humic substances in seawater. Limnology and Oceanography, 54(2): 610-619.

Le Gall, A.-C. and van den Berg, C.M.G., 1993. Cathodic stripping voltammetry of glutathione in natural waters. Analyst, 118: 1411-1415.

Le Gall, A.-C. and van den Berg, C.M.G., 1998. Folic acid and glutathione in the water column of the North East Atlantic. Deep-Sea Research Part I-Oceanographic Research Papers, 45: 1903-1918.

Leal, M.F.C. and Van den Berg, C.M.G., 1998. Evidence for strong copper(I) complexation by organic ligands in seawater. Aquatic Geochemistry, 4(1): 49-75.

Li, Y.-H., Burkhardt, L. and Teraoka, H., 1984. Desorption and coagulation of trace elements during estuarine mixing. Geochimica et Cosmochimica Acta, 48: 1879-1884.

Liu, X. and Millero, F.J., 1999. The solubility of iron hydroxide in sodium chloride solutions. Geochimica et Cosmochimica Acta, 63(19-20): 3487-3497.

Luther III, G.W. and Ferdelman, T.G., 1993. Voltammetric characterization of iron(II) sulfide complexes in laboratory solutions and in marine waters and porewaters. Environmental Science & Technology, 27(6): 1154-1163.

Macrellis, H.M., Trick, C.G., Rue, E.L., Smith, G. and Bruland, K.W., 2001. Collection and detection of natural iron-binding ligands from seawater. Marine Chemistry, 76(3): 175-187.

Mawji, E. et al., 2011. Production of siderophore type chelates in Atlantic Ocean waters enriched with different carbon and nitrogen sources. Marine Chemistry, 124(1-4): 90-99.

Moffett, J.W. and Dupont, C., 2007. Cu complexation by organic ligands in the sub-arctic NW Pacific and Bering Sea. Deep-Sea Research Part I-Oceanographic Research Papers, 54(4): 586-595.

Moffett, J.W., Zika, R.G. and Brand, L.E., 1990. Distribution and potential sources and sinks of copper chelators in the Sargasso Sea. Deep-Sea Research Part A-Oceanographic Research Papers, 37: 27-36.

Muller, F.L.L. and Batchelli, S., 2013. Copper binding by terrestrial versus marine organic ligands in the coastal plume of River Thurso, North Scotland. Estuarine, Coastal and Shelf Science, 133: 137-146.

Oldham, V.E., Swenson, M.M. and Buck, K.N., 2014. Spatial variability of total dissolved copper and copper speciation in the inshore waters of Bermuda. Marine Pollution Bulletin, 79(1-2): 314-320.

Omanović, D., Garnier, C. and Pižeta, I., 2015. ProMCC: An all-in-one tool for trace metal complexation studies. Marine Chemistry, 173(0): 25-39.

Plavsic, M. et al., 2009. Determination of the Copper Complexing Ligands in the Krka River Estuary. Fresenius Environmental Bulletin, 18(3): 327-334.

Rijkenberg, M.J.A. et al., 2006. Iron-binding ligands in Dutch estuaries are not affected by UV induced photochemical degradation. Marine Chemistry, 100(1-2): 11-23.

Rozan, T.F., Lassman, M.E., Ridge, D.P. and Luther III, G.W., 2000. Evidence for iron, copper and zinc complexation as multinuclear sulphide clusters in oxic rivers. Nature, 406(6798): 879-882.

Rue, E. and Bruland, K., 2001. Domoic acid binds iron and copper: a possible role for the toxin produced by the marine diatom Pseudo-nitzschia. Marine Chemistry, 76(1-2): 127-134.

Rue, E.L. and Bruland, K.W., 1995. Complexation of iron(III) by natural organic-ligands in the central north pacific as determined by a new competitive ligand equilibration adsorptive cathodic stripping voltammetric method. Marine Chemistry, 50(1-4): 117-138.

Sander, S.G., Buck, K.N. and Wells, M., 2014. The effect of natural organic ligands on trace metal speciation in San Francisco Bay: Implications for water quality criteria. Marine Chemistry(0).

Schlosser, C. and Croot, P.L., 2009. Controls on seawater Fe(III) solubility in the Mauritanian upwelling zone. Geophysical Research Letters, 36.

Shank, G.C., Skrabal, S.A., Whitehead, R.F., Avery, G.B. and Kieber, R.J., 2004. River discharge of strong Cu-complexing ligands to South Atlantic Bight waters. Marine Chemistry, 88(1-2): 41-51.

Sholkovitz, E.R., Boyle, E.A. and Price, N.B., 1978. Removal of dissolved humic acids and iron during estuarine mixing. Earth and Planetary Science Letters, 40(1): 130-136.

Skrabal, S.A., Donat, J.R. and Burdige, D.J., 1997. Fluxes of copper-complexing ligands from estuarine sediments. Limnology and Oceanography, 42(5): 992-996.

Soli, A.L. and Byrne, R.H., 1989. Temperature dependence of Cu(II) carbonate complexation in natural seawater. Limnology and Oceanography, 34: 239-244.

Tang, D.G., Hung, C.C., Warnken, K.W. and Santschi, P.H., 2000. The distribution of biogenic thiols in surface waters of Galveston Bay. Limnology and Oceanography, 45(6): 1289-1297.

Turner, A., Nimmo, M. and Thuresson, K.A., 1998. Speciation and sorptive behaviour of nickel in an organic-rich estuary (Beaulieu, UK). Marine Chemistry, 63(1-2): 105-118.

Turner, D.R., Whitfield, M. and Dickson, A.G., 1981. The equilibrium speciation of dissolved components in freswater and seawater at 25oC at 1 atm. pressure. Geochimica et Cosmochimica Acta, 45: 855-882.

Turoczy, N.J. and Sherwood, J.E., 1997. Modification of the van den Berg/Ruzic method for the investigation of complexation parameters of natural waters. Analytica Chimica Acta, 354(1-3): 15-21.

Van Den Berg, C.M., 2014. UV digestion apparatus. http://pcwww.liv.ac.uk/~sn35/Site/UV_digestion_apparatus.html, pp. UV digestion apparatus.

van den Berg, C.M.G., 1982. Determination of copper complexation with natural organic ligands in seawater by equilibration with MnO2 II. Experimental procedures and application to surface seawater. Marine Chemistry, 11(4 SU -): 323-342.

van den Berg, C.M.G., 1984. Speciation of boron with Cu2+, Zn2+, Cd2+ and Pb2+ in 0.7 M KNO3 and in sea-water. Geochimica et Cosmochimica Acta, 48(12): 2613-2617.

van den Berg, C.M.G., 1995. Evidence for organic complexation of iron in seawater. Marine Chemistry, 50(1-4): 139-157.

van den Berg, C.M.G., 2006. Chemical speciation of iron in seawater by cathodic stripping voltammetry with dihydroxynaphthalene. Analytical Chemistry, 78(1): 156-163.

van den Berg, C.M.G., Merks, A.G.A. and Duursma, E.K., 1987. Organic complexation and its control of the dissolved concentrations of copper and zinc in the Scheldt estuary. Estuarine, Coastal and Shelf Science, 24(6): 785.

Velasquez, I. et al., 2011. Detection of hydroxamate siderophores in coastal and Sub-Antarctic waters off the South Eastern Coast of New Zealand. Marine Chemistry, 126(1-4): 97-107.

Weaver, R.S., Kirchman, D.L. and Hutchins, D.A., 2003. Utilization of iron/organic ligand complexes by marine bacterioplankton. Aquatic Microbial Ecology, 31(3): 227-239.

Wells, M.L., Trick, C.G., Cochlan, W.P., Hughes, M.P. and Trainer, V.L., 2005. Domoic acid: The synergy of iron, copper, and the toxicity of diatoms. Limnology and Oceanography, 50(6): 1908-1917.

Whitby, H. and van den Berg, C.M.G., 2014. Evidence for copper-binding humic substances in seawater. Marine Chemistry(published on-line).

Xue, H.B. and Sigg, L., 1999. Comparison of the complexation of Cu and Cd by humic or fulvic acids and by ligands observed in lake waters. Aquatic Geochemistry, 5(4): 313-335.

Yang, R. and Van den Berg, C.M., 2009. Metal complexation by humic substances in seawater. Environ Sci Technol, 43(19): 7192-7.

4

Chapter 4
Organic speciation of dissolved iron in estuarine and coastal waters at multiple analytical windows

This chapter is modified from: Mahmood, A., Abualhaija, M.M., van den Berg, C.M.G. and Sander, S., 2015. Organic speciation of dissolved iron in estuarine and coastal waters at multiple analytical windows. Submitted to Marine Chemistry.

4. ORGANIC SPECIATION OF DISSOLVED IRON IN ESTUARINE AND COASTAL WATERS AT MULTIPLE ANALYTICAL WINDOWS

Abstract

Competitive ligand exchange with cathodic stripping voltammetry (CLE-CSV) is commonly used to determine the speciation of iron and other metals in seawater. Here we use CLE-CSV with multiple analytical windows (MAWs) by varying the concentration of salicylaldoxime (SA) to determine the speciation of Fe in samples from the Mersey Estuary and Liverpool Bay. Data fittings obtained from individual titrations, simultaneously analysis of all windows using KINETEQL Multiwindow Solver (KMS) and KMS using single window were compared giving good agreements. The same results from different fitting approaches (within the standard deviation) were obtained and were compared with earlier published results (Abualhaija et al., 2015). Individual titration fitting as well as the MAW fitting demonstrated the presence of only one ligand in all samples. The ligand concentration behaved non-conservatively with increasing salinity, and was in excess of the iron concentration throughout the salinity range tested; it co-varied with the concentration of iron-binding humic substances (HS). Measurement of the composition of dissolved organic carbon (DOC) using 2-dimensional fluorescence scans indicates the presence of terrestrial as well as microbial sources of organic matter in the estuary. The fraction of HS in the DOC amounted to between 47 and 25 % between salinities of 19 and 31

4.1. Introduction

Iron (Fe) is an essential micronutrient for marine phytoplankton as it controls primary productivity in large regions of the open ocean; consequently it has a major influence on the global carbon cycle and climate (Boyd and Ellwood, 2010). The availability of this trace metal to biota is dependent on its speciation (Brand et al., 1983). The inorganic complexation of iron in natural waters is well known (Hudson et al., 1992). It is well established that iron is 99% bound to organic ligands in the ocean (Rue and Bruland, 1995; van den Berg, 1995), however, the composition and source of these ligands remain largely unknown (ligand soup) (Hunter and Boyd, 2007). The iron binding ligands may consist of specific compounds, such as siderophores produced by bacteria to enhance their iron acquisition, phytochelatins produced by organisms in response to toxic metal exposure, and of bioremineralization products like HS and exopolymeric substances (Boyd and Ellwood, 2010; Hassler et al., 2011; Wells et al., 2013).

Competitive ligand exchange–cathodic stripping voltammetry (CLE-CSV) is commonly used for metal complexation study. CLE-CSV measures the presence of natural metal complexing ligands because of the suppression of the response of the metal with an added competing ligand (AL). Several competing ligands with known stability constants for Fe such as 1-nitroso-2- naphthol (1N2N) (Gledhill and van den Berg, 1994; van den Berg, 1995), salicylaldoxime (SA) (Abualhaija and van den Berg, 2014; Rue and Bruland, 1995), 2-(2-thiazolylazo)-p-cresol (TAC) (Croot and Johansson, 2000) and 2,3-dihydroxynaphthalene (DHN) (van den Berg, 2006) have been used to determine the iron speciation.

Possible ligands are siderophores, exopolymer saccharides, heme and porphyrins (Gledhill and Buck, 2012; Hassler et al., 2011; Hunter and Boyd, 2007; Ibisanmi et al., 2011). Other possibilities are degradation products released during the decomposition of organic matter, bacterial degradation of sinking particles, photolysis ligand products of some high-affinity marine siderophores and bioremineralization products like humic substances, which have been suggested as weaker ligands (Hunter and Boyd, 2007; Wells et al., 2013).

In CLE-CSV the selection of the analytical window affects the detection of complexation parameters (Kogut and Voelker, 2001; van den Berg and Donat, 1992), where the window is determined by the complex stability of the competing ligand and the limit of detection. It has been suggested that the metal speciation can be improved by varying the detection window

(Pižeta et al., 2015). It is estimated that natural organic complexes are measured if the α-coefficient of the unknown complex (α_{ML}) is within a decade of either side of the α-coefficient of the competing ligands (α_{MAL}) (Ibisanmi et al., 2011; van den Berg et al., 1990). The effect of varying the detection window has been studied for Cu speciation in coastal (van den Berg et al., 1990; van den Berg and Donat, 1992) and estuarine waters (Buck and Bruland, 2005; Sander et al., 2015a) and for iron in seawater (Bundy et al., 2014; Ibisanmi et al., 2011) and estuarine-influenced shelf region (Bundy et al., 2015). Some of this work used TAC as competing ligand for Fe speciation (Ibisanmi et al., 2011) and SA was used by other work (Bundy et al., 2014; Bundy et al., 2015).

Other than the detection window, data analysis also has key importance in speciation results. Traditionally, the methods used for the determination of total ligand concentration and stability constants involve the fitting of titration data using linearization (Ružić, 1982; van den Berg, 1982) which is easily implemented in spread-sheet software, and non-linear data fitting can also be used (Gerringa et al., 1995) which may have the advantage to fit more than one ligand to the data. New approaches have also been suggested for simultaneous data-fitting of several detection windows (Hudson et al., 2003; Sander et al., 2011) and has been used for copper and iron (Bundy et al., 2015).

Early work (Boyle et al., 1977; Sholkovitz, 1976; Sholkovitz et al., 1978) on Fe across salinity gradients in estuarine systems described the scavenging of Fe (as iron oxyhydroxides) and humic substances (HS) due to co-precipitation at the mixing end of freshwaters and brackish waters, removing more than 90% of the dFe and lowering its concentration from 0.5–10 µmol/L in freshwaters (Nagai et al., 2007), to the 1–20 nmol/L range in coastal water (Laglera and van den Berg, 2009). The solubility of inorganic iron in seawater is extremely low (0.01 nmol/L) due to the formation of $Fe(OH)_3$ (Liu and Millero, 1999), which is about ~100 fold less than the concentration of Fe (0.1–0.8 nmol/L in seawater (Johnson et al., 1997; Kuma et al., 1996; Laglera and van den Berg, 2009). The aim of the present study was to measure the Fe-binding ligand parameters in Mersey River estuary and Liverpool Bay using MAWs.

We have tested here the KINETEQL Multiwindow Solver (KMS) (Hudson, 2014), to fit the speciation parameters of the MAW complexometric titrations as a unified dataset to calculate L_T and K'_{MLi} for *i* discrete ligand classes. We used recently optimised procedures and

stability constants for iron speciation in estuarine waters in the presence of SA (Abualhaija and van den Berg, 2014; Abualhaija et al., 2015). We compare the MAW data analysis to that obtained using individual titration using MCC software (Omanović et al., 2015) which compares curve fitting as well as linearization methods. The results are compared with earlier single window results (Abualhaija et al., 2015). The sources and sinks of Fe-binding ligand were analysed using a 2-D fluorescence spectroscopy technique.

4.2. Materials and Methods

4.2.1. Sampling site and sample collection

The Mersey estuary is located in north-west of England and extends from Warrington, where it receives freshwater from the River Mersey, to Liverpool Bay (47 km to the west) (Fig. 4.1). The estuary is divided into four zones: the upper estuary, the inner estuary, the narrows, and the outer estuary. The majority of the freshwater entering the estuary is from the rivers Mersey and Weaver, which drain a catchment area of approximately 4600 km^2. The estuary has a tidal range of up to 10 m, and the volume of water at high tide (35×10^7 m^3) is 50 times than that at low tide (0.7×10^7 m^3), resulting in a pronounced marine influence (Wilson et al., 2005).

Altogether 6 samples (station 1 – station 6) were collected from the Mersey estuary and one sample from Liverpool Bay (Fig. 4.1) during two cruises with the Liverpool University research vessel, *R.V. Marisa* in May 2013 (estuary) and April 2014 (Liverpool Bay).

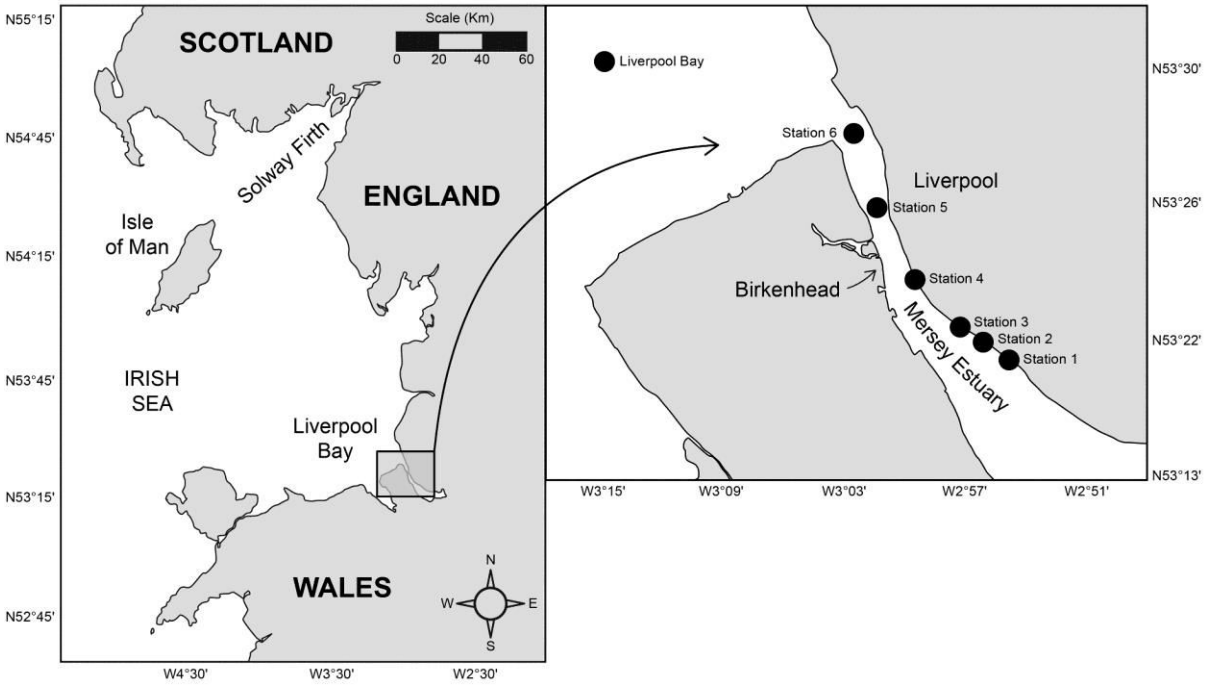

Figure 4.1. Map of sample locations in the Mersey estuary and Liverpool Bay

The hydrographic data for all the samples is given in Table 4.1. Samples were collected from near Pierhead at salinity 18.81 towards the mouth of the estuary with salinity 30.88. The seawater end-member sample was collected from Liverpool Bay at outgoing tide and had a salinity of 32.2. The average water temperature was 10.7 ± 0.23 °C.

Table 4.1. Hydrographic data for all the samples collected from Mersey estuary and Liverpool bay. Stations 1-6 were sampled May 2013 in the Mersey estuary, and the Liverpool Bay station was sampled in April 2014.

Stations	Salinity at 25°C	Time (GMT)	LAT (N)	LON (W)	Water depth (m)	Temp. (°C)
Station1	18.81	08:50	53° 21.527	2° 55.909	2.6	10.42
Station2	20.00	09:20	53° 21.889	2° 56.673	3.5	10.51
Station3	22.18	09:49	53° 22.171	2° 57.402	6.5	10.61
Station4	26.25	10:20	53° 23.821	2° 59.847	8.0	10.87
Station5	28.82	10:53	53° 25.211	3° 01.136	13.8	10.99
Station6	30.88	11:27	53° 26.792	3° 02.102	18.2	10.86
Liverpool Bay	32.20	11.53	53° 31.970	3° 21.077	24.0	10.86

Sample containers (1 L, low-density polyethylene (LDPE) bottles (Nalgene) were cleaned by soaking in 1 % detergent (Citranox, Fischer, UK) (one week), rinsed with milli-Q, soaked in 1 M HCl (two weeks), washed with milli-Q and left filled with 0.1 % HCl. 5 L carboys were high-density PE and were rinsed with 0.1 M HCl (reagent grade, Fischer UK) and MQ.

The samples for speciation analysis at MAWs were collected by peristaltic pumping into a 5 L polyethylene carboy, which was rinsed 3 times with the same water before filling. The suspended matter was allowed to settle overnight in the laboratory and the supernatant water was filtered through a 0.2 µm filter (Sartobran cartridge, Whatman) using a vacuum pump and stored in LDPE bottles in the dark at 4 °C until analysis (Batchelli et al., 2010). Separate samples from surface and subsurface (100 mL) were collected for fluorescence analysis, DOC and total dissolved nitrogen (TDN) measurements. For fluorescence analysis, the samples were filtered through pre-combusted GF/F filters (nominal pore size 0.7 mm) in an acid washed glass filtration assembly whereas samples for DOC and TDN were filtered using 0.2 µm filter. The filtrates were wrapped in aluminium foil, stored in the dark at 4 °C and were analysed within 5 days of samples collection.

Our MAW samples were collected concurrently with subsets of samples collected by (Abualhaija et al., 2015) to investigate the competition between copper and iron for humic ligands in estuarine waters. The author performed the speciation analysis using a single window (5 µM SA).

4.2.2. Reagents

All sample manipulation was done in a Class 100 laminar airflow bench at room temperature. Milli-Q (Millipore U.K) of 18.2 MΩ. cm resistivity was used to prepare reagents and dilutions. Iron solutions of different concentration were prepared by diluting 1000 ppm atomic absorption standard solutions (BDH, UK) and acidified to pH 2 with HCl. HCl (Trace analysis grade) and ammonia (electronic MOS grade) were purchased from Fisher Scientific and were used to adjust the pH. A stock solution of 0.1 M salicylaldoxime (SA) was prepared by dissolving SA in 0.1 M HCl. The SA was 98% purity from Acros organics, Fisher Scientific. The pH buffer contained 1 M boric acid and ~0.3 M ammonia in Milli-Q and gave pH 8.15 when added to seawater. Suwannee river HA (Standard II 2S101H) standard was from the

International Humic Substances Society (IHSS) and used for calibration. The stock solution contained 0.1 g HS /L in MQ water and was stored in the dark at 4 °C. pH measurements were done using a Metrohm model 713 pH Meter, and were calibrated against NBS pH buffers 4, 7 and 9.

4.2.3. Voltammetric equipment

Voltammetric apparatus consisted of a Metrohm 663 VA Stand connected to a μAutolab potentiostat, which was computer-controlled using the GPES 4.9 software. A hanging mercury drop electrode (HMDE) was used as working electrode; the reference electrode was Ag | AgCl | 3M KCl, while a glassy carbon rod was the auxiliary electrode. The apparatus was pressurised using compressed air at 1 bar; the mercury was filtered approximately every 2 months to remove Hg-oxides. Voltammetric measurements were made using the differential-pulse mode. Each sample was scanned 3 times, and an average value was taken as a peak height.

4.2.4. Determination of dissolved iron (dFe)

Samples were acidified and UV-digested to remove interfering surfactants and complexing ligands prior of measuring the dFe concentration: UV-digestion was 1 h using home-built apparatus with a 125-W high pressure mercury vapour lamp in PTFE-capped quartz tubes (Abualhaija and van den Berg, 2014). An aliquot of 10 ml was pipetted in a PTFE voltammetric cup, and the pH was neutralised using ammonia and pH buffer. The dFe concentration was measured by cathodic-stripping voltammetry (CSV) using 5 μM SA and 0.01 M borate buffer (Abualhaija and van den Berg, 2014). The water was air-purged (2 min.) prior to analysis to ensure saturation with air-O_2 to maximise the sensitivity (Abualhaija and van den Berg, 2014). The software was adapted to discard two (as opposed to 4) mercury drops prior to using the third mercury drop.

4.2.5. dFe speciation analysis

Fe-speciation was done by CLE-CSV in the presence of SA as a competing ligand (Buck

et al., 2007; Rue and Bruland, 1995) using the recalibrated method in the presence of air and overnight equilibration (Abualhaija and van den Berg, 2014). 200 mL of the sample were pre-mixed with buffer (2 ml 1 M borate buffer) and SA (final concentration between 5 and 50 µM) in a 250-ml Teflon bottle. Fe was added to capped polyethylene vials (Sterilin) in 12 steps; the 0-added Fe aliquot was in triplicate. 10-mL aliquots of seawater were pipetted into these vials and allowed to equilibrate overnight (Abualhaija and van den Berg, 2014). The detection window was varied in separate titrations by using [SA] of 5, 10, 15, 25 and 50 µM (W1 - W5). The vials were conditioned 3 times to the range of Fe concentrations used and sample salinity. The vials were used consistently in the same sequence and were not rinsed between repeated titrations for the same sample. Fe standard additions were the same for each sample across all windows. The vials were MQ-rinsed between samples. Reproducibility of repeated titrations, and regular increases in the response (smooth titrations), indicated that conditioning was complete. Rather than diluting the samples which could possibly change the speciation, a shorter deposition time (30 to 60 sec.) was used to stay within the linear range for low salinity samples (from stations 1 - 4), as those stations had high concentration of dFe. All titrations for a particular sample were measured at the same deposition time, except for one titration (sample from station 6, 5 µM SA) which was measured at a lower deposition time. In order to use the data for simultaneous analysis of all analytical windows, the titration data (station 6, 5 µM SA) was corrected using the ratio obtained from the modelled data (model is discussed in result and discussion section). The detection limit of the voltammeter was taken as 0.01 nA.

4.2.6. Calculation of $\alpha_{Fe'SA}$ at varying concentrations of SA

The conditional stability constants for complexation of Fe´ with SA vary as follows with salinity (Abualhaija et al., 2015).

$$K'_{Fe'SA} = (-2.98 \pm 0.18) \times 10^4 \times Sal + (4.60 \pm 0.04) \times 10^6 \quad (1)$$

$$\log B'_{Fe'SA2} = (-1.41 \pm 0.06) \times \log Sal + (12.85 \pm 0.07) \quad (2)$$

Values for the constants were calculated for all the samples collected at different salinities and used to calculate a value for $\alpha_{Fe'SA}$ from:

$$\alpha_{Fe'SA} = K'_{Fe'SA}[SA] + B'_{Fe'SA2}[SA]^2 \quad (3)$$

Values for log $\alpha_{Fe'}$, the inorganic α-coefficient of Fe in seawater, were calculated for each salinity at pH_{NBS} 8.15. These were between 10.3, at the lowest salinity, and 10.0 at the highest salinity.

4.2.7. Data processing of the ligand titrations

4.2.7.1. Data processing of individual titrations

The sensitivity (S) (nA /nM of Fe) of each complexing ligand titration was estimated from the slope of the CSV response at the highest three Fe additions. The data fitting for individual titration was performed using linearization and curve-fitting of the MCC software (Omanović et al., 2015) for one or two ligand model.

4.2.7.2. Simultaneous analysis of MAW data

The sensitivity of each individual complexing ligand titration was determined by internal calibration. As for each sample, titrations were performed by applying five different analytical windows i.e. 5, 10, 15, 25 and 50 µM SA (W1 - W5), thus, five different sensitivities were obtained from applied analytical windows to each sample (Table 4.2). The analytical window yielded the highest sensitivity (S_{max}) was used to set the R_{AL} (Hudson et al., 2003) (R_{AL} = ratio of sensitivity at a given analytical window to the highest sensitivity (S_{max})). For windows with lower sensitivities, the sensitivities were normalized (R_{AL}) to the maximum sensitivity using experimentally determined values for each sensitivity. For example, for the sample collected from station 1, the obtained sensitivities for five different analytical windows were 1.29, 1.16, 1.14, 1.12 and 0.51 (Table 4.2). The highest sensitivity (S_{max} = 1.29) obtained from 5 µM SA window, thus, being the highest, (S_{max} = 1.29) was used to set the R_{AL} for this window as 1 and the R_{AL} values (R_{AL} = S/ S_{max}) other applied analytical windows to the same samples were calculated as 0.9, 0.88, 0.87 and 0.4.

After fixing the R_{AL}, KMS speciation model (Hudson, 2014) was used for the simultaneous analysis of all the data obtained by applying MAWs to the same sample. In KMS model, a two-step optimization sequence was utilized to run the MAW data sets. The first step to run the model by given inputs which include the observed current (Ip), total

[dFe], added [SA], conditional stability constant of dFe with SA (K'_{FeSA} and K'_{FeSA2}), $\alpha_{Fe'}$, S_{max} as an initial sensitivity and the R_{AL} values calculated for all the windows. Besides that, initial guesses were also given for the parameters to be determined (K'_{FeLi} , $[L_T]$ and S_{fitted}). After running the first step, in second step, the values of the fitted parameters (K'_{FeLi} , $[L_T]$ and S_{fitted}) were optimised by repeatedly running the data-fitting program. The optimisation was iterated with different initial guess values to minimise the root-mean-square error (RMSE) between the observed current (Ip) and the calculated current (Ip^{calc}) using the Solver function.

4.2.8. Determination of humic substances (HS) and organic matter

The concentration of Fe-binding humics was determined by CSV method (Laglera et al., 2007) at pH_{NBS} 8.15 in the presence of bromate, and calibrated on the mg /L scale against Suwannee River HA. Fe was added (50 nM) to saturate all the free HS to maximise the sensitivity.

To track the sources and quality of dissolved organic matter (DOM), fluorescence indices were calculated for all the surface and subsurface samples using a Horiba (Jobin Yvon) spectrofluorimeter FluoroMax-4 with a 1 cm path-length quartz cuvette. The MQ blank was subtracted from all the scans. Three fluorescence indices were determined as follows: the fluorescence index (FI) (Johnson et al., 2011; McKnight et al., 2001), the humidification index (HIX) (Zsolnay et al., 1999) and the index for freshly produced autochthonous DOM or biological index (BIX) (Huguet et al., 2009).

FI Indices were calculated using following relationships:

$$FI = \frac{Icorrected\ (370 : 450)}{Icorrected\ (370 : 500)}$$

where FI is the ratio of corrected fluorescence intensities at 370:450 and 370:500 (excitation: emission wavelengths in nm). The FI index serves as a proxy for the relative amount of DOM derived from ex situ as well in situ sources (McKnight et al., 2001). Values of 1.4 or less are typical for isolated humic substances or samples with dominantly terrestrial origin, with greater DOM aromaticity, while values of 1.9 or higher are demonstrative of microbial sources and lower aromatic carbon content (Johnson et al., 2011; McKnight et al., 2001).

The emission-based biological index (BIX) was determined at an excitation wavelength of 310 nm. This index is used to assess the relative contribution of microbially-derived DOM in water samples (Huguet et al., 2009). Values > 1 correspond to freshly produced DOM of biological or microbial origin, whereas values of 0.6 and lower will contain little biological material (Huguet et al., 2009; Jaffé et al., 2004).

$$BIX = \frac{Icorrected\ (310:380)}{Icorrected\ (310:430)}$$

where Icorrected is the corrected fluorescence intensity at 310:380 and 310:430 (excitation: emission wavelengths in nm).

Another emission-based index, the humidification index (HIX) was calculated from the ratio of two integrated sections of an emission scan at an excitation wavelength of 255 nm:

$$HIX = \frac{Sum\ of\ Intensities\ (430-480)}{Sum\ of\ Intensities\ (300-340)}$$

Humification of DOM alters the structure of the molecules of organic matter, which leads to an increase in the DOM aromaticity thus reducing its availability for microbial utilization. Low HIX values (<10) correspond to relatively non-humified DOM derived from biomass (Banaitis et al., 2006; Ohno et al., 2007). Humic substances isolated from soils, surface waters and coal show ranges of HIX values of 10 - 30, 20 - 50 and >50, respectively (Birdwell and Engel, 2010). HIX has direct correlation with DOM aromaticity and inverse correlation with carbohydrate content (Kalbitz et al., 2003). Literature values with FI range (1.2 - 1.6) along with HIX range (5 - 20) and BIX (0.58 - 1.22) is typical for organic matter released from sediment (Birdwell and Engel, 2010). Low values of HIX and high values of BIX and FI in water represent fluorescence that is water soluble, extracellular substances excreted by microorganisms, detritus resulting from cell death, and aquatic organic matter less humified than surface water organics, possibly due to a lack of exposure to solar radiation (Stedmon and Markager, 2005).

To measure DOC and TDN, aliquots of 0.2 µm filtered samples were acidified to pH 2 and concentrations were measured by high temperature catalytic combustion using a Shimadzu TOC-VCPH/CPN Total Organic Carbon Analyser equipped with an ASI-V autosampler and a TNM-1 module. Prior to analysis, the acidified samples were purged with synthetic air to remove dissolved inorganic carbon. L-arginine solutions ranging from 5 to

500 µmol C/L and 6.6 to 333.3 µmol N/L, respectively, were used for calibration and deep Atlantic seawater reference material (DSR, D.A. Hansell, and University of Miami, Florida, USA) was measured during each run to ensure the instrumental precision and accuracy.

4.3. Results and discussions

4.3.1. Investigating the effect of increasing detection window onto titrations through modelling

We have modelled titrations of seawater with iron at various detection windows. The ligand concentration in the water was set to 50 nM and log $K'_{Fe'L}$ to 11.6, which is realistic for estuarine waters, and we used recently calibrated constants for FeSA and $FeSA_2$ (Abualhaija et al., 2015). The results of modelling data are presented in Fig. 4.2 which shows that the detection window at 5 µM SA has the greatest whereas 50 µM SA window has the lowest sensitivity. The modelled data also shows (Fig. 4.2) that whilst the detection window at 5 µM SA has the greatest sensitivity (steepest increase in the peak height when the iron concentration is greater than the ligand concentration), the relative peak heights are reversed for lower iron concentrations: the peak height is lowest at 5 µM SA and greatest at 50 µM SA when [Fe] < 50 nM. At low Fe concentrations ([Fe] < L_T), and at high (SA), dissociation of FeL compensates for the decreased sensitivity (insert b, Fig. 4.2). The model shows that titrations at 5 µM SA show the inflection point at ligand saturation more clearly than at higher [SA], which should improve the quantification of L; on the other hand, a higher peak height at higher [SA] when [Fe] < L could improve the quantification of the complex stability.

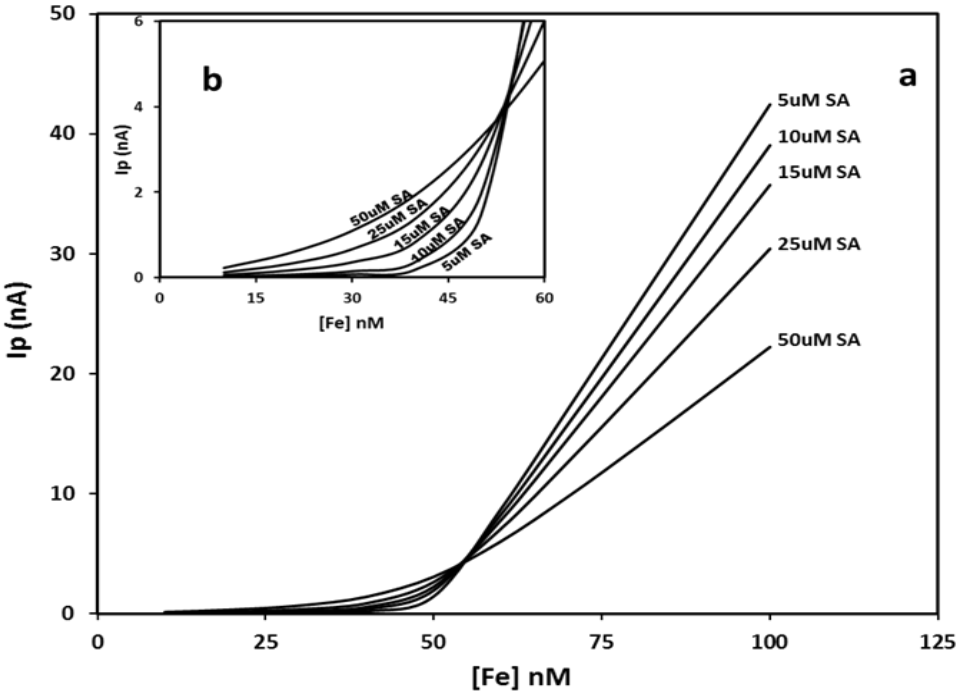

Figure 4.2. Modelled titrations at varying detection windows. a) The α-coefficient for FeSA was varied by increasing [SA] from 5 to 50 µM SA. Highest sensitivity is obtained at highest [SA] (50 µM SA) when Fe < L whereas at Fe ≥ L, the highest sensitivity was obtained at lowest window (5 µM SA); b) the zoomed portion of modelled titrations when Fe < 50 nM.

4.3.2. Complexing ligand determination in estuarine water at various detection Windows

The complexing ligand concentration in each sample was determined by titrations at 5 detection windows defined by setting the concentration of the competing ligand (SA) at 5, 10, 15, 25 and 50 µM. The complete dataset for each sample consisted of five titration curves, except the Liverpool bay sample, which was titrated at two detection windows (5 and 15 µM SA). The α-coefficient for Fe complexation with SA at each concentration of SA and salinity are summarised in Table 4.2. The α-coefficient varied by a factor of ~21 at a salinity of 18.8 (from $\alpha_{Fe'SA}$ = 23 to 485), and a factor of ~16 at a salinity of 31 (from 20 to 325) (Table 4.2).

Table 4.2. Fe-speciation parameters obtained from individual analytical window applied to each station using van den Berg (vdB) linearization (ProMCC program).

	Analytical Window	($\alpha Fe'SA$)	$logK'_{Fe'L}$	$[L_T]$	Slope	[Fe´]
Station 1*	5 µM SA	23.0	11.75±0.15	113±7.1	1.29	5.16E-21
	10 µM SA	52.8	12.02±0.16	119±8.8	1.16	2.23E-21
	15 µM SA	86.1	12.46±0.15	99.1±2.9	1.14	1.79E-21
	25 µM SA	171.8	12.50±0.12	115±5.0	1.12	8.4E-22
	50 µM SA	485.1	11.60±0.17	138±15.0	0.51	4.07E-21
	Average		**12.1±0.4**	**117±14**		
Station 2*	5 µM SA	22.6	11.52±0.09	84.1±3.9	0.97	6.08E-22
	10 µM SA	50.5	11.57±0.09	95.1±5.9	0.82	3.79E-21
	15 µM SA	83.5	11.90±0.15	81.7±5.8	1.02	2.66E-21
	25 µM SA	165.0	11.87±0.23	65.8±3.1	0.60	7.69E-21
	50 µM SA	460	10.30±0.08	77.2±6.3	0.23	1.37E-19
	Average		**11.4±0.7**	**80.8±10.7**		
Station 3*	5 µM SA	22.0	10.30±0.04	63.0±2.8	1.02	7.79E-20
	10 µM SA	48.4	10.70±0.01	67.6±0.1	1.00	8.88E-20
	15 µM SA	79.3	10.90±0.01	63.2±0.1	1.26	2.41E-20
	25 µM SA	154.6	10.60±0.01	68.0±0.3	0.82	1.41E-20
	50 µM SA	421	11.06±0.04	90.0±3.0	0.71	7.95E-21
	Average		**10.5±0.3**	**70.4±11.2**		
Station 4**	5 µM SA	20.9	12.61±0.40	47.8±3.9	1.45	4.79E-22
	10 µM SA	45.3	11.73±0.04	54.3±1.0	1.65	2.96E-21
	15 µM SA	73.2	13.30±0.01	50.9±0.1	2.45	1.02E-22
	25 µM SA	139.7	12.04±0.06	61.5±2.5	2.72	1.24E-21
	50 µM SA	368	12.62±0.18	50.8±4.4	1.01	4.37E-22
	Average		**12.4±0.6**	**53.1±5.2**		
Station 5***	5 µM SA	20.3	11.70±0.42	38.2±3.6	0.93	4.28E-21
	10 µM SA	43.6	11.76±0.10	41.1±0.1	1.44	3.79E-21
	15 µM SA	70.1	12.40±0.14	43.0±2.6	1.34	7.44E-22
	25 µM SA	132.3	12.20±0.01	41.8±0.1	1.90	1.66E-21
	50 µM SA	342	12.07±0.01	43.9±0.1	0.77	1.49E-21
	Average		**12.0±0.3**	**41.6±2.2**		
Station 6****	5 µM SA	19.8	12.23±0.30	30.8±2.5	3.42	1.62E-22
	10 µM SA	42.5	11.90±0.15	36.0±2.8	3.32	2.02E-22
	15 µM SA	67.9	12.85±0.43	31.0±3.9	3.28	3.78E-23
	25 µM SA	127.2	12.63±0.30	32.1±3.0	2.71	5.16E-23
	50 µM SA	325	12.59±0.10	41.4±2.9	1.87	3.02E-23
	Average		**12.4±0.4**	**34.3±4.5**		
Liverpool Bay***	5 µM SA	19.5	11.48±0.3	5.07±0.18	10.02	5.94E-20
	15 µM SA	66.6	11.64±0.06	8.40±0.30	8.65	3.07E-21
	Average		**11.6±0.2**	**6.7±2.4**		

*Deposition times: 30sec. **Deposition time: 60sec.

*** Deposition time: 90sec. ****Deposition time:120sec.

The titrations from two samples (station 2, salinity 20; station 6, salinity 31) are shown in Fig. 4.3. For sample from station 2, the expected order of the curves (which is also the order of the sensitivities) was not achieved as the greater sensitivity (S) was observed for 15 µM SA rather than at 5 µM SA (Fig. 4.3 and Table 4.2): S (15 µM SA) > S (5 µM SA) > S (10 µM SA) > S (25 µ M SA) whereas the expected order of curves was attained for sample from station 6: S (5 µM SA) > S (10 µM SA) > S (15 µM SA) > S (25 µM SA > S (50 µM SA). The obtained irregular variation in S was ascribed to possible surfactant effects including humic substances and other organic matter in the water, which apparently had a different influence at different concentrations of SA. For all the samples, the difference between the sensitivities at 5, 10 and 15 µM SA was small at stations 1, 2, 3, 5 and 7 (Liverpool Bay) whereas the expected decrease from [SA] > 5 µM was observed for stations 1, 6 and 7.

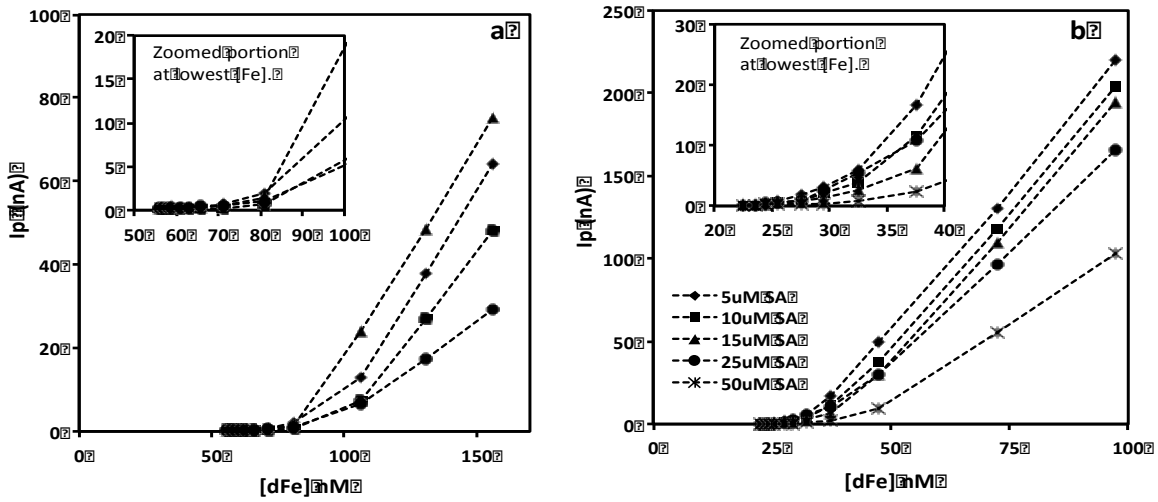

Figure 4.3. Titrations of complexing ligands from two different stations of Mersey estuary; a) Sample from station 2 ligand titration performed at 4 detection windows (5 - 25 µM SA) as 50 µM SA window was not used for simultaneous analysis of data, the maximum sensitivity was obtained at 15 µM SA window; b) Ligand titrations performed to sample collected from station 6, expected curve of sensitivities obtained.

Another complicating factor in titrations using SA is that the sensitivity decreases with increasing SA concentration due to competition by $FeSA_2$ which is non-electroactive (Abualhaija and van den Berg, 2014). This is counter to intuition as the α-coefficient for complexation of Fe with SA increases with increasing [SA] whilst at the same time the sensitivity decreases when [SA] > 5 µM (at salinity ~35). Also, it differs from the change in the CSV-sensitivity for Cu which always increases with increasing [SA] (Lucia et al., 1994).

4.3.3. Data fitting of individual titrations

Ligand concentrations and stability constants were fitted to individual titrations by linear and non-linear data fitting at each detection window using MCC software (Omanović et al., 2015) which compares three different procedures and also corrects S for under-saturation of L. The results for the individual titrations at each detection window are summarized in Table 4.2. Each titration consisted of 12 data points which is sufficient for fitting up to two ligands (Gerringa et al., 2014) depending on the data quality. It was attempted to fit titrations data to one and two ligands. To fit the data for one ligand model, van den Berg linearization approach was chosen. Concentrations of labile Fe were calculated from the peak-height and the sensitivity (S) which is equivalent to [Fe-SA], the sum of [FeSA] and [$FeSA_2$], and free Fe ([Fe´]). The plots of [labile Fe] / [FeL] versus [labile Fe] (Ružić, 1982; van den Berg, 1982) were linear for all titrations of individual samples, indicating that a single ligand was dominating the speciation of Fe over the tested detection window in each sample. To verify whether nevertheless two ligands could be resolved, titrations were also analysed by non-linear data fitting. Data fitting was not improved by fitting more than one ligand to the titrations: in each case the standard deviation increased, and the concentration of one of the ligands was inconsistent between samples and unrealistically large or small. This confirmed that in each sample a single ligand was responsible for complexation with Fe, with any other ligands having an insignificant effect on the Fe speciation.

If more than one ligand is present in the water, and if these are not resolved by individual titrations, then a trend would be expected when the detection window is varied (van den Berg and Donat, 1992): a higher detection window would be expected to find a shift in the value of the complex stability or in the ligand concentration, or both. The α-coefficient for complexation of various metals has been shown to increase with the detection window and titrations at different detection windows appeared to show this for copper (van den Berg and Donat, 1992). Our present work did not show such a trend: comparison of the values for [L], $K'_{Fe'L}$ and [Fe´] (Table 4.2) from individual titrations at increasing detection window showed experimental variability but no systematic trends, suggesting that Fe speciation is here dominated by just one ligand. Further, the ligand concentration in each sample was calculated by averaging the result of the five titrations, and was found to have a standard deviation of typically 16 % or less (Table 4.2, Fig. 4.4),

except for the Liverpool bay station which had a standard deviation of 36 % at a much lower ligand concentration. The consistency of the ligand concentrations also suggests that the same ligand was found at each detection window, and that any other ligand (which could be expected to be present) was not detected either because it has a much lower concentration than the main ligand, or binds the metal much weaker so that competition is negligible, or both.

A different data fitting method (Hudson, 2014) was used to simultaneously fit all titrations carried out at different concentrations of SA to verify whether more than one ligand could be fitted using that software.

4.3.4. Data fitting using KMS model

The KMS program fits values for the parameters (L and K for one or more ligands) by minimization using Solver of the residual error of the modelled and real data (Hudson, 2014). An advantage of this program is that it uses all the data points obtained at various concentrations of the competing ligand (SA), simultaneously and therefore has up to ~60 data pairs to calculate the complexing ligand parameters for *i* discrete ligand classes (For example, for simultaneous fitting, the total data points used for different stations were as follow: sample from station 1, 60 data pairs; 64 data pairs for station 3 and 4 each whereas 47 data pairs were used for station 2 & 5 (only (W1 - W4) were used , W5 was excluded from simultaneous fitting); 55 data pairs for station 6 and for Liverpool Bay 21 data pairs from two windows). A drawback is that the program does not produce a standard deviation and instead we used the residual error to verify whether data-fits for more than one ligand improved the data fitting (Sander et al., 2011). The initial data-guess was varied to check its effect on the values found and the effect on the calculated ligand concentration was very small (the spread is shown in Table 4.3 and Fig. 4.4), much less than the standard deviations of the individual data-fits. Attempts were also made to fit the data for four parameters ($\log K'_{FeL1}$, $\log K'_{FeL2}$, $[L_1]$ and S_{fitted}) excluding the estimations for $[L_2]$, but no improvement was observed in RMSE value. Other than that, the obtained values for $\log K'_{FeL2}$ were very small (data not shown). Further, the data from each sample was attempted to fit for five parameters (($\log K'_{FeL1}$ $\log K'_{FeL2}$, $[L_1]$, $[L_2]$ and S_{fitted}), but this caused the residual error to increase confirming the absence of a significant second ligand. Forcing a data-fit to two

ligands was found to produce large variability in the concentrations found for L_2 with repeated calculations. The two-ligand data fittings were therefore considered to be unrealistic and confirmed the individual titration fitting that a single ligand dominated the speciation of Fe (Table 4.3). The presence of any other ligand class was undetectable either due to much lower concentration of that ligand than the main ligand or due to much weaker binding strength of that ligand for Fe, or both.

For each sample, other than simultaneous analysis of all the titrations as a unified dataset, the KMS model was also run for 5 µM SA (W1) window only from each station. The R_{AL} was taken as 1 for individual window analysis and the obtained results were compared with simultaneous analysis of all windows as unified dataset (Table 4.3).

Comparison of the ligand concentrations obtained using KMS (W1 – W5), KMS (W1) and the averaged results obtained from individual titrations showed good agreement (Fig. 4.4 and Table 4.3). Further, the results were also compared with results reported by Abualhaija et al. (2015) (Fig. 4.4 and Table 4.3). The difference between the ligand concentration of the different data fitting methods was <15 % but it was systematic: The results obtained from simultaneous fitting of all the windows were, on average 10 % higher than the values obtained from single window (W1) for all the stations whereas the difference was ≈ 25 % for Liverpool Bay sample. The range in the values obtained by varying the initial guess-values using KMS was narrow (range < 1 %), compared to an experimental standard deviation of 10 – 30 % in the ligand concentrations in the individual titrations (Table 4.3). The value obtained using KMS was often within the experimental standard deviation. It is tempting to suggest that the MAW titrations may have led to better optimization of the sensitivity but the comparative titrations at various detection windows (Table 4.2) showed no systematic increase when the detection window was increased. The KMS values obtained from simultaneous analysis of all the windows as a unified dataset as well as KMS (W1) results are used here for further interpretation of the data.

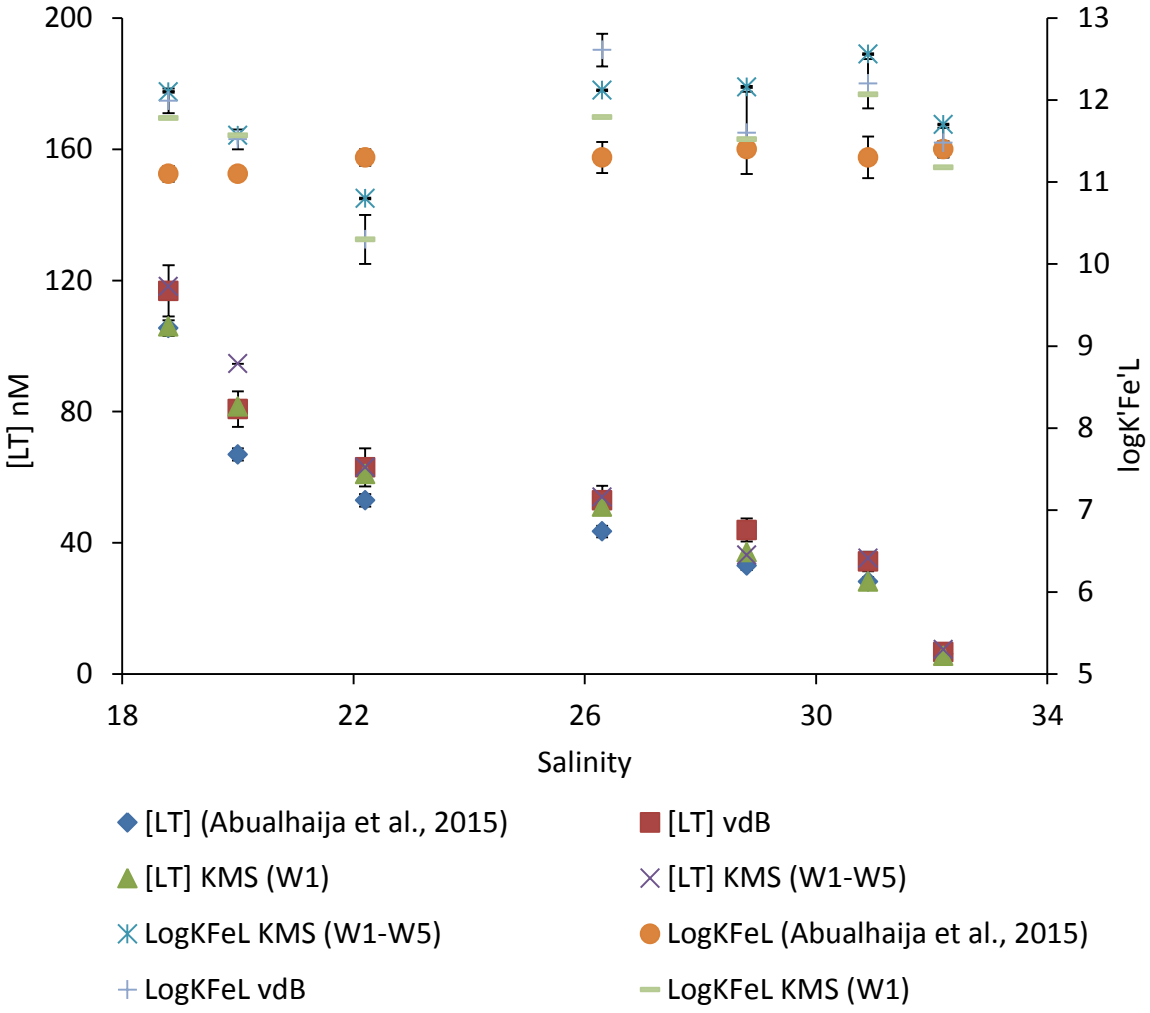

Figure 4.4. Comparison of Fe complexing ligand parameters through the estuary as calculated from MAWs using the average of individual titrations fitted by van den Berg linearization (MCC), using the simultaneous fitting of MAWs (W1 – W5) by KMS, using the single window (W1) fitted in KMS. Earlier published results on same samples by (Abualhaija et al., 2015) also included in the comparison.

Table 4.3. Comparison of Fe-speciation parameters obtained for each station; 1) averaged parameters obtained from individual analytical window from vdB linearization (MCC software); 2) parameters obtained by analysing 5 µM SA (W1) analytical window for one ligand model in KMS; 3) simultaneous analysis of all (meaningful) analytical windows using a one ligand model in KMS. None of the stations showed a significantly better fit for two ligand model and results are thus not considered reliable and are not reported; 4) our results were compared with earlier published results (Abualhaija et al., 2015).

		(Abualhaija et al., 2015) vdB Linearization (MCC)		vdB linearization (MCC) (average value from the individual titrations)		KMS (W1) 5 µM (SA)					KMS (W1-W5)				
Stations	**dFe (nM)**	**$[L_T]$**	**$logK'_{Fe'L}$**	**$[L_T]$**	**$logK'_{Fe'L}$**	**$[L_T]$**	**$logK'_{Fe'L}$**	**S_{Fitted}**	**S**	**RMSE**	**$[L_T]$**	**$logK'_{Fe'L}$**	**S_{Fitted}**	**S_{max}**	**RMSE**
Station 1	83.5±3.8	105±1.0	11.1±0.09	117±14	11.99±0.15	105.96±0.80	11.8	1.08	1.29	0.10	118.20±0.80	12.1	1.08	1.29	0.38
Station 2*	51.0±1.2	67±0.8	11.1±0.06	80.8±10.7	11.52±0.12	81.54±0.003	11.6	1.07	0.97	0.06	94.60±0.01	11.6	1.07	1.02	0.28
Station 3	40.3±0.5	53±1	11.3±0.13	70.4±11.2	10.30±0.30	61.00±0.01	10.3	1.07	1.02	0.04	57.22±0.01	10.8	1.25	1.26	0.26
Station 4	35.0±1.0	43±0.5	11.30±0.07	53.1±5.2	12.61±0.40	47.50±0.10	11.9	1.07	1.43	0.13	52.60±0.01	12.3	1.80	2.75	0.33
Station 5*	20.1±2.8	33±0.3	11.40±0.05	41.6±2.2	11.60±0.50	37.20±0.08	11.5	0.93	1.07	0.15	36.23±0.08	12.2	1.70	1.93	0.27
Station 6	22.5±1.3	28±0.1	11.3±0.11	34.3±4.5	12.20±0.30	28.20±0.01	12.1	2.10	3.32	0.12	35.33±0.01	12.6	3.63	3.42	0.40
Liverpool Bay	4.8±0.5	6±0.1	11.30±0.06	6.7±2.4	11.48±0.20	5.57±0.01	11.2	9.75	10.02	0.02	7.49±0.01	11.7	9.75	10.02	0.21
Average			11.2±0.1		11.7±0.7		11.5±0.6					11.9±0.6			

* Four windows (W1 –W4), excluding W5, were used for simultaneous analysis in KMS

4.3.5. Variations in log K

The complex stability of Fe-L complexes ($logK'_{Fe'L}$) in the present study was found between 10.8 and 12.6 for (KMS (W1-W5)) and in the range from (10.3 - 12.1) for KMS (W1), and was without a systematic salinity trend (Table 4.3 and Fig. 4.4). Averaging of the $logK'_{Fe'L}$ values gave a value of 11.9 ± 0.6 for (KMS (W1 - W5)) and 11.5 ± 0.6 for KMS (W1). This complex stability is similar to that (between 11.1 and 11.6) for terrestrial humic acid (Abualhaija and van den Berg, 2014; Laglera and van den Berg, 2009) and similar to that (11.3) for terrestrial humic substances in estuarine, black-river waters (Batchelli et al., 2010). Similar complex stability (between 11 and 12) has been found elsewhere for ligands in coastal waters (Bundy et al., 2015), estuarine waters (Croot and Johansson, 2000; Gerringa et al., 2007; Gledhill et al., 2015) and oceanic waters (Ibisanmi et al., 2011; Sander et al., 2015c; Velasquez et al., 2011). The ligands from estuarine origin therefore are similar to terrestrial HS. Nevertheless, ligands with values for log $K'_{Fe'L}$>12 have been found in estuarine-influenced shelf waters (Buck et al. 2007). Therefore the reported variability for complex stability is high.

The spread of reported complex stabilities for ocean waters is even larger than in estuarine water; 9-11 (Gledhill and van den Berg, 1994), 13 (Rue and Bruland, 1995), 12 (Boye et al., 2001), 11.5 (Ibisanmi et al., 2011), 11-14 (Witter et al., 2000), and 10.3 to 11.4 (Buck and Bruland, 2007). But the more recent papers from oceanic waters (Buck and Bruland, 2007; Ibisanmi et al., 2011; Sander et al., 2015c) reported complex stability in between 11 to 12, which is a narrower range than in earlier published papers (complex stability in a range of 9 to 14) (Gledhill and van den Berg, 1994; Rue and Bruland, 1995; van den Berg, 1995; Witter et al., 2000), the recent studies are reporting a complex stability for ligands that is similar to that found for terrestrial HS. However, it may be too early to generalise complex stability as the complex stability of SA has been calibrated only very recently in seawater (Abualhaija and van den Berg, 2014) and extended to estuarine water (Abualhaija et al., 2015).

4.3.6. Comparison of dFe with ligands

The MAW speciation experiments showed that these estuarine waters are dominated by one ligand and that this ligand class originates in low salinity waters and are diluted by seawater. (Abualhaija et al., 2015) have shown that iron and the ligand concentration co-vary in the Mersey waters, their concentration decreasing in a non-linear fashion with increasing salinity at a constant ratio of 0.8, which means that ~20 % of the ligand is free. We have compared our KMS (W1 – W5) and (KMS (W1)) results with earlier reported results (Abualhaija et al., 2015) (Fig. 4.5a). The results obtained from KMS (W1) (y = 0.75x) were in close agreement with earlier reported results by (Abualhaija et al., 2015) whereas the calculated ligand concentration was 15% greater (y = 0.65x) when all the windows were analysed simultaneously in KMS.

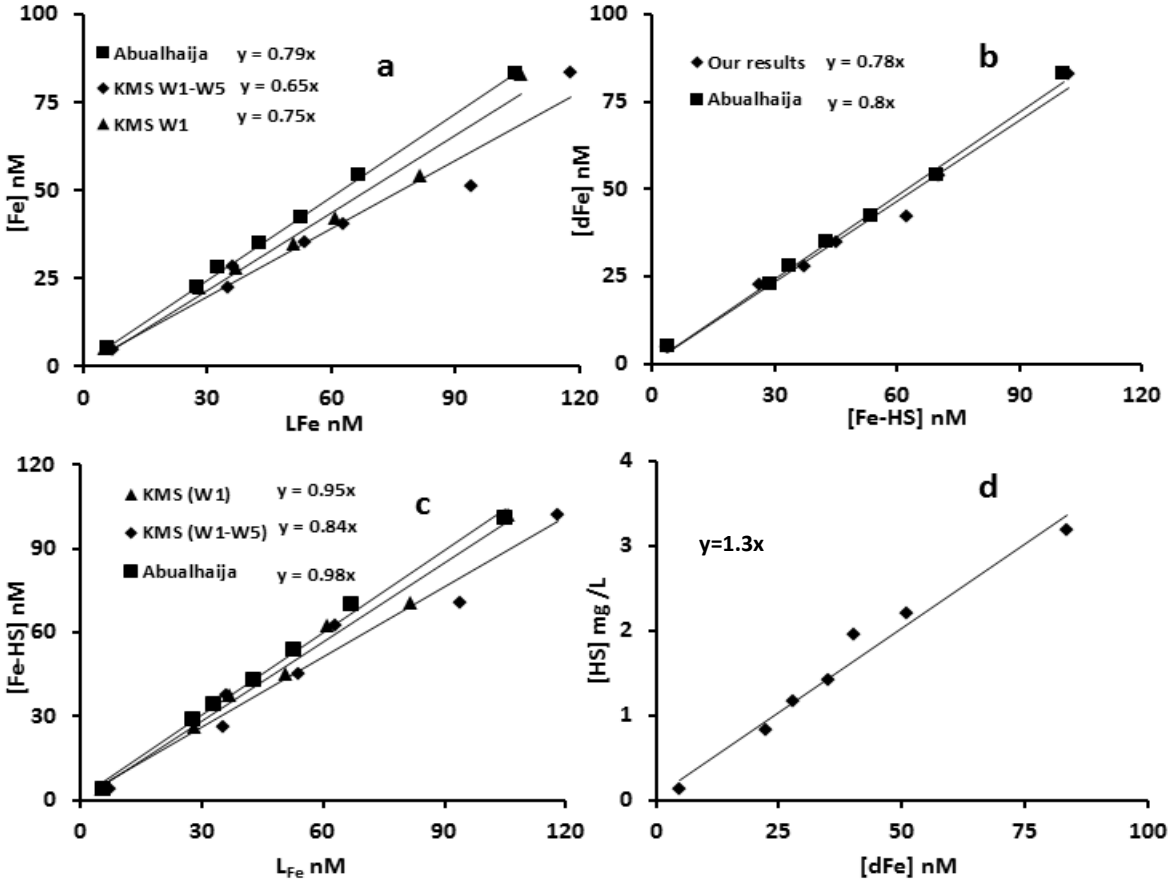

Figure 4.5. Plot showing the correlations **a)** [dFe] nM with [L_T] nM obtained from simultaneous MAW (W1 – W5) fitting by KMS, single window (W1) fitted by KMS and [L_T] nM published by (Abualhaija et al., 2015); **b)** [dFe] nM as a function of [Fe-HS] nM and compared with earlier published results by (Abualhaija et al., 2015); **c)** [Fe-HS] nM as function of [L_T] nM obtained from simultaneous fitting of MAWs (W1 – W5) by KMS, single window (W1) fitted by KMS and [L_T] nM published by (Abualhaija et al., 2015); **d)** [HS] mg /L as a function of [dFe] nM.

Previous studies have shown that 1 mg HS was equivalent to 30.6 ± 0.6 nM of Fe-binding ligands (Abualhaija and van den Berg, 2014). This value was used to convert voltammetrically measured Fe-binding HS into nM. A diagram of [Fe-HS] as function of [L_T] obtained from KMS (W1) shows a linear relationship with a slope of near unity (y = 0.95x) with an intercept that is <1 nM ligands giving a good indication that nearly the entire ligand concentration for Fe consists of HS. The slope value found from [Fe-HS] plot with [L_T] obtained from KMS (W1 – W5) was slightly low (y = 0.84x) (Fig. 4.5c), probably due to excess ligand concentrations detected by simultaneous analysis of all the dataset. A plot of [Fe-HS] (nM scale) as function of Fe (Fig. 4.5b) shows a linear relationship with a slope of (y = 0.78x) which is similar to the slope of ligands (KMS (W1)) with [Fe] (Fig. 4.5a), confirming that the major portion of ligands that control Fe in the Mersey estuary are humic substances. Our results are in agreement with earlier published results (Abualhaija et al., 2015).

Within the Mersey river estuary, the dFe speciation is highly controlled by a large excess of [L_T] with log $K'_{Fe'L}$ in the range of 10.8 - 12.5. The concentration of both dFe and [L_T] was highest at lowest salinity (18.8), then the concentration declined dramatically from station 1 to station 2 almost 39 % decrease in the concentration of dFe and around 21 % in [L_T] was seen. The relevant work conducted for such kind of environment has revealed that the loss of dissolved Fe is most obvious for lower salinities likely due of flocculation of dFe at these salinities (Boyle et al., 1977; Sholkovitz, 1976; Sholkovitz et al., 1978). The mixing pattern of [L_T] with salinity suggests that organic ligands were conservative at station 1 but suddenly a small increase in salinity turned their conservative behavior into non-conservative. From station 2 to onward, a small gradual decrease in [L_T] along with [dFe] within the estuary was noticed. Since the concentrations of both dFe and [L_T] are highly correlated so it is anticipated that L could also be lost due to flocculation at lower salinity and later on due to dilution. From the correlation (Fig. 4.5a, $r^2 \simeq 0.97$; Fig. 4.5b, $r^2 \simeq 0.98$), it is also evident that [L_T] were fully saturated with dFe thus supporting the earlier work which suggested that DOM especially humic acid plays an important role in the flocculation of Fe during river–ocean mixing through estuaries.

Previous work on estuarine and river waters (Buck et al., 2007; Bundy et al., 2015; Jones et al., 2011; Powell and Wilson-Finelli, 2003) reported strong organic complexation of Fe. Some work found only one ligand class in rivers (Jones et al., 2011; Powell and Wilson-

Finelli, 2003). Pore water of sediments was thought to be the dominant source of Fe-complexing ligands in the Satilla River estuary (Jones et al., 2011). The concentration of iron has been found to co-vary with the ligand (Buck et al., 2007) and the ligands are thought to be affected by photochemical processes (Powell and Wilson-Finelli, 2003). Coastal sources of a strong Fe-binding ligand have been suggested (Bundy et al., 2014) but also a low-salinity source (Bundy et al., 2015) with removal at higher salinity.

4.3.7. Composition and sources of DOM in the Mersey estuary and Liverpool Bay

A measurement of DOC was used to elucidate the composition of dissolved organic matter and was compare to the detected ligands. The Fe-binding HS had been determined after saturation with Fe, which should be equal to the total HS (Laglera et al., 2007) and has in the past been shown to give comparable HS concentrations as found using UV absorbance. DOC was determined after sample acidification to remove inorganic carbon and to stabilise the organic matter.

The voltammetrically detected Fe-binding HS was calibrated on the mg /L scale of SRHA and was converted to the mg C scale using a ratio of 1 mg of SRHA = 0.52 mg C/L (http://www.humicsubstances.org/elements.html). A plot of HS (mg C /L) as function of the concentration of DOC (mg C /L) was straight with a slope of 0.56 but with a significant intercept on the DOC axis: [HS] = 0.56 x DOC – 0.68 (DOC and HS as mg C/L). Extrapolation to low concentrations of DOC, in the seawater end-member, would give a residual concentration of 1.21 mg C /L DOC when HS is near zero (Fig 4.6a).

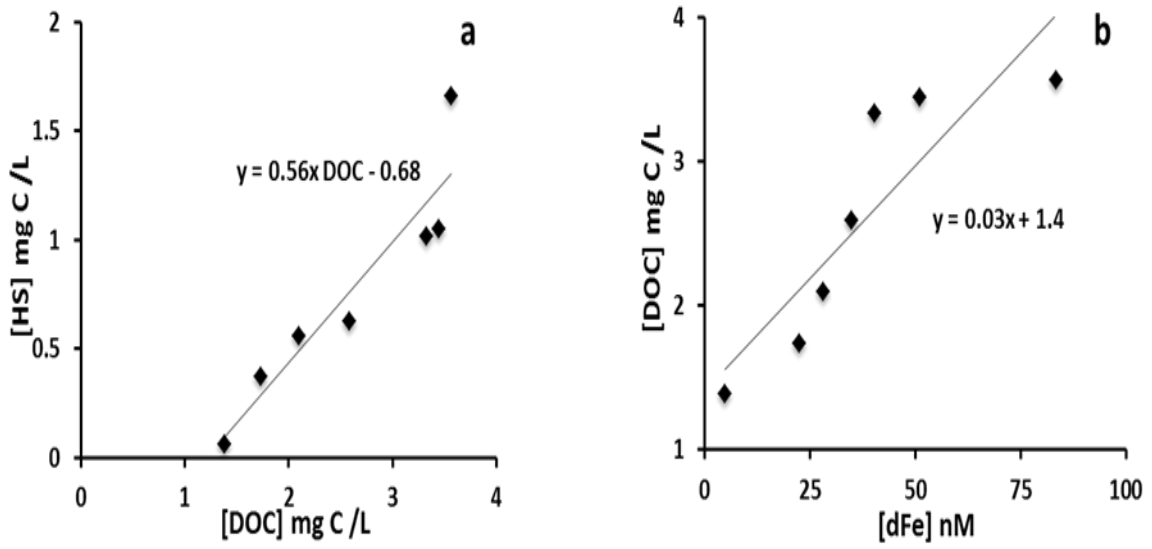

Figure 4.6. a) Voltammetrically measured Fe-binding [HS] mg C /L as function of the concentration of [DOC] mg C /L; b) [DOC] mg C /L as a function of [dFe] nM.

The fraction of DOC as HS (as mg C/L) decreased from 47 % at the low salinity (Sal) end (Sal 18.8) to 25 % at Sal 30.9, and to 5 % of DOC in the Liverpool bay sample (Sal 32.2) Table 4.4. The data suggests a non-conservative mixing behaviour of the HS compared to DOC in these estuarine waters (Fig. 4.6a). The DOC was found to decrease in a linear manner with the salinity to a low of 1.2 mg C /L at the high salinity end, which is a little higher than that (~0.8 mg C /L of DOC) in open Atlantic waters (Lomas et al., 2013) which makes sense as this is shelf water. The DOC therefore shows a simple dilution of high-DOC estuarine with low-DOC seawater. The decrease in the proportion of DOC occurring as HS during this dilution stage indicates that the HS is subject to a removal process compared to a conservative DOC.

Table 4.4: [DOC] mg C/L, [HS] mg C/L, [HS] mg/L, [TDN] mg N/L, K'FeSA and B'FeSA2 values for all the samples collected from the Mersey estuary and Liverpool Bay samples:

Stations	LogK'FeSA	LogB'FeSA2	DOC mg C/L	HS mg/L	HS mg C/L	% of HS of DOC	TDN mg N/L
Station 1	16.61	21.05	3.57	3.19±0.21	1.66	46.5	4.23
Station 2	16.60	21.02	3.45	2.2±0.3	1.14	33.2	3.77
Station 3	16.60	20.95	3.33	1.95±0.30	1.01	30.5	3.47
Station 4	16.58	20.85	2.59	1.41±0.21	0.73	28.3	2.28
Station 5	16.57	20.79	2.10	1.17±0.20	0.61	29.0	1.11
Station 6	16.57	20.75	1.74	0.82±0.17	0.43	24.5	0.60
Liverpool Bay	16.56	20.72	1.40	0.12±0.02	0.06	4.5	0.42

To track the sources of organic ligands that control the distribution of Fe in Mersey estuary, fluorescence indices FI, HIX and BIX were calculated for the entire surface and some subsurface waters samples (Table 4.1S). All the surface water samples have FI ~1.6 which means that the sources were consistent with mixed sources from allochthonous (terrestrial) as well as autochthonous (microbial) origin throughout the estuary. The subsurface water samples from stations 2 and 4 have FI values 1.92 and 1.89 respectively, which is representative of microbial sources of DOM. HIX values range from (11.06 - 11.74) for all the surface and subsurface waters samples except for two subsurface water stations (station 4 and 6), which had lower values of 9.6 and 6.7. The lower HIX values suggest that the DOM could be microbially-derived with lower aromaticity and higher N contents (Birdwell and Engel, 2010). The similar HIX values in the surface water indicate that these have terrestrial humic substances. The BIX value calculated for the entire surface and subsurface waters samples was ~0.75 suggesting that there was a contribution of sedimentary organic matter to the water too.

Accumulation of sediments takes place in rivers during time of either low flow or change in flow. When the flow changes, the accumulated sediment is weathered and carried along with the associated porewaters until the coastal zone (Powell and Wilson-Finelli, 2003). Reducing sediments release Fe and Fe-complexing ligands to surface water in upwelling system (Jones et al., 2011; Taillefert et al., 2000). Due to shallow nature of Liverpool Bay and strong tidal and wind mixing in estuary, Mersey estuary and Liverpool Bay is subjected to short-lived or intermittent periods of stratification. As a result, a complete drawdown of nutrients takes place throughout the water column (Greenwood et al., 2011). Thus, as shown by the BIX value, a fraction of Fe and Fe-complexing ligands could be contributed from the sediment.

Bacteria in both marine and freshwater systems are known to produce siderophores (Haygood et al., 1993; Macrellis et al., 2001) with log $K'_{Fe'L} = 11.5 - 11.9$. Many of the siderophores that have been identified in aquatic systems appear to originate from freshwater cyanobacteria (Bundy et al., 2015; Ito et al., 2004) and heterotrophic bacteria (Gledhill et al., 2004; Mawji et al., 2011). (Bundy et al. 2015) reported more than two ligand classes in estuarine-influenced shelf waters and suggested that bacteria could be largely responsible for the production of siderophores in San Francisco Bay contributing for strong

ligand pool in low salinity waters whereas HS account a small fractions of ligands out of total ligand pool. Unlike previous studies who reported the production of stronger L1 in situ (Rue and Bruland, 1995), recent studies suggested the terrestrial or in situ microbial sources of stronger Fe-binding ligands (Bundy et al., 2014). Marine siderophores, like their terrestrial counterparts, have recently been shown to play a dissolutive role in obtaining Fe from particles (Borer et al., 2005), a process which get enhanced in the presence of light and likely due to the photoreactivity of some marine siderophore functional groups (Barbeau et al., 2001; Buck et al., 2007). Presence of DOM in our samples from microbial sources could both be produced either in situ or at low salinity waters and persisted until Liverpool Bay.

4.3.8. dFe, Fe-binding HS, DOC, TDN and L as a function of salinity

The concentrations of humics determined as Fe-HS by voltammetry (mg /L was converted to mg C/L using a ratio of 0.52 mg C/L for each mg of HA), DOC (mg C /L), [L_T] nM and [dFe] nM /L and [TDN] mg N /L was plotted as a function of salinity (Fig. 4.7). As it is evident from the plot that all of the environmental variables ([Fe-HS], [TDN], [dFe] and [L_T]) except [DOC] have shown non-conservative mixing pattern with salinity. The concentration of these variables was decreased with increasing salinity. The dFe and HS are known to co-precipitate across salinity gradients in estuarine systems but the measured ligands also followed the similar mixing pattern as shown by dFe and HS giving an indication that measured ligands could be HS. The iron also co-varied with the DOC but in a non-linear fashion (Fig. 4.6b), in agreement with the different behaviour of DOC and HS (Fig. 4.6a).

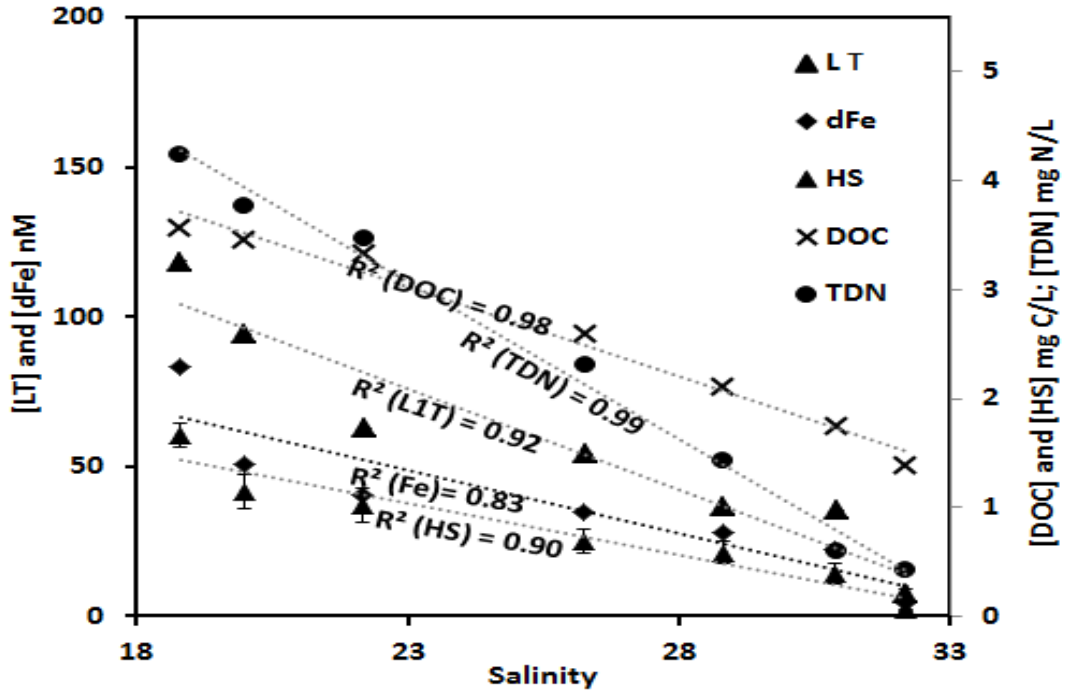

Figure 4.7. Concentrations of humics determined as Fe-binding HS by voltammetry, [HS] mg C /L, [DOC] mg C /L, [L_T] nM /L obtained from KMS (W1 – W5) and [dFe] nM /L and [TDN] mg N /L versus salinity.

4.4. Conclusion

The comparable conditional stability constant value (11.9 ± 0.6, 11.5 ± 0.6) obtained for the ligand class present in the Mersey estuary and Liverpool Bay was in the range reported earlier for terrestrial humic acid, terrestrial HS and siderophores produced by bacteria in freshwater and marine environment. The fluorescence data confirmed the presence of dissolved organic matter in these waters from terrestrial and microbial origin and is largely of constant composition throughout the estuary. This confirms our finding of a constant source of Fe-complexing ligand throughout the estuary, which was found at each detection window and that these mixed sources of dissolved organic matter might be having similar binding strength for Fe, could be responsible for Fe-speciation in this estuarine water. The BIX data indicated the presence of Fe and Fe-complexing ligands in Mersey estuary and Liverpool Bay from the upwelling of sediments pore water. From the same stations, parallel samples were collected for characterization of the dissolved organic matter (DOM) using state of the art technique, electron spray ionization Fourier-transform-ion-cyclotron resonance (ESI-FT-ICR) mass spectrometry (manuscript in preparation) which also confirmed

the presence of DOM from terrestrial sources as well as DOM flux from sediment pore waters.

The concentration of iron-binding ligands (Table 4.3) decreased from 118 nM at Sal 18.8 to 35 nM at Sal 30.9, with a further, steeper, decrease to 7.5 nM for the Liverpool Bay sample. Unfortunately, we do not have a sample from lower salinity (< 18) but it is quite possible that the complexation between dFe and Fe-binding ligands started much earlier in low salinity waters and Fe remained strongly complexed to those ligands throughout the estuary and remained stable, unless removed due to flocculation/co-precipitation along with HS. The Liverpool Bay sample was taken about 15 miles away from the mouth of the estuary in water with much less tidal flow: suspended particulate matter was therefore largely removed by settling and this would have removed dissolved iron and HS as a result of scavenging. This explains the lower concentration of HS, ligands and Fe in this sample.

We used here the approach of multiple analytical windows (MAW) in an attempt to obtain a better estimate for the sensitivity (S) at the higher concentration of the added ligand (AL, which was here SA). This approach goes back to the suggestion that overload titrations (at very high AL) would outcompete natural ligands and then the peak height should increase linearly with the added metal (Kogut and Voelker, 2001) (here Fe, but previously Cu). At the time this was shown to work for Cu complexation with humic substances, but natural waters contain ligands (thiols) that bind Cu much stronger (Laglera and van den Berg, 2003) and which to some extent invalidate the assumption that the response is going to be linear at high concentration of SA. Therefore the response still has to be corrected for un-saturation of L also at high SA. At least with Cu and SA, the sensitivity increases with the concentration of SA, so the measurements have a high sensitivity.

Similarly in this work we varied the analytical window by varying the concentration of SA but in this case we measured the Fe-SA species. At the highest concentration of [SA], the SA should be able to outcompete the ambient natural ligands to produce a linear response as function of the Fe concentration and thus facilitate the calibration of the sensitivity S. However, because the response for Fe relies specifically on adsorption of FeSA, the response goes down when [SA] > 5 µM due to the formation of Fe-SA_2 which is not electro-active (Abualhaija and van den Berg, 2014). This decrease seriously hampers the MAW approach for Fe as demonstrated in this study. The MAW approach has been shown to be useful to

facilitate calibration of S when the sensitivity increases with [AL] such as for the Cu-SA technique. This work shows that MAW method does not provide this advantage for the system of Fe-SA due to the decreasing sensitivity with increasing concentration of SA. Secondly, the titrations at constant concentrations of SA (single analytical window (SAW) titrations) gave the same result (same ligand concentration and complex stability) as the MAW titrations. This suggests that the ambient ligands in these estuarine and coastal waters were dominated by just one ligand. Furthermore the data-fitting using several approaches (data linearization as well as curve fitting methods) gave the same result for the experimental data, suggesting that the speciation of iron is quite robust.

To facilitate the use of a high detection window to obtain a good estimate for the senstivity S, it would be convenient to use a different added ligand that has a higher sensitivity when its concentration is increased.

Acknowledgements

AM received a scholarship from the University of Otago and travel support from the NZ Prime Minister Science Prize. Royal Society International Exchange Scheme – 2013/R1 and New Zealand MBIE programme C01X1005 funded the study.

4.5. References

Abualhaija, M.M. and van den Berg, C.M., 2014. Chemical speciation of iron in seawater using catalytic cathodic stripping voltammetry with ligand competition against salicylaldoxime. Marine Chemistry, 164: 60-74.

Abualhaija, M.M., Whitby, H. and van den Berg, C.M., 2015. Competition between copper and iron for humic ligands in estuarine waters. Marine Chemistry, 172: 46-56.

Banaitis, M.R. et al., 2006. Investigating sorption-driven dissolved organic matter fractionation by multidimensional fluorescence spectroscopy and PARAFAC. Journal of colloid and interface science, 304(1): 271-276.

Barbeau, K., Rue, E.L., Bruland, K.W. and Butler, A., 2001. Photochemical cycling of iron in the surface ocean mediated by microbial iron(iii)-binding ligands. Nature, 413(6854): 409-413.

Batchelli, S., Muller, F.L., Chang, K.-C. and Lee, C.-L., 2010. Evidence for strong but dynamic iron–humic colloidal associations in humic-rich coastal waters. Environmental science & technology, 44(22): 8485-8490.

Birdwell, J.E. and Engel, A.S., 2010. Characterization of dissolved organic matter in cave and spring waters using UV–Vis absorbance and fluorescence spectroscopy. Organic Geochemistry, 41(3): 270-280.

Borer, P.M., Sulzberger, B., Reichard, P. and Kraemer, S.M., 2005. Effect of siderophores on the light-induced dissolution of colloidal iron(III) (hydr)oxides. Marine Chemistry, 93(2–4): 179-193.

Boyd, P. and Ellwood, M., 2010. The biogeochemical cycle of iron in the ocean. Nature Geoscience, 3(10): 675-682.

Boye, M. et al., 2001. Organic complexation of iron in the Southern Ocean. Deep Sea Research Part I: Oceanographic Research Papers, 48(6): 1477-1497.

Boyle, E., Edmond, J. and Sholkovitz, E., 1977. The mechanism of iron removal in estuaries. Geochimica et Cosmochimica Acta, 41(9): 1313-1324.

Buck, K.N. and Bruland, K.W., 2005. Copper speciation in San Francisco Bay: A novel approach using multiple analytical windows. Marine Chemistry, 96(1): 185-198.

Buck, K.N. and Bruland, K.W., 2007. The physicochemical speciation of dissolved iron in the Bering Sea, Alaska. Limnology and Oceanography, 52(5): 1800-1808.

Buck, K.N., Lohan, M.C., Berger, C.J. and Bruland, K.W., 2007. Dissolved iron speciation in two distinct river plumes and an estuary: Implications for riverine iron supply. Limnology and Oceanography, 52(2): 843-855.

Bundy, R.M. et al., 2015. Iron-binding ligands and humic substances in the San Francisco Bay estuary and estuarine-influenced shelf regions of coastal California. Marine Chemistry, 173: 183-194.

Bundy, R.M., Biller, D.V., Buck, K.N., Bruland, K.W. and Barbeau, K.A., 2014. Distinct pools of dissolved iron-binding ligands in the surface and benthic boundary layer of the California Current. Limnology and Oceanography, 59(3): 769-787.

Croot, P. and Johansson, M., 2000. Determination of iron speciation by cathodic stripping voltammetry in seawater using the competing ligand 2-(2-Thiazolylazo)-p-cresol (TAC). Electroanalysis, 12(8): 565-576.

Gerringa, L., Herman, P. and Poortvliet, T., 1995. Comparison of the linear van den Berg/Ružić transformation and a non-linear fit of the Langmuir isotherm applied to Cu speciation data in the estuarine environment. Marine Chemistry, 48(2): 131-142.

Gerringa, L.J., Rijkenberg, M.J., Thuróczy, C.-E. and Maas, L.R., 2014. A critical look at the calculation of the binding characteristics and concentration of iron complexing ligands in seawater with suggested improvements. Environmental Chemistry, 11(2): 114-136.

Gerringa, L.J.A. et al., 2007. Kinetic study reveals weak Fe-binding ligand, which affects the solubility of Fe in the Scheldt estuary. Marine Chemistry, 103(1–2): 30-45.

Gledhill, M., Achterberg, E.P., Li, K., Mohamed, K.N. and Rijkenberg, M.J.A., 2015. Influence of ocean acidification on the complexation of iron and copper by organic ligands in estuarine waters. Marine Chemistry(0).

Gledhill, M. and Buck, K.N., 2012. The organic complexation of iron in the marine environment: a review. Frontiers in microbiology, 3.

Gledhill, M. et al., 2004. Production of siderophore type chelates by mixed bacterioplankton populations in nutrient enriched seawater incubations. Marine Chemistry, 88(1–2): 75-83.

Gledhill, M. and van den Berg, C.M., 1994. Determination of complexation of iron (III) with natural organic complexing ligands in seawater using cathodic stripping voltammetry. Marine Chemistry, 47(1): 41-54.

Greenwood, N. et al., 2011. Spatial and temporal variability in nutrient concentrations in Liverpool Bay, a temperate latitude region of freshwater influence. Ocean Dynamics, 61(12): 2181-2199.

Hassler, C.S., Schoemann, V., Nichols, C.M., Butler, E.C. and Boyd, P.W., 2011. Saccharides enhance iron bioavailability to Southern Ocean phytoplankton. Proceedings of the National Academy of Sciences, 108(3): 1076-1081.

Haygood, M.G., Holt, P.D. and Butler, A., 1993. Aerobactin production by a planktonic marine Vibrio sp. Limnology and Oceanography, 38(5): 1091-1097.

Hudson, R.J., Covault, D.T. and Morel, F.M., 1992. Investigations of iron coordination and redox reactions in seawater using 59 Fe radiometry and ion-pair solvent extraction of amphiphilic iron complexes. Marine Chemistry, 38(3): 209-235.

Hudson, R.J., Rue, E.L. and Bruland, K.W., 2003. Modeling complexometric titrations of natural water samples. Environmental science & technology, 37(8): 1553-1562.

Hudson, R.J.M., 2014. Software: KINETEQL Multiwindow Solver (KMS), Version 1.0. https://sites.google.com/site/kineteql/.

Huguet, A. et al., 2009. Properties of fluorescent dissolved organic matter in the Gironde Estuary. Organic Geochemistry, 40(6): 706-719.

Hunter, K.A. and Boyd, P.W., 2007. Iron-binding ligands and their role in the ocean biogeochemistry of iron. Environmental Chemistry, 4(4): 221-232.

Ibisanmi, E., Sander, S.G., Boyd, P.W., Bowie, A.R. and Hunter, K.A., 2011. Vertical distributions of iron-(III) complexing ligands in the Southern Ocean. Deep Sea Research Part II: Topical Studies in Oceanography, 58(21): 2113-2125.

Ito, Y., Ishida, K., Okada, S. and Murakami, M., 2004. The absolute stereochemistry of anachelins, siderophores from the cyanobacterium Anabaena cylindrica. Tetrahedron, 60(41): 9075-9080.

Jaffé, R. et al., 2004. Source characterization of dissolved organic matter in a subtropical mangrove-dominated estuary by fluorescence analysis. Marine Chemistry, 84(3): 195-210.

Johnson, K.S., Gordon, R.M. and Coale, K.H., 1997. What controls dissolved iron concentrations in the world ocean? Marine Chemistry, 57(3): 137-161.

Johnson, M.S., Couto, E.G., Abdo, M. and Lehmann, J., 2011. Fluorescence index as an indicator of dissolved organic carbon quality in hydrologic flowpaths of forested tropical watersheds. Biogeochemistry, 105(1-3): 149-157.

Jones, M.E., Beckler, J.S. and Taillefert, M., 2011. The flux of soluble organic-iron(III) complexes from sediments represents a source of stable iron(III) to estuarine waters and to the continental shelf. Limnology and Oceanography, 56(5): 1811-1823.

Kalbitz, K., Schmerwitz, J., Schwesig, D. and Matzner, E., 2003. Biodegradation of soil-derived dissolved organic matter as related to its properties. Geoderma, 113(3): 273-291.

Kogut, M.B. and Voelker, B.M., 2001. Strong copper-binding behavior of terrestrial humic substances in seawater. Environmental Science and Technology, 35(6): 1149-1156.

Kuma, K., Nishioka, J. and Matsunaga, K., 1996. Controls on iron (III) hydroxide solubility in seawater: the influence of pH and natural organic chelators. Limnology and Oceanography, 41(3): 396-407.

Laglera, L.M., Battaglia, G. and van den Berg, C.M.G., 2007. Determination of humic substances in natural waters by cathodic stripping voltammetry of their complexes with iron. Analytica Chimica Acta, 599(1): 58-66.

Laglera, L.M. and van den Berg, C.M.G., 2003. Copper complexation by thiol compounds in estuarine waters. Marine Chemistry, 82(1-2): 71-89.

Laglera, L.M. and van den Berg, C.M.G., 2009. Evidence for geochemical control of iron by humic substances in seawater. Limnology and Oceanography, 54(2): 610-619.

Liu, X. and Millero, F.J., 1999. The solubility of iron hydroxide in sodium chloride solutions. Geochimica et Cosmochimica Acta, 63(19): 3487-3497.

Lomas, M. et al., 2013. Two decades and counting: 24-years of sustained open ocean biogeochemical measurements in the Sargasso Sea. Deep Sea Research Part II: Topical Studies in Oceanography, 93: 16-32.

Lucia, M., Campos, A. and van den Berg, C.M., 1994. Determination of copper complexation in sea water by cathodic stripping voltammetry and ligand competition with salicylaldoxime. Analytica Chimica Acta, 284(3): 481-496.

Macrellis, H.M., Trick, C.G., Rue, E.L., Smith, G. and Bruland, K.W., 2001. Collection and detection of natural iron-binding ligands from seawater. Marine Chemistry, 76(3): 175-187.

Mawji, E. et al., 2011. Production of siderophore type chelates in Atlantic Ocean waters enriched with different carbon and nitrogen sources. Marine Chemistry, 124(1–4): 90-99.

McKnight, D.M. et al., 2001. Spectrofluorometric characterization of dissolved organic matter for indication of precursor organic material and aromaticity. Limnology and Oceanography, 46(1): 38-48.

Nagai, T., Imai, A., Matsushige, K., Yokoi, K. and Fukushima, T., 2007. Dissolved iron and its speciation in a shallow eutrophic lake and its inflowing rivers. Water research, 41(4): 775-784.

Ohno, T., Fernandez, I.J., Hiradate, S. and Sherman, J.F., 2007. Effects of soil acidification and forest type on water soluble soil organic matter properties. Geoderma, 140(1): 176-187.

Omanović, D., Garnier, C. and Pižeta, I., 2015. ProMCC: an all-in-one tool for trace metal complexation studies. Marine chemistry, 173: 25-39.

Pižeta, I. et al., 2015. Interpretation of complexometric titration data: An intercomparison of methods for estimating models of trace metal complexation by natural organic ligands. Marine Chemistry, 173(0): 3-24.

Powell, R.T. and Wilson-Finelli, A., 2003. Importance of organic Fe complexing ligands in the Mississippi River plume. Estuarine, Coastal and Shelf Science, 58(4): 757-763.

Rue, E.L. and Bruland, K.W., 1995. Complexation of iron (III) by natural organic ligands in the Central North Pacific as determined by a new competitive ligand equilibration/adsorptive cathodic stripping voltammetric method. Marine Chemistry, 50(1): 117-138.

Ružić, I., 1982. Theoretical aspects of the direct titration of natural waters and its information yield for trace metal speciation. Analytica Chimica Acta, 140(1): 99-113.

Sander, S.G., Buck, K.N. and Wells, M., 2015a. The effect of natural organic ligands on trace metal speciation in San Francisco Bay: Implications for water quality criteria. Marine Chemistry, 173(0): 269-281.

Sander, S.G., Hunter, K.A., Harms, H. and Wells, M., 2011. Numerical approach to speciation and estimation of parameters used in modeling trace metal bioavailability. Environmental science & technology, 45(15): 6388-6395.

Sander, S.G. et al., 2015c. Spatial and seasonal variations of iron speciation in surface waters of the Subantarctic front and the Otago Continental Shelf. Marine Chemistry, 173: 114-124.

Scatchard, G., 1949. The attractions of proteins for small molecules and ions. Annals of the New York Academy of Sciences, 51(4): 660-672.

Sholkovitz, E., 1976. Flocculation of dissolved organic and inorganic matter during the mixing of river water and seawater. Geochimica et Cosmochimica Acta, 40(7): 831-845.

Sholkovitz, E., Boyle, E. and Price, N., 1978. The removal of dissolved humic acids and iron during estuarine mixing. Earth and Planetary Science Letters, 40(1): 130-136.

Stedmon, C.A. and Markager, S., 2005. Resolving the variability in dissolved organic matter fluorescence in a temperate estuary and its catchment using PARAFAC analysis. Limnology and Oceanography, 50(2): 686-697.

Taillefert, M., Bono, A. and Luther, G., 2000. Reactivity of freshly formed Fe (III) in synthetic solutions and (pore) waters: voltammetric evidence of an aging process. Environmental science & technology, 34(11): 2169-2177.

van den Berg, C., Nimmo, M., Daly, P. and Turner, D., 1990. Effects of the detection window on the determination of organic copper speciation in estuarine waters. Analytica Chimica Acta, 232: 149-159.

van den Berg, C.M., 1995. Evidence for organic complexation of iron in seawater. Marine Chemistry, 50(1): 139-157.

van den Berg, C.M., 2006. Chemical speciation of iron in seawater by cathodic stripping voltammetry with dihydroxynaphthalene. Analytical chemistry, 78(1): 156-163.

van den Berg, C.M. and Donat, J.R., 1992. Determination and data evaluation of copper complexation by organic ligands in sea water using cathodic stripping voltammetry at varying detection windows. Analytica Chimica Acta, 257(2): 281-291.

van den Berg, C.M.G., 1982. Determination of copper complexation with natural organic ligands in seawater by equilibration with MnO2 I. Theory. Marine Chemistry, 11(4): 307-322.

Velasquez, I. et al., 2011. Detection of hydroxamate siderophores in coastal and Sub-Antarctic waters off the South Eastern Coast of New Zealand. Marine Chemistry, 126(1): 97-107.

Wells, M., Buck, K.N. and Sander, S.G., 2013. New approach to analysis of voltammetric ligand titration data improves understanding of metal speciation in natural waters. Limnology and Oceanography: Methods, 11(9): 450-465.

Witter, A.E., Hutchins, D.A., Butler, A. and Luther, G.W., 2000. Determination of conditional stability constants and kinetic constants for strong model Fe-binding ligands in seawater. Marine Chemistry, 69(1): 1-17.

Zsolnay, A., Baigar, E., Jimenez, M., Steinweg, B. and Saccomandi, F., 1999. Differentiating with fluorescence spectroscopy the sources of dissolved organic matter in soils subjected to drying. Chemosphere, 38(1): 45-50.

Chapter 4
Supplementary data

Table 4.1S. Fluorescence Indices calculated for all the surface and subsurface water samples along with DOC and TDN values collected from the Mersey estuary and Liverpool Bay.

Stations	BIX	HIX	FI	DOC mg C/L	TDN mg N/L
Station 1 surface	0,76	11,07	1,60	3,57	4,23
Station 2 deep	0,75	11,10	1,92	3,41	3,77
Station 2 Surface	0,76	11,06	1,59	3,45	3,77
Station 3 Surface	ND	ND	ND	3,33	3,47
Station 4 deep	0,75	9,56	1,89	2,86	2,30
Station 4 Surface	0,75	11,74	1,59	2,59	2,28
Station 5 deep	0,75	11,14	1,58	2,02	1,42
Station 5 surface	0,75	11,20	1,58	2,10	1,11
Station 6 deep	0,76	6,75	1,59	1,80	0,60
Station 6 Surface	0,75	11,26	1,58	1,74	0,60
Liverpool Bay	0,75	11,06	1,68	1.39	0,42

5

Chapter 5
Identification of iron-binding substances in the oceans

5. IDENTIFICATION OF IRON-BINDING SUBSTANCES IN THE OCEANS

Iron-limitation of the primary productivity in large parts of the global ocean (Martin and Fitzwater, 1988) makes iron arguably the most important trace metal in the ocean. Its bioavailability is mediated by the form (speciation) in which the iron occurs (Hassler et al., 2011b). Similar iron concentrations in the deep Pacific and Atlantic (Biller and Bruland, 2012) are consistent with a major impact of scavenging, the residual Fe being controlled by complexation with organic ligands (Völker and Tagliabue, 2015). Organic complexation plays a key role in the geochemistry and bioavailability of iron but surprisingly the composition of the organic ligands responsible for the binding of Fe is largely unknown. Likely candidates for the identity of Fe-binding ligands include siderophores (specific Fe-binding compounds produced by bacteria) (Hutchins et al., 1999), exopolysaccharides (EPS) (Hassler et al., 2011a) (released by bacteria) and humic substances (Laglera and van den Berg, 2009). Here we demonstrate that iron-binding humic substances account for 95-98 % of the unknown ligands in the ocean and on the shelf. This revolutionary finding challenges the paradigm that iron-binding ligands largely originate from in-situ production by microorganisms and much facilitates the modeling of the background ligand concentration that controls the global oceanic distribution of Fe.

The solubility of inorganic Fe in seawater is ~10 pM due to formation of solid Fe-hydroxides (Liu and Millero, 1999) but the overall solubility of Fe is raised to the nM level as a result of complexation with dissolved organic matter (Kuma et al., 1998).

Organic Fe-binding ligands in seawater can originate from several sources including waste products from microorganisms, exo-cellular products, breakdown products and terrestrial organics. These organics are either in-situ produced (marine origin), or derived from land (terrestrial origin) or both. Organic complexation, including by exopolymer substances, affects the availability of Fe to marine microorganisms (Hassler et al., 2015). Marine microbes are an obvious source of chlorophyll, heme, porphyrins, thiols, phytochelatins, siderophores and other compounds in the ocean water column that are in principle capable of binding various metals including Fe. However, these microbial

compounds are readily broken down (Morel and Price, 2003) and it is therefore not at all clear that any one of these remains at sufficient levels to bind the Fe in the deeper waters. Secondly these compounds originate from the organisms and are therefore already saturated with iron and other metal ions, and would not be a source of free ligands. Therefore it is not a given that the microbes add to the pool of free ligands.

The residual concentration of Fe in the deep ocean is in the range of ~0.5 – 0.8 nM (Biller and Bruland, 2012); considering that scavenging acts on Fe throughout the oceanic water column, the ligand concentration can be expected to be greater than that of the residual Fe, suggesting a background concentration of ligands of perhaps ~1 nM or more. Data on iron-binding ligands is still scarce but concentrations have been found of ~1-2 nM in ocean waters (Boye et al., 2006; Ibisanmi et al., 2011; Rue and Bruland, 1995) which are consistent with the background Fe concentration in the deep waters. Whilst the siderophores and the EPS may be produced in-situ, the humics are by nature from terrestrial origin in view of their high concentration in estuarine waters (Laglera and van den Berg, 2009), and decreasing fluorescent humic matter with increasing salinity (Stolpe et al., 2014). Knowing the composition of the most important ligands would much facilitate modeling the global oceanic iron distribution and possible effects of global change (pH and warming) on iron availability and its geochemistry.

Using new methods, developed or updated in our laboratory, we have determined the concentrations of iron-complexing ligands and humic substances in a transect in continental shelf waters and in a profile of the water column of the NE Atlantic. Using these methods it has previously been demonstrated that iron and copper are associated with humic substances in estuarine and near-coastal waters (Abualhaija et al., 2015; Laglera et al., 2007; Whitby and van den Berg, 2015), and that the iron binding humic species are transported from the estuary to the sea at a steadily diminishing concentration (Laglera and van den Berg, 2009). Fluorescence data suggests that humic-like compounds occur widespread in ocean waters (Heller et al., 2013). If these compounds are the same as the iron-binding humics found in estuarine waters, then potentially these are an important ligand ocean-wide.

The salinity range of the shelf samples was narrow (between 35.2 and 35.6), showing only minor coastal influence, explaining a lack of salinity trends in the data. Fe

concentrations were between 0.24 and 0.93 nM (Table 5.1S), more similar to ocean waters than coastal waters although they were collected over the shelf from a depth of ~3 m in a water depth of ~100 m. Concentrations at the beginning and end of the transect were somewhat higher than in between (Fig. 5.1). The low concentrations of iron suggest that the water was recently pushed onto the shelf with little history of sedimentary inputs.

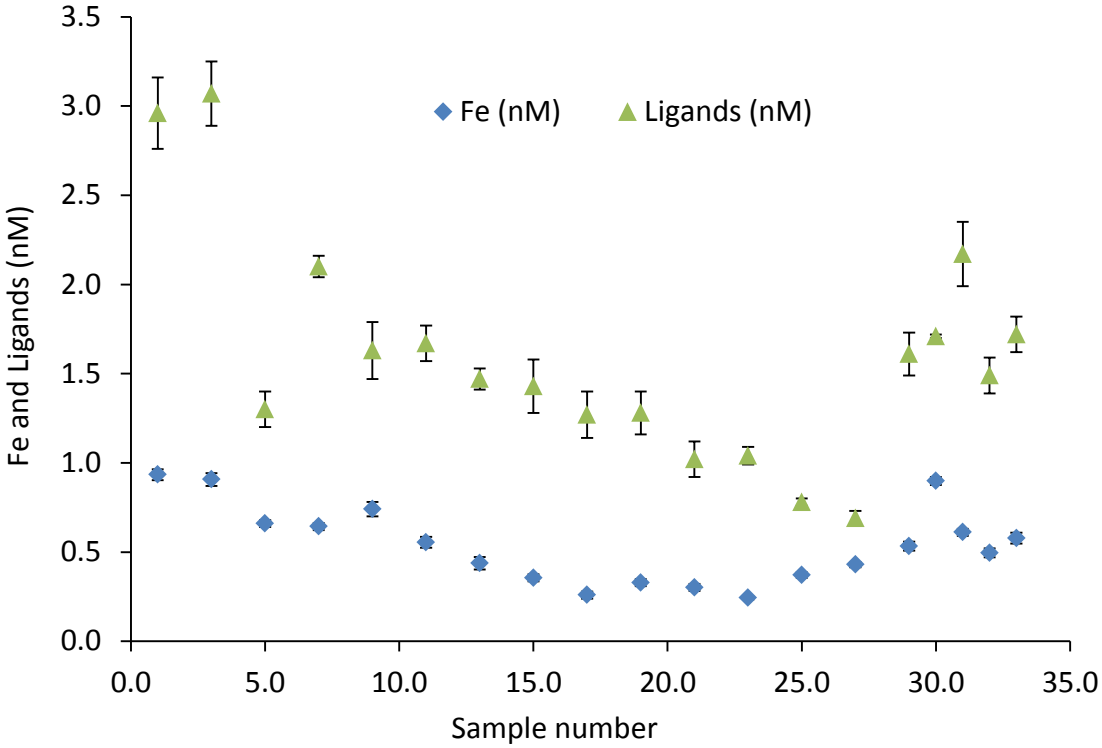

Figure 5.1. Concentrations of Fe and Fe- binding ligands (nM) in the shelf samples as function of sample number

Iron binding ligand concentrations were between 0.7 and 3.1 nM (Table 5.1S), and greater than the iron concentration in all samples. The ligand concentration in excess of the iron concentration was about 1.1 ± 0.5 nM. The excess was not constant, the difference being greater at the beginning and end of the sample series, where the Fe concentration was higher too (Fig. 5.1). A possible reason for this is the scavenged behaviour of Fe: the Fe is scavenged either because its inorganic species (Fe') exceeds the solubility limit of ~10 pM, or because it is taken up by micro-organisms, or because it adsorbs on sinking particulate material. All these processes are reacting with inorganic Fe and therefore tend to slow down if the Fe is complexed with dissolved organic matter, which would explain that there is more

residual Fe with higher ligand concentrations when the Fe is being scavenged. This hypothesis is supported by co-variation between the iron and ligand concentrations with a slope of ~0.27±0.05 (Fig. 5.2S), which suggests that the residual concentration of Fe in the shelf waters is controlled by the ligand concentration. The ratio of ligand over Fe in the shelf waters was 3.1 ± 0.9 indicating a significant excess of ligand over metal, sufficient to retain Fe in a complexed state. The average concentration of inorganic iron (Fe') in the shelf waters was 3.2 ± 1.1 pM amounting to 0.6 % of the average concentration of iron of 0.5 ± 0.2 nM, which was 31% of the average ligand concentration of 1.6 ± 0.6 nM.

5.1. Iron binding ligands in the Atlantic water column

The distribution of Fe in the water column of the Atlantic (Fig. 5.2 and Table 5.2S) shows Fe generally increasing with depth between 0.10 and 0.65 nM, in agreement with other data for these waters (Gerringa et al., 2015). The Fe in the frozen samples was 1 – 8 % less than in the acidified samples (Fig. 5.2A), caused by adsorption on the wall of the bottles containing the unacidified frozen samples (Gerringa et al., 2014). Apart from this small systematic difference the agreement is very good considering that the iron was determined by two different techniques and laboratories.

The ligand concentration in the water column was between 1.45 and 2.13 nM (Fig. 5.2A and Table 5.2S). These ligand concentrations are not unusual for ocean waters (Boye et al., 2006; Boye et al., 2001; Buck et al., 2015) and similar to those found in nearby Atlantic waters (Boye et al., 2006; Boye et al., 2001; Buck et al., 2015; Gerringa et al., 2015). The ligand determinations were unequivocal in that they could be fitted to only a single ligand in all samples of the Atlantic water column and the shelf. The standard deviation of the ligand concentrations was 0.08 nM at ligand concentrations of 1.7 nM, suggesting a limit of detection of < 0.2 nM. Example titrations and the data linearization as evidence for the presence of only one ligand are shown in Fig. 5.3S.

The complex stability can be used to see if there are changes in the ligand composition between the shelf and the open ocean, or from the surface to the deep. The complex stability of the Fe species in the Atlantic and over the shelf is identical within a narrow range of log $K'_{Fe'L}$ values of 11.2 ±0.1 (Atlantic profile) and 11.2 ±0.2 for the shelf samples. This may

suggests that the same ligand dominate the iron speciation (for iron in excess of 0.2 nM) in the entire water column and also in the shelf waters 2000 miles away. The complex stability is similar to that (11.1 to 11.6) for reference humic substances (riverine origin) added to seawater (Abualhaija and van den Berg, 2014; Laglera and van den Berg, 2009), and for humic-like substances found in estuarine waters (11.1 to 11.9) (Abualhaija et al., 2015; Batchelli et al., 2010) and (10.4-11.1) for exopolymeric substances isolated from ocean waters (Hassler et al., 2015), a strong similarity between the ligands in the Atlantic and the shelf and humic acid-like substances with the evidence comes from the similarity between the concentrations of the iron-binding ligands and the humics suggests that the humic substances may account for the large fraction of iron-binding ligands. The concentration of inorganic iron (Fe') was found to increase from 0.4 pM at a depth of 26 m) to 3.3 pM at a depth of 3346 m (Fig. 5.2B); the increase was regular apart from two outliers of around 3 pM at intermediate depth. This increase is driven by the increase in dissolved Fe from 0.1 nM at the surface to 0.7 nM in the deep water. The background concentration of 0.4 and 0.6 pM Fe' in the surface waters are relevant because culture experiments have shown that oceanic diatoms are inhibited when Fe' < 3 pM (Sunda and Huntsman, 1995). The low concentration of Fe' would support the suggestion that there is iron-limitation in this region (Mohamed et al., 2011), unless the organically bound iron is made available as a result of photochemical reduction.

5.2. Comparison of the concentration of iron-binding ligands and humics

We determined the concentration of iron-binding humic substances in the same samples as used for the speciation study, using an independent method making use of the voltammetric response that is specific for the humics in presence of excess iron. The concentration of humic substances in the Atlantic was found to closely follow that of the ligands (Fig. 5.2A) showing that the humics are subject to the same source(s) and sink(s) as the unknown iron binding ligands, and on the whole the concentration of iron-binding humics was very similar to that of the ligands.

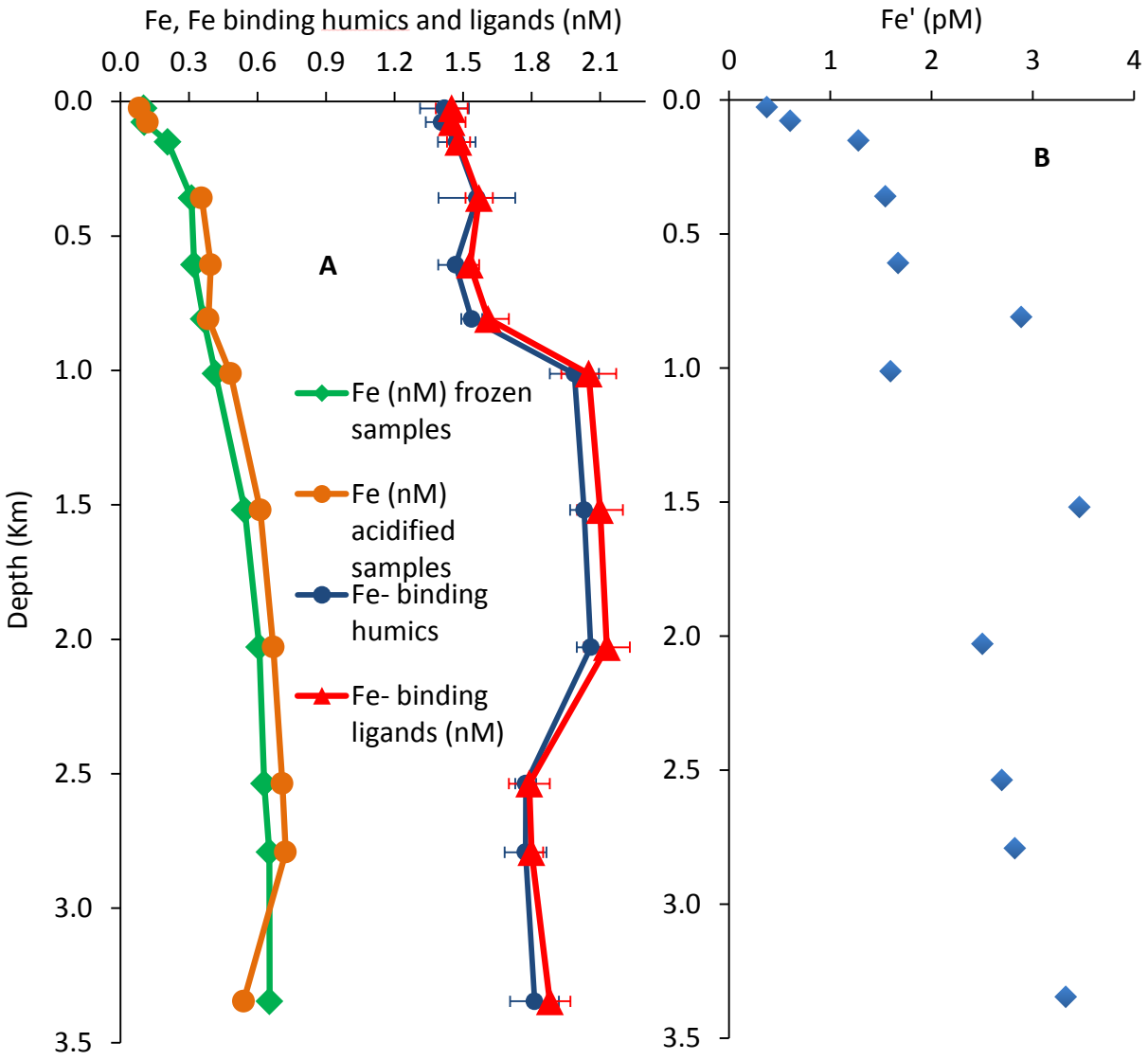

Figure 5.2. A) Concentrations of Fe, Fe binding humics and Ligands (nM scale) as function of sampling depth (km). B) Concentration of inorganic iron (Fe') (pM) as function of sampling depth (km) in the Atlantic samples.

A diagram of the iron-binding humics as function of the ligand concentration (Fig. 5.3) shows straight lines with a slope of 0.98±0.04 for the shelf samples and of 0.95±0.03 for the Atlantic samples. The two data sets overlap, with the shelf samples covering a larger range (Fig. 5.3). The relationship between the concentration of iron-binding humics and complexing ligands is very close, and the concentration of the iron-binding humics can account for a major proportion of the total ligand concentration for iron.

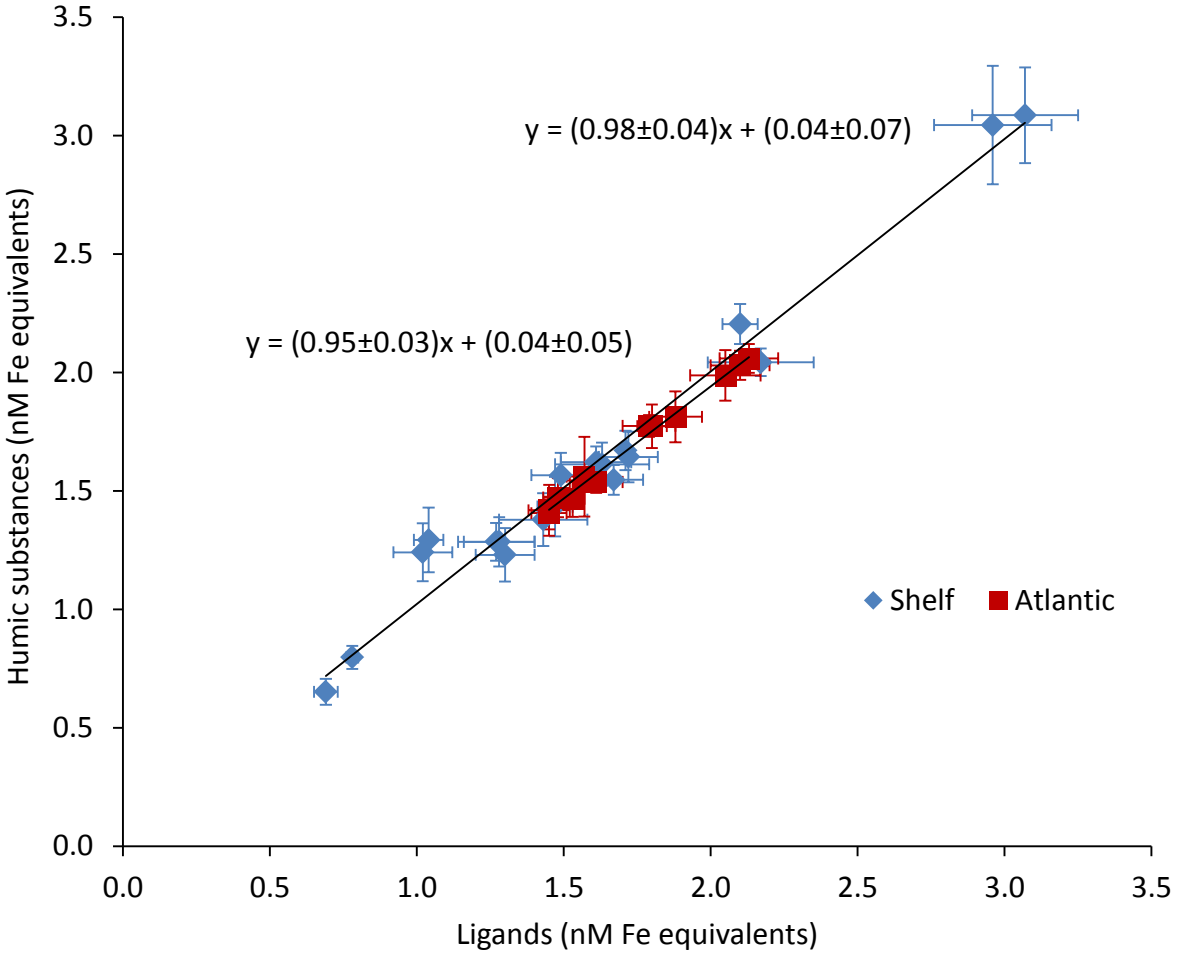

Figure 5.3. Comparison between concentration of Fe-binding humics (HS) (nM scale) and the concentration of Fe-binding ligands (L) (nM) in the Shelf and Atlantic samples. The Fe-binding ligand concentration is virtually the same as the concentration of Fe-binding humics in the Shelf and Atlantic samples.

In view of the systematic difference between the distribution of the ligands and the humics in the oceanic water column (Fig. 5.2A) it is possible to ascribe the difference (40 ±30 pM) to a low concentration of ligands similar to siderophores, which were not detected by the titrations. Ligands in this concentration range (<0.2 nM) would have been missed by the method used here if their concentration was less than that of iron. Experiments using additions up to 4 nM of desferrioxamine-B as an example of a siderophore showed that these did not produce a humic-like signal suggesting that siderophore-like substances (thought to occur at ~20 pM levels (Mawji et al., 2008)) would not have been detected by the voltammetric technique used, and could still be controlling a significant fraction of the iron.

The slightly higher excess ligand concentration in surface waters (Fig. 5.2) can be ascribed to biological activity as microbes apparently take up Fe but not the ligands. It has been suggested that strong ligands are produced in situ by biological production, whereas weak ligands are from terrestrial sources, degradation product released from the decomposition of organic matter, photolysis of some high affinity strong ligands (such as siderophores) and biomineralisation products (Hunter and Boyd, 2007; Rue and Bruland, 1995). (Bundy et al., 2015) suggested that the biological production in San Francisco bay is largely responsible for a strong ligand pool whereas humic substances account for a small fraction out of the total ligand pool. However, our measurements do not support the presence of more than one ligand.

Although this work shows that HS are largely responsible for iron complexation, it is not clear from where the HS originate. Their distribution throughout the water column suggests they are recalcitrant (not readily broken down). They could be from microbial breakdown, or organic matter in the sea, or from land. Also it could be that marine humic substances are produced in situ by biological production (i.e. exopolysaccharides) in addition to terrestrial humics and indistinguishable from these. It is possible that the CSV method for the determination of Fe-HS is not specific to humic substances, as any other ligand (with a similar complexation property as that of the HS) could be electrochemically active with the addition of iron and give a voltammetric response similar to HS, which could overlap with the HS response. Further work is required to study the association between Fe, humic substances and any other ligand (such as EPS) expected to give a humic like response and the contribution of this ligand to Fe-binding ligands, and secondly, to identify the main sources of these HS-like ligands.

The identification of the predominant iron-binding ligands as humic substances suggests that specific iron-binding compounds (siderophores) produced by bacteria may contribute for only small fraction of the ligands in the oceans and shelf, whereas the humics play the controlling role with respect to the solubility and global transport of iron, and also with respect to the general chemistry of iron. However, it is not clear if the HS are from terrestrial origin or are produced in-situ in the sea.

Acknowledgements

The research of Mahmoud Abualhajia was funded by the University of Jordan. Micha Rijkenberg was funded by the Dutch National Program for Sea and Coastal Research (ZKO, project number 839.08.410) of the Netherlands Organisation for Scientific Research (NWO, www.nwo.nl/en).

5.3. Method section

5.3.1. Determination of the iron complexing ligand concentrations

Iron and iron-complexing ligands were determined by cathodic stripping voltammetry (CSV) in the presence of salicylaldoxime (SA) using a newly optimised method (Abualhaija and van den Berg, 2014). In brief: approximately 160 ml sample was pre-mixed with 0.01 M borate buffer and 5 µM SA. 10 ml aliquots of the solution were pipetted into 14 15-mL PFA (perfluoroalkoxy alkane) (Savillex, Cole-Parmer) vials with lid, containing Fe additions from 0 nM to 10 nM. These were then left to equilibrate overnight. The labile Fe concentration was then determined by CSV in a PTFE voltammetric cell using 120 or 180s deposition time. The deposition potential was 0 V, followed by the scan to -1 V. The PFA Savillex vials were conditioned to the titrations by setting up and discarding the first titration 3 times. The fourth one was measured and was repeated to check for further improvement. The voltammetric cell was conditioned 3 times with seawater with SA without added Fe prior to the start of each titration. The overnight equilibration is essential to prevent possible overestimation of the complex stability and incorrect data fitting: a short equilibration time of between 15 and 30 min as used in some recent work (Buck et al., 2015; Bundy et al., 2014) could be the reason for non-linearity in the data treatment, incorrectly suggesting the presence of more than one ligand due to slow dissociation of FeL.

Data interpretation was using the van den Berg/Ruzic linearization procedure (Ruzic, 1982; van den Berg, 1982) with correction of the sensitivity for under-saturation of the ligand (Turoczy and Sherwood, 1997). A first estimate for S was from the last three data points which was subsequently corrected in an iterative manner for ligand under-saturation. Comparative calculations were carried out using alternative modeling software (MCC) (Omanović et al., 2015). Concentrations of inorganic iron (Fe') were calculated using a quadratic equation from the determined concentrations of the ligands, iron concentration and the complex stability.

The titrations were interpreted using newly calibrated values for the complex stability of FeSA and $FeSA_2$ ($\log K'_{Fe'SA} = 6.52$ and $\log B'_{Fe'SA2} = 10.72$ on the scale of Fe' (Abualhaija and van den Berg, 2014). A value of 10^{10} was used for the side reaction coefficient of inorganic complexation of Fe in seawater of pH_{NBS} 8.18. The optimised experimental conditions include measurements at a concentration of 5 µM SA and in the presence of air which means that

the pH was stabilised by the carbonate system at pH_{NBS} 8.18 for seawater in air-equilibrium (Abualhaija and van den Berg, 2014), in addition to an added borate/ammonia buffer which had been set to the same pH. The measurement conditions were therefore consistent with the calibrated conditions and the results reproducible.

5.3.2. Determination of iron-binding humic concentrations

The concentration of iron-binding humic substances was determined by an independent CSV method (Laglera et al., 2007) . 50 nM Fe was added to saturate the humics and measurement was at the natural pH of seawater in the presence of air, borate/ammonia buffer, and 0.4 M bromate. Calibration was by standard additions of Suwannee River humic acid (SRHA) reference material (Standard II 2S101H). The deposition potential was 0 V, and the deposition time was between 120 and 180 s. The concentration of humics was converted from the µg L^{-1} scale to the nanomolar scale using a value of 30.6 nanomole/mg for the ratio at which iron is bound by SRHA and riverine and estuarine humics (Abualhaija and van den Berg, 2014).

5.3.3. Determination of the total dissolved iron concentrations

The concentration of dissolved iron was determined in samples that had been stored frozen and subsequently defrosted. Aliquots of 30 mL were acidified to pH 2 and left overnight in the presence of 5 µM SA. Then 10 mL of the acidified sample aliquot was placed in the voltammetric cell, the pH was neutralized with ammonia, and 10 mM of the borate buffer was added. Voltammetric parameters were a deposition time of between 60 and 120 s at 0 V, followed by the scan to -1 V (Abualhaija and van den Berg, 2014).

5.3.4. Sample containers and analytical apparatus

Analytical equipment consisted of a µAutolab-III potentiostat (Ecochemie, Netherlands), a hanging mercury drop electrode (Metrohm VA663), a double junction Ag/AgCl reference electrode with a salt bridge containing 3 M KCl, and a glassy carbon counter electrode. The electrode stand was pressurised using air in order to ensure that the

concentration of dissolved oxygen was constant during the measurements.

5.3.5. Sampling area and sample storage

Shelf seawater samples from the Celtic sea were collected on board the RSS *Discovery* as part of the shelf sea biogeochemistry program in April 2014, whereas depth profile ocean samples were collected from station 4 (Long: -43.563141, Lat: 55.726905) in the western North Atlantic during the GEOTRACES cruise 64PE358 (RV Pelagia) in August 2012. Shelf surface samples (16 underway samples: Fig. 5.1S) were collected using a towed 'fish' at ~ 2-3 m and pumped into the clean laboratory using a Teflon diaphragm pump. In addition, three shelf samples were collected using trace metal OTE bottles deployed on a Ti-CTD frame from sites indicated as CTD202 (one sample at 90 m depth) and CTD78 (samples at 161 and 195 m) (Fig. 5.1S). Ocean samples were collected using 24 ultra trace-metal clean PVDF samplers of 27 L mounted on an all titanium frame and deployed in deep ocean waters with a Kevlar hydrowire. All shelf and ocean samples were filtered in-line using a 0.2 µm cartridge filter (Sartobran) into 0.5 L sample bottles (LDPE, Nalgene) and stored frozen until analysis.

5.4. References

Abualhaija, M.M. and van den Berg, C.M.G., 2014. Chemical speciation of iron in seawater using catalytic cathodic stripping voltammetry with ligand competition against salicylaldoxime. Marine Chemistry, 164(0): 60-74.

Abualhaija, M.M., Whitby, H. and van den Berg, C.M.G., 2015. Competition between copper and iron for humic ligands in estuarine waters. Marine Chemistry, 172(0): 46-56.

Batchelli, S., Muller, F.L.L., Chang, K.C. and Lee, C.L., 2010. Evidence for Strong but Dynamic Iron-Humic Colloidal Associations in Humic-Rich Coastal Waters. Environmental Science & Technology, 44(22): 8485-8490.

Biller, D.V. and Bruland, K.W., 2012. Analysis of Mn, Fe, Co, Ni, Cu, Zn, Cd, and Pb in seawater using the Nobias-chelate PA1 resin and magnetic sector inductively coupled plasma mass spectrometry (ICP-MS). Marine Chemistry, 130: 12-20.

Boye, M. et al., 2006. The chemical speciation of iron in the north-east Atlantic Ocean. Deep Sea Research I: Oceanographic Research Papers, 53(4): 667-683.

Boye, M. et al., 2001. Organic complexation of iron in the Southern Ocean. Deep-Sea Research Part I-Oceanographic Research Papers, 48(6): 1477-1497.

Buck, K.N., Sohst, B. and Sedwick, P.N., 2015. The organic complexation of dissolved iron along the U.S. GEOTRACES (GA03) North Atlantic Section. Deep-Sea Research Part II: Topical Studies in Oceanography, 116: 152-165.

Bundy, R.M., Biller, D.V., Buck, K.N., Bruland, K.W. and Barbeau, K.A., 2014. Distinct pools of dissolved iron-binding ligands in the surface and benthic boundary layer of the California Current. Limnology and Oceanography, 59(3): 769-787.

Gerringa, L.J.A., Rijkenberg, M.J.A., Schoemann, V., Laan, P. and de Baar, H.J.W., 2015. Organic complexation of iron in the West Atlantic Ocean. Marine Chemistry(0).

Gerringa, L.J.A., Rijkenberg, M.J.A., Thuroczy, C.E. and Maas, L.R.M., 2014. A critical look at the calculation of the binding characteristics and concentration of iron complexing ligands in seawater with suggested improvements. Environmental Chemistry, 11(2): 114-136.

Hassler, C.S., Alasonati, E., Nichols, C.A.M. and Slaveykova, V.I., 2011a. Exopolysaccharides produced by bacteria isolated from the pelagic Southern Ocean - Role in Fe binding, chemical reactivity, and bioavailability. Marine Chemistry, 123(1-4): 88-98.

Hassler, C.S. et al., 2015. Iron associated with exopolymeric substances is highly bioavailable to oceanic phytoplankton. Marine Chemistry, 173(0): 136-147.

Hassler, C.S., Schoemann, V., Nichols, C.M., Butler, E.C.V. and Boyd, P.W., 2011b. Saccharides enhance iron bioavailability to Southern Ocean phytoplankton. Proceedings of the National Academy of Sciences of the United States of America, 108(3): 1076-1081.

Heller, M.I., Gaiero, D.M. and Croot, P.L., 2013. Basin scale survey of marine humic fluorescence in the Atlantic: Relationship to iron solubility and H2O2. Global Biogeochemical Cycles, 27(1): 88-100.

Hutchins, D.A., Witter, A.E., Butler, A. and Luther, G.W., III, 1999. Competition among marine phytoplankton for different chelated iron species. Nature, 400(6747): 858-861.

Ibisanmi, E., Sander, S.G., Boyd, P.W., Bowie, A.R. and Hunter, K.A., 2011. Vertical distributions of iron-(III) complexing ligands in the Southern Ocean. Deep-Sea Research Part II-Topical Studies in Oceanography, 58(21-22): 2113-2125.

Kuma, K., Katsumoto, A., Kawakami, H., Takatori, F. and Matsunaga, K., 1998. Spatial variability of Fe(III) hydroxide solubility in the water column of the northern North Pacific Ocean. Deep-Sea Research Part I-Oceanographic Research Papers, 45(1): 91-113.

Laglera, L.M., Battaglia, G. and van den Berg, C.M.G., 2007. Determination of humic substances in natural waters by cathodic stripping voltammetry of their complexes with iron. Analytica Chimica Acta, 599(1): 58-66.

Laglera, L.M. and van den Berg, C.M.G., 2009. Evidence for geochemical control of iron by humic substances in seawater. Limnology and Oceanography, 54(2): 610-619.

Liu, X. and Millero, F.J., 1999. The solubility of iron hydroxide in sodium chloride solutions. Geochimica et Cosmochimica Acta, 63(19-20): 3487-3497.

Martin, J.H. and Fitzwater, S.E., 1988. Iron deficiency limits phytoplankton growth in the northeast Pacific subarctic. Nature, 331: 341-343.

Mawji, E. et al., 2008. Hydroxamate Siderophores: Occurrence and Importance in the Atlantic Ocean. Environmental Science & Technology, 42(23): 8675-8680.

Mohamed, K.N., Steigenberger, S., Nielsdottir, M.C., Gledhill, M. and Achterberg, E.P., 2011. Dissolved iron(III) speciation in the high latitude North Atlantic Ocean. Deep-Sea Research Part I-Oceanographic Research Papers, 58(11): 1049-1059.

Morel, F.M.M. and Price, N.M., 2003. The Biogeochemical Cycles of Trace Metals in the Oceans. Science, 300(5621): 944-947.

Omanović, D., Garnier, C. and Pižeta, I., 2015. ProMCC: An all-in-one tool for trace metal complexation studies. Marine Chemistry, 173(0): 25-39.

Rue, E.L. and Bruland, K.W., 1995. Complexation of iron(III) by natural organic-ligands in the central north pacific as determined by a new competitive ligand equilibration adsorptive cathodic stripping voltammetric method. Marine Chemistry, 50(1-4): 117-138.

Ruzic, I., 1982. Theoretical aspects of the direct titration of natural waters and its information yield for trace metal speciation. Analytica Chimica Acta, 140: 99-113.

Stolpe, B., Zhou, Z.Z., Guo, L.D. and Shiller, A.M., 2014. Colloidal size distribution of humic- and protein-like fluorescent organic matter in the northern Gulf of Mexico. Marine Chemistry, 164: 25-37.

Sunda, W.G. and Huntsman, S.A., 1995. Iron uptake and growth limitation in oceanic and coastal phytoplankton. Marine Chemistry, 50(1-4): 189-206.

Turoczy, N.J. and Sherwood, J.E., 1997. Modification of the van den Berg/Ruzic method for the investigation of complexation parameters of natural waters. Analytica Chimica Acta, 354(1-3): 15-21.

van den Berg, C.M.G., 1982. Determination of copper complexation with natural organic ligands in seawater by equilibration with MnO2 I. Theory. Marine Chemistry, 11(4 SU -): 307-322.

Völker, C. and Tagliabue, A., 2015. Modeling organic iron-binding ligands in a three-dimensional biogeochemical ocean model. Marine Chemistry, 173(0): 67-77.

Whitby, H. and van den Berg, C.M.G., 2015. Evidence for copper-binding humic substances in seawater. Marine Chemistry, 173(0): 282-290.

Chapter 5

Supplementary data

Figures:

Figure 5.1S. Map of sample locations. Transect (U1 to U30) and CTD (202 and78) samples from the Shelf waters in the Celtic sea.

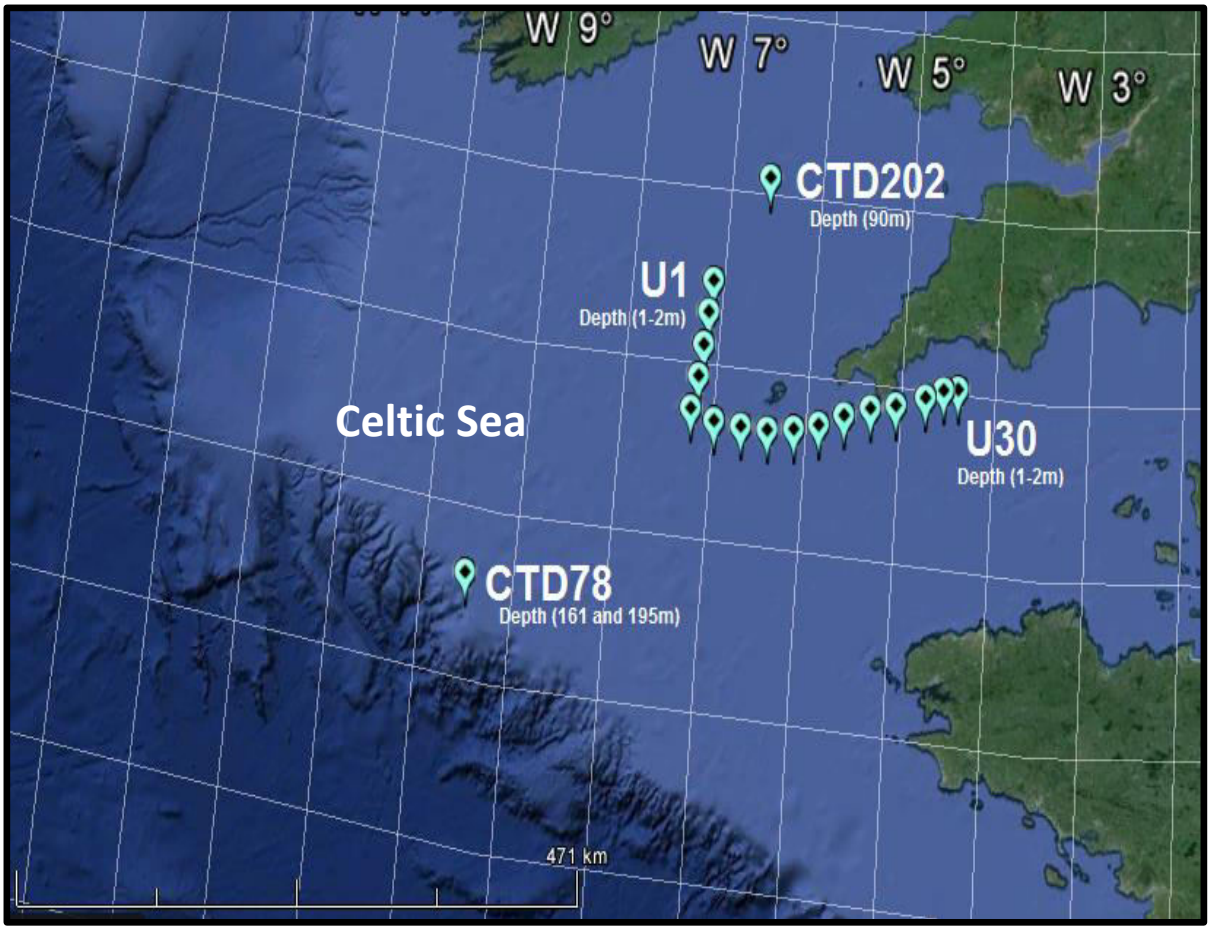

Figure 5.2S. A) Fe concentration (nM) as function of Fe- binding ligands concentration (nM) in shelf samples. B) Fe concentration (nM) versus Fe- binding ligands concentration (nM) in the Atlantic samples.

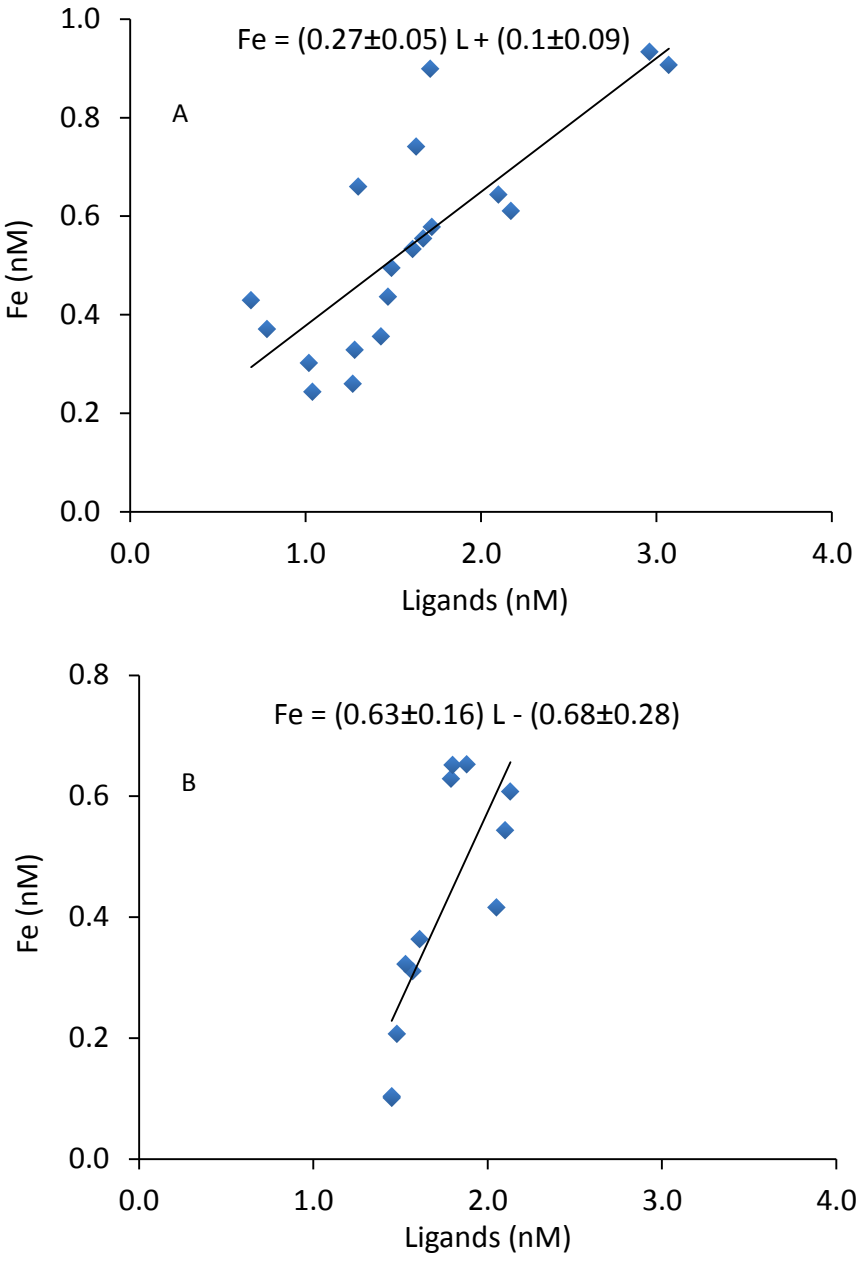

Figure 5.3S. Examples of complexing ligand titration. A,C) Peak height as function of the concentration of total dissolved Fe. B,D) Linearisation of the data.

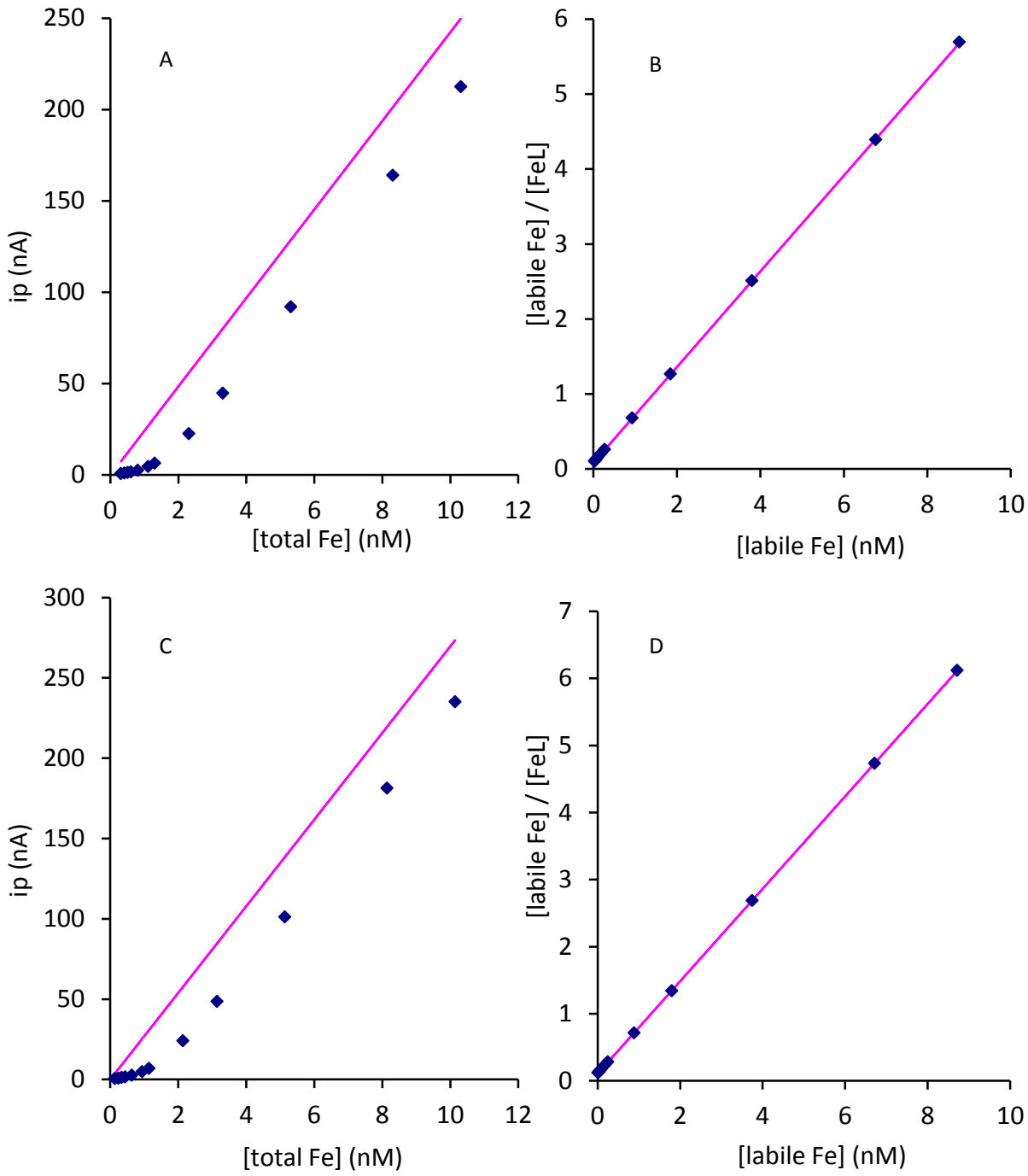

Tables:

Table 5.1S. Shelf data: Humic substance concentrations (HS) were converted from the µg/l scale to the nM scale using a binding capacity of 30.6 nM Fe/mg HA (Abualhaija and van den Berg, 2014).

Station	Depth (m)	Salinity	Fe (nM)	HS (µg/l)	L (nM)	Log $K'_{Fe'L}$	HS (nM)	Fe' (pM)
U1	2 – 3	35.2	0.93	99.5	2.96	11.0	3.04	4.6
U3	2 – 3	35.3	0.91	100.9	3.07	11.0	3.09	4.2
U5	2 – 3	35.3	0.66	40.2	1.30	11.2	1.23	5.1
U7	2 – 3	35.4	0.64	72.0	2.10	11.0	2.20	4.4
U9	2 – 3	35.4	0.74	52.7	1.63	11.2	1.61	5.2
U11	2 – 3	35.4	0.55	50.6	1.67	11.2	1.55	3.1
U13	2 – 3	35.3	0.44	46.9	1.47	11.3	1.43	2.1
U15	2 – 3	35.4	0.36	45.1	1.43	11.0	1.38	3.3
U17	2 – 3	35.3	0.26	42.0	1.27	11.0	1.29	2.5
U19	2 – 3	35.4	0.33	42.0	1.28	11.0	1.29	3.4
U21	2 – 3	35.3	0.30	40.6	1.02	11.1	1.24	2.6
U23	2 – 3	35.2	0.24	42.3	1.04	11.1	1.29	1.9
U25	2 – 3	35.3	0.37	26.1	0.78	11.4	0.80	2.8
U27	2 – 3	35.3	0.43	21.3	0.69	11.6	0.65	4.0
U29	2 – 3	35.3	0.53	53.0	1.61	11.3	1.62	1.6
U30	2 – 3	35.3	0.90	54.6	1.71	11.6	1.67	2.8
CTD202.ros1	90	35.2	0.61	66.8	2.17	11.0	2.04	2.0
CTD78.ros3	161	35.6	0.50	51.2	1.49	11.2	1.57	3.1
CTD78.ros16	195	35.6	0.58	53.7	1.72	11.3	1.64	2.5

Table 5.2S. Atlantic data: Vertical profile of Geotraces station 4 in the NE Atlantic.

Sample number	Depth (km)	Fe (nM)	HS (µg/l)	L (nM)	Log $K'_{Fe'L}$	HS (nM)	Fe' (pM)
23	0.026	0.10	46.4	1.45	11.3	1.42	0.4
21	0.077	0.10	46.0	1.45	11.1	1.41	0.6
19	0.151	0.21	48.1	1.48	11.1	1.47	1.3
16	0.359	0.31	51.0	1.57	11.2	1.56	1.6
14	0.607	0.32	48.0	1.53	11.2	1.47	1.7
12	0.808	0.36	50.3	1.61	11.0	1.54	2.9
11	1.012	0.42	65.0	2.05	11.1	1.99	1.6
9	1.519	0.54	66.4	2.10	11.0	2.03	3.5
7	2.029	0.61	67.3	2.13	11.2	2.06	2.5
5	2.537	0.63	58.0	1.79	11.3	1.77	2.7
4	2.792	0.65	58.0	1.80	11.3	1.77	2.8
2	3.346	0.65	59.3	1.88	11.2	1.81	3.3

6

Chapter 6

General conclusions and future perspectives

6. GENERAL CONCLUSIONS AND FUTURE PERSPECTIVES

6.1. General conclusions

1. Experiments showed that the CSV sensitivity is much improved in the presence of dissolved oxygen (DO) through a catalytic effect (Fe^{II} acts as catalyst for the reduction of DO). Furthermore, the optimum sensitivity was obtained at 5 µM SA (~5 x less than the pre-existing method). Interpretation of the experiments showed that the complex responsible for adsorption on the mercury drop electrode is FeSA, whereas the $FeSA_2$ species does not adsorb. This is important because it means that using a concentration of 25 – 30 µM SA (as advocated in previous work) causes a greatly reduced sensitivity.

2. The kinetic determination of the dissociation rate of Fe complex with the natural ligands showed that the dissociation rate has a half-life of 9 min, which means that a reaction time of > 1 h is required after the addition of SA to be close to equilibrium. This is much longer than the equilibrium time of 15-30 min suggested by previous work.

3. Calibration of the stability constants (log $K'_{Fe'SA}$ and log $B'_{Fe'SA2}$) showed a very good agreement with and without EDTA. The similarity of these constants indicates that the complexation of Fe with hydroxide and EDTA is well understood.

4. The pH optimization experiments of the CSV method using SA showed that the sensitivity decreases with decreasing pH. This hinders the use of the SA method at lower pH and could be a reason for using a different competitive ligand.

5. Based on the competition experiments between copper and iron for natural ligands (which was identified as humic substance), it can be concluded that copper competes with iron for complexation with natural ligands in estuarine and coastal waters.

6. The competition effect was occurring already at low copper additions suggesting that the competition reactions between Fe and Cu should be taken into account in the study of the bioavailability of both metals to marine microorganisms.

7. The MAW experiments showed that all samples from the Mersey estuary and Liverpool bay contained only one ligand in spite of the large amount of organic matter.

8. The similarity of the concentration of iron binding humic substances and complexing ligands in samples from estuarine, coastal, shelf and ocean waters, combined with the similarity of the complex stability, and the evidence that only one ligand is present, suggests that humic substances may be the dominant ligand in these waters.

6.2. Perspectives resulting from this work

The new conditions for the chemical speciation of iron using the SA method that are recommended in the present study (air-blanketing and if necessary air-purging if samples are not already in equilibrium with air, a lower concentration of SA than pre-existing method (Buck et al., 2007; Rue and Bruland, 1995)), give better sensitivity, and stable conditions also when samples derive from anoxic waters and much facilitates the speciation procedure and the method to determine dissolved Fe. This could solve the problem of decreasing FeSA response found in some previous work (Buck et al., 2007; Rue and Bruland, 1995).

The equilibration time (typically overnight) between SA and Fe complexed with L suggested by the present study is essential to avoid possible underestimation of the Fe that is bound by the added SA and overestimation of the complex stability of FeL, and thus incorrect data fitting: a too short equilibration time was used in some previous and recent work (Buck et al., 2007; Buck et al., 2015; Bundy et al., 2015; Bundy et al., 2014; Rue and Bruland, 1995) using the old SA method, and could be the reason for non-linearity in the

data treatment, incorrectly suggesting the presence of more than one ligand.

This kinetic effect also has implications for field work in that measurements have to include ample equilibration time (typically overnight and in presence of SA and added Fe) which means that titrations cannot be just equilibrated 15 minutes after the SA addition as done in some work currently (Buck et al., 2015). This will affect the procedures used in the field as it is slower so you cannot do so many titrations and you cannot do this automatically (Gerringa et al., 2014).

The new calibrated values for $K'_{Fe'SA}$ and $B'_{Fe'SA2}$ obtained over a large range of salinity between 4 and 35 give a significantly larger value for the α-coefficient for complexation of Fe by SA than the previous values calculated based on $B'_{Fe'SA2}$ only (Buck et al., 2007). It is of importance to use the correct stability constants when the detection window is varied as the ratio of the new and old α-coefficients varies with the concentration of SA: the ratio changes from 7.3 to 1.6 (Sal 35), or from 11.9 to 9.4 (Sal 2) when [SA] is raised from 5 to 30 µM. Using the old constants could lead to a shift in the detected $K'_{Fe'L}$ with the detection window and non-linearity of the data fitting. Again, this could lead to incorrect interpretation of data in terms of two or more ligands (Bundy et al., 2015; Bundy et al., 2014).

Some work has suggested the presence of more than one ligand. A quick survey shows that all this work used either incorrect stability constants (Bundy et al., 2014), only a very short equilibration time (Buck et al., 2007; Bundy et al., 2014), or both. These factors can be the reason for incorrectly finding two or more ligands.

Natural organic ligands in seawater have been hypothesized as consisting of several compounds (ligand soup) (Hunter and Boyd, 2007), and more than one ligand has been found using CSV (Buck and Bruland, 2007; Buck et al., 2015; Bundy et al., 2015; Bundy et al., 2014; Cullen et al., 2006; Rue and Bruland, 1995). The distinction between these classes depended on the detection window (binding strength of the added competing ligand) and the method of measurement, and it is difficult to distinct between these classes if there is overlapping in their complex stability (log $K'_{Fe'L}$). There is a need for new complexation titration experiments to be done at very low Fe concentration using longer deposition time and lowering the iron additions at the end of the titration (to avoid the saturation of mercury

drop electrode) to confirm whether a second ligand could be present, this may need to use a higher detection window taking into account the lower sensitivity using the improved SA method at higher concentration of SA.

The identification of the Fe-binding ligands as humic substances challenges the paradigm that iron-binding ligands largely originate from in-situ production by microorganisms. However, it is not known from where the HS originate. They could be from microbial breakdown or from land. So there could still be a marine source as well as a terrestrial source. It has to be further investigated if any other ligand (like EPS) could give a humic like response and therefore contribute to the pool of Fe-binding ligands.

Copper additions to Fe complexed with natural ligands demonstrated competition between Cu and Fe for natural ligands, when added copper outcompeted iron and displaced it from FeL and therefore increased Fe' (Abualhaija et al., 2015). Consequently competition by Cu can be expected to affect the availability of Fe to microorganisms in seawater. Iron (Fe) and copper (Cu) are known to occur complexed with organic matter and this complexation for both metals affects their geochemistry and bioavailability. Both metals are essential metals for microorganism and interaction between them is quite possible and can be expected to affect their bioavailability and complexation with organic matter. It has been shown that the uptake rate of organically bound iron by phytoplankton is dependent on copper availability (Maldonado., et al., 2006) where the Fe (II) produced by reductases is re-oxidized by a copper containing ferroxidase during the Fe transport to the cell membrane (Maldonado., et al., 2006). Further work is required to confirm whether the relationship between Cu and Fe plays a role in open sea conditions, and whether other metals can compete with Fe for natural ligands.

A major finding of the re-calibration of the stability constants for complexation of SA with Fe is that only the FeSA adsorbs, whereas FeSA2 does not adsorb. Maximum sensitivity is obtained at 5 µM SA and it drops rapidly with increasing [SA]. This affects the method of multiple detection windows (MAW) in which the concentration of SA is raised to be able to outcompete natural ligands as done for copper. The MAW method does not work well for iron because of the decreasing sensitivity at high [SA]. A careful study of iron speciation in estuarine waters using the MAW method (Mahmood et al., 2015) shows that any way there

was only one ligand for Fe (HS) in estuarine waters, though it cannot be excluded that the situation is different in other estuaries.

Another major finding was that the sensitivity of the SA method decreases with a slight decrease in pH. This means that it is difficult to impossible to use the method to study Fe speciation at lower pH and it may be necessary to develop a procedure using a different ligand, but otherwise similar to SA.

6.3. References

Abualhaija, M.M., Whitby, H. and van den Berg, C.M.G., 2015. Competition between copper and iron for humic ligands in estuarine waters. Marine Chemistry, 172(0): 46-56.

Buck, K.N. and Bruland, K.W., 2007. The physicochemical speciation of dissolved iron in the Bering Sea, Alaska. Limnology and Oceanography, 52(5): 1800-1808.

Buck, K.N., Lohan, M.C., Berger, C.J.M. and Bruland, K.W., 2007. Dissolved iron speciation in two distinct river plumes and an estuary; implications for riverine iron supply. Limnology and Oceanography, 52(2): 843-855.

Buck, K.N., Sohst, B. and Sedwick, P.N., 2015. The organic complexation of dissolved iron along the U.S. GEOTRACES (GA03) North Atlantic Section. Deep Sea Research Part II: Topical Studies in Oceanography, 116(0): 152-165.

Bundy, R.M. et al., 2015. Iron-binding ligands and humic substances in the San Francisco Bay estuary and estuarine-influenced shelf regions of coastal California. Marine Chemistry, 173: 183-194.

Bundy, R.M., Biller, D.V., Buck, K.N., Bruland, K.W. and Barbeau, K.A., 2014. Distinct pools of dissolved iron-binding ligands in the surface and benthic boundary layer of the California Current. Limnology and Oceanography, 59(3): 769-787.

Cullen, J.T., Bergquist, B.A. and Moffett, J.W., 2006. Thermodynamic characterization of the partitioning of iron between soluble and colloidal species in the Atlantic Ocean. Marine Chemistry, 98(2–4): 295-303.

Gerringa, L.J.A., Rijkenberg, M.J.A., Thuroczy, C.E. and Maas, L.R.M., 2014. A critical look at the calculation of the binding characteristics and concentration of iron complexing ligands in seawater with suggested improvements. Environmental Chemistry, 11(2): 114-136.

Hunter, K.A. and Boyd, P.W., 2007. Iron-binding ligands and their role in the ocean biogeochemistry of iron. Environmental Chemistry, 4(4): 221-232.

Mahmood, A., Abualhaija, M.M., van den Berg, C.M.G. and Sander, S., 2015. Organic speciation of dissolved iron in estuarine and coastal waters at multiple analytical windows. Marine Chemistry, Submitted.

Maldonado, M.T. et al., 2006. Copper-dependent iron transport in coastal and oceanic diatoms. Limnology and Oceanography, 51(4): 1729-1743.

Rue, E.L. and Bruland, K.W., 1995. Complexation of iron(III) by natural organic-ligands in the central north pacific as determined by a new competitive ligand equilibration adsorptive cathodic stripping voltammetric method. Marine Chemistry, 50(1-4): 117-138.